Title

Nuclear Structure Dependent Radiative Corrections to Gamow-Teller Transitions and Proton-Proton Fusion

Author

Hambleton, Katherine Ann

Publication Date

2024

Peer reviewed|Thesis/dissertation

Nuclear Structure Dependent Radiative Corrections to Gamow-Teller Transitions and Proton-Proton Fusion

by

Katherine Hambleton

A dissertation submitted in partial satisfaction of the

requirements for the degree of

Doctor of Philosophy

in

Physics

in the

Graduate Division

of the

University of California, Berkeley

Committee in charge:

Professor Wick Haxton, Chair
Professor Hitoshi Murayama
Professor Kai Vetter

Fall 2024

Nuclear Structure Dependent Radiative Corrections to Gamow-Teller Transitions and Proton-Proton Fusion

Abstract

Nuclear Structure Dependent Radiative Corrections to Gamow-Teller Transitions and Proton-Proton Fusion

by

Katherine Hambleton

Doctor of Philosophy in Physics

University of California, Berkeley

Professor Wick Haxton, Chair

Precision in semileptonic weak nuclear interactions has become an important topic, with applications to both high-energy and solar physics. We can search for physics beyond the standard model by checking CKM unitarity using superallowed Fermi beta decay. This is one of the most precise tests of the standard model. With better measurements of the axial form factor g_A, the neutron lifetime can also become a competitive test of CKM unitarity. In solar physics, the rate of pp-fusion can be used in the luminosity constraint to test for new physics in the sun.

The radiative correction to superallowed Fermi beta decay comes from a box diagram involving the axial-vector weak current. It is known that the spin-flip transitions generated by the magnetic moment and Gamow-Teller operators are modified by the nuclear environment. Nuclear shell model calculations of these transitions consistently give larger results than what is seen in experiments. This is corrected by phenomenological "quenching factors" which suppress the rates to match experiment. In the analysis done by Towner and Hardy, they accounted for this effect by modifying the free-nucleon Born correction by a product of these quenching factors.

Their analysis was challenged in a 2019 paper by Seng Gorchtein and Ramsey-Musolf, who claim that this analysis is flawed due to the fact that the quasi-elastic contribution has been shown not to require this quenching correction. They provide a formula for the quasi-elastic part of the box diagram, which involves nuclear structure corrections due to Pauli blocking and the nucleon removal energy.

The goal of this thesis is to focus on a smaller nuclear system, in which the calculation does not suffer from these issues. Instead of focusing on Fermi decay, which has been the focus of much of the field, we analyze the case of *pp*-fusion which is mediated by a Gamow-Teller interaction. We also are able to confirm the approximation claimed in a 2003 analysis done

by Kurylov Ramsey-Musolf and Vogel. In particular, we will be able to directly calculate the two-body contribution, Figure 1b in their paper.

Since much of the focus has been on Fermi decays, and much less has been written about Gamow-Teller transitions, we go through the analysis for both the one-body Born contribution and the two-body nuclear structure correction. We give a new analysis of the Born correction for Gamow-Teller transitions, which is slightly different from that of Hayen 2021. This contribution is important for comparing the measured value of g_A in neutron decay to the one calculated in lattice QCD. We also derive new formulas for the two-body nuclear structure correction, in analogy with the analysis of Fermi decays by Towner 1992. Using the standard two-body density matrix technique, these formulas can be used to calculate the nuclear structure correction to Gamow-Teller transitions in larger nuclear systems.

We calculate the nuclear structure correction in *pp*-fusion in three different ways. First, we apply our new formulas for the two-body nuclear structure correction. This result depends on the approximation scheme outlined in Jaus and Rasche 1990 and Towner 1992, where we ignore the nuclear environment effects on the Green's function. Our result is slightly smaller than the estimate given by Kurylov and collaborators, due to a partial cancellation between the spin and the tensor terms and the narrow momentum space wavefunction of the initial *pp*-state.

We then give a new method which does not rely on approximating the nuclear Green's function. This involves expanding the box diagram in terms of all possible intermediate states. We are able to check that this works by verifying the completeness relation, which must be exactly satisfied if all intermediate states are included. This is the main reason we are limited to small nuclear systems, such as the two and three body system.

Once we expand the box diagram in terms of intermediate states, we are then able to directly calculate the effect of the nuclear environment through the nuclear Green's function. We find a significant enhancement over the previous calculation - much larger than one would expect from the non-relativistic $1/M_N$ power counting. This effect is due to a persistent energy gap at low momentum transfer, coming from the binding energy of the deuteron.

Using our detailed knowledge of the system, we are then able to derive an approximate form of the result - the "modified normal ordering" scheme. We pick an average value of the nuclear energy, which is allowed to depend on the loop momentum. This approximation scheme allows us to remove the intermediate states and normal order the currents, thus allowing us to separate out the one-body and two-body parts.

In addition to narrowing the uncertainty in the *pp*-fusion cross section, the analysis done here is one concrete demonstration of the method outlined in Seng Gorchtein and Ramsey-Musolf's 2019 paper. While we were not able to resolve the issue of how to handle the phenomenological quenching factors in larger systems, the work done here can provide some insight into what an alternative method might look like.

To my parents, Jeff and Margaret Hambleton

For always believing in me, and for supporting me through this long and difficult journey.

Contents

List of Figures

List of Tables

Acknowledgments

I would like to thank my advisor Wick Haxton for helping me find a problem in the intersection of nuclear, high energy, and solar physics. Thanks to his guidance, I was able to navigate my way through this confusing problem and come out the other side with interesting new results which should be interesting to the wider community.

I would also like to thank Professor Michael Ramsey-Musolf for giving me the initial insight into this problem. Although we didn't necessarily see eye-to-eye on how best to tackle the problem, I would not have been able to get my footing and start making progress without his input.

I would also like to thank my friends and colleagues, Ken McElvain and Evan Rule, for discussing the project with me and allowing me to bounce ideas off of them. And also my late friend Maddie Dickens, who helped me through very lonely and difficult times at the start of my time at Berkeley.

Chapter 1

Semileptonic Weak Interactions

The topic of this thesis is the *order-α electromagnetic radiative corrections to weak nuclear processes*. In the first two sections, I hope to provide the reader with the required context to understand exactly what is being discussed and why it matters. We will begin by reviewing the structure of the weak interactions, and how they are modified by the strong force. This will set the stage for discussing the radiative corrections in Section 2.

Electromagnetism

As far as we know today, there are four basic forces in nature. Gravity governs the behaviour of massive objects on large scales, and it will not be important here. Electromagnetism is the most important force for the physics of our everyday lives. It is responsible for all the various chemical reactions, all of our electronic devices, and our ability to see. Less familiar to us are the two nuclear forces - the strong and weak forces.

The strength of electromagnetic interactions is controlled by the *fine structure constant* α.

$$\alpha = \frac{e^2}{4\pi\varepsilon_0\hbar c} \approx \frac{1}{137} \tag{1.0.1}$$

At the quantum level, α appears in every calculation which involves the electromagnetic interaction. For example, electrons are bound to nuclei by the coulomb attraction between electrons and protons. The energy levels of Hydrogen-like ions involve the fine structure constant, α.

$$E_n = -\frac{Z^2 m_e \alpha^2 c^2}{2n^2} \tag{1.0.2}$$

Where Z is the charge of the nucleus. Plugging in the electron mass $m_e c^2 \approx 511$ keV, for $Z = n = 1$ we arrive at the ground state energy of Hydrogen, 13.6 eV. We can also find α in the Bohr radius, which tells us roughly the size of the atomic cloud.

$$a_0 = \frac{\hbar}{m_e \alpha c} \tag{1.0.3}$$

Which is about 0.5 Å, or 0.5×10^{-10} m. (Hereafter we set $\hbar = c = \varepsilon_0 = 1$, unless otherwise stated.)

In quantum field theory, the theory of charged particles interacting with the electromagnetic field is known as *quantum electrodynamics*, or QED. The most powerful computational tool at our disposal is called *perturbation theory*. This involves taking any process, and analyzing the result in a power series in α. For example, if the rate of some process in QED is $f(\alpha)$, then the perturbative expansion to order α^2 would be

$$f(\alpha) = f_0 + f_1\alpha + f_2\alpha^2 + \mathcal{O}(\alpha^3). \tag{1.0.4}$$

The $\mathcal{O}(\alpha^3)$ represents everything we are leaving out of our calculation. Since α is about $\frac{1}{100}$, the terms we are neglecting are suppressed by at least $\alpha^3 \approx \frac{1}{1{,}000{,}000}$. Thus, we are able to get a very good approximation to the result by considering only the first few terms. We say that QED is *perturbative* at low energies.

We can use QED to compute things like electromagnetic decay rates and scattering cross sections. The perturbation series can be represented using *Feynman diagrams*, which can be directly converted into a probability amplitude by using the Feynman rules. Examples of such diagrams are shown in Figure 1.1.

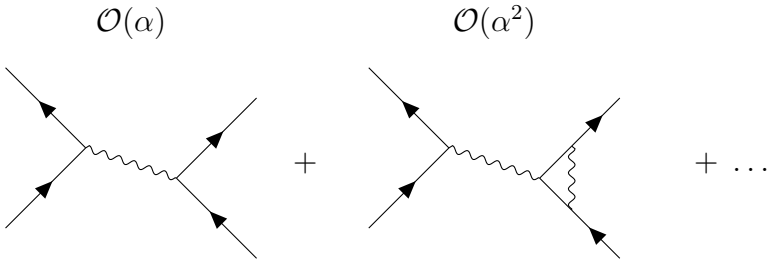

Figure 1.1: Examples of Feynman diagrams used to calculate the electromagnetic scattering amplitude. The dots represent an infinite series of additional terms with more photon exchanges.

At lowest order in perturbation theory, we can approximate electromagnetic scattering by considering one-photon exchange. The one-photon exchange approximation would be corrected by a two-photon exchange contribution, and so on. Each additional photon which is exchanged comes at the cost of another factor of α, which is about 1%. We are able to approximate the sum of infinitely many terms in Figure 1.1 by truncating the sum at a given order in α. The terms we neglect are suppressed by an additional power of α, and this allows us to estimate the uncertainty in our answer.

Strong Nuclear Force

The strong nuclear force is what binds quarks into nucleons. It also holds nuclei together - overwhelming the electrostatic repulsion of the positively charged protons. In contrast to electromagnetism, the strong interactions are *non-perturbative* at low energies. The simple Feynman diagrams shown in Figure 1.1 do not give us a good approximation - no matter

how many terms we include. The non-perturbative nature of the strong interactions has historically made them far more mysterious than electromagnetism and gravity.

Nuclear physics began with the discovery of radioactivity in the late 1800's, which categorized α, β, γ rays according to how easily they were stopped by matter (α here refers to α-particles, not the fine structure constant). When electrons in atoms jump between energy levels of Equation 1.0.2, they give off photons in the eV range (visible, ultraviolet), up to the keV range (X-rays). Nuclear transitions give off gamma rays, with energies about a thousand times greater than atomic transitions. Throughout this work, we will typically be working with energies in MeV.

$$\text{MeV} = 1000 \text{ keV} = 10^6 \text{ eV} \tag{1.0.5}$$

Nuclei themselves were discovered by shooting α particles at a thin gold foil. Most of the α's would pass straight through, with only slight deflection. Occasionally, they would seem to hit something which would cause them to be deflected back by almost 180°. In 1911, Ernest Rutherford was able to explain this by supposing the existence of a small, central, positive charge - which we now call the nucleus. The size of the nucleus is about 10^5 times smaller than the atomic cloud in Equation 1.0.3, and it is typically measured in femtometers (fm).

$$\text{fm} = 10^{-5} \text{ Å} = 10^{-15} \text{ m} \tag{1.0.6}$$

If we scaled up the atom to be the size of the main UC Berkeley campus, the nucleus would be roughly the size of a coffee bean.

Rutherford went on to show that all nuclei were made up of Hydrogen nuclei - which we now call protons. For some time, it was believed that the only elementary particles were electrons and protons. The discovery of the neutron would take another 20 years, when in 1932 James Chadwick was able to reliably produce neutrons by bombarding ^{9}Be by α particles.

Between the late 1950's and the early 1960's, there was a zoo of new "elementary particles" being discovered one after the other. New strongly interacting particles were split into two groups according to their statistics: mesons (Bosons) and bayons (Fermions). (Masses given in MeV from [Pat+16].)

$$\begin{aligned} \text{Mesons: } & \pi^{\pm}(140), \pi^0(135), K^{\pm}(494), K^0(498), \eta(548), \rho(775), \omega(783) \dots \\ \text{Baryons: } & p^+(938), n^0(940), \Lambda^0(1116), \Delta(1232), \Sigma^+(1189), \Sigma^0(1193), \Sigma^-(1197), \Xi^0(1315), \dots \end{aligned} \tag{1.0.7}$$

These further were categorized according to their mass and symmetry properties. In addition to the usual charge, spin, and parity, there were new symmetries known as *isospin* and *strangeness*.

This was not understood until 1964 when Gell-Mann and Zweig independently suggested that all of these strongly interacting particles were made up of yet-undiscovered elementary spin 1/2 particles called *quarks*. These quarks carry a new kind of charge, called *colour charge*, and interact by exchanging massless *gluons* - the strong force equivalent of the

photon. These quarks and gluons could never be seen individually due to a phenomenon known as *colour confinement*, which states that only colour neutral particles can be observed in nature.

Weak Nuclear Force

The weak nuclear force appears to be nothing like the forces we have discussed thus far. It doesn't bind anything together. It doesn't push things around like the gravitational or electromagnetic forces. It has no immediately observable impact in our daily lives. So what exactly does the weak force *do*?

The weak nuclear force causes nuclear beta decay. In nuclear beta decay, a neutron becomes a proton (or vice-versa). In order to compensate for the difference in electric charge, an electron (or positron) is emitted so that electric charge is conserved overall. In 1911, experiments performed by Lise Meitner and Otto Hahn showed that the electron is emitted with a continuous energy spectrum - implying some energy was lost.

$$ {}^{A}Z \to {}^{A}(Z \pm 1) + e^{\mp} + (\text{missing energy}) \tag{1.0.8} $$

In 1930, Wolfgang Pauli suggested that a yet-undiscovered new particle might carry away the missing energy in beta decay. This particle is a light, electrically neutral, spin 1/2 particle called the "neutrino". For example, consider the decay of the radioactive isotope Oxygen-14.

$$ {}^{14}\mathrm{O} \to {}^{14}\mathrm{N} + e^{+} + \nu_e \tag{1.0.9} $$

Free neutrons - those not bound in nuclei - also decay via the weak interaction. This was first demonstrated in 1948, just after World War II, by Arthur Snell and Leonard Miller who estimated a neutron half-life somewhere between 15 and 27 minutes. The neutron is heavier than the proton by approximately $M_n - M_p \approx 1.3$ MeV, which is large enough to allow free neutrons to decay via the weak interaction.

$$ n \to p^{+} + e^{-} + \bar{\nu}_e \tag{1.0.10} $$

The weak interaction which is most relevant for our daily lives occurs in the core of the Sun, where the density and temperature are so extreme that two protons can overcome the repulsive coulomb force and fuse together. In proton-proton fusion, one of the protons turns into a neutron through the weak interaction. The bound state of a proton and a neutron is called deuterium, d, also known as ^{2}H or "heavy hydrogen".

$$ p + p \to d + e^{+} + \nu_e \tag{1.0.11} $$

The weak interaction might seem remote and inconsequential, but it is in fact partially responsible for providing energy to all life on Earth through hydrogen burning. We will say much more about the *pp*-fusion reaction in Section 3.3.

Muon Decay

While nuclear beta decay is the earliest known example of a weak process, it is not the simplest example. We cannot ignore the effect of the strong interactions, and this makes calculating the rate of nuclear beta decay more complicated in general.

The simplest example of a weak decay process is *muon decay*. Muons are constantly being produced as high energy cosmic rays collide with the upper atmosphere. Because they only decay via the weak interaction, muons have a relatively long lifetime. Muons produced by cosmic rays can be easily detected on the Earth's surface, or even deep underground. Famously, in 1965 Luis Alvarez suggested using these naturally occurring cosmic ray muons as a non-invasive method to image the Egyptian pyramids to search for hidden chambers.

The muon is a member of the *lepton* family, which are elementary spin 1/2 particles that are not effected by the strong force. The muon is essentially a heavier cousin of the electron. They have the same electric charge, but the muon is about $m_\mu \approx 207 m_e$ times heavier. The muon is able to decay via the weak interaction.

$$\mu^- \to \nu_\mu + e^- + \bar{\nu}_e \tag{1.0.12}$$

Because muons are not effected by the strong force, this is a particularly simple and important decay process for studying the weak interactions.

By comparing muon decay to nuclear beta decay, we can learn about the interplay between the strong force and the weak force in nuclei.

Fermi's Theory of Weak Interactions

I now would like to describe the theory of the weak interactions, which will be the basis for the rest of this thesis. Rather than simply write down the answer, I will give a bit of the historical background which led to our current understanding.

In 1934, Enrico Fermi published his theory of beta decay [Fer34] (English translation [Wil68]). Fermi purposed the following interaction to mediate nuclear beta decay (written in modern notation).

$$\mathcal{L} = -\frac{G}{\sqrt{2}}[\bar{p}\gamma^\mu n][\bar{e}\gamma_\mu \nu_e] + \text{h.c} \tag{1.0.13}$$

Fermi's weak interaction has zero range - occurring all at the one point. The interaction is mediated by a vector current, in analogy with the electromagnetic current (Equation 1.1.9). For small velocities, Fermi's interaction reduces to a simple scalar operator. The most probable beta decay in Fermi's theory occurs when there is no change in nuclear spin, $\Delta J = 0$.

Fermi's selection rule turned out to be too restrictive to fit the data. In 1936, Gamow and Teller would purpose an additional interaction in order to explain angular momentum

selection rules seen in experiments [GT36]. For small nucleon velocities, the Gamow-Teller operator involves the spin of the nucleon (in two-component notation).

$$\chi_p^\dagger \vec{\sigma} \chi_n \tag{1.0.14}$$

Where σ are the usual Pauli spin matrices. Gamow-Teller transitions would allow for a change in nuclear spin without an any change in the parity of the nucleus.

The spin operator is a axial-vector - it does not transform under a parity transformation like an ordinary vector. Having both vector and axial-vector interactions opens the door to parity violation in the weak interactions, but it would take another 20 years before this fact was appreciated. In Winter 1956, Lee and Yang would purpose an experiment to put parity violation to the test [LY56b]. Lee and Yang point out that, in order to observe parity violation, one needs to form a pseudo-scalar out of the measured quantities. They suggested aligning nuclear spins, and then looking at the angular distribution of the emitted electrons.

$$N(\theta)d\theta = (\text{const}) \left(1 + A\frac{\vec{p}_e \cdot \langle \vec{J} \rangle}{E_e J}\right) \sin\theta d\theta \tag{1.0.15}$$

Where $\langle \vec{J} \rangle$ is the expectation value of nuclear spin. Under a parity transformation, the direction of the spin remains the same while the direction of the electron momentum flips. The coefficient A is due to the interference between parity-conserving and parity-violating interactions.

Immediately after Lee and Yang's work, Chien-Shiung Wu and her team conducted the famous *Wu experiment* which demonstrated that parity symmetry is violated in beta decay [Wu+57]. She did this by depositing the radioactive isotope ^{60}Co on a paramagnetic crystal layer of cerium magnesium nitrate. At extremely low temperatures, the large anisotropic magnetic field of the crystal aligns the spins of the ^{60}Co nuclei. They were able to demonstrate that the electrons have a much higher chance to be emitted in the opposite direction to nuclear spin.

Not only was parity violated in the weak interactions, but it was badly violated. This would be the clue which would allow physicists to finally discover the correct form of the weak interactions. The answer turns out to be surprisingly simple - take Fermi's original interaction Equation 1.0.13 and replace all of the fields with *left-handed* fields. We can write this using a projection operator.

$$e_L \equiv \frac{1}{2}(1 - \gamma^5)e \tag{1.0.16}$$

This is known as $V-A$ *theory*, first appearing in a paper by Feynman and Gell-Mann [FG58] but first proposed Sudarshan and Marshak. The reason for this name is that we can write the left-handed weak currents in terms of the vector current, $V^\lambda = \bar{\psi}_2 \gamma^\lambda \psi_1$, and the axial-vector current, $A^\lambda = \bar{\psi}_2 \gamma^\lambda \gamma^5 \psi_1$.

$$V^\lambda - A^\lambda = \bar{\psi}_2 \gamma^\lambda (1 - \gamma^5) \psi_1 \tag{1.0.17}$$

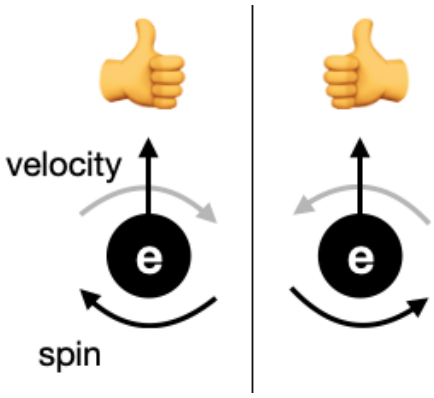

Figure 1.2: Parity symmetry exchanges left-and-right handed particles. Handedness, or helicity, is the relation between a particle's linear motion and it's spin. A particle is *left-handed* if you curl your fingers on your left hand in the direction of the spin, and your thumb points in the direction of motion.

The fermion fields ψ_1 and ψ_2 are pairs of fermions which are coupled in the weak interaction. For example, the weak current acts on the pairs (n, p), (e, ν_e) and (μ, ν_μ) as shown in Figure 1.3.

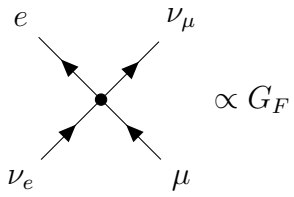

Figure 1.3: Four Fermion interaction which mediates muon decay.

The interaction Lagrangian corresponding to the vertex in Figure 1.3 is given by

$$\mathcal{L} = -\frac{G_F}{\sqrt{2}}[\bar{e}\gamma^\lambda(1-\gamma^5)\nu_e][\bar{\nu}_\mu\gamma_\lambda(1-\gamma^5)\mu] \tag{1.0.18}$$

Because the muon is so simple, it is now straightforward to calculate the muon decay rate. One thing we are interested in is the energy spectrum of the emitted electron (setting $m_e \to 0$ for simplicity).

$$\Gamma = \frac{G_F^2}{12\pi^3}\int_0^{E_{\max}} dE_e\, E_e^2 m_\mu\,(3m_\mu - 4E_e) \tag{1.0.19}$$

With $E_{\max} = \frac{1}{2}m_\mu$. Historically, this energy spectrum played an important role in constraining the structure of the weak interactions [Mic52]. Integrating over the electron energy gives

the famous result for the muon decay rate (the inverse lifetime).

$$\frac{1}{\tau_\mu} = \Gamma = \frac{G_F^2 m_\mu^5}{192\pi^3} \tag{1.0.20}$$

By carefully measuring the value of the muon lifetime, $\tau \approx 2.2\mu s$, and doing a more careful analysis of the theoretical decay rate, we can calculate the constant G_F [Pat+16].

$$G_F = 1.1663787(6) \times 10^{-5}\ \text{GeV}^{-2} \tag{1.0.21}$$

This is known as Fermi's constant.

The smallness of this constant is responsible for the weakness of the weak interactions. We can get an idea of this by doing some order of magnitude calculations using simple dimensional analysis. Weak cross sections are roughly on the order of

$$\sigma_{\text{weak}} \sim G_F^2 E^2 \sim (5 \times 10^{-17}\ \text{mb}) \times \left(\frac{E}{\text{MeV}}\right)^2 \tag{1.0.22}$$

We can compare this to electromagnetic cross sections, which go like

$$\sigma_{\text{EM}} \sim \frac{\alpha^2}{E^2} \approx (20\ \text{mb}) \times \left(\frac{\text{MeV}}{E}\right)^2 \tag{1.0.23}$$

Weak cross sections are about 6 to 18 orders of magnitude smaller, depending on the energy. This is why neutrinos are so difficult to detect, since they only interact via the weak force.

When the theory of weak interactions was first being developed, there was experimental evidence which suggested that all of the various four-Fermion interactions were governed by approximately the same constant, G_F. This was clearly a sign that something deeper was connecting all of the observed weak processes. However, there was no known mechanism at the time which would explain why this should be the case. This is the fundamental question of *weak universality*.

> *Do all of the four-Fermion interactions have the same $V - A$ structure with the same coupling constant G_F?*

For example, it was known experimentally that muon decay and neutron decay were governed by almost the same Fermi constant. Is it the case that neutron decay is goverened by the same type of interaction Lagrangian as in Equation 1.0.18 with the same constant G_F?

$$\mathcal{L} \stackrel{?}{=} -\frac{G_F}{\sqrt{2}}[\bar{p}\gamma^\lambda(1-\gamma^5)n][\bar{e}\gamma_\lambda(1-\gamma^5)\nu_e] \tag{1.0.24}$$

There are several problems with this simple interpretation of weak universality which came up over the course of the development of the standard model.

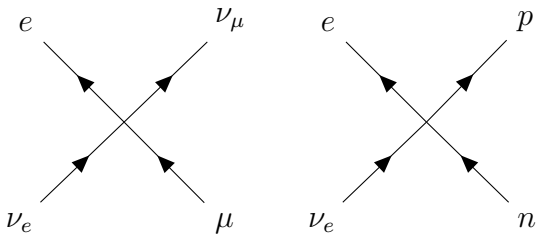

Figure 1.4: Four-Fermi interactions which mediate muon decay (left) and free neutron decay (right).

1. Unlike the muon, the neutron is a *composite particle* - it is made up of quarks and gluons held together by the strong interaction. The simple $V-A$ structure is modified by the presence of the strong interactions. The strong interactions do not effect the vector current, but they do renomalize the axial-vector component of the current. This is explored in Section 1.2

2. The light up-and-down valence quarks which compose the neutron are not paired in the same straightforward way the lepton pairs (e, ν_e) and (μ, ν_μ) are. Instead, the quark pairings are modified by the CKM matrix. This is explored in Section 1.1

3. The tree-level decay rates are modified by electromagnetic radiative corrections, which differ between the two decays. In the four Fermion theory, it was shown that the radiative corrections to neutron decay depended on an ultraviolet regulator, which rendered them ambiguous. This is explored in Section 2

1.1 Weak Interactions in The Standard Model

The four-fermion $V-A$ interaction in Equation 1.0.18 is not the final theory of the weak interactions. It is a manifestation of a deeper theory which was worked out between 1964 and 1967. This was the culmination of the work done by many people, and in particular Glashow, Salam, and Weinberg who were awarded the 1979 Nobel Prize in Physics for their work.

The four-fermion interaction does not actually occur at one point, as in Fermi's original theory. Instead, it is mediated by a heavy boson - the W-boson - as shown in Figure 1.5. The W-bosons in this context are usually called "intermediate vector bosons". The W is not directly observed in weak decays because it is so massive, with $M_W = 80.385(15)$ GeV [Pat+16]. This explains why observe an effective four-Fermion interaction.

In the Glashow-Salam-Weinberg model of the weak interactions, the $W^\pm$ bosons and the newly predicted Z^0 boson are *gauge bosons* of a $U(1)_Y \times SU(2)_L$ gauge group which also includes electromagnetism. Thus the electromagnetic and weak forces become one unified

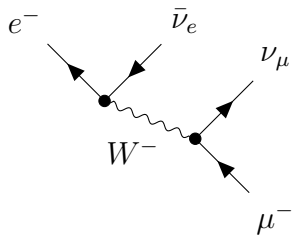

Figure 1.5: A muon decays into a neutrino via the emission of a highly virtual W-boson, which then produces an electron and another neutrino.

electroweak force. This is shocking - on the surface, these theories could not be more different. How could they be manifestations of one underlying force?

The reason they appear so different is that the photon is massless, while the W and Z bosons are very heavy. The traditional view is that gauge theories demand massless gauge bosons, like the photon. However, in the 1960s people found a way around this using *spontaneous symmetry breaking*. When the gauge symmetry is spontaneously broken, the associated gauge bosons can acquire mass through the *Higgs mechanism*. This is the basis for the Glashow-Salam-Weinberg model that I now wish to describe.

Gauge Symmetry

The standard model is based on gauge theory, which has its roots in electromagnetism. Gauss' law for magnetism states that the divergence of the magnetic field is zero, $\nabla \cdot \vec{B} = 0$. This is automatically satisfied if we introduce a *vector potential*.

$$\vec{B} = \nabla \times \vec{A} \tag{1.1.1}$$

(A here refers to the gauge potential, not the weak axial-vector current). The vector potential itself is unphysical - only the magnetic field is observable. Our choice of $\vec{A}$ is not unique, because we can add the gradient of any function to it and get the same magnetic field.

$$\vec{A}'(\vec{x}, t) = \vec{A}(\vec{x}, t) - \nabla\lambda(\vec{x}) \tag{1.1.2}$$

We can extend this argument further in a manner consistent with Lorentz covariance. We can define both $\vec{E}$ and $\vec{B}$ in terms of the *gauge field*, $A^\mu = (\phi, \vec{A})$.

$$\vec{E} = -\nabla\phi - \frac{\partial \vec{A}}{\partial t}, \quad \vec{B} = \nabla \times \vec{A} \tag{1.1.3}$$

Again this choice of A^μ is not unique. We can choose any scalar function $\lambda(\vec{x}, t)$ and the $\vec{E}, \vec{B}$ fields are invariant under the *gauge transformation*

$$A'_\mu = A_\mu + \partial_\mu\lambda. \tag{1.1.4}$$

In quantum electrodynamics, this gauge freedom plays a crucial role in determining the interactions. We can write the Lagrangian as

$$\mathcal{L} = -\frac{1}{4}F_{\mu\nu}F^{\mu\nu} + i\bar{\psi}\not{D}\psi + m\bar{\psi}\psi \tag{1.1.5}$$

where $F^{\mu\nu}$ is a rank-two Lorentz covariant tensor made up of $\vec{E}$ and $\vec{B}$ fields, which can be written in terms of derivatives of A^μ

$$F_{\mu\nu} = \partial_\mu A_\nu - \partial_\nu A_\mu \tag{1.1.6}$$

and D_μ is the gauge covariant derivative for a fermion with charge Q.

$$D_\mu = \partial_\mu - ieQA_\mu \tag{1.1.7}$$

This Lagrangian has gauge freedom. We can redefine the fermion field by performing a local $U(1)$ transformation determined by the function $\lambda(\vec{x}, t)$, and the gauge field transforms accordingly.

$$\psi \to e^{ieQ\lambda}\psi, \quad A_\mu \to A_\mu + \partial_\mu\lambda \tag{1.1.8}$$

The gauge covariant derivative is constructed such that $D_\mu\psi$ transforms the same way as ψ under this transformation. The ordinary derivative $\partial_\mu\psi$ picks up derivatives of the function λ, but these are exactly cancelled by the change in the gauge field.

Expanding out the gauge covariant derivative, we pick up a term which represents the interaction of the electromagnetic field with the fermion

$$\mathcal{L} \supset eQA_\mu\bar{\psi}\gamma^\mu\psi = eA_\mu J^\mu \tag{1.1.9}$$

This leads us to identify $J^\mu = Q\bar{\psi}\gamma^\mu\psi$ with the usual electromagnetic current. Minimizing the action with respect to the photon field A gives us Maxwell's equations of electromagnetism.

The photon - the particle created by the gauge field A^μ - is massless. Giving a mass to the photon by including a term $m_\gamma^2 A^\mu A_\mu$ explicitly breaks gauge invariance. How then is it the case that the vector bosons of the weak interaction, the W^μ and Z^μ, are massive? In the Glashow-Salam-Weinberg model, the gauge symmetry is broken via *spontaneous symmetry breaking*. The gauge bosons are then able to acquire a mass via the *Higgs mechanism*. With the final piece of this puzzle - the Higgs boson - being observed at the Large Hadron Collider in 2012, this has been often dubbed the most successful theory in physics.

Standard Model - Electroweak Sector

The standard model of particle physics is based on $U(1)_Y \times SU(2)_L \times SU(3)_c$ gauge symmetry. The $U(1)_Y$ of hypercharge is an abelian gauge field just like in ordinary quantum electrodynamics. The $SU(2)_L$ gauge symmetry acts on pairs of left handed fields - hence the subscript L. It also acts on the higgs doublet, which will be crucially important. We will write these fields in capital letters to represent that they are $SU(2)_L$ doublets.

$$L_i = \begin{pmatrix} \nu_{Li} \\ e_{Li} \end{pmatrix}, \quad Q_i = \begin{pmatrix} u_{Li} \\ d'_{Li} \end{pmatrix}, \quad \Phi = \begin{pmatrix} \phi^+ \\ \phi^0 \end{pmatrix} \tag{1.1.10}$$

The index i on the lepton and quark fields is the flavour index. The associated right handed fields are not charged under $SU(2)_L$.

$$e_{Ri}, \quad u_{Ri}, \quad d_{Ri} \tag{1.1.11}$$

These fields which are charged under $U(1)_Y \times SU(2)_L$ are acted upon by the gauge covariant derivative (following [PS95] Chapter 20.2)

$$D_\mu = \partial_\mu - igW_\mu^a T^a - ig'YB_\mu \tag{1.1.12}$$

Here the operator Y gives the hypercharge of the field and $T^a = \frac{\sigma^a}{2}$ are the generators of the $SU(2)$ transformation. The hypercharges can be worked out from the relation to electric charge.

$$Q = T^3 + Y \tag{1.1.13}$$

The magic happens when we include the Coleman-Weinberg potential for the higgs field.

$$V(\Phi) = -\mu^2 \Phi^\dagger \Phi + \frac{\lambda}{2}(\Phi^\dagger \Phi)^2 \tag{1.1.14}$$

The minimum of this potential occurs at

$$\Phi^\dagger \Phi = \frac{v^2}{2} \tag{1.1.15}$$

where $v^2/2 = \mu^2/\lambda$ is called the *vacuum expectation value*, or VEV for short. This is not simply a point in field space, but an entire space of minima. We can parameterize the space of minima using a local $U(2)$ transformation.

$$\Phi = U(x)\frac{1}{\sqrt{2}}\begin{pmatrix} 0 \\ v \end{pmatrix} \equiv U(x)\Phi_0 \tag{1.1.16}$$

The $U(1)_Y \times SU(2)_L$ gauge symmetry is *spontaneously broken* by the ground state of the theory down to $U(1)_{\text{EM}}$ of electromagnetism. The only surviving symmetry generator which leaves the ground state invariant is the combination $T^3 + Y$.

$$\exp\left(i(T^3 + Y)\lambda(x)\right)\Phi_0 = \Phi_0 \tag{1.1.17}$$

The remaining 3 degrees of freedom which rotate Φ_0 can be eliminated by a choice of gauge, called *unitary gauge*. In this gauge choice, the extra degrees of freedom of the higgs doublet are transferred to the longitudinal components of the three massive vector bosons, $W^\pm$ and Z. We can see how this works by expanding out the higgs kinetic term and inserting the VEV.

$$D_\mu \Phi = \left(\partial_\mu \Phi - igW_\mu^a T^a - i\frac{1}{2}g'B_\mu\right)\Phi \to -i\frac{v}{2}\begin{pmatrix} gW_\mu^+ \\ -\sqrt{\frac{g^2+(g')^2}{2}}Z_\mu \end{pmatrix} \tag{1.1.18}$$

Where $W^{\pm} = \frac{1}{\sqrt{2}}(W^1 \mp iW^2)$, and Z is defined by a field redefinition

$$Z = \frac{1}{\sqrt{g^2 + (g')^2}}(gW^3 - g'B) \equiv \cos\theta_W W^3 - \sin\theta_W B \tag{1.1.19}$$

The angle θ_W is known as the *weak mixing angle*.

The kinetic term for the higgs gives us mass terms for the vector bosons

$$D_\mu \Phi^\dagger D^\mu \Phi \to \frac{v^2}{4}\left(g^2 W^+_\mu W^{-\mu} + \frac{1}{2}(g^2 + (g')^2) Z_\mu Z^\mu\right) \tag{1.1.20}$$

The first term gives masses to the $W^{\pm}$ bosons set by $M_W = gv/2$. The second term gives mass to the Z boson with $M_Z = \sqrt{g^2 + (g')^2} \times v/2$. The photon is the remaining linearly independent combination.

$$A = \frac{1}{\sqrt{g^2 + (g')^2}}(g'W^3 + gB) = \sin\theta_W W^3 + \cos\theta_W B \tag{1.1.21}$$

The photon remains massless even after electroweak symmetry breaking.

The Higgs field also gives mass to the fermions of the standard model through the Yukawa couplings. (with $\tilde{\Phi} = i\sigma^2 \Phi^*$)

$$\mathcal{L} \supset -y^e_{ij} \bar{L}_i \Phi e_{Rj} - y^u_{ij} \bar{Q}_i \tilde{\Phi} u_{Rj} - y^d_{ij} \bar{Q}_i \Phi d_{Rj} + \text{h.c} \tag{1.1.22}$$

The matrices y^e, y^u, and y^d are the Yukawa coupling constants between the Higgs and the fermions. Plugging in the ground state of the Higgs field gives us the fermion mass matrices (with $m = \frac{v}{\sqrt{2}} y$).

$$\mathcal{L} \supset -m^e_{ij} \bar{e}_{Li} e_{Rj} - m^u_{ij} \bar{u}_{Li} u_{Rj} - m^d_{ij} \bar{d}_{Li} d_{Rj} + \text{h.c} \tag{1.1.23}$$

We perform another set of field redefinitions in flavour space to diagonalize the mass matrices. Since the neutrinos are massless in this model (neutrinos do have a small mass, but that will not concern us in this thesis), we are able to transform the neutrino fields and the electron-type fields in the same way

$$e_{Li} \to U^e_{ij} e_{Lj}, \quad \nu_{Li} \to U^e_{ij} \nu_{Lj} \tag{1.1.24}$$

However, since the up-type and down-type quarks have their own separate mass matrices, they are not diagonalized by the same field redefinition.

$$u_{Li} \to U^u_{ij} u_{Lj}, \quad d_{Li} \to U^d_{ij} d_{Lj} \tag{1.1.25}$$

This mismatch results in the *Cabibbo-Kobayashi-Maskawa matrix*, or CKM matrix V_{ij}. We define the fields d'_i as follows.

$$d'_i = [(U^u)^\dagger U^d]_{ij} d_j \equiv V_{ij} d_j \tag{1.1.26}$$

The CKM matrix in the standard model is unitary by definition, and this has specific experimental consequences.

Just as we did for the case of electromagnetism in Equation 1.1.9, we can use the gauge covariant derivative for the fermion fields to write down the electroweak currents. Plugging in the redefined fields W, Z, and A into the gauge covariant derivative Equation 1.1.12, we find

$$D_\mu = \partial_\mu - i\frac{g}{\sqrt{2}}\left(W_\mu^+ T^+ + W_\mu^- T^-\right) - i\frac{g}{\cos\theta_W}\left(T^3 - \sin^2\theta_W Q\right) Z_\mu - ieQA_\mu \tag{1.1.27}$$

Where $e = g\sin\theta_W$.

Plugging in the various fermion fields gives us the weak charged currents, neutral currents, and electromagnetic currents. For example, the weak charge-changing current for the leptons is

$$\frac{g}{2\sqrt{2}} W_\mu^+ \bar{\nu}_i \gamma^\mu (1-\gamma^5) e_i = \frac{g}{2\sqrt{2}} W_\mu^+ j_W^{\mu+} \tag{1.1.28}$$

where we expanded out the left handed field in terms of the $V-A$ currents. In the limit that the momentum transfer is much smaller than the W boson mass, the exchange of a W boson can be approximated by a contact four-Fermi interaction

$$\begin{aligned} \Delta\mathcal{L} = \frac{g^2}{8} j_W^\mu \frac{1}{q^2 - M_W^2}\left(\eta_{\mu\nu} - \frac{q_\mu q_\nu}{M_W^2}\right) j_W^\nu \\ \rightarrow -\frac{g^2}{8M_W^2} j_W^\mu j_{W\mu} \end{aligned} \tag{1.1.29}$$

Comparing this against Fermi's contact interaction in Equation 1.0.18, we find the relation to the Fermi constant.

$$\frac{G_F}{\sqrt{2}} = \frac{g^2}{8M_W^2} \tag{1.1.30}$$

When we have a weak interaction involving the quarks, we pick up an additional factor from the CKM matrix. For example, the charge-changing current for the light quark fields picks up an additional factor V_{ud}.

$$\frac{g}{2\sqrt{2}} W_\mu^+ \bar{u}\gamma^\mu (1-\gamma^5) V_{ud} d = V_{ud}\frac{g}{2\sqrt{2}} W_\mu^+ J_W^{\mu+} \tag{1.1.31}$$

This answers one of our two central questions about weak universality.

The Fermi constant in nuclear beta decay is modified by a factor V_{ud}.

This is typically called $G_V \equiv V_{ud} G_F$, since it is the coefficient of the vector current. This idea was first put forward by Cabbibo [Cab63]. Cabibbo hypothesized that the strangeness changing weak current was related by an angle θ_C, now known as the Cabbibo angle.

$$J_\mu = \cos\theta_C (V_\mu^{(\Delta S=0)} - A_\mu^{(\Delta S=0)}) + \sin\theta_C (V_\mu^{(\Delta S=1)} - A_\mu^{(\Delta S=1)}) \tag{1.1.32}$$

In terms of the CKM matrix, this model has $V_{ud} = \cos\theta_C$ and $V_{us} = \sin\theta_C$. This explained why strangeness changing decays were so much slower than expected - this was due to the smallness of $\sin\theta_C$.

Cabibbo estimated this parameter by looking at the ratio of the decay rate of the charged kaon and pion. Since π^+ and K^+ are both spinless and parity-odd, the matrix element must take a very simple form.

$$\langle\Omega|A^\lambda(x)|\pi^+, p_\pi\rangle = f_\pi p_\pi^\lambda e^{-ip_\pi x} \tag{1.1.33}$$

where f_π is the pion form factor, evaluated at the pion mass. Calculating the decay rate is a simple exercise. The result is

$$\Gamma(\pi^+ \to \mu^+ + \nu_\mu) = \frac{G_F^2 \cos^2\theta_C f_\pi^2}{8\pi}\left(1 - \frac{m_\mu^2}{m_\pi^2}\right)^2 \left(\frac{m_\mu^2}{m_\pi^2}\right) m_\pi^3 \tag{1.1.34}$$

The same logic applies for the charged kaon. The difference is that the kaon decay changes strangeness by one unit, so it comes with a factor $\sin^2\theta_C$ instead of the cosine. Thus, Cabibbo was able to estimate the parameter θ_C by comparing these two decays.

$$\tan^2\theta_C = \frac{\Gamma(K^+ \to \mu^+ + \nu_\mu)}{\Gamma(\pi^+ \to \mu^+ + \nu_\mu)} \times \frac{f_\pi^2}{f_K^2}\frac{(1 - m_\mu^2/m_\pi^2)^2 m_\pi}{(1 - m_\mu^2/m_K^2)^2 m_K} \tag{1.1.35}$$

The form factors must come from experiment or from lattice QCD. If we ignore that issue and set $f_K/f_\pi = 1$ as was done in [Cab63], we get $\theta_C \approx 15°$. A better approximation uses $f_K/f_\pi \approx 1.19$, which gives a more accurate value of $\theta_C \approx 13.4°$

Since the CKM matrix is unitary in the standard model, we have the constraint

$$|V_{ud}|^2 + |V_{us}|^2 + |V_{ub}|^2 = 1 \quad \text{(SM value)}. \tag{1.1.36}$$

This is known as *top row unitarity*, since this corresponds to the top row of the CKM matrix. Violations of CKM unitarity would imply new physics, such as a fourth quark generation.

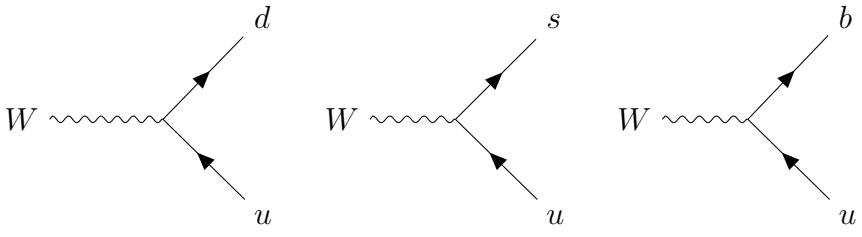

$|V_{ud}| \approx 0.97$ $|V_{us}| \approx 0.22$ $|V_{ub}| \approx 4 \times 10^{-3}$

Figure 1.6: Matrix elements in the top row of the CKM matrix [Pat+16].

We can measure the largest term, V_{ud}, by measuring G_V in nuclear beta decays and comparing this to G_F measured in muon decay. Similarly, we can measure V_{us} in strangeness changing decays such as Kaon decay. The last term V_{ub} can in principle be measured from B-meson decays, but $|V_{ub}|^2$ is smaller than the current uncertainty estimates for top row unitarity so it can be ignored [HT15] [Pat+16]. Tests of CKM unitarity provide one of the most stringent tests of the standard model, and we will discuss this more in Section 3.1.

1.2 Weak Charge-Changing Nucleon Form Factors

Our most powerful tool for dealing with electromagnetic and weak interactions is perturbation theory. The strong interactions cannot be handled this way - we are forced to keep the strong interactions to all orders. The nucleons are a complicated bound state of quarks and gluons which interact through the strong interactions, and this means we cannot use the quark currents in Equation 1.1.31 in nucleons.

We can capture the effects of the strong interactions in nucleons by using *nucleon form factors*. The nucleon form factors add another layer of uncertainty to our calculations. However, despite the difficulty of dealing with the strong interactions, we will find that we can constrain at least some of the form factors. We will do this by exploiting the various symmetries of the strong interactions.

Quantum Chromodynamics

Our theory of strong interactions is known as *quantum chromodynamics*, or QCD. The QCD Lagrangian (not including gauge fixing terms) can be written as ([Wei96] Chapter 18.7)

$$\mathcal{L}_{\text{QCD}} = -\frac{1}{4}G^{\mu\nu a}G^{a}_{\mu\nu} + \sum_n \bar{\psi}_n(i\not{D} - m_n)\psi_n \tag{1.2.1}$$

Where $G^a_{\mu\nu}$ is the gluon field strength tensor, and ψ_n are the quark fields. The quark fields transform in the fundamental representation of the QCD gauge group $SU(3)_c$. The index n goes over all of the quark flavours.

The strong coupling constant $\alpha_s = \frac{g_s^2}{4\pi}$ and the quark masses m_n in the Equation 1.2.1 are not fixed constants, but they depend on the energy scale we are interested in. The strong coupling constant depends on the energy scale according to ([PS95] Chapter 17.2)

$$\frac{dg_s}{d\log\mu} = \beta(g_s) = -\frac{g_s^3}{(4\pi)^2}\left(\frac{11}{3}N - \frac{2}{3}n_f\right) \tag{1.2.2}$$

If the β function is negative, then the coupling constant α_s gets smaller at high energies. Plugging in $N = 3$ for QCD and the number of quark flavours is $n_f = 6$, we see that the strong interactions become perturbative at high energies. This is known as *asymptotic freedom*.

Let us examine the symmetries of the QCD Lagrangian Equation 1.2.1. As usual, we have translational invariance and Lorentz invariance. The QCD Lagrangian also has discrete

symmetries of parity, time reversal, and charge conjugation. This is not so straightforward, however, since we could add a term which violates these symmetries known as the *theta term* ([Wei96] Chapter 23.6).

$$\Delta\mathcal{L} = -\frac{\theta}{64\pi^2}\varepsilon^{\mu\nu\lambda\rho}G^a_{\mu\nu}G^a_{\lambda\rho} \tag{1.2.3}$$

Such a term would lead to a P and T-violating neutron electric dipole moment, which has thus far not been observed. The limits on θ from neutron electric dipole moments are currently $\theta \lesssim 10^{-10}$ [Pat+16]. Explaining the small - possibly zero - value of this constant is known as the *strong CP problem*. We will take it as an experimental fact that strong interactions conserve parity, time reversal, and charge conjugation.

The strong interactions conserve the number of quarks of each flavour, minus the number of corresponding antiquarks. We can rotate each quark flavour by an independent phase $\psi_n \to e^{i\theta}\psi_n$ and the QCD Lagrangian is invariant. This corresponds to $U(1)^6$ symmetry - one for each quark flavour.

$$U(1)_u \times U(1)_d \times U(1)_s \times U(1)_c \times U(1)_b \times U(1)_t \tag{1.2.4}$$

However, we can actually do much better than this. In order to get a better understanding, we need to look at the values of the quark masses m_n.

As was stated previously, the values of quark masses depend on the energy scale. It is convenient to define the quark masses at high energies where QCD is perturbative. The quark masses are reported in the $\overline{\text{MS}}$ scheme at 2 GeV, where they are known to about 10%. [Pat+16]. The lightest three quarks are the u, d, s quarks.

$$m_u = 2.2^{+0.6}_{-0.4}\text{ MeV},\ m_d = 4.7^{+0.5}_{-0.4}\text{ MeV},\ m_s = 96^{+8}_{-4}\text{ MeV} \tag{1.2.5}$$

There is a significant jump in mass between the three light quarks and the three heavy quarks. The heavy quarks c, b, t are all heavier than the nucleons themselves.

$$m_c = 1.27(3)\text{ GeV},\ m_b = 4.18^{+0.04}_{-0.03}\text{ GeV},\ m_t = 173.21(86)\text{ GeV} \tag{1.2.6}$$

The top quark is heavy enough that its mass can be measured directly at the LHC.

The lightest quarks, the u and d quark, are much lighter than the scale of nuclear physics. Following Chapter 19.4 of [Wei96], we consider the limit where we set the light quark masses to zero - the so-called *chiral limit*. In the absence of quark mass terms, we can write the Lagrangian for the light quark fields in terms of left and right handed fields separately.

$$\bar{u}_L i\not{D} u_L + \bar{u}_R i\not{D} u_R + \bar{d}_L i\not{D} d_L + \bar{d}_R i\not{D} d_R \tag{1.2.7}$$

This Lagrangian is invariant under $U(2)_L \times U(2)_R$, which rotates the right handed and left handed fields separately.

$$\begin{pmatrix} u_R \\ d_R \end{pmatrix} \to U_R \begin{pmatrix} u_R \\ d_R \end{pmatrix}, \quad \begin{pmatrix} u_L \\ d_L \end{pmatrix} \to U_L \begin{pmatrix} u_L \\ d_L \end{pmatrix} \tag{1.2.8}$$

Alternatively, we can write this as

$$U(1)_V \times U(1)_A \times SU(2)_V \times SU(2)_A. \tag{1.2.9}$$

The overall $U(1)_V$ corresponds to conserved baryon number, which is an exact symmetry of the strong interactions. The axial $U(1)_A$ is strongly broken by large gauge transformations called *instantons*, in a phenomenon known as the *chiral anomaly*. A $SU(2)_V \times SU(2)_A$ transformation can be written as

$$\exp\left(i\theta_V^a \tau^a + i\theta_A^a \tau^a \gamma^5\right) \begin{pmatrix} u \\ d \end{pmatrix} \tag{1.2.10}$$

Where τ^a are the Pauli matrices. We can use Noether's theorem ([PS95] Chapter 9.6) to derive the conserved current associated with these transformations.

$$V^{\mu a} = \bar{q}\gamma^\mu \tau^a q, \quad A^{\mu a} = \bar{q}\gamma^\mu \gamma^5 \tau^a q \tag{1.2.11}$$

Where $q = \binom{u}{d}$ is the quark doublet. We see that the weak charge changing currents Equation 1.1.31 are identical to the Noether currents, where we take the linear combination corresponding to raising and lowering operators, $\tau^\pm = \frac{1}{2}(\tau^1 \pm i\tau^2)$.

The conserved charges associated with these currents are

$$Q_V^a = \int d^3x\, \bar{q}\gamma^0 \tau^a q, \quad Q_A^a = \int d^3x\, \bar{q}\gamma^0 \gamma^5 \tau^a q \tag{1.2.12}$$

These operators generate the infinitesimal $SU(2)_V \times SU(2)_A$ transformations of the quarks.

$$[Q_V^a, q] = \tau^a q, \quad [Q_A^a, q] = \tau^a \gamma^5 q \tag{1.2.13}$$

If the $SU(2)_V \times SU(2)_A$ were an exact and unbroken symmetry of the strong interactions, then the spectrum would exhibit a parity-doubling. If we have a hadronic state $|h\rangle$, then we would automatically have another state $Q_A^a |h\rangle$ with opposite parity but the same strangeness, baryon number, and spin. Since this parity doubling is not observed, the symmetry must be spontaneously broken down to a subgroup $SU(2)_V$. Proving that the symmetry is actually spontaneously broken in this way involves the details of the strong interactions, but we can derive its consequences by simply assuming that the symmetry is spontenously broken.

$$SU(2)_V \times SU(2)_A \to SU(2)_V \tag{1.2.14}$$

This remaining $SU(2)_V$ is known as *isospin symmetry*. It is broken by electromagnetic interactions, since the up-and-down quarks have different electric charges. It is also broken by the light quark mass difference, but this is also treated as an electromagnetic correction. Thus we take isospin to be a symmetry of the strong interactions.

Since the chiral $SU(2)_A$ symmetry is spontaneously broken by the ground state of the strong interactions, there must be approximately massless Goldstone Bosons with negative

parity, zero spin, zero strangeness, zero baryon number, and unit isospin. This has exactly the same quantum numbers as the pion, which is the lightest of all the hadron states. We are led to the conclusion that the pion is the Goldstone Boson associated with the spontaneous breaking of chiral symmetry.

Nucleon Form Factors

Now that we have explored the symmetries of the strong interactions, we return to the question of the weak interactions in strongly interacting systems. Our goal is to find the matrix elements of the weak charge changing current Equation 1.1.31 between nucleon states. The currents in the nucleon are modified by form factors. We will begin by reviewing how this works for the electromagnetic form factors.

The electromagnetic currents at the quark level are

$$J^{\mu}_{em}(x) = \frac{2}{3}\bar{u}\gamma^{\mu}u - \frac{1}{3}\bar{d}\gamma^{\mu}d - \frac{1}{3}\bar{s}\gamma^{\mu}s \tag{1.2.15}$$

Contributions from the heavier c, b, t quarks can be ignored when considering nucleon form factors. The strange quarks do contribute to the electromagnetic form factors at the 1% level, depending on the momentum transfer.

We can express the matrix element of the electromagnetic current as a general vertex function Γ^{μ}.

$$\langle N(p_f s_f)|J^{\mu}_{em}(x)|N(p_i s_i)\rangle = \bar{u}_{s_f}(p_f)\Gamma^{\mu}_{em}(p_f, p_i)u_{s_i}(p_i)e^{iqx} \tag{1.2.16}$$

where $N = \{n, p\}$. The electromagnetic current is exactly conserved in the strong interactions. Current conservation implies that the matrix element dotted into q is zero.

$$q_{\mu}\Gamma^{\mu}_{em}(p', p) = 0 \tag{1.2.17}$$

where $q = p' - p$ is the momentum transferred to the nucleon.

The current operator is Hermitian, and that imposes a hermiticity constraint on the current matrix element [Wei95].

$$\Gamma^{\mu}(p', p) = \gamma^0\Gamma^{\mu}(p, p')^{\dagger}\gamma^0 \tag{1.2.18}$$

This fixes all of the factors of i so that the form factors are real.

The strong interactions also conserve parity, and that places yet another constraint on the matrix element. The electromagnetic current is parity even, so we require

$$\gamma^0\Gamma^{\mu}(\mathcal{P}p', \mathcal{P}p)\gamma^0 = \eta_P\mathcal{P}^{\mu}{}_{\nu}\Gamma^{\nu}(p', p) \tag{1.2.19}$$

with $\eta_P = +1$. The matrix $\mathcal{P}^{\mu}{}_{\nu} = \mathrm{diag}(+1, -1, -1, -1)$ represents the action of spatial inversion on vectors.

The strong interactions are invariant under time reversal. The electromagnetic current is even under time reversal, and this implies another relation for the matrix element.

$$\gamma^3\gamma^1\Gamma^{\mu}(\mathcal{P}p', \mathcal{P}p)^*\gamma^1\gamma^3 = \eta_T\mathcal{P}^{\mu}{}_{\nu}\Gamma^{\nu}(p', p) \tag{1.2.20}$$

with $\eta_T = +1$.

And finally, the strong interactions are invariant under charge conjugation symmetry (with $C = i\gamma^0\gamma^2$)

$$-C\Gamma^\mu(-p,-p')^T C = \eta_C \Gamma^\mu(p',p) \tag{1.2.21}$$

with $\eta_C = -1$. The phases are not independent, but are related to the hermiticity condition Equation 1.2.18 by the CPT theorem.

Finally, we recognize that the operators we choose are not unique. We have the usual Gordon identity.

$$\bar{u}(p_f)\gamma^\mu u(p_i) = \bar{u}(p_f)\left[\frac{(p_i+p_f)^\mu}{2M_N} + i\frac{\sigma^{\mu\nu}q_\nu}{2M_N}\right]u(p_i) \tag{1.2.22}$$

The conventional choice is to eliminate the $(p_i+p_f)^\mu$ term and replace it with the other two operator structures.

$$\Gamma^\mu_{em}(p',p) = \gamma^\mu F_1^{(N)}(Q^2) + \frac{i\sigma^{\mu\nu}q_\nu}{2M_N}F_2^{(N)}(Q^2) \tag{1.2.23}$$

with $N = \{n,p\}$. The form factors are lorentz scalar functions of the spacelike four-momentum transfer squared, $Q^2 \equiv -q^2$.

The F_1 form factors are constrained by the conservation of electric charge. The total electric charge is the spatial integral of the charge density.

$$Q_{em} = \int d^3x\, J^0_{em}(\vec{x}) \tag{1.2.24}$$

This implies an exact relation for the electromagnetic form factors F_1^N at zero momentum transfer.

$$F_1^{(p)}(0) = 1, \quad F_1^{(n)}(0) = 0 \tag{1.2.25}$$

The F_2 form factors are not constrained by symmetry - even at zero momentum transfer. The form factors F_2 are the first big hint that composite particles behave very differently from fundamental particles. For example, the electron is considered to be a fundamental particle. Its magnetic moment is very close to the so-called "Dirac" value, which would correspond to $F_1 = 1$ and $F_2 = 0$. The electron magnetic moment is known to one part in ten trillion. The accepted value is [Pat+16]

$$\mu_e = 1.001\,159\,652\,180\,62(12) \tag{1.2.26}$$

in units of the Borh magneton, $\mu_B = -\frac{e}{2m_e}$. The observation that this value is very close to 1 indicates that the electron is a fundamental particle.

The nucleon magnetic moments must be measured, or computed using lattice QCD. The F_2 form factors are related to the nucleon magnetic moments by [Pat+16]

$$\begin{aligned} 1 + F_2^{(p)}(0) = \mu_p &= 2.792\,847\,351(9) \\ F_2^{(n)}(0) = \mu_n &= -1.913\,042\,7(5) \end{aligned} \tag{1.2.27}$$

The nucleon magnetic moments are given in units of the nuclear magneton, $\mu_N = \frac{e}{2m_p}$. The huge difference between the nucleon magnetic moments and Dirac value point to the complicated internal structure of the nucleons.

It will be useful to define isovector and isoscalar form factors by looking at the difference between the proton and the neutron. We write the electromagnetic form factors in terms of $\tau^3 = \tau_z$.

$$F_{1,2}^{(N)} = \frac{1}{2}(F_{1,2}^{(0)} + F_{1,2}^{(1)}\tau^3) \tag{1.2.28}$$

The isospin operators τ^a act on the nucleon isospin doublet.

$$N = \begin{pmatrix} p \\ n \end{pmatrix} \tag{1.2.29}$$

At first glance, this looks like a simple change of notation. The advantage comes that we can write Equation 1.2.23 for both of the nucleons in one line.

$$\Gamma_{em}^{\mu}(p', p) = \left(\frac{1}{2}F_1^{(0)}(Q^2) + \frac{\tau^3}{2}F_1^{(1)}(Q^2)\right)\gamma^{\mu} + \left(\frac{1}{2}F_2^{(0)}(Q^2) + \frac{\tau^3}{2}F_2^{(1)}(Q^2)\right)\frac{i\sigma^{\mu\nu}q_{\nu}}{2M_N} \tag{1.2.30}$$

We now want to apply this same reasoning to the weak charge changing currents which mediate nuclear beta decay. The charge changing quark current is given by

$$J_W^{+\mu}(x) = \bar{u}\gamma^{\mu}(1-\gamma^5)d = V^{+\mu} - A^{+\mu} \tag{1.2.31}$$

(Note that the CKM matrix is not included in the definition). The current which lowers the charge is given by the hermitian conjugate.

$$J_W^{-\mu}(x) = \bar{d}\gamma^{\mu}(1-\gamma^5)u = V^{-\mu} - A^{-\mu} \tag{1.2.32}$$

Importantly, we note that the charge changing current itself is not hermitian! This means we cannot use the hermiticity condition Equation 1.2.18 to fix the factors of i, as we did for the electromagnetic current. It also does not transform simply under charge conjugation. The best we can do is enforce parity and time reversal, Equations 1.2.19 and 1.2.20. The charged current has mixed parity, so we consider the vector and axial-vector parts separately.

We consider the terms which transform the same way as the underlying quark current under parity and time reversal. The vector current has $\eta_P = \eta_T = 1$.

$$\langle n(p_f s_f)|V^{+\mu}(x)|p(p_i s_i)\rangle = \bar{u}(p_f)\left[\gamma^{\mu}F_1(Q^2) + \frac{i\sigma^{\mu\nu}q_{\nu}}{2M_N}F_2(Q^2) + \frac{q^{\mu}}{M_N}F_S(Q^2)\right]u(p_i)e^{iqx} \tag{1.2.33}$$

And for the axial current has $\eta_P = -1$ and $\eta_T = +1$. Note that the choice of operators for the axial form factors are also not unique, since we have an axial-vector Gordon identity. The conventional choice is [WAL75]

$$\langle n(p_f s_f)|A^{+\mu}(x)|p(p_i s_i)\rangle = \bar{u}(p_f)\left[\gamma^{\mu}\gamma^5 F_A(Q^2) + \frac{q^{\mu}}{M_N}\gamma^5 F_P(Q^2) + \frac{i\sigma^{\mu\nu}\gamma^5 q_{\nu}}{2M_N}F_T(Q^2)\right]u(p_i)e^{iqx} \tag{1.2.34}$$

Assuming time reversal symmetry Equation 1.2.20, all of the form factors are real.

The strong interactions are also invariant under charge conjugation and isospin symmetry. We cannot enforce straightforward charge conjugation as in Equation 1.2.21 because it swaps $J^{+\mu}$ and $J^{-\mu}$. However, we can apply a cleverly chosen mixture of charge conjugation and an isospin rotation. This is known as *G-parity*, which was first introduced by Lee and Yang in 1956 [LY56a]. First, we rotate by π around the 2-direction in isospin space

$$e^{i(\pi/2)\tau^2} = \varepsilon = i\tau^2 = \begin{pmatrix} 0 & 1 \\ -1 & 0 \end{pmatrix} \tag{1.2.35}$$

This plays an important role in the theory of $SU(2)$. In particular, the transpose of the Pauli matrices is given by

$$(\tau^a)^T = \varepsilon\tau^a\varepsilon \tag{1.2.36}$$

Applying this to the nucleon doublet gives the transformation $N \to \varepsilon N$. Then we apply charge conjugation to the result.

$$\begin{pmatrix} p \\ n \end{pmatrix} \xrightarrow{G} \begin{pmatrix} C\bar{n}^T \\ -C\bar{p}^T \end{pmatrix} \tag{1.2.37}$$

The quark doublet transforms under G-parity as

$$U_G^\dagger q U_G = \varepsilon C \bar{q}^T \tag{1.2.38}$$

with $q = \binom{u}{d}$. The vector current transforms with $\eta_G = +1$.

$$U_G^\dagger \bar{q}\gamma^\mu\tau^+ q U_G = +\bar{q}\gamma^\mu\tau^+ q \tag{1.2.39}$$

And the axial current transforms with G-parity $\eta_G = -1$.

$$U_G^\dagger \bar{q}\gamma^\mu\gamma^5\tau^+ q U_G = -\bar{q}\gamma^\mu\gamma^5\tau^+ q \tag{1.2.40}$$

In general, the matrix element transforms under G-parity as

$$-\varepsilon^T C\Gamma^\mu(-p,-p')^T C\varepsilon = \eta_G\Gamma^\mu(p',p) \tag{1.2.41}$$

Using this general formula, it is a simple exercise to check how each of the terms in Equations 1.2.33 and 1.2.34 transform under G-parity. The scalar and tensor terms transform in the opposite way from the underlying quark currents. Assuming isospin and charge conjugation symmetry, we must have

$$F_S = F_T = 0 \tag{1.2.42}$$

This was first pointed out by Weinberg in 1958 [Wei58], who labeled these *second class currents*. There is currently no evidence that these terms play a role in beta decay processes.

We can take a different approach and get to the same answer, following [WAL75]. Taking the hermitian conjugate, we find that the scalar and tensor terms come with a different sign in $V^{-\mu}$ and $A^{-\mu}$.

$$\begin{aligned}\langle n(p_f s_f)|V^{-\mu}(x)|p(p_i s_i)\rangle &= \bar{u}(p_f)\left[\gamma^\mu F_1 + \frac{i\sigma^{\mu\nu}q_\nu}{2M_N}F_2 - \frac{q^\mu}{M_N}F_S\right]u(p_i)e^{iqx} \\ \langle n(p_f s_f)|A^{-\mu}(x)|p(p_i s_i)\rangle &= \bar{u}(p_f)\left[\gamma^\mu\gamma^5 F_A + \frac{q^\mu}{M_N}\gamma^5 F_P - \frac{i\sigma^{\mu\nu}\gamma^5 q_\nu}{2M_N}F_T\right]u(p_i)e^{iqx}\end{aligned} \tag{1.2.43}$$

However, the charged currents should transform as an isovector as in Equation 1.2.11. Therefore we should be able to use the Wigner Eckart theorem in isospin space to relate $V^{+\mu}$ to $V^{-\mu}$ and $A^{+\mu}$ to $A^{-\mu}$. The trick is to write the isovector operator using the spherical vector e_q ([Edm57] Chapter 5.1)

$$\tau^+ = -\frac{1}{\sqrt{2}}\tau_{1,1}, \quad \tau^z = \tau_{1,0}, \quad \tau^- = \frac{1}{\sqrt{2}}\tau_{1,-1} \tag{1.2.44}$$

where $\tau_{1,q} = \vec{\tau}\cdot\vec{e_q}$. Matrix elements can then be related to the reduced matrix element in isospin space ([Edm57] Chapter 5.4).

$$\langle 1/2,1/2|V^{+\mu}|1/2,-1/2\rangle = \langle 1/2,-1/2|V^{-\mu}|1/2,1/2\rangle = \frac{1}{\sqrt{6}}\langle 1/2||V_1^\mu||1/2\rangle \tag{1.2.45}$$

The same reasoning applies for the axial-vector current, which also transforms like an isovector. The only way for this to be the case is for the scalar and tensor terms to vanish [WAL75].

$$F_S = F_T = 0 \tag{1.2.46}$$

Further, we can use this same line of reasoning to relate the vector part of the charged currents to the isovector part of the electromagnetic currents. Using the same formula from Edmonds, we find (suppressing the momentum and spin)

$$\langle p|V_{1,0}^\mu|p\rangle = -\langle n|V_{1,0}^\mu|n\rangle = \frac{1}{\sqrt{6}}\langle 1/2||V_1^\mu||1/2\rangle \tag{1.2.47}$$

Separate the electromagnetic current into a isoscalar and an isovector part.

$$J_{em}^\mu = J_{em}^{\mu(0)} + J_{em}^{\mu(1)} \tag{1.2.48}$$

The isoscalar part is invariant under isospin rotations

$$J_{em}^{\mu(0)} = \frac{1}{6}\bar{u}\gamma^\mu u + \frac{1}{6}\bar{d}\gamma^\mu d - \frac{1}{3}\bar{s}\gamma^\mu s \tag{1.2.49}$$

and the isovector part can be related to $V_{1,0}^\mu$.

$$\begin{aligned}J_{em}^{\mu(1)} &= \frac{1}{2}\bar{u}\gamma^\mu u - \frac{1}{2}\bar{d}\gamma^\mu d \\ &= \frac{1}{2}\bar{q}\gamma^\mu\tau^3 q \\ &= \frac{1}{2}V_{1,0}^\mu\end{aligned} \tag{1.2.50}$$

Notice that the factor of 1/2 appears in both Equation 1.2.50 and in the definition of the isovector form factor 1.2.28. This gives us a direct relation between the charge changing form factors $F_{1,2}$ and the isovector electromagnetic form factors.

$$F_{1,2} = F_{1,2}^{(1)} \tag{1.2.51}$$

In particular, this means ([Wal04] Chapter 42.10)

$$F_1(q^2 = 0) = 1, \quad F_2(q^2 = 0) = (\mu_p - 1) - \mu_n \tag{1.2.52}$$

This is known as the *conserved vector current* hypothesis, or CVC, which was first proposed by Feynman and Gell-Mann [FG58].

The vector part of the $V - A$ weak current is the same as the isovector part of the electromagnetic current.

If we suppose that $SU(2)_V \times SU(2)_A$ were an exact and unbroken symmetry, then the axial currents $A^{\mu a}$ would be conserved. The implication for the nucleon axial current matrix element is (recall $Q^2 = -q^2$)

$$q_\mu \langle p|A^\mu(0)|n\rangle = \bar{u}_p \left[F_A(Q^2)\not{q}\gamma^5 + \frac{1}{M_N} q^2 \gamma^5 F_P(Q^2)\right] u_n = 0 \tag{1.2.53}$$

Using the Dirac equation for the proton and neutron spinors, this implies

$$2M_N F_A(Q^2) + \frac{1}{M_N} q^2 F_P(Q^2) = 0 \tag{1.2.54}$$

At $q^2 = 0$, since $F_A(0) \neq 0$ and $M_N \neq 0$ this implies that the pseudoscalar form factor has a pole at $q^2 = 0$.

$$F_P(Q^2) \approx \frac{2M_N^2}{Q^2} F_A(Q^2) \quad \text{(Massless pion limit)} \tag{1.2.55}$$

This is corrected by the non-zero pion mass. A more rigorous derivation ([Wei96] Chapter 19.4) would instead give us

$$F_P(Q^2) \approx \frac{2M_N^2}{m_\pi^2 + Q^2} F_A(Q^2) \tag{1.2.56}$$

This argument was first put forward by Nambu in 1960. The axial-vector current is not conserved, but it is broken by terms of order m_π^2. This is known as *partially conserved axial current*, or PCAC ([Wal04] Chapter 45.2). Equation 1.2.56 is an example of *pole dominance*, and it is one of a wider class of approximate relations can be derived.

The last form factor we need is $F_A(Q^2)$. If the axial $SU(2)_A$ symmetry were conserved, then we would have $F_A(Q^2 = 0) = 1$. However, the symmetry breaking means this will have some value different from 1. We define g_A to be the value of the form factor at $Q^2 = 0$.

$$F_A(Q^2 = 0) \equiv g_A \tag{1.2.57}$$

We now have the answer to our second question about weak universality.

The axial part of the $V - A$ weak current is modified by a factor of g_A for nuclei.

Unfortunately, there is no simple identity or relation which sets the value of g_A. It must be either measured, or come from an exact QCD calculation such as in lattice QCD.

In summary, we can write the weak current between nucleons as W to distinguish it form the electromagnetic vertex Γ.

$$\langle p(p_f s_f)|J_W^{\lambda+}(x)|n(p_i s_i)\rangle = \bar{u}(p_f)W^{\lambda}(p_f, p_i)u(p_i)e^{iqx} \tag{1.2.58}$$

We write this in isospin space in analogy with Equation 1.2.30.

$$W^{\lambda}(p_f, p_i) = \left[\gamma^{\mu}F_1(Q^2) + \frac{i\sigma^{\mu\nu}q_{\nu}}{2M_N}F_2(Q^2) - \gamma^{\mu}\gamma^5 F_A(Q^2) - \frac{q^{\mu}}{M_N}\gamma^5 F_P(Q^2)\right]\tau^+ \tag{1.2.59}$$

Note that the parity-violating terms come with a minus sign, which reflects the minus sign in the axial-vector part of the $V - A$ weak current.

1.3 Superallowed Nuclear Beta Decay

We can now use the four-Fermion interaction to derive the rate of nuclear beta decay. If we assume the emitted leptons are free Dirac particles, then we could write

$$\langle p_e, p_\nu|\bar{e}(x)\gamma_\lambda(1-\gamma^5)\nu(x)|\Omega\rangle = e^{i(p_e+p_\nu)x}\bar{u}(p_e)\gamma_\lambda(1-\gamma^5)v(k_\nu) \tag{1.3.1}$$

If we ignore nuclear recoil, then we can write the beta decay amplitude as

$$\mathcal{M} = \frac{G_F V_{ud}}{\sqrt{2}}\bar{u}(p_e)\gamma_\lambda(1-\gamma^5)v(k_\nu)\int d^3x e^{-i\vec{q}\cdot\vec{x}}\,\langle f_{\mathcal{N}}|V^{\lambda}(x) - A^{\lambda}(x)|i_{\mathcal{N}}\rangle \tag{1.3.2}$$

The term inside the integral is generally referred to as a *nuclear matrix element*. In principle, we can use the nuclear form factors Equations 1.2.33 and 1.2.34 and plug them into a nuclear model and calculate the decay rate. However, this typically comes with a lot of uncertainties. We now wish to discuss a special case where much of these uncertainties associated with the nuclear model disappear.

Superallowed Fermi β-decay is a special type of nuclear beta decay. Nuclear beta decay is called "allowed" if the leptons are emitted with no net angular momentum, $l = 0$. The momentum $\vec{q} = \vec{k}_e + \vec{k}_\nu$ in Equation 1.3.2 is the total momentum carried by the leptons. In nuclear beta decay, this is typically $q \approx 1 - 5$ MeV. On the other hand, the nuclear size is about $R_\mathcal{N} \approx 2 - 5$ fm. Thus the product $qR_\mathcal{N}$ is about $0.01 - 0.1$ for nuclei below $A \lesssim 30$. Thus we can ignore this and take the long-wavelength limit, where we replace the exponential by 1.

$$e^{-i\vec{q}\cdot\vec{x}} \approx 1 \quad \Leftrightarrow \quad \text{Long-Wavelength Limit} \tag{1.3.3}$$

This is typically referred to in this context as the *allowed approximation*. Decays in which the leptons do carry angular momentum $l \neq 0$ are called "forbidden" because they are suppressed by $(qR_\mathcal{N})^l$.

Keeping terms to zeroth order in nucleon velocity, we can write the one-body currents in Equations 1.2.33 and 1.2.34 as

$$V^0(\vec{x}) = \sum_a \tau_a^+ \delta^3(\vec{x} - \vec{x}_a), \quad \vec{A}(\vec{x}) = g_A \sum_a \tau_a^+ \vec{\sigma}_a \delta^3(\vec{x} - \vec{x}_a) \tag{1.3.4}$$

Where the sum over a goes over all of the protons and neutrons in the nucleus. The coefficient g_A comes from the axial form factor at low momentum transfer in Equation 1.2.57. In the allowed approximation, these decays are mediated by the so-called "Fermi" (F) and "Gamow-Teller" (GT) operators.

$$\begin{aligned} \text{(F)} : \int d^3x\, V^0(\vec{x}) &= \sum_a \tau_a^+, \\ \text{(GT)} : \int d^3x\, \vec{A}(\vec{x}) &= g_A \sum_a \tau_a^+ \vec{\sigma}_a \end{aligned} \tag{1.3.5}$$

Importantly, if the nucleus undergoes a spin $0^+ \to 0^+$ transition, then only the Fermi operator can contribute. In this limit, the Fermi operator is equal to the isospin raising operator.

$$\int d^3x\, V^0(\vec{x}) = \sum_a \tau_a^+ = T^+ \tag{1.3.6}$$

If we assume isospin symmetry, then this operator should take us between nuclear states which are in the same isospin multiplet. In this case, the nuclear structure of the initial and final nucleus are identical - provided we ignore the difference between protons and neutrons. A simplified illustration of this is shown in Figure 1.7. Beta decays of this type are called *superallowed Fermi beta decays*.

In the isospin symmetric approximation, the matrix element of the isospin raising operator is completely fixed by the $SU(2)$ group theory.

$$M_F = \langle TM_T'|T^+|TM_T\rangle = \sqrt{T(T+1) - M_T(M_T+1)} \tag{1.3.7}$$

This means that, in the isospin symmetric approximation, the decay rate for superallowed β-decay is independent of nuclear structure!

From the above argument, we can use superallowed Fermi β-decay to extract the value of G_V without worrying about our nuclear model. Historically speaking, this is what led to the theory of *conserved vector current* (CVC) which we discussed in the previous section. Feynman and Gell-Mann [FG58] calculated G_V using superallowed Fermi β-decay of $^{14}\mathrm{O} \to {}^{14}\mathrm{N}^*$ and then compared that to G_F measured in muon decay. Because the β-decay only involves the vector current, they hypothesized that the vector part of the weak current is conserved by the strong interactions.

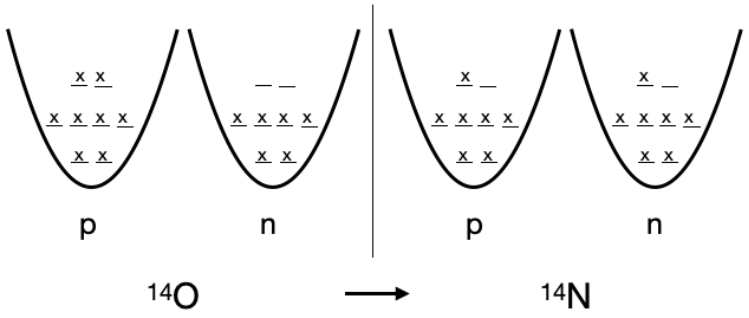

Figure 1.7: Simplified cartoon of the nuclear structure for the superallowed beta decay from $^{14}\mathrm{O}$ to $^{14}\mathrm{N}^*$. The x's represent occupation of a one-body nuclear energy level by either a proton or a neutron. Not shown are the angular momentum and isospin couplings. The ground state of $^{14}\mathrm{N}$ has $J^\pi = 1^+$, and the superallowed beta decay goes to the 0^+ first excited state.

We can now go ahead and compute the decay rate for superallowed beta decay from the amplitude 1.3.2. We start with the usual formula for the decay rate (the nuclear states are normalized to 1).

$$\Gamma = \int \frac{d^3p_e}{(2\pi)^3 2E_e} \frac{d^3p_\nu}{(2\pi)^3 2E_\nu} (2\pi)\delta(E_e + E_\nu - \Delta E_{\mathcal{N}})|\mathcal{M}|^2 \tag{1.3.8}$$

where $\Delta E_{\mathcal{N}}$ is the total change in the nuclear energy. Doing the lepton traces, plugging in the Fermi matrix element, and integrating over angles gives

$$\Gamma = \frac{G_V^2 |M_F|^2}{2\pi^3} \int_0^{\Delta E_{\mathcal{N}}} E_e E_\nu^2 p_e \, dE_e \tag{1.3.9}$$

The integral gives us the total lepton phase space. This is typically written in terms of $W = E_e/m_e$ and $W_0 = \Delta E_{\mathcal{N}}/m_e$.

$$\Gamma = \frac{G_V^2 |M_F|^2 m_e^5}{2\pi^3} \int_0^{W_0} W(W_0 - W)^2 \sqrt{W^2 - 1} \, dW \tag{1.3.10}$$

However, this formula is missing a large correction which comes from the distortion of the electron wavefunction.

Beta decays involve charge particles which interact via the electromagnetic interaction. Electrons emitted in beta decay are not plane waves, but instead get distorted by the coulomb field of the nucleus. The *Fermi function* represents the distortion of the emitted electron wave in the presence of the coulomb field of the daughter nucleus. Since the nucleus is so much smaller than the wavelength of the emitted electron/positron, we can approximate this effect by squaring the coulomb wavefunction at the origin ([New82] Chapter 14)

$$|\psi(\vec{r}=0)|^2 = \frac{2\pi\eta}{e^{2\pi\eta}-1} \quad \text{(NR limit)} \tag{1.3.11}$$

where $\eta = \pm Z\alpha/v$, v is the electron velocity, and Z is the charge of the daughter nucleus. We take the plus sign for a positron, and the minus sign for an electron. Since the electron is typically relativistic in beta decay, we need to solve the full relativistic Dirac equation and we find [Hay+18]

$$F(Z,W) = 4(2pR)^{2(\gamma-1)} e^{-\pi\eta} \frac{|\Gamma(\gamma+i\eta)|^2}{|\Gamma(1+2\gamma)|^2} \tag{1.3.12}$$

where $\gamma = \sqrt{1-(Z\alpha)^2}$. In the limit $\gamma \to 1$ we recover the simple non-relativistic formula. However, the relativistic version introduces a nuclear size parameter R since the relativistic wavefunction has a slight divergence at the origin. The choice of R gets lumped in together with other *finite nuclear size* corrections.

The Fermi function is combined with the lepton phase space into the *statistical rate function* ([Kra88] Chapter 9.3).

$$f(Z,W_0) = \int_0^{W_0} F(Z,W) W (W_0 - W)^2 \sqrt{W^2-1}\, dW \tag{1.3.13}$$

It is also conventional to write the decay rate in terms of the half-life $t_{1/2} = \log(2)/\Gamma_{\text{tot}}$. We also need to know the branching ratio R for superallowed β-decay, and the electron capture fraction P_{EC}. We can define a partial half-life as [HT15]

$$t = \frac{t_{1/2}}{R}(1+P_{\text{EC}}). \tag{1.3.14}$$

The product of these is defined as the ft value of the decay. We find the celebrated formula for superallowed beta decay.

$$ft = \frac{2\pi^3 \log(2)}{G_V^2 |M_F|^2 m_e^5} \tag{1.3.15}$$

For states with $T=1$, Equation 1.3.7 simply gives $M_F = \sqrt{2}$. Using this equation, we can measure the ft values for numerous different beta decays and extract G_V. Then we can compare this to G_F measured in muon decay to extract V_{ud}.

Results for various superallowed beta decays are given in Table 1.1. Although there is broad agreement between the ft values, we can see that they do not all agree within the

Decay	ft (s)
$^{10}\mathrm{C} \to {}^{10}\mathrm{B}$	3043.0 ± 4.3
$^{14}\mathrm{O} \to {}^{14}\mathrm{N}$	3042.2 ± 2.7
$^{22}\mathrm{Mg} \to {}^{22}\mathrm{Na}$	3051.9 ± 7.2
$^{26m}\mathrm{Al} \to {}^{26}\mathrm{Mg}$	3037.38 ± 0.58
$^{34}\mathrm{Cl} \to {}^{34}\mathrm{S}$	$3049.43^{+0.88}_{-0.95}$
$^{38m}\mathrm{K} \to {}^{38}\mathrm{Ar}$	3051.45 ± 0.92
$^{42}\mathrm{Sc} \to {}^{42}\mathrm{Ca}$	3047.5 ± 1.4
$^{46}\mathrm{V} \to {}^{46}\mathrm{Ti}$	$3050.32^{+0.44}_{-0.46}$
$^{54}\mathrm{Co} \to {}^{54}\mathrm{Fe}$	$3050.7^{+1.1}_{-1.5}$
$^{62}\mathrm{Ga} \to {}^{62}\mathrm{Zn}$	3074.0 ± 1.5
$^{74}\mathrm{Rb} \to {}^{74}\mathrm{Kr}$	3082.7 ± 6.5

Table 1.1: Measured ft values for various superallowed beta decays [HT15]

error bars. Even worse, we can use this together with the value of $V_{us} = \sin\theta_C \approx 0.22$ we found in Equation 1.1.35 and we find a range of values

$$|V_{ud}|^2 + |V_{us}|^2 \approx 1.028 \pm 0.003 \tag{1.3.16}$$

Which is a clear violation of CKM unitarity (Equation 1.1.36)!

We might think that the problem lies with our assumption of isospin symmetry. We can define a correction δ_C such that

$$|M_F|^2 = 2(1 - \delta_C) \tag{1.3.17}$$

where 2 is the isospin symmetric value. These corrections are model dependent, and are discussed in [TH02]. However, these corrections take us in the wrong direction for CKM unitarity. Clearly this is not the whole story. In the next section, we will explain how radiative corrections provide the solution to this problem.

Chapter 2

Radiative Corrections to Weak Nuclear Processes

In the last section, we mentioned corrections due to the electron moving through the static Coulomnb field of the daughter nucleus. This is encapsulated by the the Fermi function in Equations 1.3.11 and 1.3.12. In addition to the effects of the static Coulomb field, there are radiative corrections due to photon emission and virtual photon exchange. These are the topic of the present section.

In this thesis, we will be investigating the "*order* α" electromagnetic radiative corrections to weak nuclear processes - usually written as $\mathcal{O}(\alpha)$. As we discussed in the beginning of Section 1, α controls the strength of the electromagnetic interactions. Since $\alpha \approx 1/137$, these corrections typically change the result at the 1% level. Radiative corrections with two loops would be order α^2, and enter at the level of 0.01%. Examples of such loop diagrams are shown in Figure 2.1.

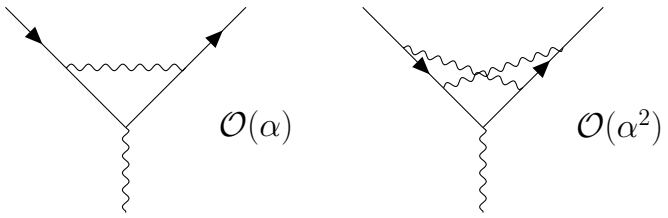

Figure 2.1: Examples of virtual photon exchange which would contribute at $\mathcal{O}(\alpha)$ (left) and $\mathcal{O}(\alpha^2)$ (right).

The theory of radiative corrections has historically been problematic due to the presence of self interactions. If an electron is able to emit a photon, and also absorb a photon, then the electron is able to interact with itself through a diagram such as in Figure 2.2. Such possibilities cannot simply be excluded in quantum field theory, so they must be dealt with in another way.

Figure 2.2: Self energy diagram in QED which naively leads to an infinite result, in which an electron emits and absorbs a photon.

The solution to the problem is *regularization and renormalization*. Instead of dealing with the original Lagrangian in equation 1.1.5, we define renormalized fields (following [Wei95] Chapter 10 and [PS95] Chapter 7)

$$\begin{aligned} \psi_{\mathrm{B}} &= \sqrt{Z_\psi}\psi \\ A_{\mathrm{B},\mu} &= \sqrt{Z_A}A_\mu \end{aligned} \tag{2.0.1}$$

Where the subscript "B" refers to the original "bare field". The fields without the subscript will refer to the renormalized field for the remainder of this section. In terms of the renormalized field, the QED lagrangian becomes

$$\mathcal{L}_{\mathrm{QED}} = -\frac{1}{4}Z_A F^{\mu\nu}F_{\mu\nu} + Z_\psi\bar{\psi}(i\partial\!\!\!/ - \sqrt{Z_A}e_B A\!\!\!/ - m_B)\psi \tag{2.0.2}$$

At zeroth order in the interactions, the renormalization constants are simply equal to 1. Therefore we also define a shift away from 1, which will be at least order α.

$$\begin{aligned} \delta_\psi &= Z_\psi - 1 \\ \delta_A &= Z_A - 1 \end{aligned} \tag{2.0.3}$$

The self energy diagram Figure 2.2 shifts the location of the pole away from the bare mass m_{B}, and we define a pole mass

$$Z_\psi m_{\mathrm{B}} = m + \delta_m \tag{2.0.4}$$

Defining m to be the location of the pole in the propagator is known as the *on-shell renormalization scheme*.

Finally, the electromagnetic coupling constant e gets renormalized by the interactions. However, the renormalization of the coupling constant cannot depend on the species of fermion we are considering - it must be universal for all charged particles. Therefore, the electromagnetic coupling only gets renormalized by Z_A

$$\sqrt{Z_A}e_{\mathrm{B}} = e \tag{2.0.5}$$

This can also be derived using the Ward identity.

Putting this all together, we can divide the Lagrangian into ordinary terms and *counter terms*.

$$\begin{aligned} \mathcal{L} = &-\frac{1}{4}F^{\mu\nu}F_{\mu\nu} + \bar{\psi}(i\partial\!\!\!/ - eA\!\!\!/ - m)\psi \\ &-\frac{1}{4}\delta_A F^{\mu\nu}F_{\mu\nu} + \bar{\psi}(\delta_\psi i\partial\!\!\!/ - \delta_\psi eA\!\!\!/ - \delta_m)\psi \end{aligned} \tag{2.0.6}$$

The counter terms are treated as higher order in α, and they are used to soak up the problematic infinities which occur in diagrams like Figure 2.2.

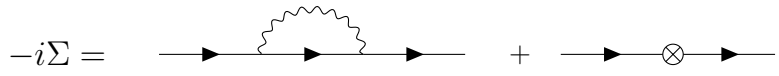

Figure 2.3: The self-energy contribution from the loop gets a correction from the counter terms, such that the renormalization conditions are satisfied.

The full propagator for the electron gets modified by the presence of self energy diagrams as follows

$$S(p) = \int d^4x e^{ipx} \langle \Omega | T\psi(x)\bar{\psi}(0)|\Omega\rangle = \frac{i}{\not{p} - m - \Sigma(\not{p})} \tag{2.0.7}$$

Here Σ represents the *one particle irreducible* diagrams (1PI), which cannot be separated into two parts by cutting a single internal line. An example of one such 1PI diagram is Figure 2.2. The loop contribution gets corrected by the counter term contribution as in Figure 2.3.

$$-i\Sigma = -i\Sigma^{\text{loop}} + i\not{p}\delta_\psi - i\delta_m \tag{2.0.8}$$

In the on-shell renormalization scheme, the counter terms are chosen such that the pole of the propagator Equation 2.0.7 has a pole of unit residue at $\not{p} = m$.

Since the loop contribution gives an infinite result, we cannot simply set $\delta_\psi = \delta_m = \infty$. We need to choose a *regularization procedure* in order to make sense of these divergent results. A simple choice for these purposes is the Pauli-Villars regulator, which introduces a UV mass scale Λ. We also need to include a small photon mass λ to control IR divergences.

By direct computation, the wavefunction renormalization at one loop is

$$Z_\psi = 1 - \frac{\alpha}{2\pi}\left(\frac{1}{2}\log\left(\frac{\Lambda^2}{m^2}\right) + \frac{9}{4} - \log\left(\frac{m^2}{\lambda^2}\right)\right). \tag{2.0.9}$$

We see that we cannot simply set $\Lambda = \infty$ and $\lambda = 0$ because the wavefunction renormalization would diverge logarithmically.

Note that this counter term also shows up in the correction to the electromagnetic interaction. The loop diagram in Figure 2.4 gives a correction to the electron form factors F_1 and F_2 we defined in Equation 1.2.23.

$$\bar{u}(p_f)\Gamma^\mu_{\text{loop}}(p_f, p_i)u(p_i) = F_1^{\text{loop}}\bar{u}_f\gamma^\mu u_i + F_2^{\text{loop}}\frac{i\bar{u}_f\sigma^{\mu\nu}q_\nu u_i}{2m} \tag{2.0.10}$$

The form factor F_2 is UV and IR finite, and gives the famous Schwinger correction to the magnetic moment.

$$\mu_e = 1 + \frac{\alpha}{2\pi} \approx 1.001\,161 \quad \text{(at one loop)} \tag{2.0.11}$$

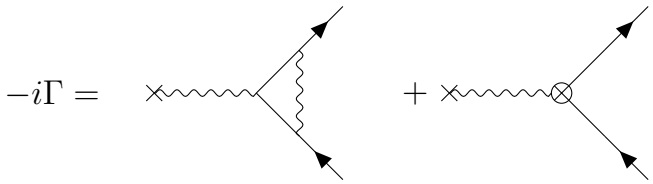

Figure 2.4: The electromagnetic vertex gets corrected by virtual photon exchange, and this is accompanied by a counter term which cancels the UV divergence.

This is quite close to the measured value in Equation 1.2.26. On the other hand, the F_1^{loop} term diverges both in the UV and the IR. By including the counter term in Equation 2.0.9, the UV divergence is cancelled exactly. In particular, the correction to the form factor F_1 is exactly equal to zero at zero momentum transfer.

$$\delta_\psi + F_1^{\text{loop}}(q^2 = 0) = 0 \tag{2.0.12}$$

This is a result of the Ward-Takahashi identity, which relates the electromagnetic vertex to the propagator Equation 2.0.7.

$$-i(p_f - p_i)_\mu \Gamma^\mu(p_f, p_i) = S(p_f)^{-1} - S(p_i)^{-1} \tag{2.0.13}$$

At $q^2 \neq 0$, the form factor F_1^{loop} is also plagued by an IR divergence - it depends on the fictitious mass of the photon λ which we included to render the integrals finite. These are not cancelled by a counter term in the same way the UV divergence is. Instead, they are cancelled by accounting for the emission of low energy photons in the final state. These are known as *bremsstrahlung* contributions, and they contribute to the overall rate in a way which cancels the dependence on the IR regulator λ.

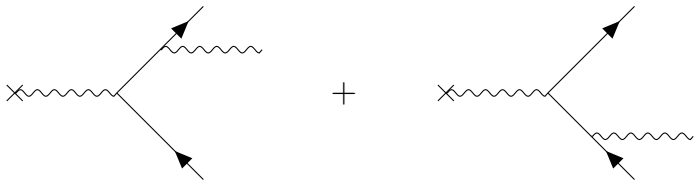

Figure 2.5: In addition to virtual photon exchange, it is possible that there are unobserved low-energy photons produced in the final state.

Radiative Corrections to Muon Decay

As we discussed in Section 1, we can learn a lot about nuclear beta decay by comparing it to the much simpler process of muon decay. Therefore, it makes sense to start by considering the $\mathcal{O}(\alpha)$ radiative corrections to muon decay. The $\mathcal{O}(\alpha)$ correction has been known since the

late 50's [Ber58][KS59]. We can compute it by simply applying the tricks we have discussed in this section so far.

The interaction Lagrangian which mediates muon decay Equation 1.0.18 gets modified by the wavefunction renormalization constants for the electron and the muon (the neutrinos are not renormalized by electromagnetic interactions).

$$\mathcal{L}' = -\sqrt{Z_e Z_\mu}\frac{G_F}{\sqrt{2}}[\bar{e}\gamma^\lambda(1-\gamma^5)\nu_e][\bar{\nu}_\mu\gamma_\lambda(1-\gamma^5)\mu] \tag{2.0.14}$$

Where Z_e and Z_μ are given by 2.0.9 with m_e and m_μ, respectively. The counter term is then proportional to $\sqrt{Z_e Z_\mu} - 1$.

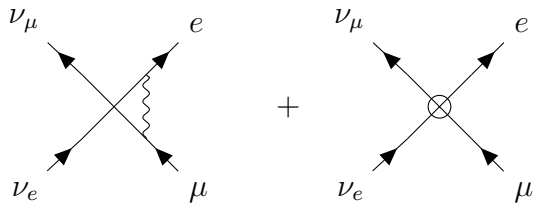

Figure 2.6: One loop contribution to the muon decay amplitude, plus the corresponding counter-term.

The loop contribution to the amplitude can be written down immediately from the Feynman rules.

$$\begin{aligned}\mathcal{M}_{\text{loop}} = -ie^2\frac{G_F}{\sqrt{2}}\int\frac{d^4k}{(2\pi)^4}\frac{1}{k^2-\lambda^2+i\epsilon}&\frac{\bar{u}(p_e)\gamma^\alpha(\not{p}_e+\not{k}+m_e)\gamma^\lambda(1-\gamma^5)v(p_{\nu_e})}{(p_e+k)^2-m_e^2+i\epsilon}\\ &\times\frac{\bar{u}(p_{\nu_\mu})\gamma_\lambda(1-\gamma^5)(\not{p}_\mu+\not{k}+m_\mu)\gamma_\alpha u(p_\mu)}{(p_\mu+k)^2-m_\mu^2+i\epsilon}\end{aligned} \tag{2.0.15}$$

We would like to do the usual contractions of the gamma matrices, but as it is written currently the lepton propagators occur in different fermion bilinears. We can cast this in a more useful form by using *Fierz rearrangement*.

$$\begin{aligned}u_1\bar{u}_2 = \frac{1}{4}\Big[&(\bar{u}_2u_1)\mathbf{1} + (\bar{u}_2\gamma_\mu u_1)\gamma^\mu + \frac{1}{2}(\bar{u}_2\sigma_{\mu\nu}u_1)\sigma^{\mu\nu}\\ &-(\bar{u}_2\gamma_\mu\gamma^5u_1)\gamma^\mu\gamma^5 + (\bar{u}_2\gamma^5u_1)\gamma^5\Big]\end{aligned} \tag{2.0.16}$$

Now the magic happens. Due to the presence of the $(1-\gamma^5)$'s, the only terms which survive have an odd number of γ matrices. Only the vector and axial-vector terms survive. We use this to put the neutrino spinors together.

$$\gamma^\lambda(1-\gamma^5)v\bar{u}\gamma_\lambda(1-\gamma^5) = -\gamma^\mu(1-\gamma^5)\left[\bar{u}\gamma_\mu(1-\gamma^5)v\right] \tag{2.0.17}$$

After doing the rearrangement, we have

$$\begin{aligned}\mathcal{M}_{\text{loop}} &= +ie^2\frac{G_V}{\sqrt{2}}\left[\bar{u}(p_{\nu_\mu})\gamma_\lambda(1-\gamma^5)v(p_{\nu_e})\right] \\ \times\int\frac{d^4k}{(2\pi)^4}&\frac{\bar{u}(p_e)\gamma^\alpha(\not{p}_e+\not{k}+m_e)\gamma^\lambda(1-\gamma^5)(\not{p}_\mu+\not{k}+m_\mu)\gamma_\alpha u(p_\mu)}{[k^2-\lambda^2+i\epsilon][(p_e+k)^2-m_e^2+i\epsilon][(p_\mu+k)^2-m_\mu^2+i\epsilon]}\end{aligned} \tag{2.0.18}$$

What follows is a grind of gamma matrix algebra and feynman parameter integrals. We can organize the terms according to the form factors we defined in Equations 1.2.33 and 1.2.34. We need to be very careful about keeping terms with m_e to avoid infrared divergences in the limit $m_e \to 0$. Without going into all of those details, we can pick out the UV divergent terms. Only the vector and axial-vector form factors F_1 and F_A end up being UV divergent. The coefficient of the UV divergent logarithm is simple to calculate.

$$\mathcal{M}_{\text{loop}} = \mathcal{M}_{\text{tree}} \times \frac{\alpha}{2\pi}\frac{1}{2}\log\left(\frac{\Lambda^2}{m_\mu^2}\right) + (\text{UV finite terms}) \tag{2.0.19}$$

Where $\mathcal{M}_{\text{tree}}$ is the tree-level amplitude. This is exactly the same log which shows up in the wavefunction renormalization Equation 2.0.9, but with the opposite sign. The UV divergence is exactly cancelled by including the counter-term proportional to $(\sqrt{Z_e Z_\mu}-1)$. Thus the muon decay is finite to order α. In fact, the same Fierz rearrangement argument [BS62] [SF13] implies an even stronger condition.

Electromagnetic radiative corrections to muon decay are finite to all orders in α.

The result at one loop is given by

$$\frac{1}{\tau_\mu} = \frac{G_F^2 m_\mu^5}{192\pi^3}F\left(\frac{m_e^2}{m_\mu^2}\right)\times\left[1+\frac{\alpha}{2\pi}\left(\frac{25}{4}-\pi^2\right)\right] \tag{2.0.20}$$

where $F(x) = 1-8x-12x^2\log x+8x^3-x^4$ is a tree level phase space correction factor when we keep the electron mass which we ignored in Equation 1.0.20.

Radiative Corrections to Neutron Decay

Now we can try to apply the same treatment to free neutron decay. However, will run into a problem which was first encountered in the late 50s [BFS56][Ber58][KS59]. Unlike the case of muon decay, the neutron decay has a different helicity structure compared to the ordinary electromagnetic vertex. This is shown in Figure 2.7.

Let's see this by explicit calculation. For the sake of clarity, we take the electromagnetic vertex to be the fundamental vertex with $F_1 = 1$ and $F_2 = 0$ for the proton, and let $g_A = 1$ for simplicity. Note that we pick up an additional minus sign from the product of the charges

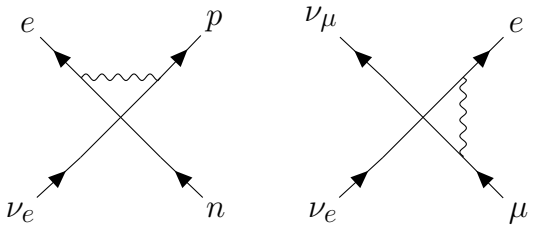

Figure 2.7: Comparison of the helicity structure of the vertex correction in muon and neutron decay, which explains the UV divergence in the case of neutron decay.

$q_e q_p = -1$. The loop correction in this case is

$$\mathcal{M}_{\text{loop}} = +ie^2 \frac{G_V}{\sqrt{2}} \int \frac{d^4k}{(2\pi)^4} \frac{1}{k^2 - \lambda^2 + i\epsilon} \frac{\bar{u}_e \gamma_\mu (\not{p}_e - \not{k} + m_e) \gamma_\lambda (1-\gamma^5) v_\nu}{(p_e - k)^2 - m_e^2 + i\epsilon} \times \frac{\bar{u}_p \gamma^\mu (\not{p}_2 + \not{k} + M_p) \gamma^\lambda (1-\gamma^5) u_n}{(p_2 + k)^2 - M_p^2 + i\epsilon} \tag{2.0.21}$$

where p_1 is the initial neutron momentum, and p_2 is the final proton momentum. Again we want to do the Fierz rearrangement, but there is a problem. In order to put the electron and proton spinors together, we first need to do a charge conjugation. Crucially, this changes $(1-\gamma^5)$ into $(1+\gamma^5)$ - this is the source of the problem.

$$\mathcal{M}_{\text{loop}} = +ie^2 \frac{G_V}{\sqrt{2}} \int \frac{d^4k}{(2\pi)^4} \frac{1}{k^2 - \lambda^2 + i\epsilon} \frac{\bar{u}_e \gamma_\mu (\not{p}_e - \not{k} + m_e) \gamma_\lambda (1-\gamma^5) v_\nu}{(p_e - k)^2 - m_e^2 + i\epsilon} \frac{\bar{v}_n \gamma^\lambda (1+\gamma^5) (\not{p}_2 + \not{k} - M_p) \gamma^\mu v_p}{(p_2 + k)^2 - M_p^2 + i\epsilon} \tag{2.0.22}$$

Now the Fierz rearrangement produces scalar and pseudo-scalar terms.

$$\gamma_\lambda (1-\gamma^5) v_\nu \bar{v}_n \gamma^\lambda (1+\gamma^5) = 2(1+\gamma^5) \left[\bar{v}_n (1-\gamma^5) v_\nu \right] \tag{2.0.23}$$

Going through the motions again, we find something completely different compared to the muon case.

$$\mathcal{M}_{\text{loop}} = \mathcal{M}_{\text{tree}} \times \frac{\alpha}{2\pi} 2 \log \left(\frac{\Lambda^2}{M_p^2} \right) + (\text{UV finite terms}) \tag{2.0.24}$$

Adding the counter-term proportional to $(\sqrt{Z_p Z_e} - 1)$ no longer cancels the UV divergence. Instead, we get a well known factor of 3/2.

$$\mathcal{M}_{\text{loop}} + (\sqrt{Z_p Z_e} - 1)\mathcal{M}_{\text{tree}} = \mathcal{M}_{\text{tree}} \times \frac{\alpha}{2\pi} \frac{3}{2} \log \left(\frac{\Lambda^2}{M_p^2} \right) + (\text{UV finite terms}) \tag{2.0.25}$$

This leads us to the following conclusion.

Electromagnetic radiative corrections to neutron decay in the 4-fermion theory depend on the ultraviolet regulator, rendering them ambiguous.

In fact, we can extend this argument and consider the generic reaction

$$A + \nu_e \to B + e \tag{2.0.26}$$

where A and B are particles which interact via the fundamental left-handed weak interaction, $\bar{\psi}_A \gamma^\lambda (1 - \gamma^5) \psi_B$. These might be (μ, ν_μ), or (n, p) or the quarks (d, u). We suppose they have electric charges q_A and q_B, subject to charge conservation $q_A - q_B = -1$. In general, we get three vertex corrections. These are shown in Figure 2.8.

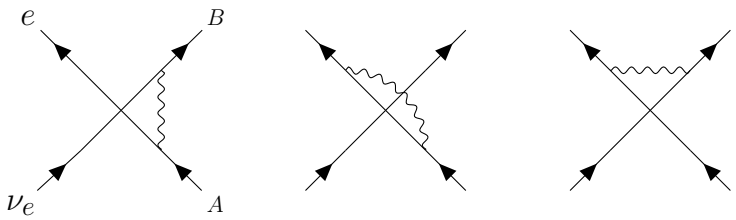

Figure 2.8: Feynman diagrams for virtual photon exchange for any charged particles A, B involved in the radiative corrections to the process $A + \nu_e \to B + e$.

The corresponding counter-term now involves the wavefunction correction from the three charged particles, $\sqrt{Z_A Z_B Z_e} - 1$. In this case, the UV divergence (including the counter-term) is equal to

$$\mathcal{M}_{\text{loop}} + \mathcal{M}_{\text{ct}} = \mathcal{M}_{\text{tree}} \times \frac{\alpha}{2\pi} \frac{3}{4} (1 + 2\bar{Q}) \log \left(\frac{\Lambda^2}{M^2} \right) + (\text{UV finite terms}) \tag{2.0.27}$$

where $\bar{Q} = \frac{q_A + q_B}{2}$ is the average of the electric charges, and M is the relevant mass scale. This can be derived rigorously using the current algebra approach [AND67][Sir78]. The UV divergence is only cancelled when $\bar{Q} = -1/2$, which just happens to be the case for muon decay. For neutron decay, we have $\bar{Q} = 1/2$ and this leads to the coefficient $3/2$ we derived earlier. On the other hand, their quark counterparts (u, d) give $\bar{Q} = 1/6$.

This ambiguity would make early attempts at establishing weak universality impossible. There were competing speculations at the time as to what might cure this divergence. Some argued that the strong interactions might provide a natural UV cutoff to the theory. However, this was shown not to be the case. Even without a complete theory of the strong interactions, new methods using current algebra showed that the divergent part remains to all orders in the strong interactions [AND67].

Others argued that this problem would be solved by introducing a massive vector boson - appropriately called W - which might mediate the weak interactions. They couldn't yet detect the W-boson directly since it was presumed to be heavy, and its mass would provide a natural regulator by setting $\Lambda = M_W$. Calculations by Lee [Lee62] show this was plausible using an early model of the intermediate vector boson. Thus the problem of electroweak radiative corrections and universality of the weak interaction played an important role in motivating the development of renormalizable weak interactions.

2.1 Sirlin's Inner vs Outer Corrections

As we have seen, the radiative corrections to neutron decay are not so straightforward. The result is sensitive to the UV regulator in Equation 2.0.25. The radiative correction also depends on the nuclear structure. We can see a hint of the nuclear model dependence in the $\bar{Q}$ term in Equation 2.0.27, which is different if we take nucleons $\bar{Q} = 1/2$ or quarks $\bar{Q} = 1/6$. We need a way to untangle this mess, and separate out the parts we know from the parts we don't know.

In his seminal 1967 paper [Sir67], Sirlin isolates the general properties of the radiative correction which are independent of the details of strong interactions and the underlying UV physics. These are called the "outer corrections". The basic premise of Sirlin's separation can be understood by looking at Equation 2.0.21, and applying a simple on-shell spinor identity.

$$\bar{u}_p \gamma^\mu (\not{p}_2 + \not{k} + M_p) = \bar{u}_p [(2p_2 + k)^\mu - i\sigma^{\mu\nu} k_\nu] \tag{2.1.1}$$

Roughly speaking, first term $(2p_2 + k)^\mu$ is the "outer correction", and the remainder term $-i\sigma^{\mu\nu}k_\nu$ is the "inner correction". The outer correction is proportional to the tree-level weak vertex, it contains the IR divergence, and it is UV finite when it is combined with the counter term. The inner correction contains the problematic UV divergence, but it is IR finite and automatically gauge invariant.

The method consists of separating out all terms of order $1/k$ in a gauge invariant manner. It is shown that, at order α, all of the terms which explicitly depend on the electron energy E and electron mass m_e can be rigorously computed. In particular, the shape of the allowed electron spectrum is given by a single universal function $g(E, E_m, m_e)$.

Following [Sir67], we write the nucleon weak vertex as $W_\lambda(p_2, p_1)$. The tree level amplitude is

$$\mathcal{M}_{\text{tree}} = \frac{G_V}{\sqrt{2}} [\bar{u}_e \gamma^\lambda (1 - \gamma^5) v_\nu][\bar{u}_p W_\lambda(p_2, p_1) u_n] \tag{2.1.2}$$

Where p_1 is the momentum of the incoming neutron, and p_2 is the momentum of the outgoing proton. The exact structure of the weak vertex is not needed for Sirlin's argument.

Consider all diagrams in Figure 2.9 in which the virtual photon attaches to the lepton line and the hadronic line. We can write the amplitude symbolically as

$$\mathcal{M}_{\text{box}} = -e^2 \frac{G_V}{\sqrt{2}} \int \frac{d^4k}{(2\pi)^4} D^{\mu\nu}(k) \frac{[\bar{u}_e \gamma_\nu (\not{p}_e - \not{k} + m_e) \gamma^\lambda (1 - \gamma^5) v_\nu]}{(p_e - k)^2 - m_e^2 + i\epsilon} T_{\mu\lambda}(p_2, p_1, k) \tag{2.1.3}$$

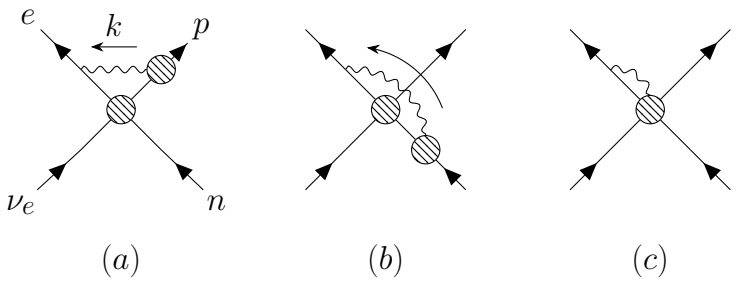

Figure 2.9: "Box Diagram" where the virtual photon attaches to the lepton line and the hadronic line. In the last diagram, the virtual photon attaches to the proper weak vertex.

We define a the time ordered product of the currents as

$$T^{\mu\lambda}(p_f, p_i, k) = -i \int d^4x e^{ikx} \langle p_f | T J^{\mu}_{em}(x) J^{\lambda}_{W}(0) | p_i \rangle \tag{2.1.4}$$

This quantity is also referred to as the generalized Compton tensor, since it is the time ordered product of the electromagnetic currents which enters into the amplitude for Compton scattering.

As we argued in the lead up to Equation 2.1.1, the outer correction should come from Figure 2.9 (a) in which a virtual photon is exchanged between the proton and the electron. We represent the electromagnetic vertex by $\Gamma^{(N)}_{\mu}(p', p)$. This amplitude can be written as

$$\begin{aligned}\mathcal{M}(a) = +ie^2 \frac{G_V}{\sqrt{2}} \int \frac{d^4k}{(2\pi)^4} D^{\mu\nu}(k) \frac{[\bar{u}_e \gamma_\nu (\not{p}_e - \not{k} + m_e) \gamma^\lambda (1-\gamma^5) v_\nu]}{(p_e - k)^2 - m_e^2 + i\epsilon} \\ \times [\bar{u}_p \Gamma^{(p)}_{\mu}(p_2, p_2 + k) S(p_2 + k) W_\lambda(p_2 + k, p_1) u_n]\end{aligned} \tag{2.1.5}$$

where $D^{\mu\nu}(k)$ is the photon propagator in Feynman gauge

$$D^{\mu\nu}(k) = \frac{-i\eta^{\mu\nu}}{k^2 - \lambda^2 + i\epsilon} \tag{2.1.6}$$

and $S(p)$ is the fully dressed renormalized propagator for the proton, Equation 2.0.7.

The first step in separating out the strong-interaction dependant part is introducing the "proton electromagnetic form factor", $F^{(p)}_{\mu}(p_2, p_2 + k)$, which is defined by the relation

$$\bar{u}_p \Gamma^{(p)}_{\mu}(p_2, p_2 + k) S(p_2 + k) = \bar{u}_p F^{(p)}_{\mu}(p_2, p_2 + k) S_0(p_2 + k) \tag{2.1.7}$$

Here, $S_0(p)$ is the free propagator, $S_0(p) = i[\not{p} - M_p]^{-1}$. The key lies in the Ward–Takahashi identity, Equation 2.0.13. We also need to use the on-shell renormalization conditions for the propagator, which imply

$$\bar{u}(p) S(p)^{-1} = \bar{u}(p) S_0(p)^{-1} = 0 \quad \text{(on-shell)} \tag{2.1.8}$$

After some clever rearrangement, we arrive at the Ward-Takahashi identity for F_μ.

$$\begin{aligned} k^\mu F_\mu^{(p)}(p, p+k) &= \not{k} \\ F_\mu^{(p)}(p,p) &= \gamma_\mu \end{aligned} \tag{2.1.9}$$

This suggests writing F_μ as a simple γ_μ, plus a correction term.

$$F_\mu^{(p)}(p', p) = \gamma_\mu + X_\mu^{(p)}(p', p) \tag{2.1.10}$$

Crucially, the correction term vanishes when dotted into k^μ and it goes to zero when $k \to 0$.

$$\begin{aligned} k^\mu X_\mu(p, p+k) &= 0 \\ X_\mu(p,p) &= 0 \end{aligned} \tag{2.1.11}$$

Plug in the free propagator, and use the identity Equation 2.1.1. Now we can pick out a term proportional to the tree level amplitude which also contains the IR divergence.

$$\begin{aligned} &\bar{u}_p \Gamma_\mu^{(p)}(p_2, p_2+k) S(p_2+k) W_\lambda(p_2+k, p_1) u_n \\ &= \frac{i}{k^2 + 2p_2 \cdot k + i\epsilon} \bar{u}_p \left[(2p_2 + k)_\mu W_\lambda(p_2, p_1) + R_{\mu\lambda}^{(p)}(p_2, p_1, k) \right] u_n \end{aligned} \tag{2.1.12}$$

The remainder term $R_{\mu\lambda}^{(p)}$ is everything which is left over.

$$\begin{aligned} R_{\mu\lambda}^{(p)}(p_2, p_1, k) = (2p_2 + k)_\mu [W_\lambda(p_2 + k, p_1) - W_\lambda(p_2, p_1)] \\ - i\sigma_{\mu\nu} k^\nu W_\lambda(p_2 + k, p_1) \\ + X_\mu^{(p)}(p_2, p_2 + k)(\not{p}_2 + \not{k} + M_p) W_\lambda(p_2 + k, p_1) \end{aligned} \tag{2.1.13}$$

Crucially, the remainder term is regular as $k \to 0$. This means that the limit

$$\lim_{k \to 0} \frac{1}{k^2 + 2p_2 \cdot k} R_{\mu\lambda}^{(p)}(p_2, p_1, k) \tag{2.1.14}$$

exists. However, there is still the problem of gauge invariance. The remainder term is not gauge invariant, but it satisfies

$$\frac{k^\mu}{k^2 + 2p_2 \cdot k} R_{\mu\lambda}^{(p)}(p_2, p_1, k) = W_\lambda(p_2 + k, p_1) - W_\lambda(p_2, p_1) \tag{2.1.15}$$

When the weak vertex depends on the momentum transfer, we cannot ignore this term.

Now we can repeat this same analysis for the vertex correction where the photon attaches to the neutron line Figure 2.9 (b). The difference here is that the neutron has no electric charge, so we simply have

$$\begin{aligned} k^\mu F_\mu^{(n)}(p - k, p) &= 0 \\ F_\mu^{(n)}(p,p) &= 0 \end{aligned} \tag{2.1.16}$$

Finally, we need to consider the possibility that a photon attaches to an internal line of the proper weak vertex. Let $G_{\mu\lambda}(p_2, p_1, k)$ be the matrix element for a photon emitted from any internal line of the proper weak vertex, Figure 2.9 (c). The amplitude for this process is

$$\mathcal{M}(c) = -e^2 \frac{G_V}{\sqrt{2}} \int \frac{d^4k}{(2\pi)^4} D^{\mu\nu}(k) \frac{[\bar{u}_e \gamma_\nu (\not{p}_e - \not{k} + m_e)\gamma^\lambda (1-\gamma^5) v_\nu]}{(p_e - k)^2 - m_e^2 + i\epsilon} \bar{u}_p G_{\mu\lambda}(p_2, p_1, k) u_n \tag{2.1.17}$$

We can derive the divergence of $G_{\mu\lambda}$ by considering all diagrams in which a photon can be emitted, and using the Ward identity. A photon can be emitted from the electron line, the proton line, the neutron line, or from the weak vertex.

$$\begin{aligned}
\mathcal{M}_\mu =& (-1)e \frac{\bar{u}_e \gamma_\mu (\not{p}_e + \not{k} + m_e)\gamma_\lambda (1-\gamma^5) v_\nu}{k^2 + 2p_e \cdot k} \bar{u}_p W^\lambda(p_2, p_1) u_n \\
&+ e[\bar{u}_e \gamma_\lambda (1-\gamma^5) v_\nu] \bar{u}_p F_\mu^{(p)}(p_2, p_2 + k) \frac{\not{p}_2 + \not{k} + M_p}{k^2 + 2p_2 \cdot k} W^\lambda(p_2 + k, p_1) u_n \\
&+ e[\bar{u}_e \gamma_\lambda (1-\gamma^5) v_\nu] \bar{u}_p W^\lambda(p_2, p_1 - k) \frac{(\not{p}_1 - \not{k} + M_n)}{k^2 - 2p_1 \cdot k} F_\mu^{(n)}(p_1 - k, p_1) u_n \\
&+ e[\bar{u}_e \gamma^\lambda (1-\gamma^5) v_\nu] \bar{u}_p G_{\mu\lambda}(p_2, p_1, k) u_n
\end{aligned} \tag{2.1.18}$$

The minus sign for the first line is due to the negative electron charge. We require $k^\mu \mathcal{M}_\mu = 0$ for gauge invariance. Dot this into k^μ and use the Ward identity for the proton and neutron vertex functions Equations 2.1.9 and 2.1.16. Use basic on-shell spinor identities to eliminate the various propagators, and we are left with a simple relation for $G_{\mu\lambda}$.

$$k^\mu G_{\mu\lambda}(p_2, p_1, k) = W^\lambda(p_2, p_1) - W^\lambda(p_2 + k, p_1) \tag{2.1.19}$$

This exactly cancels the gauge dependence we found in $R_{\mu\lambda}^{(p)}$, which renders the inner correction gauge invariant! Another fundamental property of $G_{\mu\lambda}(p_2, p_1, k)$ is that it is regular as $k \to 0$. This can be seen in a number of ways [Sir67], but we will not go into the details.

Putting this together, we can express the virtual photon exchange with the electron Equation 2.1.3 by separating out the outer correction from the generalized compton tensor Equation 2.1.4.

$$T_{\mu\lambda}(p_2, p_1, k) = \frac{(2p_2 + k)_\mu}{k^2 + 2p_2 \cdot k + i\epsilon} \bar{u}_p W_\lambda(p_2, p_1) u_n + \hat{T}_{\mu\lambda}(p_2, p_1, k) \tag{2.1.20}$$

This is directly analogous to the simple minded rewriting Equation 2.1.1. The first term in the bracket contains the entire IR divergence, and it is proportional to the tree-level nuclear matrix element. This term gets lumped into the outer correction.

On the other hand, the remainder term is IR finite and contains all of the nuclear structure dependence.

$$\hat{T}_{\mu\lambda}(p_2, p_1, k) = \bar{u}_p \left[\frac{R_{\mu\lambda}^{(p)}(p_2, p_1, k)}{k^2 + 2p_2 \cdot k + i\epsilon} + G_{\mu\lambda}(p_2, p_1, k) + \frac{R_{\mu\lambda}^{(n)}(p_2, p_1, k)}{k^2 - 2p_1 \cdot k + i\epsilon} \right] u_n \tag{2.1.21}$$

As we have already seen, this particular combination is also gauge invariant.

$$k^{\mu}\hat{T}_{\mu\lambda}(p_2, p_1, k) = 0 \tag{2.1.22}$$

This is represents the inner correction.

Including the wavefunction renormalization Equation 2.0.9 as we described in the previous section, we can show that the outer correction is UV finite. Including the inner bremsstrahlung diagrams, we get a result which is well defined. We can now write the corrected electron spectrum to order α for unpolarized neutron decay as

$$N(E)dE = \tilde{\xi}N_0(E)dE\left[1 + \frac{\alpha}{2\pi}g(E, E_m, m)\right] \tag{2.1.23}$$

Where $N_0(E)$ is the uncorrected electron spectrum, which by definition includes the Fermi function 1.3.12.

$$N_0(E) = \frac{|M_{\mathrm{F}}|^2 + g_A^2|M_{\mathrm{GT}}|^2}{2\pi^3}E[E_m - E]^2 pF(Z, E) \tag{2.1.24}$$

E_m is the end-point energy of the electron spectrum - the maximum energy which the emitted electron can have. The outer correction is expressed in terms of the complicated function $g(E, E_m, m)$.

$$\begin{aligned} g(E, E_m, m) =& 3\log\frac{M_p}{m_e} - \frac{3}{4} + \frac{4}{\beta}L\left(\frac{2\beta}{1+\beta}\right) \\ &+4\left(\frac{\tanh^{-1}\beta}{\beta} - 1\right)\left[\frac{E_m - E}{3E} - \frac{3}{2} + \log\left(\frac{2(E_m - E)}{m_e}\right)\right] \\ &+\frac{1}{\beta}\tanh^{-1}\beta\left[2(1+\beta^2) + \frac{(E_m - E)^2}{6E^2} - 4\tanh^{-1}\beta\right] \end{aligned} \tag{2.1.25}$$

Here $L(x)$ is the Spence function.

$$L(x) = \int_0^x \frac{dt}{t}\log(1-t) \tag{2.1.26}$$

The remaining inner correction shifts the Fermi and Gamow-Teller matrix elements differently.

$$(1 + \Delta_{\mathrm{F}})|M_{\mathrm{F}}|^2 + g_A^2(1 + \Delta_{\mathrm{GT}})|M_{\mathrm{GT}}|^2 \tag{2.1.27}$$

But they do not effect the shape of the beta spectrum, provided we ignore terms of order $\alpha(E/M_p)\log(M_p/E)$ and $\alpha q/M_p$.

2.2 Matching onto the UV Complete Description

In the first part of Section 2, we gave a hand-wavey argument as to why the divergent part of the amplitude for neutron decay is proportional to $(1 + 2\bar{Q})$. This argument can be made

more precise to show that this is the correct behaviour independent of the strong interactions. We will prove this following [Abe+68], focusing on the most relevant parts of the argument.

We now employ a clever re-writing of the lepton covariant in Equation 2.1.3. First, use the on-shell condition to combine the m_e and $\not{p}_e$ terms. Then for the $\not{k}$ term, use the identity for the product of three gamma matrices.

$$\gamma^\mu\gamma^\nu\gamma^\sigma = \eta^{\mu\nu}\gamma^\sigma - \eta^{\mu\sigma}\gamma^\nu + \eta^{\nu\sigma}\gamma^\mu + i\varepsilon^{\mu\nu\sigma\lambda}\gamma_\lambda\gamma^5 \tag{2.2.1}$$

This gives us

$$\begin{aligned} &\bar{u}_e\gamma^\mu(\not{p}_e - \not{k} + m_e)\gamma^\lambda(1-\gamma^5)v_\nu \\ &= \bar{u}_e(2p_e^\mu\gamma^\lambda - k^\mu\gamma^\lambda + \eta^{\mu\lambda}\not{k} - k^\lambda\gamma^\mu - i\varepsilon^{\mu\lambda\alpha\beta}k_\alpha\gamma_\beta)(1-\gamma^5)v_\nu \\ &= (2p_e - k)^\mu L^\lambda + \eta^{\mu\lambda}k\cdot L - k^\lambda L^\mu - i\varepsilon^{\mu\lambda\alpha\beta}k_\alpha L_\beta \end{aligned} \tag{2.2.2}$$

Where $L^\lambda = \bar{u}_e\gamma^\lambda(1-\gamma^5)v_\nu$ is the tree-level lepton matrix element. We also combined the γ^5's in the last term using $\gamma^5(1-\gamma^5) = -(1-\gamma^5)$.

The first term with the electron momentum does not contribute to the divergent part, so we will ignore that term for now. Then we are left with the following four terms.

$$k_\mu T^{\mu\lambda}, \quad k_\lambda T^{\mu\lambda}, \quad \eta_{\mu\lambda}T^{\mu\lambda}, \quad \varepsilon_{\mu\lambda\alpha\beta}k^\alpha T^{\mu\lambda} \tag{2.2.3}$$

Lets focus on the first term, which is the inner product of the photon momentum with the $T^{\mu\lambda}$. Doing the usual integration by parts trick, we pick up a term which involves the equal time commutator of the currents.

$$\begin{aligned} k_\mu T^{\mu\lambda}(p_f, p_i, k) = &\int d^4x\, e^{ikx}\,\langle p_f|T\frac{\partial}{\partial x^\mu}J^\mu_{em}(x)J^\lambda_W(0)|p_i\rangle \\ &+ \int d^3x e^{-i\vec{k}\cdot\vec{x}}\,\langle p_f|[J^0_{em}(\vec{x}), J^\lambda_W(\vec{0})]_{\text{ETC}}|p_i\rangle \end{aligned} \tag{2.2.4}$$

The first term gives zero by ordinary current conservation. However, the second term is not zero! In order to calculate it, we need the equal time commutator of the currents.

$$[J^0_{em}(\vec{x}), J^\lambda_W(\vec{y})]_{\text{ETC}} = \delta^3(\vec{x}-\vec{y})J^\lambda_W(\vec{x}) \tag{2.2.5}$$

Lets think about why this makes sense. The weak current changes a neutron into a proton, and raises the charge by 1. If we integrate over d^3x, then this says that the total charge changes by +1 which is what we expect. Therefore, we find

$$k_\mu T^{\mu\lambda}(p_f, p_i, k) = \langle p_i|J^\lambda_W(0)|p_i\rangle \tag{2.2.6}$$

Note that this is proportional to the tree level nuclear matrix element. This confirms what we already found in Equation 2.1.20. This appears to violate gauge invariance, but if all of the various loop diagrams are added together terms proportional to the photon momentum $D_{\mu\nu}(k) \to k_\mu k_\nu$ all cancel [Abe+68].

For the second term, we can play the same game. However, the axial-vector current is not conserved. We pick up an additional term from the divergence of the axial-vector current.

$$M^{\mu}(p_f, p_i, k) = \int d^4x\, e^{ikx}\, \langle p_f | T J^{\mu}_{em}(x) D(0) | p_i \rangle \tag{2.2.7}$$

Where $D(x) = \partial \cdot A(x)$. We also need to use translation invariance to rewrite Equation 2.1.4 as

$$T^{\mu\lambda}(p_f, p_i, k) = -i \int d^4x\, e^{-i(k+p_f-p_i)x}\, \langle p_f | T J^{\mu}_{em}(0) J^{\lambda}_{W}(x) | p_i \rangle \tag{2.2.8}$$

Playing the same game then, we find

$$(k + p_f - p_i)_{\lambda} T^{\mu\lambda}(p_i, p_f, k) = \langle p_f | J^{\mu}_{W}(0) | p_i \rangle + M^{\mu}(p_f, p_i, k) \tag{2.2.9}$$

The remaining two terms which involve $\eta_{\mu\lambda} T^{\mu\lambda}$ and $\varepsilon_{\mu\lambda\alpha\beta} k^{\alpha} T^{\lambda\mu}$ are not so straightforward to calculate. However, we can get at the high energy asymptotic behaviour using the method described in [Bjo66]. We can rewrite the time ordered product using the integral form of the theta function.

$$\theta(t) = \int \frac{dz}{2\pi} \frac{i}{z + i\epsilon} e^{-izt} \tag{2.2.10}$$

We can expand the time ordered product in integral form by introducing a dummy variable s.

$$\begin{aligned} T^{\mu\lambda}(p_f, p_i, k) = &\int \frac{ds}{2\pi} \frac{1}{s - k^0 + i\epsilon} \int d^4x e^{ist - i\vec{k}\cdot\vec{x}}\, \langle p_f | J^{\lambda}_{W}(0) J^{\mu}_{em}(x) | p_i \rangle \\ &+ \int \frac{ds}{2\pi} \frac{1}{-s + k^0 + i\epsilon} \int d^4x e^{ist - i\vec{k}\cdot\vec{x}}\, \langle p_f | J^{\mu}_{em}(x) J^{\lambda}_{W}(0) | p_i \rangle \end{aligned} \tag{2.2.11}$$

In the limit $k^0 \to \infty$, we can drop other terms in the denominators and then integrate over s to get delta function in time. The two terms combine into an equal-time commutator.

$$\lim_{k^0 \to \infty} T^{\mu\lambda}(p_f, p_i, k) = \frac{1}{k^0} \int d^3x e^{-i\vec{k}\cdot\vec{x}}\, \langle p_f | [J^{\mu}_{em}(\vec{x}), J^{\lambda}_{W}(\vec{0})]_{\mathrm{ETC}} | p_i \rangle \tag{2.2.12}$$

We need to plug in an explicit form of the currents. We express these in isospin space.

$$J^{\mu}_{em}(x) = \bar{\Psi} \gamma^{\mu} T^{Q} \Psi, \quad J^{\mu}_{W}(x) = \bar{\Psi} \gamma^{\mu} (1 - \gamma^5) T^{+} \Psi \tag{2.2.13}$$

Where T^Q gives the charge of the fermion, and T^+ is the usual isospin raising operator.

$$T^{Q} = \begin{pmatrix} Q_+ & 0 \\ 0 & Q_- \end{pmatrix}, \quad T^{+} = \begin{pmatrix} 0 & 1 \\ 0 & 0 \end{pmatrix} \tag{2.2.14}$$

Separating out the vector and axial-vector parts of the current, the commutation relations for the currents are

$$\begin{aligned} [J^{\mu}_{em}(\vec{x}), V^{\lambda}(\vec{y})]_{\mathrm{ETC}} = &Q_+ \delta^3(\vec{x} - \vec{y}) \bar{\Psi} \gamma^{\mu} \gamma^0 \gamma^{\lambda} T^{+} \Psi \\ &- Q_- \delta^3(\vec{x} - \vec{y}) \bar{\Psi} \gamma^{\lambda} \gamma^0 \gamma^{\mu} T^{+} \Psi \end{aligned} \tag{2.2.15}$$

and

$$\begin{aligned}[J^{\mu}_{em}(\vec{x}), A^{\lambda}(\vec{y})]_{\text{ETC}} = Q_{+}\delta^{3}(\vec{x}-\vec{y})\bar{\Psi}\gamma^{\mu}\gamma^{0}\gamma^{\lambda}\gamma^{5}T^{+}\Psi \\ -Q_{-}\delta^{3}(\vec{x}-\vec{y})\bar{\Psi}\gamma^{\lambda}\gamma^{0}\gamma^{\mu}\gamma^{5}T^{+}\Psi\end{aligned} \tag{2.2.16}$$

We can use these to directly calculate the contribution from the remaining terms. Using the ordinary gamma matrix contraction, we have

$$\begin{aligned}\eta_{\mu\lambda}[J^{\mu}_{em}(\vec{x}), V^{\lambda}(\vec{y})]_{\text{ETC}} = -2\delta^{3}(\vec{x}-\vec{y})(Q_{+}-Q_{-})V^{0}(\vec{x}) \\ \eta_{\mu\lambda}[J^{\mu}_{em}(\vec{x}), A^{\lambda}(\vec{y})]_{\text{ETC}} = -2\delta^{3}(\vec{x}-\vec{y})(Q_{+}-Q_{-})A^{0}(\vec{x})\end{aligned} \tag{2.2.17}$$

Where $Q_{+}-Q_{-}=1$, independent of the model. Plugging this in, we have

$$\lim_{k^{0}\to\infty}\eta_{\mu\lambda}T^{\mu\lambda}(p_f,p_i,k) = -2\frac{1}{k^{0}}\langle p_f|J^{0}_{W}(0)|p_i\rangle \tag{2.2.18}$$

Put this in a covariant form using any form which has the same asymptotic behaviour. Following [Abe+68] we take

$$\lim_{k^{2}\to\infty}\eta_{\mu\lambda}T^{\mu\lambda}(p_f,p_i,k) = -2\frac{k_{\lambda}\langle p_f|J^{\lambda}_{W}(0)|p_i\rangle}{k^{2}+2p_f\cdot k+i\epsilon} \tag{2.2.19}$$

Lastly, we have the term which involves the anti-symmetric Levi-Civita tensor. We make use of the following identity, which can be easily checked.

$$\varepsilon^{\mu\nu\alpha\beta}\gamma_{\alpha}\gamma_{0}\gamma_{\beta} = 2i(\delta^{\mu}_{0}\delta^{\nu}_{\rho}-\delta^{\nu}_{0}\delta^{\mu}_{\rho})\gamma^{\rho}\gamma^{5} \tag{2.2.20}$$

Note that the order of the indices are flipped in the second term of Equation 2.2.15. This picks up a minus sign which cancels the original minus sign from the commutator. Instead of getting $(Q_{+}-Q_{-})$, we get the sum $(Q_{+}+Q_{-})$ which is model dependent. The presence of the γ^{5} also changes the vector current into the axial current, and vice versa.

$$\begin{aligned}\varepsilon_{\mu\lambda\alpha\beta}[J^{\mu}_{em}(\vec{x}), V^{\lambda}(\vec{y})]_{\text{ETC}} = 4i\bar{Q}(\delta^{0}_{\alpha}\delta^{\kappa}_{\beta}-\delta^{0}_{\beta}\delta^{\kappa}_{\alpha})\delta^{3}(\vec{x}-\vec{y})A_{\kappa}(\vec{x}) \\ \varepsilon_{\mu\lambda\alpha\beta}[J^{\mu}_{em}(\vec{x}), A^{\lambda}(\vec{y})]_{\text{ETC}} = 4i\bar{Q}(\delta^{0}_{\alpha}\delta^{\kappa}_{\beta}-\delta^{0}_{\beta}\delta^{\kappa}_{\alpha})\delta^{3}(\vec{x}-\vec{y})V_{\kappa}(\vec{x})\end{aligned} \tag{2.2.21}$$

If we want to compute the corrections to the Fermi matrix element (the vector operator), this term gives involves the axial-vector current. Conversely, if we want to compute the corrections to the Gamow-Teller matrix element, this term would give us a correction involving the vector current. This fact will be very important for the rest of the thesis.

Plugging this in to our asymptotic formula, we have

$$\lim_{k^{0}\to\infty}\varepsilon_{\mu\lambda\alpha\beta}k^{\alpha}T^{\mu\lambda}(p_f,p_i,k) = -i4\bar{Q}[\eta_{\alpha\beta}-\delta^{0}_{\beta}\delta^{0}_{\alpha}]\langle p_f|J^{\alpha}_{W}(0)|p_i\rangle \tag{2.2.22}$$

Again we can put this into a covariant form by matching the asymptotic form. However, the presence of the $\bar{Q}$ makes this more complicated. At low momentum transfer, the degrees of

freedom are the nucleons with $\bar{Q} = 1/2$. At high energy, this changes to the quark degrees of freedom with $\bar{Q} = 1/6$. This implies the existence of a cross-over point - an energy scale at which this asymptotic regime takes over. The asymptotic form we take involves this new mass scale.

$$\lim_{k^2\to\infty} \varepsilon_{\mu\lambda\alpha\beta} k^\alpha T^{\mu\lambda}(p_f, p_i, k) = -i4\bar{Q}\frac{k^2}{k^2 - M_A^2}\left(\eta_{\alpha\beta} - \frac{k_\beta k_\alpha}{k^2}\right) J_W^\alpha(0) \tag{2.2.23}$$

In [Abe+68], they make an argument that this pole is related to the A_1 vector meson with $M_A \sim 1.2$ GeV.

Putting all of these terms together, we can pick out the divergent term just as we did in Section 2. The result is

$$\mathcal{M}_{\text{box}}\Big|_{\text{divergent}} = \mathcal{M}_0 \frac{\alpha}{2\pi}\left(\frac{5}{2} + 3\bar{Q}\right)\frac{1}{2}\log\left(\frac{\Lambda^2}{M^2}\right) \tag{2.2.24}$$

In [Abe+68] they continue this line of reasoning and include the term where the photon only attaches to the hadron line and the wavefunction renormalization. Without going through those details, it turns out the answer is the same as we found from the wavefunction correction in Equation 2.0.25. Therefore we confirm naive result we found in 2.0.27.

$$\mathcal{M}_{\text{loop}} + \mathcal{M}_{\text{ct}}\Big|_{\text{divergent}} = \mathcal{M}_0 \frac{\alpha}{2\pi}\frac{3}{4}\left(1 + 2\bar{Q}\right)\log\left(\frac{\Lambda^2}{M^2}\right) \tag{2.2.25}$$

Going beyond the local four Fermion theory, we know from the standard model that the weak interaction vertex is mediated by the W-boson. We can replace the photon propagators with

$$\frac{1}{k^2} \to \frac{1}{k^2}\frac{M_W^2}{M_W^2 - k^2} \tag{2.2.26}$$

Here we ignore the overall momentum transfer $p_f - p_i$, which is much smaller than M_W. This sets a natural cut-off at $\Lambda = M_W$.

The contribution from the vector part of the box diagram is independent of the dynamics of the strong interactions. On the other hand, the contribution induced by the axial current Equation 2.2.23 is model dependent. In the asymptotic regime, it is proportional to $\bar{Q}$.

$$\mathcal{M}_A^{\text{box}} = \mathcal{M}_0 \frac{\alpha}{2\pi}\left[\frac{3}{2}\bar{Q}\log\left(\frac{M_W^2}{M_A^2}\right) + C\right] \tag{2.2.27}$$

Here M_A is the scale at which the asymptotic regime Equation 2.2.23 takes over, and C is the remaining non-asymptotic contribution [Sir78].

In [Sir78], they also calculate the contribution from Z-boson exchanges. This gives

$$\mathcal{M}_{(Z)}^{\text{box}} = \mathcal{M}_0 \frac{\alpha}{4\pi}\left(\frac{R}{R-1}\right)\log R\left[3/2\cot^2\theta_W + 3\bar{Q}\tan^2\theta_W\right] \tag{2.2.28}$$

Where $R = M_W^2/M_Z^2$. The first term is shared in common with the muon decay, and gets absorbed into the renormalization of G_F. On the other hand, the term proportional to $\bar{Q}$ is different and must be accounted for.

We can now compare the radiative corrections for muon decay to that of superallowed fermi decay [Sir78].

$$\frac{1}{\tau_\mu} = \frac{\hat{G}_\mu m_\mu^5}{192\pi^3}\left[1 - \frac{8m_e^2}{m_\mu^2}\right] \times \left(1 + \frac{3}{5}\frac{m_\mu^2}{M_W^2} + \frac{\alpha}{2\pi}\left[\frac{25}{4} - \pi^2 - \frac{3}{2}\tan^2\theta_W \frac{R}{R-1}\log R + \dots\right]\right) \tag{2.2.29}$$

$$\begin{aligned} Pd^3p_e = \hat{P}_0 d^3p_e \Bigg(1 + \frac{\alpha}{2\pi}\Bigg[&3\log\frac{M_W}{M_p} + g(E, E_m) + 6\bar{Q}\log\frac{M_W}{M_A} + 2C \\ &+ 3\bar{Q}\tan^2\theta_W \frac{R}{R-1}\log R + \mathcal{A}_g + \dots\Bigg]\Bigg) \end{aligned} \tag{2.2.30}$$

We can now absorb the terms associated with field renormalization of W and the Z exchange graphs into the definition of G_μ

$$G_\mu = \hat{G}_\mu\left[1 - \frac{3\alpha}{8\pi}\tan^2\theta_W \frac{R}{R-1}\log R + \dots\right] \tag{2.2.31}$$

In terms of this renormalized Fermi coefficient, we have

$$\frac{1}{\tau_\mu} = \frac{G_\mu m_\mu^5}{192\pi^3}\left[1 - \frac{8m_e^2}{m_\mu^2}\right] \times \left(1 + \frac{3}{5}\frac{m_\mu^2}{M_W^2} + \frac{\alpha}{2\pi}\left[\frac{25}{4} - \pi^2\right]\right) \tag{2.2.32}$$

and

$$Pd^3p_e = P_0 d^3p_e\left(1 + \frac{\alpha}{2\pi}\left[3\log\frac{M_Z}{M_p} + g(E, E_m) + 6\bar{Q}\log\frac{M_Z}{M_A} + 2C + \mathcal{A}_g\right]\right) \tag{2.2.33}$$

Where we used $R/(R-1)\tan^2\theta_W = -1$. Note that $\bar{Q}$ comes from the quark model, so $\bar{Q} = 1/6$ in this case. It is common to swap out the M_Z for an M_p. We also separate out the part of the radiative correction which depends on the electron energy.

$$Pd^3p_e = P_0 d^3p_e\left[1 + \frac{\alpha}{2\pi}g(E, E_m)\right]\left(1 + \frac{\alpha}{2\pi}\left[4\log\frac{M_Z}{M_p} + \log\frac{M_p}{M_A} + 2C + \mathcal{A}_g\right]\right) \tag{2.2.34}$$

The first bracket is Sirlin's outer correction Equation 2.1.25, and the second term in parenthesis is the inner correction - now rendered finite.

Chapter 3

Precision in Weak Nuclear Processes

If we want to compute the rate of a weak nuclear process, we need to take the weak currents 1.2.33 and 1.2.34 and evaluate them in a particular nucleus. This involves a nuclear matrix element, which depends on our model of the nucleus. The uncertainty of the nuclear matrix element typically dominates the theoretical error budget. One might then wonder why we should worry about $\mathcal{O}(\alpha)$ radiative corrections.

As we have seen in section 1.3, there are cases where the nuclear model dependence mostly goes away. In particular, for superallowed Fermi beta decay, the nuclear matrix element is fixed by isospin symmetry. Without radiative corrections, we found a value of V_{ud} which was inconsistent with CKM unitarity. In section 3.1, we will see how this issue is resolved by including radiative corrections.

When we deal with a Gamow-Teller interaction, then we also have the issue of uncertainties associated with the nucleon axial form factor g_A in Equation 1.2.57. However, recent measurements in in the Perkeo III experiment have greatly reduced the uncertainty here [Mär+19]. The nuclear matrix element for a GT transition is no longer fixed by symmetry, so in general that uncertainty will dominate. However, we can consider simple nuclear systems such as free neutron decay. Another example where precision is important is in *pp*-fusion in the core of the sun, which will be discussed in Section 3.3.

3.1 Superallowed Fermi β-Decay and CKM Unitarity

As we discussed in section 1.3, the ft values for superallowed beta decay give a value of V_{ud} which is inconsistent with CKM unitarity. We now want to investigate how this picture is modified by radiative corrections.

We want to be able to compare all of the various decays, for example those given in Table 1.1 or those listed in [HT15]. It is helpful to modify Sirlin's original inner/outer correction to separate out the correction which is independent of the particular nucleus we are interested in. In particular, we modify Equation 2.2.34 by separating the low energy term C into a

universal Born term and a nuclear structure dependent term.

$$C = C_{\text{Born}} + C_{\text{NS}} \tag{3.1.1}$$

The Born term is readily calculated by the formula Equation 4.1.24. Most of the uncertainty comes from evaluating the nucleon form factors as a function of momentum transfer.

We can write the corrected decay rate Γ_β in terms of the uncorrected rate decay rate Γ^0_β.

$$\Gamma_\beta = \Gamma^0_\beta(1+\delta_R)(1+\Delta^V_R) \tag{3.1.2}$$

From Section 1.3, we know the uncorrected decay rate is

$$\Gamma^0_\beta = \frac{G_V^2|M_F|^2 m_e^5}{2\pi^3} f(Z, W_0) \tag{3.1.3}$$

The Fermi matrix for a superallowed Fermi transition with isospin $T = 1$ is equal to 2, with a correction factor for isospin symmetry breaking corrections.

$$|M_F|^2 = 2(1-\delta_C) \tag{3.1.4}$$

The statistical rate function $f(Z, W_0)$ includes the fermi function, and effects due to finite nuclear size and electron screening.

$$f(Z, W_0) = \int_0^{W_0} F(Z, W) W (W_0 - W)^2 \sqrt{W^2 - 1} dW \tag{3.1.5}$$

The part of the radiative correction which depends on the nucleus is given by

$$\delta_R = \frac{\alpha}{2\pi}[\bar{g}(E_m) + \delta_2 + \delta_3 + \delta_{\text{NS}}] \tag{3.1.6}$$

Here $\bar{g}$ is Sirlin's g-function Equation 2.1.25 integrated over the final beta spectrum. The terms δ_2 and δ_3 account for the leading $\mathcal{O}(Z\alpha^2)$ and $\mathcal{O}(Z^2\alpha^3)$ effects where the electron is able to interact with the coulomb field of the nucleus [JR87]. And finally δ_{NS} is the nuclear structure dependent part of the low-energy axial-vector box diagram.

$$\delta_{\text{NS}} = \frac{\alpha}{\pi} C_{\text{NS}} \tag{3.1.7}$$

The nucleus-independent part of the radiative correction is given by the second term in Equation 2.2.34 with C replaced by C_{Born}.

$$\Delta^V_R = \frac{\alpha}{2\pi}\left[4\log\frac{M_Z}{M_p} + \log\frac{M_p}{M_A} + 2C_{\text{Born}} + \mathcal{A}_g\right] \tag{3.1.8}$$

The last term $\mathcal{A}_g$ is a small correction from perturbative QCD, which was evaluated in [MS86].

Putting this together, we can again write the decay rate in terms of the ft value Equation 1.3.15. Recall that the CVC hypothesis, combined with the allowed approximation and isospin symmetry implies

$$ft = \frac{K}{G_V^2 |M_F|^2} = \text{const} \tag{3.1.9}$$

independent of the nucleus. The constant $K = 2\pi^3 \log(2)/m_e^5$ is a combination of physical constants. Now we can include all of the various corrections to this expression.

$$ft(1+\delta_R)(1+\Delta_R^V) = \frac{K}{2G_V^2(1-\delta_C)} \tag{3.1.10}$$

Following Towner and Hardy [TH02][HT15] we do one final reorganization and define a corrected $\mathcal{F}t$ value which should be the same for all superallowed transitions.

$$\mathcal{F}t \equiv ft(1+\delta_R')(1+\delta_{\rm NS}-\delta_C) = \frac{K}{2G_V^2(1+\Delta_R^V)} \tag{3.1.11}$$

We have chosen to group together the terms which depend on nuclear structure $\delta_{\rm NS} - \delta_C$ and define δ_R' without the inner correction $\delta_{\rm NS}$.

Now we want to analyze the effect this has CKM unitarity. We need to pay particular attention to the uncertainties associated with the various terms. The statistical rate function f has a very strong dependence on the maximum electron energy W_0, going like $f \sim W_0^5$. The total energy released in the decay must be measured very precisely in order to keep the experimental errors down.

The universal correction Δ_R^V was calculated in [MS06], where they chose a lower cut-off for the asymptotic regime to be $M_A = 1.2$ GeV, which is allowed to vary by a factor of two in each direction. This gave the dominant uncertainty in their calculation. The Born term $C_{\rm Born}$ depends on the nucleon form factors $F_A(Q^2)$ and $G_M(Q^2)$, and was calculated to be $C_{\rm Born} = 0.829$ (other calculations give a larger value [SGR19]). The perterbative QCD contribution is very small, calculated at $\mathcal{A}_g = -0.34$. Putting this together, [HT15] cite a value of

$$\Delta_R^V = 2.361 \pm 0.038\% \tag{3.1.12}$$

In Table 3.1, we show the nucleus dependent corrections from [HT15]. Altogether, they quote an average value of

$$\overline{\mathcal{F}t} = 3072.27(62) \tag{3.1.13}$$

The amount of uncertainty coming from each term depends on the nucleus in question. The experimental uncertainty in the uncorrected ft value differs greatly between the various decays. This comes from measuring the total energy released in the decay, the partial half-life, and the branching ratio. The largest theory contribution to the error come from the nuclear structure dependent corrections δ_C and $\delta_{\rm NS}$, which both depend on the details of the nuclear model. Very little uncertainty comes from the outer correction, δ_R'.

Decay	ft (s)	$\delta'_R(\%)$	$\delta_C - \delta_{\rm NS}(\%)$	$\mathcal{F}t$ (s)
$^{10}\mathrm{C} \to {}^{10}\mathrm{B}$	3043.0 ± 4.3	1.679	0.52 ± 0.039	3078.0 ± 4.5
$^{14}\mathrm{O} \to {}^{14}\mathrm{N}$	3042.2 ± 2.7	1.543	0.575 ± 0.056	3071.4 ± 3.2
$^{22}\mathrm{Mg} \to {}^{22}\mathrm{Na}$	3051.9 ± 7.2	1.466	0.605 ± 0.030	3077.9 ± 7.3
$^{26m}\mathrm{Al} \to {}^{26}\mathrm{Mg}$	3037.38 ± 0.58	1.478	0.305 ± 0.027	3072.9 ± 1.0
$^{34}\mathrm{Cl} \to {}^{34}\mathrm{S}$	$3049.43^{+0.88}_{-0.95}$	1.443	0.735 ± 0.048	$3070.7^{+1.7}_{-1.8}$
$^{38m}\mathrm{K} \to {}^{38}\mathrm{Ar}$	3051.45 ± 0.92	1.440	0.770 ± 0.056	3071.6 ± 2.0
$^{42}\mathrm{Sc} \to {}^{42}\mathrm{Ca}$	3047.5 ± 1.4	1.453	0.630 ± 0.059	3072.4 ± 2.3
$^{46}\mathrm{V} \to {}^{46}\mathrm{Ti}$	$3050.32^{+0.44}_{-0.46}$	1.445	0.655 ± 0.063	3074.1 ± 2.0
$^{54}\mathrm{Co} \to {}^{54}\mathrm{Fe}$	$3050.7^{+1.1}_{-1.5}$	1.443	0.805 ± 0.068	$3069.8^{+2.4}_{-2.6}$
$^{62}\mathrm{Ga} \to {}^{62}\mathrm{Zn}$	3074.0 ± 1.5	1.459	1.52 ± 0.21	3071.5 ± 6.7
$^{74}\mathrm{Rb} \to {}^{74}\mathrm{Kr}$	3082.7 ± 6.5	1.50	1.69 ± 0.27	3076 ± 11

Table 3.1: Corrected $\mathcal{F}t$ values including radiative and isospin breaking corrections [HT15]

Combining this with a very precise measurement of G_F from muon decay, Towner and Hardy cite a value for V_{ud} of [HT15]

$$|V_{ud}| = 0.974\,17(21) \tag{3.1.14}$$

The value of V_{us} can be measured in leptonic, and semi-leptonic decays. These involve calculating the kaon form factor in lattice QCD. The PDG average is $|V_{us}| = 0.2248(6)$ [Pat+16]. The last term we need is $|V_{ub}| = 4.09(39) \times 10^{-3}$, but this is much smaller than the uncertainty in top row unitarity and has very little effect. With these values, CKM unitarity is restored within the error bars [HT15].

$$|V_{ud}|^2 + |V_{us}|^2 + |V_{ub}|^2 = 0.999\,78(55) \tag{3.1.15}$$

The dominant uncertainty in V_{ud} comes from the $W\gamma$-axial vector box term in Δ_R^V. As the experimental uncertainty gets smaller, and lattice calculations of the kaon form factors improve, it will become more even more important to understand the radiative corrections.

3.2 Free Neutron Decay and Corrections to g_A

As we discussed in Section 1.2, the weak current in nucleons gets modified by the nucleon form factors. At low momentum transfer, the vector current is unaffected due to CVC. However, the axial current gets a large correction. This means we need to modify our simple $V - A$ current for nucleons according to Equation and 1.2.57.

$$V^\lambda - A^\lambda = \bar{\psi}_p \gamma^\lambda (1 - g_A \gamma^5) \psi_n \tag{3.2.1}$$

Where g_A would be equal to 1 if the axial $SU(2)_A$ symmetry was not spontaneously broken by the strong interactions.

In the last section, we explained how measurement of superallowed Fermi β-decay gives the most precise determination of V_{ud}, since it only depends on the vector current which is conserved by the strong interactions. However, one might also want to look at a much more simple process - free neutron decay. The lifetime of the neutron can be written as

$$\frac{1}{\tau_n} = \frac{G_F^2 |V_{ud}|^2}{2\pi^3} m_e^5 (1 + 3g_A^2)(1 + \delta_R)(1 + \Delta_R^V) f \tag{3.2.2}$$

Where $f = 1.6887(1)$ is a phase space factor which includes a relatively large enhancement from the Fermi function [CMS19]. The radiative corrections are the same as those in superallowed Fermi beta decay we discussed in Section 3.1.

This expression only involves the inner radiative correction to the vector current Δ_R^V because g_A is measured in neutron decay. In particular, g_A is measured by looking at the asymmetry parameter, A, which is the difference between the number of electrons emitted parallel to the neutron spin minus the number emitted in the anti-parallel direction.

$$A = \frac{N^\uparrow - N^\downarrow}{N^\uparrow + N^\downarrow} \tag{3.2.3}$$

If parity were conserved in the weak interactions, this would come out to be exactly zero. Instead, we find (up to 1% corrections)

$$A = -2\frac{g_A(g_A - 1)}{(1 + 3g_A^2)} \tag{3.2.4}$$

Note that the asymmetry parameter is independent of V_{ud}, so we can use the asymmetry parameter to calculate g_A without using inputs from superallowed β-decay.

In principal, these measurements of g_A should be compared with calculations from lattice QCD. At the present moment, these calculations face a lot of challenges and it is not known exactly how to handle systematic uncertainties. Despite this, the field has seen much improvement. In [Wal+20], they cite a 1% uncertainty in the pure QCD evaluation of g_A.

When we compare the measured value of g_A to the pure QCD value g_A^{QCD} we need to account for the electromagnetic radiative corrections. Since Δ_R^V was included in the measured value, it needs to be subtracted out and Δ_R^A needs to be added in. Thus the discrepancy between the measured value and the QCD value is the difference between the two. [Hay21]

$$g_A^{\text{eff}} = g_A^{\text{QCD}} \left[1 + \frac{1}{2}(\Delta_R^A - \Delta_R^V) + \delta_{\text{BSM}}\right] \tag{3.2.5}$$

Where δ_{BSM} are potential contributions from new physics beyond the standard model. The difference between the vector and axial-vector radiative corrections mimic the effect of BSM right handed currents. If one wants to use the lattice calculation of g_A^{QCD} to search for BSM physics, it is important to take these radiative corrections into account.

Historically, this measurement has not been nearly as precise as that of superallowed Fermi beta decay. Over the years, measurements of the neutron lifetime - and thus also g_A

- have shifted significantly. This is best exemplified in Figure 1 of [Gro+22]. The accepted value for the neutron lifetime τ_n decreased over time since the 1960s

$$\tau_n = 1010 \text{ s} \rightarrow 925 \text{ s} \rightarrow 900 \text{ s} \rightarrow 879 \text{ s} \tag{3.2.6}$$

and now sits at $\tau_n = 879$ seconds. Similarly, the accepted value of g_A has increased from

$$g_A = 1.2 \rightarrow 1.23 \rightarrow 1.25 \rightarrow 1.27 \tag{3.2.7}$$

The measurement of the neutron lifetime remains a tricky subject experimentally. There is disagreement between measurements of the lifetime using neutron beams, and the lifetime measured from trapped neutrons - so called "bottle" measurements. An overview of the different experimental techniques is summarized in [Pau09]. Although the bottle techniques cite a much smaller uncertainty, it is suspected that there may still be systematic issues with those measurements. The origin of the discrepancy remains unknown. The current accepted PDG value for g_A is [Gro+22]

$$\begin{aligned} \tau_n &= 879.4(6)\text{s} \\ g_A &= 1.2756(13) \quad \text{PDG average} \end{aligned} \tag{3.2.8}$$

More recently, neutron lifetime and asymmetry measurements have been performed by the new PERKEO III spectrometer [Mär+19]. The experiment involves a large solenoid, with one "downstream detector" and one "upstream detector" which detect electrons emitted parallel and anti-parallel to the neutron beam direction, respectively. This experiment uses a beam of cold, polarized neutrons are pulsed by a "chopper" rotating at 6000 rpm. The advantage of the pulsed beam is that it allows for the control of beam related background, edge effects, and the magnetic mirror effect. The magnetic mirror effect occurs when electrons are reflected by an increasing magnetic field, and depends on the details of the spatial profile of the magnetic field. The experiment was able to claim a 0.04% uncertainty in g_A.

$$g_A = 1.27641(56) \quad \text{PERKEO III} \tag{3.2.9}$$

Having a more precise measurement of g_A opens the door to studying processes mediated by the axial current to much higher precision. In the near future, it is possible that the neutron lifetime measurement can become competitive with superallowed Fermi β-decay in determining V_{ud} [SGR19]. This warrants more accurate theoretical calculations, including the radiative corrections.

3.3 Applications to Solar Physics

Radiative corrections have also proved important to solar physics through the determination of the proton-proton fusion cross section [Ade+11]. Being the first reaction in the *pp*-chain, is has wide reaching implications for solar models. The *pp*-fusion cross section cannot be

measured experimentally in a terrestrial laboratory, so we must rely on theoretical calculations.

About 98.4% of the suns photon luminosity comes from the *pp*-chain, with about 1.6% coming from the CNO cycle [BU88]. In the *pp*-chain, hydrogen is burned to form helium-4.

$$4p \rightarrow {}^4\mathrm{He} + 2e^+ + 2\nu_e \tag{3.3.1}$$

In the dominant branch of the *pp*-chain, called the ppI-cycle, two *pp*-fusion reactions produce two ^{3}He nuclei which themselves fuse to form ^{4}He. The ^{3}He burns rather quickly, but the initial *pp*-fusion reaction is very slow. The *pp*-fusion reaction effectively acts as a bottle-neck for the remainder of the *pp*-chain. To first approximation, the rate of energy production in the Sun is determined by the rate of *pp*-fusion.

In the ppI-cycle, every two *pp*-fusion reactions releases an amount of energy approximately equal to

$$4M(^1\mathrm{H}) - M(^4\mathrm{He}) - 2\langle E_\nu \rangle_{pp} = 26.6 \text{ MeV} \tag{3.3.2}$$

The average energy released to neutrinos is $\langle E_\nu \rangle_{pp} \approx 0.26$ MeV, which does not contribute to the photon luminosity. The reaction rate is determined by the number density of Hydrogen in the core, multiplied by the thermal cross section.

$$\frac{\text{Rate}}{\text{Volume}} = \frac{n_{\mathrm{H}}^2}{2}\langle \sigma v \rangle_{pp} \tag{3.3.3}$$

In the context of solar fusion, the thermal cross-section is typically re-expressed in terms of the so-called "astrophysical S-factor", S_{11}. The reaction rate depends on the composition and temperature profile in the core of the sun. This requires performing a hydrodynamic simulation of all of the physics happening inside the Sun. To a first approximation, we can relate the thermal cross section to the solar luminosity as follows.

$$L_\odot \sim \frac{1}{2}(26.2 \text{ MeV}) \times (\text{Rate of } pp\text{-fusion}) \tag{3.3.4}$$

This relationship is what Bethe and Critchfield used to demonstrate that proton-proton fusion is able to generate enough energy to power the sun [BC38].

Every *pp*-fusion reaction which takes place produces a so-called *pp*-neutrino. Therefore we can use the neutrino flux Φ_{pp} as a proxy for the reaction rate.

$$(\text{Rate of } pp\text{-fusion}) = 4\pi(\mathrm{AU})^2\Phi_{pp} \tag{3.3.5}$$

Assuming only the ppI-cycle takes place, we can use Equation 3.3.4 to relate the luminosity to the flux of *pp*-neutrinos.

$$\frac{L_\odot}{4\pi(\mathrm{AU})^2} \approx \frac{1}{2}(26.2 \text{ MeV})\Phi_{pp} \quad \text{ppI only} \tag{3.3.6}$$

This simple argument gets the *pp*-neutrino flux correct within 6%.

More generally, we can consider all reactions in the sun which produce neutrinos. Let Φ_i be the flux of neutrinos originating from the i-th reaction in the sun. Then we can relate the neutrino fluxes to the solar luminosity.

$$\frac{L_\odot}{4\pi(\text{AU})^2} = \sum_i \alpha_i \Phi_i \tag{3.3.7}$$

The neutrino fluxes are just a proxy for the reaction rates, this is actually conservation of energy. If we want to be more precise, we can also include non-equilibrium effects and other sources of energy loss. [Ves+20]

Measuring the mean solar luminosity is not so straightforward because of solar variability on different time scales. These days it is measured by special instruments on satellites, which collect sunlight and measure the thermal energy generated. According to the IAU 2015, the mean solar luminosity has an uncertainty of less than 0.05%. [Mam+15]

$$L_\odot = 3.8275(14) \times 10^{26} \text{ W} \tag{3.3.8}$$

In order to calculate the α_i in Equation 3.3.7, we need to use our knowledge of solar fusion reactions. In [SV90], they consider the three principal reactions of the pp-chain. We have ppI, which ends in the fusion of two ^{3}He nuclei. We can also have ^{3}He burn by combining with a ^{4}He nucleus to form ^{7}Be. In the ppII cycle, that beryllium nucleus electron captures to form ^{7}Li. In the ppIII cycle, it captures another proton to become ^{8}B, which then β^+-decays. Each of these contribute a different amount of energy to the photon luminosity.

$$\begin{aligned} \text{ppI}: &\ \nu_{pp} + \nu_{pp} + 26.2 \text{ MeV} \\ \text{ppII}: &\ \nu_{pp} + \nu_{\text{Be}} + 25.6 \text{ MeV} \\ \text{ppIII}: &\ \nu_{pp} + \nu_{\text{B}} + 19.7 \text{ MeV} \end{aligned} \tag{3.3.9}$$

We can determine the rates of the ppII and ppIII chains by measuring the flux of ^{7}Be and ^{8}B neutrinos, respectively. However, we cannot determine the rate of the ppI chain by simply measuring the *pp*-neutrinos. Each of these reactions produce at least one *pp*-neutrino. We can eliminate this double counting by subtracting off the rates of the ppII and ppIII reactions.

$$\begin{aligned} \frac{L_\odot}{4\pi(\text{AU})^2} = &\ 19.7 \text{ MeV}\Phi_{\text{B}} + 25.6 \text{ MeV}\Phi_{\text{Be}} \\ &+26.2 \text{ MeV}(\Phi_{pp} - \Phi_{\text{Be}} - \Phi_{\text{B}})/2 \end{aligned} \tag{3.3.10}$$

This argument can be extended to include all of the reactions which produce neutrinos, as is done in [Bah02] and more recently in [Ves+20]. Normalizing by the photon luminosity, and normalizing the fluxes by their order of magnitude, we can write the luminosity constraint as

$$\begin{aligned} 1 \pm 0.0004 = \frac{1}{8.5069\text{cm}^{-2}\text{s}^{-1}} \Bigg[&1.30987 \left(\frac{\Phi_{pp}}{10^{10}}\right) + 0.011921 \left(\frac{\Phi_{pep}}{10^8}\right) + 0.125525 \left(\frac{\Phi_{\text{Be}}}{10^9}\right) \\ &+0.000066 \left(\frac{\Phi_{\text{B}}}{10^6}\right) + 0.003457 \left(\frac{\Phi_{\text{N}}}{10^8}\right) + 0.02157 \left(\frac{\Phi_{\text{O}}}{10^8}\right) + 0.000024 \left(\frac{\Phi_{\text{F}}}{10^6}\right) \Bigg] \end{aligned} \tag{3.3.11}$$

The dominant contribution comes from *pp*-neutrinos which account for $92.2 \pm 0.5\%$ of the luminosity constraint. The ^{7}Be neutrinos are the next biggest contribution, at $7.4 \pm 0.1\%$. The ^{15}O neutrinos take up another 1.2%, followed by *pep* and ^{13}N neutrinos at about 0.2% each.

The ^{7}Be neutrino flux has recently been measured in Borexino phase-II with only 2% uncertainty. [Ago+19]

$$\Phi_{\mathrm{Be}} = 4.99 \pm 0.11^{+0.06}_{-0.08} \times 10^9 \mathrm{cm}^{-2}\mathrm{s}^{-1} \quad \text{Borexino} \tag{3.3.12}$$

The *pp*-neutrinos have so far only been measured at the 10% level. The theoretical value has been calculated using two different metalicities - so called high-Z and low-Z models. These give predictions for the *pp*-neutrino flux which differ by about 1%. [Vin+17]

$$\begin{aligned} \Phi_{pp} &= 5.98(1 \pm 0.006) \times 10^{10}\mathrm{cm}^{-2}\mathrm{s}^{-1} \quad \text{High-Z} \\ \Phi_{pp} &= 6.03(1 \pm 0.005) \times 10^{10}\mathrm{cm}^{-2}\mathrm{s}^{-1} \quad \text{Low-Z} \end{aligned} \tag{3.3.13}$$

In a more recent analysis by [Ves+20], they use some simple assumptions to fix the ratios of Φ_{pep}/Φ_{pp}, $\Phi_{\mathrm{O}}/\Phi_{\mathrm{N}}$, and $\Phi_{\mathrm{F}}/\Phi_{\mathrm{N}}$. Plugging in the Borexino measurement of Φ_{Be}, this leaves us with a direct relationship between Φ_{pp} and Φ_{N}.

$$\Phi_{pp} + 1.654\Phi_{\mathrm{N}} = 6.003(1 \pm 0.002) \times 10^{10}\mathrm{cm}^{-2}\mathrm{s}^{-1} \tag{3.3.14}$$

CNO neutrinos have just recently been observed for the first time at Borexino, which can then be used to fix Φ_{pp}.

$$\Phi_{pp} = 5.937^{+0.023}_{-0.032} \times 10^{10}\mathrm{cm}^{-2}\mathrm{s}^{-1} \quad \text{Luminosity Constraint} \tag{3.3.15}$$

Thus the luminosity constraint can be used to fix the flux of *pp*-neutrinos at the level of 0.5%. More accurate measurements of the CNO and ^{7}Be neutrino fluxes will reduce the uncertainty even further.

Being able to compare the *pp*-neutrino flux to the predictions of the solar model provides us with a precise test of our understanding of the sun. Recall that the luminosity constraint is really a statement about conservation of energy. If there is some new source of energy loss, for example the production of new light particles like axions, then that will show up as a violation of the luminosity constraint. At present, the *pp*-neutrinos have not been measured to high enough accuracy to test the luminosity constraint. This is why we must rely on accurate theoretical calculations of the cross sections to come up with the theoretical reaction rate.

The *pp*-fusion reaction is mediated by the axial vector weak current, due to the fact that it requires a spin-flip. Two protons in a relative $^1S_0$ state come together to form a deuteron in a mixed $^3S_1 - {}^3D_1$ state. The cross section can be written as [Sch+98]

$$\sigma_{pp}(E) = \frac{1}{(2\pi)^3} \frac{G_V^2 m_e^5}{v_{\mathrm{rel}}} f_R \sum_m |\, \langle d, m | \vec{A}_- | pp \rangle \,|^2 \tag{3.3.16}$$

where $\vec{A}_-$ is the axial-vector current which lower the charge by one unit. It is conventional to include the radiative corrections in the phase space function f_R, along with the coulomb corrections to the electron wavefunction.

The axial-vector current also includes two-body currents which are required to reproduce the GT matrix element in tritium β-decay. In [Sch+98], they argue that these two-body currents are relatively model-independent as long as the GT matrix element in tritium is reproduced. However, in [Ade+11] they argue that neglected three-body currents in tritium complicate the extraction of the two-body current. Nevertheless, they estimate that the uncertainty in the cross section is about one percent.

The radiative corrections were not calculated in [Sch+98], but they were estimated based off superallowed fermi beta decay. The outer radiative corrections to *pp*-fusion were examined in [KRV03], but the inner radiative corrections were again only estimated using a scaling argument based on superallowed fermi beta decay. In particular, one would like to know the nuclear structure dependent part $C_{\rm NS}$ which has not been calculated for this reaction. We will give the first calculation of this correction to my knowledge in Section 7.

Low Energy Neutrino Reactions

In [KRV03], they also investigate the outer radiative corrections to the inverse process - neutrino-deuteron disintegration. This is another two-nucleon process which is relevant to solar physics. In particular, it is used in the SNO experiment to measure neutrino oscillations.

Neutrinos coming to us from the sun which were originally produced in the ν_e flavour can "oscillate" into $\nu_{\mu,\tau}$ neutrinos. These effects could be enhanced by interactions with matter, such as in the sun. This is known as the Mikheyev-Smirnov-Wolfenstein (MSW) effect. If this is the case, then we should be able to detect ν_μ and ν_τ neutrinos on earth which account for the difference. These neutrinos cannot participate charge-changing reactions, but they can participate in neutral current reactions. The Sudbury Neutrino Observation (SNO) experiment set out to test this by using the following reactions [Poo02].

$$\begin{aligned} \nu_e + d &\to p + p + e^- \quad \text{(CC)} \\ \nu_x + d &\to n + p + \nu_x \quad \text{(NC)} \\ \nu_x + e^- &\to \nu_x + e^- \quad \text{(ES)} \end{aligned} \tag{3.3.17}$$

Here ν_x stands for any flavour of neutrino, and d is a deuterium nucleus - also known as heavy hydrogen or ^{2}H. If it is true that neutrinos in the Sun change flavour, then one expects to find $\Phi^{\rm CC}(\nu_e) < \Phi^{\rm ES}(\nu_x)$. This measurement is direct evidence for Solar neutrino oscillations.

The neutral current and charge current reactions involve different charged particles in the final state, so radiative corrections must be included to get an accurate comparison of the two fluxes. Initially, radiative corrections were not taken account in the cross section [Poo02]. The differences in the radiative corrections can shift the measured ratios of ν_x to ν_e, thus mimicking the effect of neutrino oscillations.

Chapter 4

One-Body Born Correction

In Section 2.2, we discussed how the anti-symmetric part of the box diagram is model dependent. In the asymptotic regime where the relevant degrees of freedom are quarks, it is governed by Equation 2.2.23 with $\bar{Q} = 1/6$. The low energy part of the box diagram below asymptotic regime we called C in Equation 2.2.27.

As we discussed in Section 3.1, it is convenient to subtract out the part of C which is independent of nuclear structure. In particular, we subtract out the *Born contribution*.

$$C = C_{\text{Born}} + C_{\text{NS}} \tag{4.0.1}$$

The Born contribution is calculated only for a single nucleon, keeping all relativistic corrections. In this section, we will calculate it in the case of both Fermi and Gamow-Teller transitions. In the following section, we will give some strategies on how one might try to compute the remaining term, C_{NS}, which will lead into the rest of the thesis.

We will want to compare the tree-level amplitude to the box diagram amplitude. This will let us pick out the correction C according to Equation 2.2.27. The tree level amplitude for beta decay Equation 1.3.2 can be written as

$$\mathcal{M}_{\text{tree}} = \frac{G_V}{\sqrt{2}} L_\lambda \langle f | J_W^\lambda | i \rangle \tag{4.0.2}$$

Where the lepton current is given by $L^\lambda = \bar{u}_e \gamma^\lambda (1-\gamma^5) v_\nu$ in the case of β^--decay. If we are instead dealing with β^+-decay, we would have $L^\lambda = \bar{u}_\nu \gamma^\lambda (1-\gamma^5) v_e$, but the results of this section are the same in either case.

The general box diagram was derived in Equation 2.1.3, using the generalized Compton tensor we defined in Equation 2.1.4.

$$\mathcal{M}_{\text{box}} = ie^2 \frac{G_V}{\sqrt{2}} \int \frac{d^4k}{(2\pi)^4} \frac{1}{(k^2 + i\epsilon)} \frac{[\bar{u}_e \gamma^\mu (\not{p}_e - \not{k} + m_e) \gamma^\lambda (1-\gamma^5) v_\nu]}{(p_e - k)^2 - m_e^2 + i\epsilon} T_{\mu\lambda}(p_f, p_i, k) \tag{4.0.3}$$

The low-energy correction C comes from the anti-symmetric part of the lepton tensor from Equation 2.2.2.

$$\bar{u}_e \gamma_\mu (\not{p}_e - \not{k} + m_e) \gamma^\lambda (1-\gamma^5) v_\nu \to -i\varepsilon^{\mu\lambda\alpha\beta} k_\alpha L_\beta \tag{4.0.4}$$

Plugging this in for the lepton covariant, the part of the box diagram we need to compute is given by

$$\mathcal{M}_{\text{box}} = e^2 \frac{G_V}{\sqrt{2}} L_\beta \int \frac{d^4k}{(2\pi)^4} \frac{1}{k^2 + i\epsilon} \frac{\varepsilon^{\mu\lambda\alpha\beta} k_\alpha}{k^2 - 2p_e \cdot k + i\epsilon} T_{\mu\lambda}(p_f, p_i, k) \tag{4.0.5}$$

This is the part of the box diagram which contributes to C in Equation 2.2.27. It is manifestly IR-finite. Using point nucleons it is UV-divergent, but this divergence is regulated by the nucleon form factors as we will discuss. Evaluating this expression will be the focus of the remainder of this thesis.

In order to match this onto the tree-level amplitude, we define an *effective hadronic current* for the box diagram as follows.

$$\mathcal{M}_{\text{box}} = \frac{\alpha}{2\pi} \frac{G_V}{\sqrt{2}} L_\beta \mathcal{J}^\beta \tag{4.0.6}$$

This allows us to factor out the constants like G_V and α, and the lepton tree-level matrix element. The effective hadronic current is then given by

$$\mathcal{J}^\beta = 8\pi^2 \int \frac{d^4k}{(2\pi)^4} \frac{1}{(k^2 + i\epsilon)} \frac{\varepsilon^{\mu\lambda\alpha\beta} k_\alpha}{(p_e - k)^2 - m_e^2 + i\epsilon} T_{\mu\lambda}(p_f, p_i, k) \tag{4.0.7}$$

Then, by comparing the tree-level amplitude to the box diagram amplitude, we can calculate C.

$$\mathcal{M}_{\text{box}} = \mathcal{M}_{\text{tree}} \times \frac{\alpha}{2\pi} C \tag{4.0.8}$$

We will now show how this works for both Fermi and Gamow-Teller transitions, as defined in Equation 1.3.5.

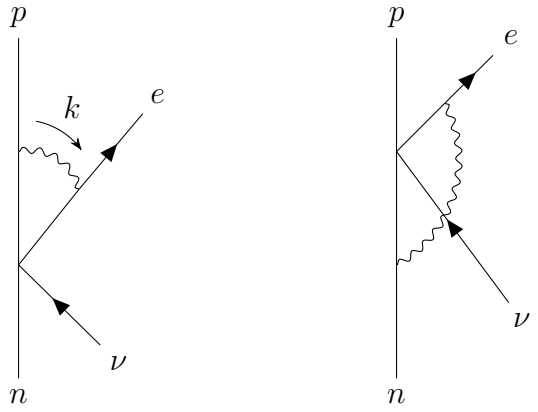

Figure 4.1: Feynman diagrams for the Born contribution C_{Born}.

In order to calculate the Born term C_{Born}, we want to replace the hadronic covariant $T^{\mu\lambda}$ in Equation 4.0.7 by single nucleon currents and propagators. This derivation closely follows what is presented in [Tow92]. In the single nucleon Born approximation, we suppose that the weak and electromagnetic currents latch onto the same nucleon. The Feynman diagram for this process is shown in Figure 4.1. We defined C_{Born} to be independent of nuclear structure, so we ignore the nucleon velocity in the nucleus. This is known in this context as the *static approximation*. Corrections to this are included in the *quasi-elastic* evaluation, which we discuss later.

The Born contribution can be evaluated from the single nucleon Feynman diagrams in Figure 4.1. We want this to be independent of any nuclear structure, so we simply use free-nucleon propagators and currents.

$$\begin{aligned} 2M_N T^{\mu\lambda}_{\text{Born}}(p,k) = &\frac{\bar{u}_p \Gamma^{(p)}_\mu(p,p+k)(\not{p}+\not{k}+M_N)W_\lambda(p+k,p)u_n}{(p+k)^2-M_N^2+i\epsilon} \\ &+\frac{\bar{u}_p W_\lambda(p,p-k)(\not{p}-\not{k}+M_N)\Gamma^{(n)}_\mu(p-k,p)u_n}{(p-k)^2-M_N^2+i\epsilon} \end{aligned} \tag{4.0.9}$$

We have to factor out the normalization of the spinors, $2M_N$. Remember that our nuclear states were normalized to 1.

By simply counting factor of loop momentum k, we see that the naive loop momentum integral is log divergent. However, we know that the description in terms of nucleons does not extent to all momentum transfers. At very high momentum transfer, we reach the perturbative QCD regime and a description in terms of quarks is more appropriate.

The natural way to enforce this momentum cut-off is through the nucleon form factors we defined in Equations 1.2.30 and 1.2.59. These go to zero at high momentum transfer, approximately following a dipole approximation.

$$G_D(Q^2) = \left(\frac{1}{1+Q^2/\Lambda^2}\right)^2 \tag{4.0.10}$$

where $Q^2 = -k^2$. The cut-off Λ is called the *dipole mass*. It can be related to the nucleon charge radius. A more data-driven approach to the nucleon form factors uses the *z-expansion*, which is discussed in Appendix A. We use these form factors to calculate the Born terms and uncertainties for Fermi and Gamow-Teller transitions.

4.1 Born Correction for Fermi Transitions

For a pure Fermi decay, we only use the Fermi operator in Equation 1.3.5. The matrix element of the Fermi operator is M_F. The amplitude only involves the time component of the lepton current.

$$\mathcal{M}_{\text{tree}} = \frac{G_V}{\sqrt{2}} L^0 M_F \tag{4.1.1}$$

Singling out the time component of the lepton current sets the index $\beta = 0$ in Equation 4.0.7. Invoking the static approximation, we also set $p_f = p_i = p$. We also ignore the external lepton momentum $p_e \to 0$. The effective hadronic current Equation 4.0.7 for the Fermi transition is

$$\mathcal{J}^0 = 8\pi^2 \int \frac{d^4k}{(2\pi)^4} \frac{1}{(k^2 + i\epsilon)^2} \epsilon^{ijk} k^k T^{ij}(p_f, p_i, k) \tag{4.1.2}$$

Then we divide by the tree level Fermi matrix element M_F to find the the correction term C^F.

$$C^F = \frac{\mathcal{J}^0}{M_F} \tag{4.1.3}$$

Here the superscript F reminds us this is the correction for Fermi transitions.

In the rest frame $p = (M_N, \vec{0})$, we can write this in a covariant form.

$$\mathcal{J}^0 = 8\pi^2 \int \frac{d^4k}{(2\pi)^4} \frac{1}{(k^2 + i\epsilon)^2} \frac{1}{M_N} \varepsilon^{\mu\lambda\alpha\beta} T_{\mu\lambda} k_\alpha p_\beta \tag{4.1.4}$$

Then we write the hadronic covariant for the nucleus in terms of the Born contribution for a single nucleon, Equation 4.0.9. The Fermi operator in Equation 1.3.5 gets modified by the same loop contribution for each nucleon in the sum.

$$T^{\mu\lambda}(p, k) = \sum_a \tau_a^+ T^{\mu\lambda}_{\text{Born}}(p, k) \tag{4.1.5}$$

The isospin raising operator gives us the tree level fermi nuclear matrix element. This cancels the fermi matrix element M_F in the denominator, leaving us with

$$C^F_{\text{Born}} = 8\pi^2 \int \frac{d^4k}{(2\pi)^4} \frac{1}{(k^2 + i\epsilon)^2} \frac{1}{M_N} \varepsilon_{\mu\lambda\alpha\beta} T^{\mu\lambda}_{\text{Born}} k^\alpha p^\beta \tag{4.1.6}$$

The vertex operators Γ and W in Equation 4.0.9 correspond to the electromagnetic and weak currents, respectively. In the case of the single-nucleon, these are given by Equations 1.2.30 and 1.2.59. The electromagnetic vertex for the proton is (keep in mind the momentum transfer at the electromagnetic interaction vertex is $-k$, not k)

$$\Gamma^\mu_{(p)}(p, p + k) \to \gamma^\mu F_1^{(p)} - i \frac{\sigma^{\mu\nu} k_\nu}{2M_N} F_2^{(p)} \tag{4.1.7}$$

And likewise for the neutron term. For the weak interaction vertex, Equation 2.2.21 tells us that we should pick out the axial-vector term.

$$W^\lambda(p + k, p) \to -\gamma^\lambda \gamma^5 F_A - \frac{k^\lambda}{M_N} \gamma^5 F_P \tag{4.1.8}$$

The pseudo-scalar term vanishes when it hits the Levi-Civita symbol in the box diagram, so we can ignore it. Any term which is symmetric under $\mu \leftrightarrow \lambda$ also vanishes. Any term proportional to p^μ, p^λ, k^μ and k^λ similarly vanish.

The rest is just straightforward Dirac algebra. For the F_1 term, use the same identity we used for the lepton part to combine the M_N and $\not{p}$ term. We can use a similar identity for the F_2 term. In total, we make the following simplifications for the Dirac matrices coming from the electromagnetic vertex Γ.

$$\begin{aligned}
\bar{u}_p\gamma^\mu(\not{p}+M_N) &= \bar{u}_p(2p^\mu) \\
\bar{u}_p\gamma^\mu\not{k} &= \bar{u}_p(k^\mu - i\sigma^{\mu\nu}k_\nu) \\
\bar{u}_p(i\sigma^{\mu\nu}k_\nu)(\not{p}+M_N) &= \bar{u}_p[2M_N(i\sigma^{\mu\nu}k_\nu) + 2p^\mu\not{k} - 2\gamma^\mu(p\cdot k)] \\
\bar{u}_p(i\sigma^{\mu\nu}k_\nu)\not{k} &= \bar{u}_p(\not{k}k^\mu - \gamma^\mu k^2)
\end{aligned} \tag{4.1.9}$$

Applying each of these simplifications gives us

$$\begin{aligned}
&\bar{u}_p\Gamma^\mu_{(p)}(p,p+k)(\not{p}+\not{k}+M_N) \\
&= \bar{u}_p\left[(F_1^{(p)}+F_2^{(p)})(-i\sigma^{\mu\nu}k_\nu) + \left(F_1^{(p)} - F_2^{(p)}\frac{\not{k}}{2M_N}\right)(2p^\mu+k^\mu) + F_2^{(p)}\frac{k^2+2p\cdot k}{2M_N}\gamma^\mu\right]
\end{aligned} \tag{4.1.10}$$

Similarly for the term where the photon attaches to the neutron line, we have

$$\begin{aligned}
&(\not{p}-\not{k}+M_N)\Gamma^\mu_{(n)}(p-k,p)u_n \\
&= \left[(F_1^{(n)}+F_2^{(n)})(-i\sigma^{\mu\nu}k_\nu) + \left(F_1^{(n)} + F_2^{(n)}\frac{\not{k}}{2M_N}\right)(2p^\mu-k^\mu) + F_2^{(n)}\frac{k^2-2p\cdot k}{2M_N}\gamma^\mu\right]u_n
\end{aligned} \tag{4.1.11}$$

Note that the second term vanishes against the Levi-Civita symbol. Keeping only the terms which don't vanish against the Levi-Civita symbol, we make the replacements

$$\begin{aligned}
(-i\sigma^{\mu\nu}k_\nu)\gamma^\lambda\gamma^5 &\to -i\varepsilon^{\mu\lambda\nu\rho}k_\nu\gamma_\rho \\
\gamma^\mu\gamma^\lambda\gamma^5 &\to -i\sigma^{\mu\lambda}\gamma^5
\end{aligned} \tag{4.1.12}$$

The terms which survive are

$$\begin{aligned}
&\bar{u}_p\Gamma^\mu_{(p)}(p,p+k)(\not{p}+\not{k}+M_N)W^\lambda(p+k,p)u_n \\
&= F_A(F_1^{(p)}+F_2^{(p)})\bar{u}_p(i\varepsilon^{\mu\lambda\nu\rho}k_\nu\gamma_\rho)u_n + F_2^{(p)}F_A\frac{k^2+2p\cdot k}{2M_N}\bar{u}_p(i\sigma^{\mu\lambda}\gamma^5)u_n
\end{aligned} \tag{4.1.13}$$

Using the static approximation, we take the initial nucleon to be at rest and we ignore recoil. This lets us simplify the matrix elements of Dirac matrices between the initial and final nucleon spinors. In this static approximation, the space components of the tensor term vanish.

$$\bar{u}_p\sigma^{ij}\gamma^5u_n \to 0 \tag{4.1.14}$$

On the other hand, the matrix element $\bar{u}_p\gamma_\rho u_n$ is only non-zero in the time direction, $\rho = 0$. Thus it is proportional to the initial nucleon momentum p.

$$\bar{u}_p\gamma^\mu u_n = 2p^\mu\chi_p^\dagger\chi_n \tag{4.1.15}$$

Where χ are the two-component Pauli spinors. Therefore the result is

$$\begin{aligned}\bar{u}_p\Gamma^\mu_{(p)}(p,p+k)(\not{p}+\not{k}+M_N)W^\lambda(p+k,p)u_n \\ = 2i\varepsilon^{\mu\lambda\nu\rho}k_\nu p_\rho F_A(F_1^{(p)}+F_2^{(p)})\chi_p^\dagger\chi_n\end{aligned} \tag{4.1.16}$$

Similarly for the term where the photon latches onto the neutron line, we make the same simplifications and we use

$$\gamma^\lambda\gamma^5(-i\sigma^{\mu\nu}k_\nu) \to -i\varepsilon^{\mu\lambda\nu\rho}k_\nu\gamma_\rho \tag{4.1.17}$$

Using the same stationary Dirac matrix element, we find

$$\begin{aligned}\bar{u}_pW^\lambda(p,p-k)(\not{p}-\not{k}+M_N)\Gamma^\mu_{(n)}(p-k,p)u_n \\ \to 2i\varepsilon^{\mu\lambda\nu\rho}k_\nu p_\rho F_A(F_1^{(n)}+F_2^{(n)})\chi_p^\dagger\chi_n\end{aligned} \tag{4.1.18}$$

Both of these terms are proportional to the magnetic Sachs form factor $G_M = F_1 + F_2$. Plugging this into the Born term, we find

$$C^F_{\text{Born}} = i8\pi^2\int\frac{d^4k}{(2\pi)^4}\frac{(\varepsilon_{\mu\lambda\alpha\beta}k^\alpha p^\beta)(\varepsilon^{\mu\lambda\nu\rho}k_\nu p_\rho)}{(k^2+i\epsilon)^2}\frac{1}{M_N^2}\left[\frac{F_AG_M^{(p)}}{(p+k)^2-M_N^2+i\epsilon}+\frac{F_AG_M^{(n)}}{(p-k)^2-M_N^2+i\epsilon}\right] \tag{4.1.19}$$

The integral is symmetric in k, and we can take $k \to -k$ in the second term and write the form factor in terms of the isoscalar form factor $G_M^{(n)} + G_M^{(p)} = G_M^{(0)}$. Then we can combine the Levi-Civita symbols using the usual product identity.

$$\varepsilon^{\mu\lambda\alpha\beta}\varepsilon_{\mu\lambda\sigma\delta} = -2(\delta^\alpha_\sigma\delta^\beta_\delta - \delta^\alpha_\delta\delta^\beta_\sigma) \tag{4.1.20}$$

With $p\cdot k = M_N\nu$ we have

$$C^F_{\text{Born}} = -i16\pi^2\int\frac{d^4k}{(2\pi)^4}\frac{(k^2-\nu^2)}{(k^2+i\epsilon)^2}\frac{F_A(-k^2)G_M^{(0)}(-k^2)}{k^2+2M_N\nu+i\epsilon} \tag{4.1.21}$$

This is essentially a more compact version of what is presented in [Tow92].

The $i\epsilon$'s in the denominators allow us to perform a Wick rotation with $\nu = i\omega$. Then go to spherical coordinates in four dimensions. The integration measure involves a radial coordinate and three angles.

$$\int d^4k = \int_0^\infty Q^3dQ\int_0^\pi\sin^2\alpha d\alpha\int_0^\pi\sin\beta d\beta\int_0^{2\pi}d\gamma \tag{4.1.22}$$

Here $Q^2 = -k^2$ is the Euclidean norm, and $\omega = Q\cos\alpha$ is the projection along the Euclidean time axis. Integrate over the other two angles, and use $dQ^2 = 2QdQ$ and $u = \cos\alpha$ and we can write the integration measure as

$$\int \frac{d^4k}{(2\pi)^4} = \frac{i}{8\pi^3}\int_0^\infty Q^2 dQ^2 \int_{-1}^1 \sqrt{1-u^2}du \tag{4.1.23}$$

Then we can do the integral over u and we are left with a simple integral over Q.

$$\begin{aligned} C^F_{\text{Born}} &= \frac{2}{\pi}\int_0^\infty dQ^2 \int_{-1}^1 du \frac{(1-u^2)^{3/2}}{(Q^2+4M_N^2u^2)} F_A(Q^2)G_M^{(0)}(Q^2) \\ &= 2\int_0^\infty \frac{dQ}{Q}\frac{1+2r}{(1+r)^2}F_A(Q^2)G_M^{(0)}(Q^2) \end{aligned} \tag{4.1.24}$$

where $r = \sqrt{1+4M_N^2/Q^2}$. This form is the one presented in [SGR19], which they arrive at using dispersion relations.

Note that this integral is divergent, unless it is regulated by the nucleon form factors. If we were to take point nucleons, then we would get a log divergence.

$$C^F_{\text{Born}} = 2\int_0^\Lambda \frac{dQ}{Q}\frac{1+2r}{(1+r)^2} = \frac{3}{2}\log\frac{\Lambda}{M_N} + \frac{9}{8} \quad \text{(point nucleons)} \tag{4.1.25}$$

This agrees with the result presented in [FK04] (their definition includes an extra factor of 2). The Born term cannot be evaluated without the inclusion of the nucleon form factors. Further, this shows that the result is sensitive to the high momentum behaviour of the nucleon form factors.

This integral can be evaluated analytically if we plug in dipole form factors for the nucleons.

$$G_M^{(0)}(Q^2) = (\mu_n+\mu_p)\left(\frac{\Lambda_V^2}{\Lambda_V^2+Q^2}\right)^2, \quad F_A(Q^2) = g_A\left(\frac{\Lambda_A^2}{\Lambda_A^2+Q^2}\right)^2 \tag{4.1.26}$$

The form factors are not perfectly described by the dipole form, and there are different measurements of the axial form factor which give different results for Λ_A. If we take $\Lambda_V = 0.84$ GeV and $\Lambda_A = 1.05(5)$ GeV, we find

$$C^{\text{F}}_{\text{Born}} = 0.892(14) \tag{4.1.27}$$

Here, the uncertainty is only due to the uncertainty in the axial form factor Λ_A.

These days, we have a more sophisticated parameterization of the nucleon form factors based on the so-called *z-expansion*. This is described in some detail in Appendix A. The z-expansion is based on a fitting procedure which produces a parameterization with uncertainties. These uncertainties give us a 1σ band which we can use to determine the uncertainty in $C^{\text{F}}_{\text{Born}}$. Following [SGR19], we calculate the uncertainty in C^F_{Born} by treating the Sachs

form factors $G_{E,M}^{(n,p)}(Q^2)$ as statistically independent, along with the axial form factor $F_A(Q^2)$. Then we calculate the change in $C_{\text{Born}}^{\text{F}}$ resulting from the change in each of these, and add the uncertainties in quadrature as usual.

Using the nucleon form factors and uncertainties described in Appendix A, we can calculate the resulting $C_{\text{Born}}^{\text{F}}$ and its uncertainties.

$$C_{\text{Born}}^{\text{F}} = 0.902(47) \tag{4.1.28}$$

This is in good agreement with the result presented in [SGR19].

4.2 Born Correction for Gamow-Teller Transitions

So far, we have discussed radiative corrections to the Fermi matrix element. The inner radiative corrections to the Gamow-Teller transitions are much less studied in the literature. Because it is much less well known, I would like to work through the entire derivation in detail.

We start by writing down the tree-level matrix element.

$$\mathcal{M}_{\text{GT}} = g_A \frac{G_V}{\sqrt{2}} \vec{L} \cdot \langle \mathbf{GT} \rangle \tag{4.2.1}$$

where $\mathbf{GT}$ is the Gamow-Teller operator in Equation 1.3.5.

$$\mathbf{GT} = \sum_a \vec{\sigma}_a \tau_a^+ \tag{4.2.2}$$

Here I define the operator without g_A so it can be factored out explicitly. Note that there is a minus sign in the axial-vector weak current, which cancels the minus sign from the metric tensor.

The tree level Gamow-Teller matrix element involves the spacial components of the lepton current, rather than the time component. For the single-nucleon case such as neutron decay, this is

$$\mathcal{M}_{\text{GT}} = g_A \frac{G_V}{\sqrt{2}} \vec{L} \cdot \left(\chi_p^\dagger \vec{\sigma} \chi_n \right) \tag{4.2.3}$$

where χ are the two-component Pauli spinors.

As before, we express the box diagram in terms of the effective hadronic current, Equation 4.0.7. In contrast to the Fermi case, we take the vector part for Gamow-Teller transitions.

$$\mathcal{M}_{\text{box}} = \frac{\alpha}{2\pi} \frac{G_V}{\sqrt{2}} L_\beta \mathcal{J}^\beta \to -\frac{\alpha}{2\pi} \frac{G_V}{\sqrt{2}} \vec{L} \cdot \vec{\mathcal{J}} \tag{4.2.4}$$

Really, we should also include the term which comes from $k_\lambda T^{\mu\lambda}$. This involves the divergence of the axial-vector current, as we showed in Equation 2.2.7. However, in [Hay21]

they show that this correction depends on the difference $(F_1^{(0)})^2-(F_1^{(1)})^2$, which is very small for small momentum transfers. Therefore we ignore this contribution.

According to the Equation 2.2.21, the box-diagram correction to Gamow-Teller transitions involves the vector part of the weak current. Before we present the full calculation, we can first take the simple point-nucleon approximation. We again use the free, single-nucleon version of the generalized Compton tensor $T^{\mu\lambda}_{\text{Born}}$, defined in Equation 4.1.5. Going through the same Dirac matrix algebra we did before, we now find

$$2M_N T^{\mu\lambda}_{\text{Born},VV}(p,k) = -i\varepsilon^{\mu\lambda\nu\rho}k_\nu \frac{\bar{u}_p\gamma_\rho\gamma^5 u_n}{(p+k)^2-M_N^2+i\epsilon} \tag{4.2.5}$$

When we plug this into the box diagram and do the contraction of the Levi-Civita symbols, we get

$$\varepsilon_{\mu\lambda\alpha\beta}k^\alpha L^\beta T^{\mu\lambda}_{\text{Born},VV}(p,k) = i\frac{1}{M_N}(k^2L_\lambda-(k\cdot L)k_\lambda)\frac{\bar{u}_p\gamma^\lambda\gamma^5 u_n}{(p+k)^2-M_N^2+i\epsilon} \tag{4.2.6}$$

Using the static approximation, we can express this in terms of the two-component Pauli spinors.

$$\varepsilon_{\mu\lambda\alpha\beta}k^\alpha L^\beta T^{\mu\lambda}_{\text{Born},VV}(p,k) = -2i\frac{(k^2\vec{L}-(k\cdot L)\vec{k})\cdot\chi_p^\dagger\vec{\sigma}\chi_n}{(p+k)^2-M_N^2+i\epsilon} \tag{4.2.7}$$

Using rotational symmetry of the loop momentum integral, we can make the following replacement.

$$k^ik^j \to \frac{1}{3}\delta^{ij}|\vec{k}|^2 \tag{4.2.8}$$

This allows us to factor out a piece which is proportional to the tree-level matrix element.

$$\varepsilon_{\mu\lambda\alpha\beta}k^\alpha L^\beta T^{\mu\lambda}_{\text{Born},VV}(p,k) \to -2i\frac{(k^2+\frac{1}{3}|\vec{k}|^2)}{(p+k)^2-M_N^2+i\epsilon}\vec{L}\cdot\chi_p^\dagger\vec{\sigma}\chi_n \tag{4.2.9}$$

Plugging this back in, we can write down the Born term for the Gamow-Teller operator in the point nucleon approximation.

$$C^{\text{GT}}_{\text{Born}} = -i\frac{16\pi^2}{g_A}\int\frac{d^4k}{(2\pi)^4}\frac{(k^2+\frac{1}{3}|\vec{k}|^2)}{(k^2+i\epsilon)^2}\frac{1}{(p+k)^2-M_N^2+i\epsilon} \tag{4.2.10}$$

Use the definition $M_N\nu = p\cdot k$, and use the fact that $|\vec{k}|^2=\nu^2-k^2$ when in the nucleon rest frame. As before, use the $i\epsilon$'s in the denominator to perform a Wick rotation using Equation 4.1.23.

$$\begin{aligned} C^{\text{GT}}_{\text{Born}} &= \frac{2}{3\pi g_A}\int_0^\infty dQ^2\int_{-1}^1 du\frac{(2+u^2)\sqrt{1-u^2}}{Q^2+4M_N^2u^2} \\ &= \frac{2}{3g_A}\int_0^\infty\frac{dQ}{Q}\frac{5+4r}{(1+r)^2} \end{aligned} \tag{4.2.11}$$

where $r = \sqrt{1 + 4M_N^2/Q^2}$. Again, the result for a point nucleon is log divergent. Integrating up to a UV cut-off Λ, we find

$$C_{\text{Born}}^{\text{GT}} = \frac{1}{g_A}\left(\frac{3}{2}\log\frac{\Lambda}{M_N} + \frac{5}{8}\right) \tag{4.2.12}$$

This is the same result reached by [FK04] using slightly different methods. As before, we need to include the nucleon form factors to get a convergent result. From this argument, we know that we will get a contribution from the $F_1^{(0)}F_1$ term of the form

$$\frac{2}{3g_V}\int_0^\infty \frac{dQ}{Q}\frac{5+4r}{(1+r)^2}F_1^{(0)}(Q^2)F_1(Q^2) \tag{4.2.13}$$

In order to get the full result, we need to do a bit more Dirac matrix algebra. The Dirac algebra is very tedious, and it adds nothing to the actual discussion. We work it out in full detail in Appendix B. Using the results from that appendix, we find the full result for the Born correction to Gamow-Teller transitions.

$$\begin{aligned} C_{\text{Born}}^{\text{GT}} = \frac{1}{g_A}\int_0^\infty \frac{dQ}{Q}\Bigg[&\frac{2(5+4r)}{3(1+r)^2}F_1^{(0)}(Q^2)F_1(Q^2) \\ &+\frac{4(2+r)}{3(1+r)^2}F_2^{(0)}(Q^2)F_1(Q^2) \\ &+\frac{4(2+r)}{3(1+r)^2}F_1^{(0)}(Q^2)F_2(Q^2) \\ &+\left(\frac{2Q^4(1-r)+M_N^2Q^2}{8M_N^4}\right)F_2^{(0)}(Q^2)F_2(Q^2)\Bigg] \end{aligned} \tag{4.2.14}$$

where $r = \sqrt{1 + 4M_N^2/Q^2}$. Recall from Section 1.2 that we can use the CVC hypothesis to relate the weak vector form factors $F_{1,2}$ to the isovector electromagnetic form factors $F_{1,2}^{(1)}$ using Equation 1.2.51. Note this has a different functional form than what is given in [Hay21], but numerically they agree within the uncertainties.

Here, we give results based on the nucleon form factors described in Appendix A. We again use the same method for calculating the uncertainties which we discussed in the previous section. We treat the Sachs form factors and F_A as statistically independent, calculate the change due to the uncertainty in each, and then add the resulting uncertainties in quadrature. The result for each individual term in Equation 4.2.14 is

$$C_{\text{Born}}^{\text{GT}} = 0.446(5) - 0.029(5) + 0.815(6) + 0.003 \tag{4.2.15}$$

Note that the last term coming from $F_2^{(0)}F_2$ is very small and can be ignored. Also note that the term coming from weak magnetism $F_1^{(0)}F_2$ is the dominant contribution. Following [Hay21], we separate out the contribution due to weak magnetism.

$$C_{\text{Born}}^{\text{GT}} = 0.416(6) + 0.817(6) \tag{4.2.16}$$

The first term is due to the usual weak vector current with F_1, and the second term comes from weak magnetism F_2. The contribution from weak magnetism is about twice as large as the other term. The full result for the Born contribution is

$$C_{\text{Born}}^{\text{GT}} = 1.233(10) \tag{4.2.17}$$

This is slightly larger than the result given in [Hay21]. The uncertainty is much smaller than the uncertainty in $C_{\text{Born}}^{\text{F}}$. This is due to the fact that $C_{\text{Born}}^{\text{GT}}$ only involves the vector form factors, which are very well known.

Chapter 5

Two-Body Nuclear Structure Dependent Correction

In addition to the Born term we looked at in the previous section, we can consider the case in which the weak and electromagnetic currents latch onto two different nucleons. The Feynman diagram for this process is shown in Figure 5.1. This two-body term depends on nuclear structure and goes into C_{NS}.

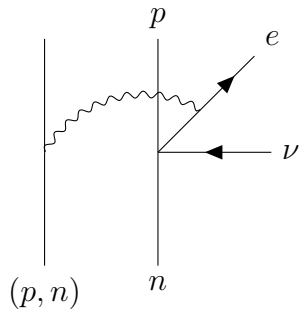

Figure 5.1: Feynman diagram for the two-body contribution to C_{NS}

Unlike the Born term, the Feynman diagram in Figure 5.1 for the two-body part has no closed loops. This means that the momentum transfer cannot be arbitrarily large. In fact, if we model the nucleus as a Fermi gas, then the momentum transfer cannot be larger than $2k_F$. We provide a sketch of the proof in Section 5.1, and an actual calculation to back up this idea is shown in Figure 5.7. Since we do not need to deal with large loop momentum, we make a non-relativistic approximation for the currents.

We want to compute the time ordered product which appears in the generalized Compton tensor, Equation 2.1.4. Expanding out the time ordered product using the identity in

Equation 2.2.10 and plugging in intermediate nuclear states, we have

$$\begin{aligned} T^{\mu\lambda}(p_f, p_i, k) &= -i \int d^4x e^{ikx} \langle p_f | T J^\mu_\gamma(x) J^\lambda_W(0) | p_i \rangle \\ &= \sum_n \frac{\langle f | J^\mu_\gamma(\vec{0}) | n \rangle \langle n | J^\lambda_W(\vec{0}) | i \rangle}{k^0 - \Delta E_n + i\epsilon} + \frac{\langle f | J^\lambda_W(\vec{0}) | n \rangle \langle n | J^\mu_\gamma(\vec{0}) | i \rangle}{-k^0 - \Delta E_n + i\epsilon} \end{aligned} \tag{5.0.1}$$

In this expression we suppress the center of mass momentum, which needs to be included in the energy ΔE_n and in the current matrix elements. In principle, we should do a sum over all nuclear states $|n\rangle$ weighted by the energy ΔE_n. Doing this full sum amounts to computing the nuclear green's function.

In order to avoid doing this explicit sum over intermediate states, Jaus, Rasche [JR90] and Towner [Tow92] argued that these energy denominators should be small, and that we can simply ignore the energy difference in the nuclear excited states ΔE_n. Using this approximation, we can ignore the time-ordering since the one-body current operators acting on two different nucleons should commute. The remaining k^0 dependence of the two terms can be combined using the Lorentzian delta function.

$$\frac{1}{k^0 + i\epsilon} - \frac{1}{k^0 - i\epsilon} = \frac{-i2\epsilon}{(k^0)^2 + \epsilon^2} \to -i2\pi\delta(k^0) \tag{5.0.2}$$

where we take the limit $\epsilon \to 0^+$. We can then pull out a delta function in k^0.

$$T^{\mu\lambda}(p_f, p_i, k) \to -i(2\pi)\delta(k^0) \int d^3x e^{-i\vec{k}\cdot\vec{x}} \langle p_f | J^\mu_{em}(\vec{x}) J^\lambda_W(\vec{0}) | p_i \rangle \Big|_{\text{2-body}} \tag{5.0.3}$$

The time ordering symbol is now gone, and the currents are evaluated at equal times. This is why we are able to pull out the two-body piece. We also ignore an overall momentum conserving delta function and write this in terms of the fourier transform currents.

$$\tilde{J}^i(\vec{k}) = \int d^3x\, e^{i\vec{k}\cdot\vec{x}} J^i(\vec{x}) \tag{5.0.4}$$

We will return to the issue of the center of mass later. Then we can make the momentum transferred by each of the currents explicit, and write

$$T^{\mu\lambda}(p_f, p_i, k) \to -i(2\pi)\delta(k^0) \langle p_f | \tilde{J}^\mu_{em}(-\vec{k}) \tilde{J}^\lambda_W(\vec{k}) | p_i \rangle \Big|_{\text{2-body}} \tag{5.0.5}$$

Then the effective hadronic current for the box diagram Equation 4.0.7, once again ignoring the electron mass and nuclear recoil, is given by

$$\mathcal{J}_\beta = -i8\pi^2 \int \frac{d^3k}{(2\pi)^3} \frac{1}{(|\vec{k}|^2 - i\epsilon)^2} \varepsilon_{\mu\lambda\alpha\beta} k^\alpha \langle p_f | \tilde{J}^\mu_{em}(-\vec{k}) \tilde{J}^\lambda_W(\vec{k}) | p_i \rangle \Big|_{\text{2-body}} \tag{5.0.6}$$

with $k^0 = 0$, due to the delta function. Note that the delta function $\delta(k^0)$ has reduced the integral to d^3k instead of d^4k.

5.1 Momentum Transfer Restrictions

The main difference between the one-body Born term we discussed in Section 4 and the two-body term is the restrictions on the momentum flow. Consider the one-body Feynman diagram for the Born term, Figure 4.1. This diagram has a closed loop, which allows the momentum transferred by the currents to be arbitrarily large. This is what led to the naive ultraviolet divergence we discussed in Section 4. On the other hand, the Feynman diagram for the two body term Figure 5.1 has no closed loops. Consequently, we will show that the loop momentum $\vec{k}$ in the two-body term is limited by the low-momentum nuclear wavefunction.

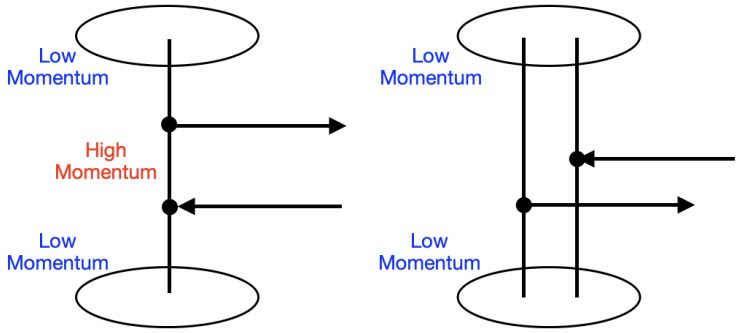

Figure 5.2: Left, momentum transfer in the one-body Feynman diagram, Figure 4.1. Right, momentum transfer in the two-body Feynman diagram, Figure 5.1.

In order to see this, consider the stripped-down version of the two Feynman diagrams shown in Figure 5.2. The two circles on the top and bottom represent the initial/final low-momentum nuclear wavefunctions. In the one-body term, the nucleon gets kicked twice by the current operators. This allows the process to go through an intermediate high-momentum state. On the other hand, the all of the nucleons in the two-body term must live inside the low-momentum wavefunction.

For simplicity, suppose we approximate the initial and final nuclear wavewfunctions by a uniform momentum distribution with some maximum momentum.

$$|\vec{p}| < k_F \quad \text{(low-momentum nuclear wavefunction)} \tag{5.1.1}$$

This is based on the usual Fermi gas approximation. This wavefunction is simply a sphere with radius k_F in momentum space, as shown in Figure 5.3. We will consider the case of two nucleons, but the argument can be easily extended.

Consider what happens when the weak and electromagnetic currents give a small kick to the nucleons, as shown in Figure 5.4. The first current can kick either nucleon 1 or 2, and the second current can also kick either nucleon 1 or 2. Because the momentum transfer is small, all nucleons remain inside the low-momentum wavefunction.

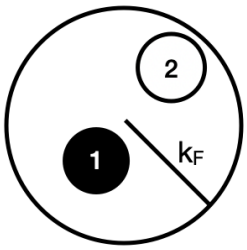

Figure 5.3: Low-momentum wavefunction of the nucleus in the Fermi sphere approximation, showing two nucleons.

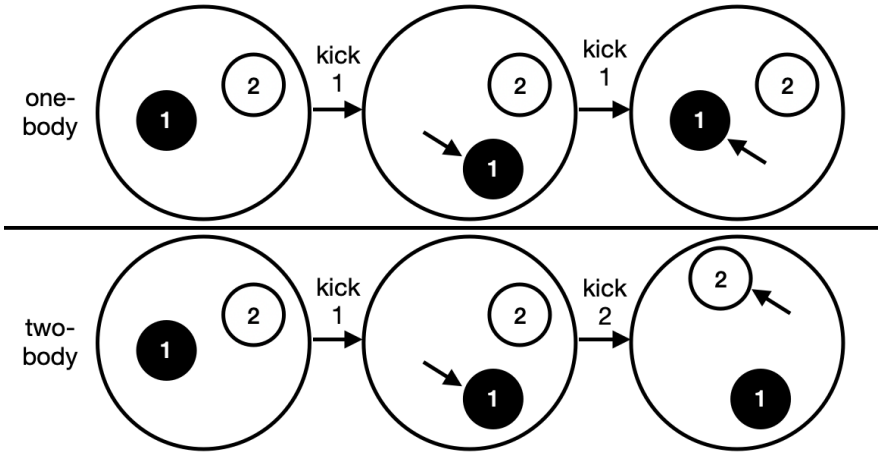

Figure 5.4: Top, one-body momentum transfer where nucleon 1 is kicked twice. Bottom, two-body momentum transfer where nucleon 1 is kicked followed by nucleon 2.

Now consider what happens when we have a large momentum transfer, as shown in Figure 5.5. In this case, the current kicks one of the nucleons outside of the low-momentum wavefunction. Then, in order to have any overlap with the final state, that same nucleon needs to be kicked back into the low-momentum wavefunction by the second current. Therefore, if we kick nucleon 1 with the first current we need to kick nucleon 1 again with the second current. This means we do not have any two-body contribution at high momentum transfer.

Using this simple Fermi sphere model, we can ask how large the momentum transfer can be for the two-body part. As we can see in Figure 5.6, the maximum momentum transfer we can have in the two-body case would send nucleons from one side of the Fermi sphere to the other. This means the nucleons get a kick equal to twice the radius of the Fermi sphere. Thus we conclude that the two-body part should die off at momentum transfers larger than

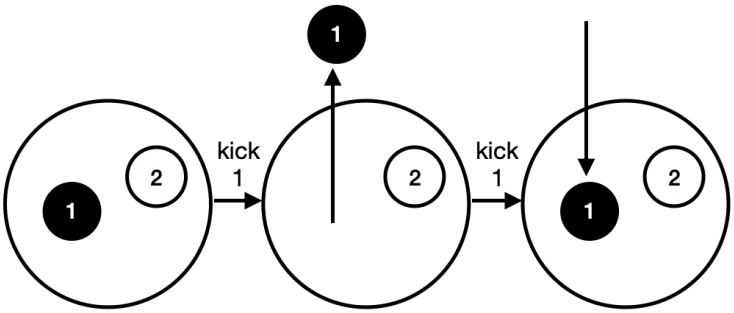

Figure 5.5: Momentum transfer diagram showing a large momentum transfer.

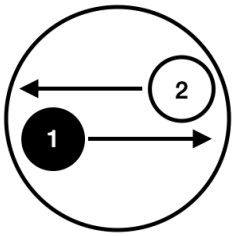

Figure 5.6: The maximum allowed momentum transfer for the two-body part.

$2k_F$.

We can see how this works using a concrete example. Following [FW66] Section 6, we focus on the *Coulomb sum rule*. We hit the initial nucleus by the charge operator, and the sum over all possible final states.

$$S(|\vec{k}|) = \sum_n |\langle n|\tilde{\rho}(\vec{k})|\psi\rangle|^2 \tag{5.1.2}$$

The charge operator $\tilde{\rho}(\vec{k})$ is the Fourier transform of the usual one-body charge operator.

$$\tilde{\rho}(\vec{k}) = \sum_a \hat{e}_a e^{i\vec{k}\cdot\vec{x}_a} \tag{5.1.3}$$

where $\hat{e}_a = \frac{1}{2}(1+\tau_a^z)$ is the charge of nucleon a. Since we are summing over all final states, we can use the completeness relation.

$$1 = \sum_n |n\rangle\langle n| \tag{5.1.4}$$

This is the key for separating out the one-body and two-body parts. Now the two charge

operators can hit each other.

$$\begin{aligned} S(|\vec{k}|) &= \langle\psi| \left(\sum_a \hat{e}_a e^{-i\vec{k}\cdot\vec{x}_a}\right)\left(\sum_b \hat{e}_b e^{i\vec{k}\cdot\vec{x}_b}\right)|\psi\rangle \\ &= \langle\psi| \sum_{a,b} \hat{e}_a\hat{e}_b e^{-i\vec{k}\cdot(\vec{x}_a-\vec{x}_b)}|\psi\rangle \end{aligned} \tag{5.1.5}$$

Then the sum can be separated into a one-body part where the currents latch onto the same nucleon, $a = b$, and a two-body part where the currents latch onto different nucleons, $a \neq b$. This is usually referred to as *normal ordering* the operators.

$$S(|\vec{k}|) = \sum_a \hat{e}_a + \langle\psi| \sum_{a\neq b} \hat{e}_a\hat{e}_b e^{-i\vec{k}\cdot(\vec{x}_a-\vec{x}_b)}|\psi\rangle \tag{5.1.6}$$

The one-body part simply gives us the sum of the charges, which is equal to Z. The exponentials cancel out, and the one-body part is independent of momentum transfer. On the other hand, the two-body part does have momentum dependence.

Consider the limiting cases of this expression. In the limit of small momentum transfer $|\vec{k}| \to 0$, the exponentials all go to 1. Then the two-body part counts ordered pairs $a \neq b$, which gives us $Z(Z-1)$.

$$S(|\vec{k}| \to 0) = Z + Z(Z-1) = Z^2 \tag{5.1.7}$$

Conversely, at high momentum $|\vec{k}| \to \infty$, the two-body term vanishes and we are left with only the one-body part.

$$S(|\vec{k}| \to \infty) = Z \tag{5.1.8}$$

Now we will focus on the case of two nucleons. Consider the isoscalar version of the Coulomb sum rule, where we replace $\hat{e}_a \to 1$ so we get something non-trivial for the deuteron where $Z = 1$. The isoscalar version of the Coulomb sum rule can be written as

$$S(|\vec{k}|) = \langle\psi| \left(e^{-i\vec{k}\cdot\vec{x}_1} + e^{-i\vec{k}\cdot\vec{x}_2}\right)\left(e^{i\vec{k}\cdot\vec{x}_1} + e^{i\vec{k}\cdot\vec{x}_2}\right)|\psi\rangle \tag{5.1.9}$$

The Coulomb sum rule essentially counts the number of ways we can hit the two nucleons. At low momentum transfer, both the one-body and two-body parts contribute as shown in Figure 5.4. We have four possibilities for how the charge operators can hit the nucleons.

$$\left.\begin{array}{c|cc} \text{1-body} & (1,1) & (2,2) \\ \hline \text{2-body} & (1,2) & (2,1) \end{array}\right\} \quad \Rightarrow \quad S(0) = 4 \tag{5.1.10}$$

This is confirmed by setting $\vec{k} = 0$ which sets all of the exponentials to 1 and we indeed get $S(0) = 4$.

Now consider what happens when the momentum transfer is large, as shown in Figure 5.5. Then the charge operators must latch onto the same nucleon, and we have no two-body part. Then there are only two possibilities for how the charge operators can hit the nucleons.

$$\text{1-body} \quad (1,1) \quad (2,2) \ \Big\} \quad \Rightarrow \quad S(|\vec{k}| \to \infty) = 2 \tag{5.1.11}$$

Let us now check this intuition with an exact calculation using the Fermi sphere model. First, we can re-write the sum rule using the relative coordinate $r = x_1 - x_2$.

$$S(|\vec{k}|) = 2 + \langle\psi| \left[e^{i\vec{k}\cdot\vec{r}} + e^{-i\vec{k}\cdot\vec{r}}\right] |\psi\rangle \tag{5.1.12}$$

The two-body part can be calculated explicitly using the momentum distribution for the nucleon relative wavefunction, $\phi(p)$.

$$S(|\vec{k}|) = 2 + 2\mathrm{Re}\int \frac{d^3p}{(2\pi)^3}\phi(\vec{p})^*\phi(\vec{p}+\vec{k}) \tag{5.1.13}$$

Assuming $\phi(p)$ is a simple Fermi sphere, we can calculate the sum rule analytically.

$$S(|\vec{k}|) = 2 + 2\left(1 - \frac{|\vec{k}|}{2k_F}\right)^2\left(1 + \frac{|\vec{k}|}{4k_F}\right)\theta(2k_F - |\vec{k}|) \tag{5.1.14}$$

The Heaviside theta function ensures that the two-body part goes to zero when $|\vec{k}| > 2k_F$. When $|\vec{k}| \to 0$, the one-and two-body parts add and we get $S(0) = 4$. Past $|\vec{k}| > 2k_F$, the two-body part vanishes and we get $S(|\vec{k}| > 2k_F) = 2$.

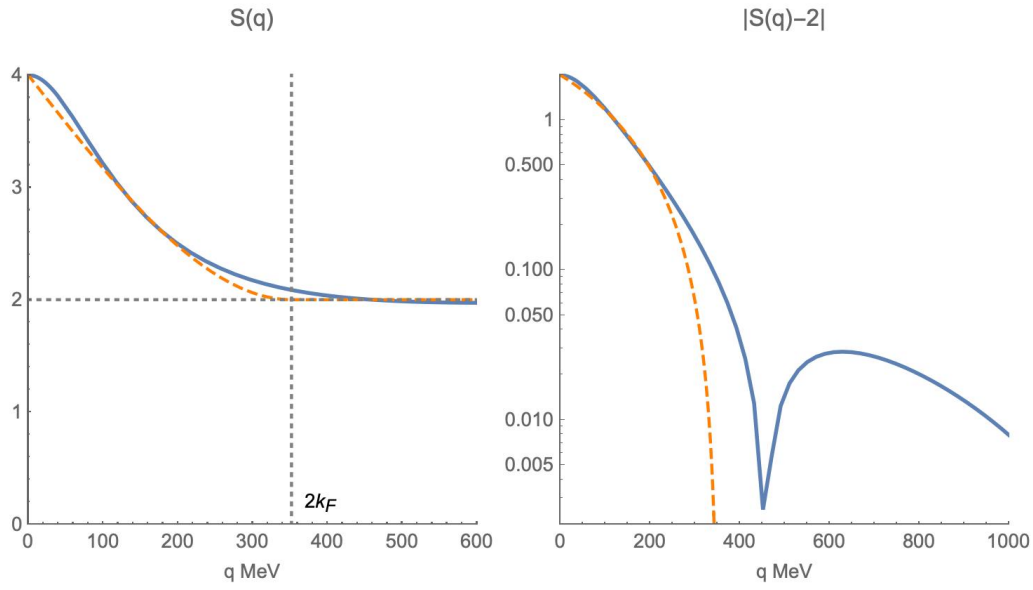

Figure 5.7: The isoscalar Coulomb sum rule for the Deuteron (solid), compared to the Fermi-gas approximation (dashed). Here we use an effective k_F which is determined by the average kinetic energy, $\langle T_r\rangle = 3k_F^2/5M_N$.

In Figure 5.7, we show the actual result for the deuteron compared to the Fermi-gas approximation. We can clearly see the limiting cases $S(0) = 4$ and $S(|\vec{k}| \to \infty) = 2$, as expected from our arguments above. The simple Fermi sphere approximation goes to zero exactly at $2k_F$, while a realistic nucleus has a long momentum tail which causes a small two-body part to persist even to high momentum transfer. We can see this behaviour in the two-body part in the right plot of Figure 5.7. In a realistic nucleus, the hard core of the nuclear potential means there is always some probability for two nucleons to be in a relative high-momentum wavefunction. Therefore, we expect this $2k_F$ momentum cut-off to be only a useful approximation.

To derive the deuteron result, use the usual decomposition of the exponential in terms of multipoles.

$$e^{i\vec{k}\cdot\vec{r}} = \sum_{LM} 4\pi i^L j_L(kr) Y_{LM}(\hat{r}) Y_{LM}(\hat{k})^* \tag{5.1.15}$$

We can calculate this by taking the $l = 0$ part which is independent of the direction of $\vec{k}$. Then we need to calculate the following radial integral.

$$S(|\vec{k}|) = 2 + 2\int_0^\infty dr\, j_0(kr)[u(r)^2 + w(r)^2] \tag{5.1.16}$$

Here, $u(r)$ and $w(r)$ are the $l = 0$ and $l = 2$ components of the deuteron wavefunction (see Figure 6.8). We will see a similar expression come up again in the context of *pp*-fusion in Equation 7.3.10.

5.2 Two-Body Contribution Fermi Transitions

Following [JR90] and [Tow92], we can calculate the two-body contribution to $C_{\rm NS}^{\rm F}$. As before, we use the static approximation and set $p_i = p_f = p$. We once again ignore the lepton momentum. Using the same arguments from Section 4.1 with the two-body hadronic covariant from Equation 5.0.6, we have

$$\mathcal{J}^0 = -i8\pi^2 \int \frac{d^3k}{(2\pi)^3} \frac{1}{(|\vec{k}|^2 - i\epsilon)^2} \epsilon^{ijk} k^k \left\langle f|\tilde{J}^i_{em}(-\vec{k})\tilde{J}^j_W(\vec{k})|i\right\rangle \Big|_{\text{2-body}} \tag{5.2.1}$$

Then the two body contribution to $C_{\rm NS}^F$ is

$$C_{\rm NS}^F = \frac{\mathcal{J}^0}{M_F} \tag{5.2.2}$$

where M_F is the Fermi matrix element from Section 1.3, which is equal to $\sqrt{2}$ in the isospin symmetric approximation for superallowed Fermi beta decay with $T = 1$.

Because the momentum integral is limited by the wavefunction, we allow ourselves to do a non-relativistic reduction of the currents. We go through the details of the non-relativistic

reduction in Appendix C. The non-relativistic reduction of the electromagnetic current Equation 1.2.30 gives us

$$J^i_{em}(\vec{x}) = \frac{1}{2M_N}\sum_a \{p^i_a, \delta^3(\vec{x}-\vec{x}_a)\}\hat{e}_a - i\epsilon^{ilm}[p^l_a, \delta^3(\vec{x}-\vec{x}_a)]\sigma^m_a\hat{\mu}_a \tag{5.2.3}$$

We have concealed the isospin operators in the definitions $\hat{e} = \frac{1}{2}(1+\tau_z)$ and $\hat{\mu} = \frac{1}{2}(\mu_s+\mu_v\tau_z)$. Likewise, the non-relativistic reduction of the weak axial-vector current in Equation 1.2.34 gives us

$$J^i_W(\vec{x}) = -g_A\sum_a \tau^+_a\sigma^i_a\delta^3(\vec{x}-\vec{x}_a) \tag{5.2.4}$$

Plug in these one-body currents and pick out the piece where the currents latch onto two different nucleons, $a \neq b$.

$$\begin{aligned} &-i\epsilon^{ijk}k^k\,\langle f|\tilde{J}^i_{em}(-\vec{k})\tilde{J}^j_W(\vec{k})|i\rangle\Big|_{\text{2-body}} \\ &= i\frac{g_A}{2M_N}\epsilon^{ijk}k^k\sum_{a\neq b}\langle f|\left[\{p^i_a, e^{-i\vec{k}\cdot\vec{x}_a}\}\hat{e}_a + i\epsilon^{ilm}k^l e^{-i\vec{k}\cdot\vec{x}_a}\sigma^m_a\hat{\mu}_a\right]\left[\tau^+_b\sigma^j_b e^{i\vec{k}\cdot\vec{x}_b}\right]|i\rangle \\ &= i\frac{g_A}{2M_N}\sum_{a\neq b}\langle f|e^{-i\vec{k}\cdot(\vec{x}_a-\vec{x}_b)}\left[2(\vec{p}_a\times\sigma_b)\cdot\vec{k}\hat{e}_a + i[(\vec{k}\cdot\sigma_a)(\vec{k}\cdot\sigma_b) - |\vec{k}|^2\sigma_a\cdot\sigma_b]\hat{\mu}_a\right]\tau^+_b|i\rangle \end{aligned} \tag{5.2.5}$$

To get the last line, we needed to use the fact that the cross product with $\vec{k}$ allows us to ignore the commutator of $\vec{p}_a$ and $e^{-i\vec{k}\cdot\vec{x}_a}$. This is close to the form presented in [JR90], except they go further and use an identity to replace $\vec{p}_a$ by the commutator of the Hamiltonian H with $\vec{x}_a$.

Following [Tow92], we can do the integral over $\vec{k}$ and convert this to an expression in position space. The integrals we need are standard.

$$\begin{aligned} \int\frac{d^3k}{(2\pi)^3}\frac{e^{-i\vec{k}\cdot\vec{r}}}{(|\vec{k}|^2-i\epsilon)^2}k^i &= -i\frac{1}{8\pi r}r^i \\ \int\frac{d^3k}{(2\pi)^3}\frac{e^{-i\vec{k}\cdot\vec{r}}}{(|\vec{k}|^2-i\epsilon)^2}k^ik^j &= \frac{1}{8\pi r}(\delta^{ij}-\hat{r}^i\hat{r}^j) \\ \int\frac{d^3k}{(2\pi)^3}\frac{e^{-i\vec{k}\cdot\vec{r}}}{(|\vec{k}|^2-i\epsilon)^2}|\vec{k}|^2 &= \frac{1}{4\pi r} \end{aligned} \tag{5.2.6}$$

Including the nucleon form factors modifies the loop momentum integrals. This does not change the structure of these expressions, but it does introduce a simple Yukawa radial function as described in [Tow92].

Assuming no form factor for the nucleons, we find (with $\vec{r} = \vec{x}_a - \vec{x}_b$)

$$C^{\text{F}}_{\text{NS}} = \frac{\pi}{\sqrt{2}}\frac{g_A}{2M_N}\sum_{a\neq b}\langle f|\left[2(\hat{r}\times\vec{p}_a)\cdot\sigma_b\hat{e}_a + \frac{1}{3r}(4\sigma_a\cdot\sigma_b + S_{ab})\hat{\mu}_a\right]\tau^+_b|i\rangle \tag{5.2.7}$$

The result we find involves three different operator structures. We have an orbital angular momentum dotted into spin, $\vec{l}_a \cdot \vec{\sigma}_b$, a spin dotted into another spin, $\sigma_a \cdot \sigma_b$, and a tensor term

$$S_{ab} = 3(\sigma_a \cdot \hat{r})(\sigma_b \cdot \hat{r}) - \sigma_a \cdot \sigma_b \tag{5.2.8}$$

As written, the exchange symmetry between a and b is obscured. We can make the exchange symmetry manifest by adding the term with a and b swapped, and writing the sum over distinct pairs with $a < b$. We also want to write this in terms of operators with manifest the exchange symmetry.

$$\begin{aligned} \vec{P} &= p_a + p_b \\ p_r &= \frac{1}{2}(p_a - p_b) \end{aligned} \tag{5.2.9}$$

Likewise with the spin and isospin operators.

$$\begin{aligned} \Sigma_{(\pm)} &= \frac{1}{2}(\sigma_a \pm \sigma_b) \\ \Xi_{(\pm)} &= \frac{1}{2}(\tau_a \pm \tau_b) \end{aligned} \tag{5.2.10}$$

We also want the expression to have good isospin, so we define the tensor product of isospin operators (this comes with an annoying minus sign).

$$\begin{aligned} T_{1,1} &= \frac{1}{2}[\tau_a \otimes \tau_b]_{1,1} = -\frac{1}{2}(\tau_a^+ \tau_b^z - \tau_a^z \tau_b^+) \\ T_{2,1} &= \frac{1}{2}[\tau_a \otimes \tau_b]_{2,1} = -\frac{1}{2}(\tau_a^+ \tau_b^z + \tau_a^z \tau_b^+) \end{aligned} \tag{5.2.11}$$

And finally, we split this up into isoscalar and isovector contributions $C_{\rm NS} = C_{\rm NS}^{(0)} + C_{\rm NS}^{(1)}$. The result is

$$\begin{aligned} C_{\rm NS}^{(0)} = \frac{\pi}{\sqrt{2}} \frac{g_A}{2M_N} \sum_{a<b} \langle f| \Bigg[&\Big(2(\hat{r} \times \vec{p}_r) \cdot \Sigma_{(+)} - (\hat{r} \times \vec{P}) \cdot \Sigma_{(-)} + \frac{\mu_s}{3r}(4\sigma_a \cdot \sigma_b + S_{ab})\Big) \Xi_{(+)}^+ \\ &+ \Big(2(\hat{r} \times \vec{p}_r) \cdot \Sigma_{(-)} - (\hat{r} \times \vec{P}) \cdot \Sigma_{(+)}\Big) \Xi_{(-)}^+ \Bigg] |i\rangle \end{aligned} \tag{5.2.12}$$

for an isoscalar photon, and

$$\begin{aligned} C_{\rm NS}^{(1)} = -\frac{\pi}{\sqrt{2}} \frac{g_A}{2M_N} \sum_{a<b} \langle f| \Bigg[&\Big(2(\hat{r} \times \vec{p}_r) \cdot \Sigma_{(+)} - (\hat{r} \times \vec{P}) \cdot \Sigma_{(-)} + \frac{\mu_v}{3r}(4\sigma_a \cdot \sigma_b + S_{ab})\Big) T_{2,1} \\ &+ \Big(2(\hat{r} \times \vec{p}_r) \cdot \Sigma_{(-)} - (\hat{r} \times \vec{P}) \cdot \Sigma_{(+)}\Big) T_{1,1} \Bigg] |i\rangle \end{aligned} \tag{5.2.13}$$

for an isovector photon. These are standard two-body operators which can be evaluated in a shell model using a two-body density matrix. The matrix elements of these operators between simple harmonic oscillator basis states is simple to compute.

5.3 Two-Body Correction to Gamow Teller Transitions

We now want to do the same calculation that was presented in [Tow92] for Fermi transitions, but apply it to Gamow-Teller transitions. In the end, we once again find simple two-body operators which can again be implemented in a shell model calculation. These are no longer scalar operators, but spin one operators. This means we need to be a bit careful about computing reduced matrix elements instead of simple matrix elements.

As usual, we start with the anti-symmetric part of the box diagram Equation 4.0.5. Once again we ignore external lepton momentum. We make the same approximations as [JR90] and [Tow92] and use the hadronic covariant in Equation 5.0.6 to separate out the two-body part.

$$\mathcal{J}_\beta = -i8\pi^2 \int \frac{d^4k}{(2\pi)^4}(2\pi)\delta(k^0)\frac{\varepsilon_{\mu\lambda\alpha\beta}k^\alpha}{(k^2+i\epsilon)^2}\left\langle f|\tilde{J}^\mu_{em}(-\vec{k})\tilde{J}^\lambda_W(\vec{k})|i\right\rangle\Big|_{\text{2-body}} \tag{5.3.1}$$

The $\delta(k^0)$ means we only have the space components of k available, so α is a spacial index. For the Gamow-Teller transition, we take the space components of the lepton matrix element. Therefore β is also a spacial index. The Levi-Civita symbol forces one of μ, λ to be a time index. We have two choices - either $\mu = 0$ or $\lambda = 0$.

$$\mathcal{J}^i = -i8\pi^2 \int \frac{d^3k}{(2\pi)^3}\frac{\epsilon^{ijk}k^j}{(|\vec{k}|^2-i\epsilon)^2}\left(\left\langle f|\tilde{J}^k_{em}(-\vec{k})\tilde{J}^0_W(\vec{k})|i\right\rangle - \left\langle f|\tilde{J}^0_{em}(-\vec{k})\tilde{J}^k_W(\vec{k})|i\right\rangle\right)\Big|_{\text{2-body}} \tag{5.3.2}$$

And then the two-body nuclear structure correction $C^{\text{GT}}_{\text{NS}}$ is given by taking the reduced matrix element.

$$C^{\text{GT}}_{\text{NS}} = -\frac{\langle|\vec{\mathcal{J}}|\rangle}{g_A\langle|\mathbf{GT}|\rangle} \tag{5.3.3}$$

The Fermi operator is a scalar, so we didn't need to bother with the reduced matrix element. However, the Gamow-Teller operator is spin 1, and this requires we take the reduced matrix element.

In the case of Fermi transitions, the two-body operators we found involved three different operator structures. Similarly for Gamow-Teller transitions, we will end up with three different operator structures - an orbital angular momentum part (l), a spin part (σ), and a tensor part (t). We now want to show how this works in detail, in analogy with the presentation in [Tow92].

Now we plug in the non-relativistic currents as before.

$$\begin{aligned} J^0_{em}(\vec{x}) &= \sum_a \hat{e}_a\delta^3(\vec{x}-\vec{x}_a) \\ J^i_{em}(\vec{x}) &= \frac{1}{2M_N}\sum_a \hat{e}_a\{p^i_a,\delta^3(\vec{x}-\vec{x}_a)\} - i\hat{\mu}_a\epsilon^{ilm}[p^l_a,\delta^3(\vec{x}-\vec{x}_a)]\sigma^m_a \end{aligned} \tag{5.3.4}$$

This time, we use the vector part of the weak current. We also use CVC which we discussed in Section 1.2. This says that the weak vector form factors are equal to the isovector electromagnetic form factors.

$$\begin{aligned} J^0_W(\vec{x}) &= \sum_a \delta^3(\vec{x}-\vec{x}_a)\tau_a^+ \\ J^i_W(\vec{x}) &= \frac{1}{2M_N}\sum_a \left[\{p_a^i, \delta^3(\vec{x}-\vec{x}_a)\} - i\mu_v\epsilon^{ilm}[p_a^l, \delta^3(\vec{x}-\vec{x}_a)]\sigma_a^m\right]\tau_a^+ \end{aligned} \tag{5.3.5}$$

Note that the term here proportional to μ_v is the contribution from weak magnetism. Just as in the case of $C^{\rm GT}_{\rm Born}$, we will find that weak magnetism provides the dominant contribution to $C^{\rm GT}_{\rm NS}$.

As before, we use the fact that $\vec{p}_a \times \vec{k}$ commutes with the exponential $e^{i\vec{k}\cdot\vec{x}_a}$, so we can factor out the exponentials without worrying about the operator ordering.

$$\begin{aligned} \mathcal{J}^i &= -i\frac{8\pi^2}{2M_N}\int \frac{d^3k}{(2\pi)^3}\frac{\epsilon^{ijk}k^j}{(|\vec{k}|^2-i\epsilon)^2} \\ &\times\left(\langle f|\sum_{a\neq b} e^{-i\vec{k}\cdot\vec{r}}\left[4p_r^k\hat{e}_a + i\mu_v\epsilon^{klm}k^l\sigma_b^m\hat{e}_a + i\epsilon^{klm}k^l\sigma_a^m\hat{\mu}_a\right]\tau_b^+|i\rangle\right) \end{aligned} \tag{5.3.6}$$

where we set $\vec{r} = \vec{x}_a - \vec{x}_b$ and $\vec{p}_r = \frac{1}{2}(\vec{p}_a - \vec{p}_b)$ as before. We combine the Levi-Civita symbol with the currents and use the usual contraction identity.

$$\begin{aligned} \vec{\mathcal{J}} &= \frac{8\pi^2}{2M_N}\int \frac{d^3k}{(2\pi)^3}\frac{1}{(|\vec{k}|^2-i\epsilon)^2} \\ &\times\left(\langle f|\sum_{a\neq b} e^{-i\vec{k}\cdot\vec{r}}\left[-i4\vec{k}\times\vec{p}_r\hat{e}_a + \mu_v\left(\vec{k}(\vec{k}\cdot\vec{\sigma}_b) - |\vec{k}|^2\vec{\sigma}_b\right)\hat{e}_a + \hat{\mu}_a\left(\vec{k}(\vec{k}\cdot\vec{\sigma}_a) - |\vec{k}|^2\vec{\sigma}_a\right)\right]\tau_b^+|i\rangle\right) \end{aligned} \tag{5.3.7}$$

Do the integral over k assuming no form factor using the same integrals Equation 5.2.6 and we find.

$$\begin{aligned} \vec{\mathcal{J}} = -\frac{\pi}{2M_N}\Bigg(\langle f|\sum_{a\neq b}\frac{1}{r}\Big[&4\vec{r}\times\vec{p}_r\hat{e}_a + \mu_v\left(\vec{\sigma}_b + \hat{r}(\hat{r}\cdot\vec{\sigma}_b)\right)\hat{e}_a \\ &+\hat{\mu}_a\left(\vec{\sigma}_a + \hat{r}(\hat{r}\cdot\vec{\sigma}_a)\right)\Big]\tau_b^+|i\rangle\Bigg) \end{aligned} \tag{5.3.8}$$

Lets pause here and examine the operator structures which are present. First, we clearly have a term which involves the orbital angular momentum, $\vec{r}\times\vec{p}_r = \vec{l}_r$. This is to be expected, since the underlying Gamow-Teller operator is a spin operator. Similarly, we have a term which is just the spin, $\vec{\sigma}$. This term will become particularly important, since it has exactly the same structure as the tree-level matrix element. Any transition which can be mediated

by the Gamow-Teller operator will pick up a correction from this term. And finally, we have a tensor operator.

$$\hat{r}(\hat{r}\cdot\vec{\sigma})-\frac{1}{3}\vec{\sigma} \tag{5.3.9}$$

This is written in such a way that is proportional to the spherical harmonic $Y_2(\hat{r})$. The applicability of this term is thus limited by the orbital angular momentum of the initial and final states.

As before, we want to write this in a form which respects the exchange symmetry $a \leftrightarrow b$. Therefore we combine this with the term with a and b swapped, and write the sum over $a < b$.

$$\begin{aligned}\vec{\mathcal{J}} = -\frac{\pi}{2M_N}\Bigg(\langle f| \sum_{a<b} \frac{1}{r}\Big[& 4(\hat{e}_a\tau_b^+ + \hat{e}_b\tau_a^+)\vec{r}\times\vec{p}_r \\ & +(\mu_v\hat{e}_b\tau_a^+ + \hat{\mu}_a\tau_b^+)\Big(\vec{\sigma}_a + \hat{r}(\hat{r}\cdot\vec{\sigma}_a)\Big) \\ & +(\mu_v\hat{e}_a\tau_b^+ + \hat{\mu}_b\tau_a^+)\Big(\vec{\sigma}_b + \hat{r}(\hat{r}\cdot\vec{\sigma}_b)\Big)\Big]\,|i\rangle \Bigg)\end{aligned} \tag{5.3.10}$$

As before, we split the contribution into an isovector photon and an isoscalar photon. We also write this in terms of the variables with proper exchange symmetry Equation 5.2.10. For an isoscalar photon, we have

$$\begin{aligned}\vec{\mathcal{J}}^{(0)} = -\frac{\pi}{2M_N}\Bigg(\langle f| \sum_{a<b} \frac{1}{r}\Big[& 4\vec{r}\times\vec{p}_r\Xi^+_{(+)} \\ & +(\mu_s+\mu_v)\Big(\vec{\Sigma}_{(+)} + \hat{r}(\hat{r}\cdot\vec{\Sigma}_{(+)})\Big)\Xi^+_{(+)} \\ & +(\mu_v-\mu_s)\Big(\vec{\Sigma}_{(-)} + \hat{r}(\hat{r}\cdot\vec{\Sigma}_{(-)})\Big)\Xi^+_{(-)}\Big]\,|i\rangle \Bigg)\end{aligned} \tag{5.3.11}$$

And for an isovector photon, we have

$$\vec{\mathcal{J}}^{(1)} = \frac{\pi}{M_N}\Bigg(\langle f| \sum_{a<b} \frac{1}{r}\Big[2\vec{r}\times\vec{p}_r + \mu_v\Big(\vec{\Sigma}_{(+)} + \hat{r}(\hat{r}\cdot\vec{\Sigma}_{(+)})\Big)\Big]T_{2,1}\,|i\rangle \Bigg) \tag{5.3.12}$$

Comparing this to the tree-level amplitude, we find the two-body correction

$$\begin{aligned}C_{\rm NS}^{\rm GT} = \frac{1}{g_A\langle|\mathbf{GT}|\rangle}\frac{\pi}{2M_N}\Bigg(\langle f|| \sum_{a<b} \frac{1}{r}\Big[& 4\vec{r}\times\vec{p}_r\Xi^+_{(+)} \\ & +(\mu_s+\mu_v)\Big(\vec{\Sigma}_{(+)} + \hat{r}(\hat{r}\cdot\vec{\Sigma}_{(+)})\Big)\Xi^+_{(+)} \\ & +(\mu_v-\mu_s)\Big(\vec{\Sigma}_{(-)} + \hat{r}(\hat{r}\cdot\vec{\Sigma}_{(-)})\Big)\Xi^+_{(-)} \\ & -4\vec{r}\times\vec{p}_r T_{2,1} \\ & -2\mu_v\Big(\vec{\Sigma}_{(+)} + \hat{r}(\hat{r}\cdot\vec{\Sigma}_{(+)})\Big)T_{2,1}\Big]\,||i\rangle \Bigg)\end{aligned} \tag{5.3.13}$$

As far as I can tell from looking in the literature, this is a new result. It is analogous to the formula we found for the two-body correction to Fermi transitions.

We can also easily check how this calculation is modified by the nucleon form factors. First, note that this calculation only involves the vector part of the weak current. Therefore we only need the vector form factors $F_{1,2}$. We assume a single dipole form factor with $\Lambda_V = 0.84$ GeV. This is a decent approximation, as we can see in Appendix A. By using the dipole form factors, we get an analytic result for the loop momentum integral. The integrals in Equation 5.2.6 get modified by functions $f(\Lambda r)$.

$$\begin{aligned}
\int \frac{d^3k}{(2\pi)^3}\frac{e^{-i\vec{k}\cdot\vec{r}}}{(|\vec{k}|^2 - i\epsilon)^2}\left(\frac{\Lambda^2}{\Lambda^2+k^2}\right)^4 k^i &= \frac{-i}{8\pi}\frac{r^i}{r}f_l(\Lambda r) \\
\int \frac{d^3k}{(2\pi)^3}\frac{e^{-i\vec{k}\cdot\vec{r}}}{(|\vec{k}|^2 - i\epsilon)^2}\left(\frac{\Lambda^2}{\Lambda^2+k^2}\right)^4 k^i k^j &= \frac{1}{8\pi r}\left(\frac{2}{3}\delta^{ij}f_\sigma(\Lambda r) + (\frac{1}{3}\delta^{ij} - \hat{r}^i\hat{r}^j)f_t(\Lambda r)\right) \\
\int \frac{d^3k}{(2\pi)^3}\frac{e^{-i\vec{k}\cdot\vec{r}}}{(|\vec{k}|^2 - i\epsilon)^2}\left(\frac{\Lambda^2}{\Lambda^2+k^2}\right)^4 |\vec{k}|^2 &= \frac{1}{4\pi r}f_\sigma(\Lambda r)
\end{aligned} \tag{5.3.14}$$

The functions f_l, f_σ, and f_t modify the orbital angular momentum, spin, and tensor operators respectively. These are straightforward to work out.

$$\begin{aligned}
f_l(x) &= 1 - \frac{8}{x^2} + \frac{e^{-x}(192+192x+72x^2+13x^3+x^4)}{24x^2} \\
f_\sigma(x) &= 1 - \frac{e^{-x}(48+33x+9x^2+x^3)}{48} \\
f_t(x) &= 1 - \frac{24}{x^2} + \frac{e^{-x}(576+576x+264x^2+72x^3+12x^4+x^5)}{24x^2}
\end{aligned} \tag{5.3.15}$$

Each of these functions go to $f(x) \to 1$ as we let $\Lambda \to \infty$. They serve to regulate the $1/r$ divergence at the origin, and smooth it out to a constant. This can be seen in Figure 5.8. These are not independent, but satisfy $f_\sigma = \frac{1}{2}(3f_l - f_t)$. The reason I give them three different names is that these are the functions which correspond to the respective operator structure.

We separate out the three different operators and how they contribute to $C_{\rm NS}^{\rm GT}$. For the orbital angular momentum operator, we have

$$C_{\rm NS}^{\rm GT}(l) = \frac{1}{g_A\langle|\mathbf{GT}|\rangle}\frac{2\pi}{M_N}\left(\langle f||\sum_{a<b}\frac{f_l(\Lambda r)}{r}\vec{r}\times\vec{p}_r\left[\Xi^+_{(+)} - T_{2,1}\right]||i\rangle\right) \tag{5.3.16}$$

For the spin operator, we have

$$\begin{aligned}
C_{\rm NS}^{\rm GT}(\sigma) = \frac{1}{g_A\langle|\mathbf{GT}|\rangle}\frac{2\pi}{3M_N}\Bigg(\langle f||\sum_{a<b}\frac{f_\sigma(\Lambda r)}{r}\Big[&(\mu_s+\mu_v)\vec{\Sigma}_{(+)}\Xi^+_{(+)} - (\mu_s-\mu_v)\vec{\Sigma}_{(-)}\Xi^+_{(-)} \\
&-2\mu_v\vec{\Sigma}_{(+)}T_{2,1}\Big]||i\rangle\Bigg)
\end{aligned} \tag{5.3.17}$$

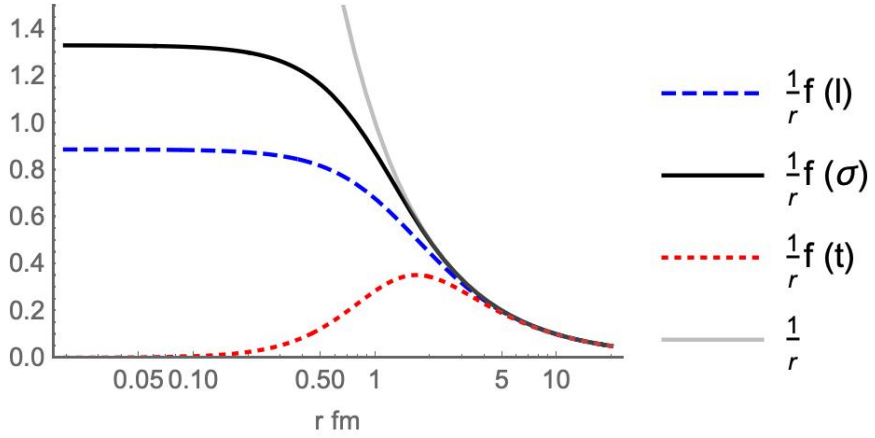

Figure 5.8: Form factors for the three operator structures in $C_{\rm NS}^{\rm GT}$ with dipole mass $\Lambda = 0.84$ GeV.

And finally the tensor part which is proportional to the spherical harmonic $Y_2(\hat{r})$ is given by

$$C_{\rm NS}^{\rm GT}(t) = \frac{1}{g_A\langle|\mathbf{GT}|\rangle}\frac{\pi}{2M_N}\Bigg(\langle f||\sum_{a<b}\frac{f_t(\Lambda r)}{r}\Big[(\mu_s+\mu_v)\Big(\hat{r}(\hat{r}\cdot\vec{\Sigma}_{(+)})-\frac{1}{3}\vec{\Sigma}_{(+)}\Big)\Xi^+_{(+)} \\ +(\mu_v-\mu_s)\Big(\hat{r}(\hat{r}\cdot\vec{\Sigma}_{(-)})-\frac{1}{3}\vec{\Sigma}_{(-)}\Big)\Xi^+_{(-)} \\ -2\mu_v\Big(\hat{r}(\hat{r}\cdot\vec{\Sigma}_{(+)})-\frac{1}{3}\vec{\Sigma}_{(+)}\Big)T_{2,1}\Big]||i\rangle\Bigg) \tag{5.3.18}$$

We will apply these formulas to proton-proton fusion in Section 7 to find a new contribution to the radiative corrections.

5.4 Further Modifications

The key to deriving the results of this section goes back to our assumption that we could ignore the nuclear energy excitation ΔE_n in Equation 5.0.1. This allowed us to remove the intermediate states using the completeness relation.

$$\sum_n |n\rangle\langle n| = 1 \tag{5.4.1}$$

Then the current operators were able to hit each other and be normal ordered. This step is required in order to separate out the two-body part.

Without that assumption, the one-body currents essentially pick up many-body corrections from the many-body Hamiltonian through the Heisenberg time evolution.

$$J(t) = e^{iHt}J_{\text{one-body}}e^{-iHt} \tag{5.4.2}$$

Or, equivalently, we have intermediate nuclear states in Equation 5.0.1 which act as an obstruction between the two current operators. The point is we can no longer simply pick out a two-body part, as we have done here. We will discuss the consequences of this in Sections 8 and 9.

For now, let us now discuss how $C_{\rm NS}$ is calculated for the determination of V_{ud}, such as in [HT15]. The results from this section are evaluated in the nuclear shell model. The states in the nuclear shell model are many-body states which are totally anti-symmetric. We can express them using a basis of single particle states $\phi_n(x)$ with a *Slater determinant*.

$$\Psi_{n_1,\ldots,n_A} = \begin{vmatrix} \phi_{n_1}(1) & \ldots & \phi_{n_1}(A) \\ \vdots & & \vdots \\ \phi_{n_A}(1) & \ldots & \phi_{n_A}(A) \end{vmatrix} \tag{5.4.3}$$

These shell models have a small model space in order to make the calculations tractable. We typically assume a fixed, inert core, and only a small number of active shells with valence nuclei.

We would like to pick the single particle wavefunctions $\phi_n(x)$ to minimize the interactions between nucleons. However, a more convenient choice is to let $\phi_n(x)$ be simple harmonic oscillator wavefunctions. These states have the unique property that they can be transformed into relative coordinates using the Moshinsky brackets.

$$|n_1 l_1(x_1), n_2 l_2(x_2), \Lambda\rangle = \sum_{NLnl} \langle NL, nl, \Lambda | n_1 l_1, n_2 l_2, \Lambda\rangle \, |NL(R), nl(r), \Lambda\rangle \tag{5.4.4}$$

Then all we need to do is compute matrix elements of the two-body operators between simple harmonic oscillator states, which is very straightforward.

There is at least one major problem with the strategy we outlined above. There are very strong, repulsive forces which keep nucleons apart at short distances. This involves high momentum components of the wavefunction which are left out of shell model calculations. These neglected high momentum components will have several consequences.

First, we need to account for the missing short range correlations between nucleons. Typically, one introduces a phenomenological correlation function to reproduce the effect of the short-range core.

$$\psi(\vec{r}_i, \vec{r}_j) \to (1 - \beta(r_{ij}))\psi(\vec{r}_i, \vec{r}_j) \tag{5.4.5}$$

In [Tow92], they modify Equations 5.2.12 and 5.2.13 by a simple hard cut-off at short distances.

$$\beta(r) = \theta(d - r), \quad d = 0.7 \text{ fm} \tag{5.4.6}$$

More sophisticated correlation functions can also be used for the same effect, for example that introduced by Miller and Spencer [MS76].

$$\beta(r) = e^{-ar^2}(1 - br^2) \tag{5.4.7}$$

with $a = 1.1$ fm^{-2} and $b = 0.68$ fm^{-2} [HS84].

In general, when we are dealing with a model space which excludes part of the Hilbert space, the current operators we used to derive Equations 5.2.12 and 5.2.13 should be replaced by *effective operators*. These effective operators would account for the missing part of the Hilbert space, and are typically fit to reproduce the correct matrix elements. In the limit that the model space expands to include the entire Hilbert space, these effective operators would get replaced by the bare operators.

In the case of the Gamow-Teller and M1 operators, it is known that the effective operators in small shell model spaces are reduced to about 80% of their bare values [Tow87][BW88]. This is known as the *quenching* of the GT and M1 operators. The effective M1 operator can be written as [Tow94]

$$\vec{\mu}^{(I)}_{\text{eff}} = g^{(I)}_{\text{L,eff}}\vec{L} + g^{(I)}_{\text{S,eff}}\vec{S} + g^{(I)}_{\text{P,eff}}[Y_2 \otimes S]_1 \tag{5.4.8}$$

The tensor term is not present in the bare one-body operator. Similarly we can write the GT matrix elements as

$$(\text{GT})_{\text{eff}} = g_{\text{LA,eff}}\vec{L} + g_{\text{A,eff}}\vec{\sigma} + g_{\text{PA,eff}}[Y_2 \otimes \sigma]_1 \tag{5.4.9}$$

The difference between the effective value and the "free-nucleon" value is called the *quenching factor*.

$$q = g_{\text{eff}}/g \tag{5.4.10}$$

In [Tow87], the quenching factors in the nuclear medium are calculated for nuclei with a closed shell plus one particle/hole, keeping second order core polarization corrections, MECs, and isobars. Those calculations were then interpolated/extrapolated to other nuclei. These effects cause a reduction in the GT and M1 matrix elements from their free nucleon values. The results are given in Table 5.1 from [Tow94]. However experimental values for the quenching are even more dramatic with $q_A \approx 0.77$ in [BW88].

	$q^{(0)}_{\text{L}}$	$q^{(0)}_{\text{S}}$	$q^{(1)}_{\text{L}}$	$q^{(1)}_{\text{S}}$	q_{A}
$A = 10$	1.042	0.897	1.173	0.927	0.878
$A = 14$	1.044	0.873	1.201	0.934	0.858
$A = 26$	1.023	0.869	1.146	0.877	0.835
$A = 34$	1.026	0.850	1.155	0.870	0.812
$A = 38$	1.028	0.840	1.159	0.866	0.801
$A = 42$	1.010	0.862	1.133	0.866	0.824
$A = 46$	1.010	0.857	1.137	0.862	0.818
$A = 50$	1.011	0.853	1.141	0.857	0.812
$A = 54$	1.011	0.849	1.145	0.854	0.807

Table 5.1: Calculated quenching factors using an interpolation/extrapolation for various nuclear masses from [Tow94]

In [Tow94], they use these quenching factors to recompute the two-body part of $C_{\rm NS}$. He also argues that the Born term Equation 4.1.24 should also be modified by the product of quenching factors.

$$\begin{aligned} C_{\rm Born}(\text{quenched}) &= q_A q_S^{(0)} C_{\rm Born}(\text{free}) \\ &= C_{\rm Born}(\text{free}) + (q_A q_S^{(0)} - 1) C_{\rm Born}(\text{free}) \end{aligned} \tag{5.4.11}$$

The second term in the last line then is combined with the two-body part to become the full nuclear structure correction, $\delta_{\rm NS}$ [TH02].

This argument was recently challenged in [SGR19]. The issue they raise is that these quenching factors are derived only for low-lying nuclear transitions. The quenching does not represent a reduction in the overall strength, but a shift from low-lying states to higher in the spectrum. The assumption that we are dealing only with low-lying states is violated in the case of the Born correction $C_{\rm Born}$.

Consider what happens when the currents latch onto the same nucleon. In this case, the energy transfer peaks at the single nucleon energy $\omega \sim Q^2/2M_N$. This corresponds to the quasi-elastic (QE) response, which is at a much higher energy than the low lying states. There is a wealth of QE electron-nucleus scattering data which indicates that, to first approximation, one gets an adequate description of the QE response using free-nucleon form factors with no quenching applied.

In [SGR19], they argue for a new approach. Rather than separate the correction into a one-body and two-body part, they argue we should separate out the low-momentum transfer part $k < 2k_F$ from the high-momentum part. The high-momentum part can then be identified with the quasi-elastic contribution, and can be calculated using free-nucleon form factors.

They calculate the quasi-elastic Born term using a modification of Equation 4.1.5 in which they allow the nucleons in to have some momentum distribution.

$$T^{\mu\lambda}_{\rm QE}(P,k) = \sum_a \tau_a^+ \int \frac{d^3p'}{(2\pi)^3} |\phi(p')|^2 f_P T^{\mu\lambda}_{\rm Born}(p',k) \tag{5.4.12}$$

They take the momentum distribution $\phi(p')$ to be a simple free Fermi gas, with a modification f_P for Pauli blocking when $|\vec{k}| < 2k_F$.

$$f_P(|\vec{k}|, k_F) = \frac{3|\vec{k}|}{4k_F}\left[1 - \frac{|\vec{k}|^2}{12k_F^2}\right] \quad \text{for} \quad |\vec{k}| < 2k_F \tag{5.4.13}$$

and $f_P = 1$ for $|\vec{k}| > 2k_F$. Their result represents a modification of the Born term by the nuclear environment.

$$C_{\rm QE} = 0.44 \pm 0.14 \tag{5.4.14}$$

This is a reduction of the free Born term by about 50%. It is interesting that the end result is about the same as the quenching factor approach in [Tow94], but the reasoning is completely

different. However, keep in mind that the low-momentum part $|\vec{k}| < 2k_F$ now involves both one-body and two-body contributions. It is this part of the correction which we wish to tackle in the next section with a new approach.

Chapter 6

Nuclear Interaction - Av18 Potential

In order to do the calculations of $C_{\rm NS}$ in the following sections, we need to be able to construct wavefunctions for the deuteron and for scattering states. For the two-body nuclear Hamiltonian in the nn, np, and pp channels, we use the Argonne v_{18} potential [WSS95], or Av18 for short. This potential is an improvement on the previous Argonne v_{14} [WSA84] potential in that it includes charge-dependent terms which violate isospin symmetry.

The wavefunction for the two body system with definite total spin s and parity $(-1)^l$ is represented in coordinate space using the coupled $(ls)j$ spinor.

$$\psi = \sum_l R_l(r)\Psi_{ls}^{jm}(\hat{r}) \tag{6.0.1}$$

Here $R_l(r)$ is the radial wavefunction in the l channel. The allowed values of l are determined by the triangle inequality $|l-s| \le j \le |l+s|$ and the parity $(-1)^l$. Since the two nucleons must get a total minus sign under exchange symmetry, the isospin is related to the spin s and the parity by

$$(-1)^{t+s+l} = -1 \quad \text{fermion antisymmetry} \tag{6.0.2}$$

For example, the ${}^1S_0$ channel has $l=0$ and $s=0$, and therefore must have isospin $t=1$. The coupled spinor is an angular momentum coupling of the ordinary spherical harmonic $Y_{lm}(\hat{r})$ and the spin wavefunction χ_{s,m_s}

$$\Psi_{ls}^{jm} = \sum_{m_l,m_s} C^{jm}_{lm_lSm_s} Y_{lm_l}(\hat{r})\chi_{sm_s} \tag{6.0.3}$$

In order to make the Schrodinger equation more simple, we will usually use the *spherical wave function* instead of the ordinary radial wavefunction.

$$\psi(\vec{r}) = \sum_l \frac{1}{r} u(r)\Psi_{ls}^{jm}(\hat{r}) \tag{6.0.4}$$

This wavefunction has the nice property that the Laplacian operator looks like the simple one-dimensional kinetic energy, plus a term for the centrifugal potential which depends on l.

$$-\nabla^2\psi = \sum_l \frac{1}{r}\left(-\frac{d^2}{dr^2} + \frac{l(l+1)}{r^2}\right) u(r)\Psi_{ls}^{jm}(\hat{r}) \tag{6.0.5}$$

Coordinate Form of the Potential

The coordinate form of the Av18 potential is broken up into three pieces. There is the electromagnetic interaction, V_{EM}, the one pion exchange potential, V_π, and a short range part which is fitted from the phase shifts, V_R.

$$V^i_{ST} = V^i_{\mathrm{EM},ST} + V^i_{\pi,ST} + V^i_{R,ST} \tag{6.0.6}$$

The electromagnetic potential is naturally very different in the pp channel versus the np and nn channels. In the pp-channel, the electromagnetic potential is taken from an analysis done by [Sto+93]. We have five different terms in the electromagnetic potential.

$$v^{\mathrm{EM}}(pp) = V_{C1}(pp) + V_{C2} + V_{DF} + V_{VP} + V_{MM}(pp) \tag{6.0.7}$$

These represent the contributions from one- and two-photon Coulomb terms, the Darwin-Foldy term, vacuum polarization, and the magnetic moment interaction. We also include form factors to represent the finite size of the nucleons. These are shown in Figure 6.1.

$$\begin{aligned}
V_{C1}(pp) &= \alpha' \frac{F_C(r)}{r} \\
V_{C2} &= -\frac{\alpha}{2M_p^2}\left[(\nabla^2 + k^2)\frac{F_C(r)}{2} + \frac{F_C(r)}{r}(\nabla^2 + k^2)\right] \approx -\frac{\alpha\alpha'}{M_p}\left[\frac{F_C(r)}{r}\right]^2 \\
V_{DF} &= -\frac{\alpha}{4M_p^2} F_\delta(r) \\
V_{VP} &= \frac{2\alpha\alpha'}{3\pi}\frac{F_C(r)}{r}\int_1^\infty dx\, e^{-2m_e r x}\left[1 + \frac{1}{2x^2}\right]\frac{\sqrt{x^2-1}}{x^2} \\
V_{MM}(pp) &= -\frac{\alpha}{4M_p^2}\mu_p^2\left[\frac{2}{3}F_\delta(r)\sigma_i\cdot\sigma_j + \frac{F_t(r)}{r^3}S_{ij}\right] - \frac{\alpha}{2M_p^2}(4\mu_p - 1)\frac{F_{ls}(r)}{r^3}L\cdot S
\end{aligned} \tag{6.0.8}$$

Here α' is an energy dependent modification of the fine structure constant.

$$\alpha' = \frac{2k\alpha}{M_p v_{\mathrm{lab}}} \tag{6.0.9}$$

Keep in mind the V_{C1} term gives us the long range $1/r$ Coulomb interaction. The presence of this term forces us to work with the Coulomb wavefunctions and use the Coulomb phase shifts.

The functions $F_C(r)$, $F_\delta(r)$, $F_l(r)$, and $F_{ls}(r)$ are form factors which regulate the interactions at short distance. They are plotted in Figure 6.1, and the full form is given in [WSS95]. The vacuum polarization term involves an integral, which can be expressed in terms of the very general Meijer G-function. This form can be directly implemented in computer algebra systems like Mathematica. However, the numerical evaluation of this function is very slow. It is much more efficient to use a polynomial approximation, as long as it's valid for the

range of r we are interested in. For $r \lesssim 100$ fm, we get a good approximation using only a second order polynomial.

$$\begin{aligned} &\int_1^\infty dx\, e^{-ax}\left[1+\frac{1}{2x^2}\right]\frac{\sqrt{x^2-1}}{x^2} \\ &\approx -\log(a) - \frac{3a(a-\pi)}{8} - \frac{5}{6} + \log(2) - \gamma \end{aligned} \tag{6.0.10}$$

where $a = 2m_e r$, and $\gamma \approx 0.577$ is the Euler-Mascheroni constant.

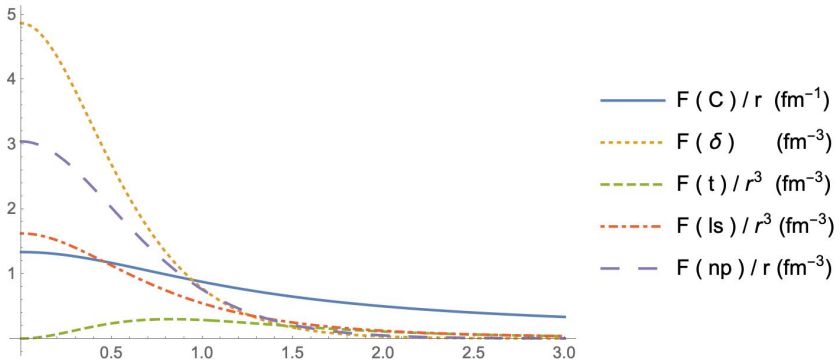

Figure 6.1: Form factors from [WSS95] used in the Av18 potential.

In the np- channel, the electromagnetic potential consists of two terms

$$v^{\mathrm{EM}}(np) = V_{C1}(np) + V_{MM}(np) \tag{6.0.11}$$

The coulomb term is due to the neutron charge distribution.

$$V_{C1}(np) = \alpha\beta_n \frac{F_{np}(r)}{r} \tag{6.0.12}$$

The function $F_{np}(r)$ dies off exponentially past $r \sim 1$ fm. The magnetic interaction is given by

$$\begin{aligned} V_{MM}(np) = &-\frac{\alpha}{4M_nM_p}\mu_n\mu_p\left[\frac{2}{3}F_\delta(r)\sigma_i\cdot\sigma_j + \frac{F_t(r)}{r^3}S_{ij}\right] \\ &-\frac{\alpha}{2M_nM_r}\mu_n\frac{F_{ls}(r)}{r^3}(L\cdot S + L\cdot A) \end{aligned} \tag{6.0.13}$$

where M_r is the reduced mass. The term $\vec{A} = \frac{1}{2}(\sigma_i - \sigma_j)$ mixes spin-singlet and spin triplet states. Its contribution is very small, and we do not include it except for the magnetic moment scattering amplitude.

Finally, for nn scattering we only have the magnetic moment term.

$$v^{\mathrm{EM}}(nn) = V_{MM}(nn) = -\frac{\alpha}{4M_n^2}\mu_n^2\left[\frac{2}{3}F_\delta(r)\sigma_i\cdot\sigma_j + \frac{F_t(r)}{r^3}S_{ij}\right] \tag{6.0.14}$$

The one pion exchange potential (OPEP) is also taken from [Sto+93]. It is given by

$$\begin{aligned} v^\pi(pp) &= f^2 v_\pi(m_{\pi^0}) \\ v^\pi(np) &= -f^2 v_\pi(m_{\pi^0}) + (-1)^{T+1} 2 f^2 v_\pi(m_{\pi^\pm}) \\ v^\pi(nn) &= f^2 v_\pi(m_{\pi^0}) \end{aligned} \tag{6.0.15}$$

Following [WSS95], we take a charge independent value of the pion form factor with $f^2 = 0.075$. The pion potential depends on the mass of the pion, which is either m_{π^0} or $m_{\pi^\pm}$.

$$v_\pi(m) = \left(\frac{m}{m_s}\right)^2 \frac{1}{3} m[Y(m,r)\sigma_i\cdot\sigma_j + T(m,r)S_{ij}] \tag{6.0.16}$$

The "scaling mass" $m_s = m_{\pi^\pm}$ is taken to be the charged pion mass, and its role is only to make the constant f dimensionless. The Yukawa functions $Y(m,r)$ and $T(m,r)$ are given by

$$\begin{aligned} Y(m,r) &= \frac{e^{-mr}}{mr}\left(1 - e^{-cr^2}\right) \\ T(m,r) &= \left(1 + \frac{3}{mr} + \frac{3}{m^2r^2}\right)\frac{e^{-mr}}{mr}\left(1 - e^{-cr^2}\right)^2 \end{aligned} \tag{6.0.17}$$

The remaining part of the potential is the short range potential, $v_{ST}^R(NN)$. It involves parameters which are fitted from the phase shifts, and it involves the five different angular momentum operators. In the NN channel with spin S and isospin T, it is given by

$$v_{ST}^R(NN) = v_{ST,NN}^c(r) + v_{ST,NN}^{l2}(r)L^2 + v_{ST,NN}^t(r)S_{ij} + v_{ST,NN}^{ls}(r)L\cdot S + v_{ST,NN}^{ls2}(r)(L\cdot S)^2 \tag{6.0.18}$$

Each of the coordinate functions is parameterized by the following functional form.

$$v_{ST,NN}^i(r) = I_{ST,NN}^i T(\mu,r)^2 + [P_{ST,NN}^i + \mu r Q_{ST,NN}^i + (\mu r)^2 R_{ST,NN}^i]W(r) \tag{6.0.19}$$

Here μ is the average of the pion masses $\mu = \frac{1}{2}(m_{\pi^0} + 2m_{\pi^\pm})$. The term T^2 has the range of the two-pion exchange potential. The function W is the Woods-Saxon function, which provides the short-range core.

$$W(r) = \left[1 + e^{(r-r_0)/a}\right]^{-1} \tag{6.0.20}$$

with $r_0 = 0.5$ fm and $a = 0.2$ fm.

The fitted parameters $I_{ST,NN}^i$, $P_{ST,NN}^i$, $Q_{ST,NN}^i$, and $R_{ST,NN}^i$ are not totally independent. In [WSS95], they impose an additional regularization condition at the origin. In coupled

channels, the fact that the $l = j - 1$ and $l = j + 1$ pieces have different behaviour at the origin can cause problems. We can fix this by forcing the tensor force to vanish at the origin.

$$v^t_{ST,NN}(r = 0) = 0 \tag{6.0.21}$$

For the other components, we use the fact that the nucleons are not point particles. As we approach $r \to 0$, we expect the potential to level off to a constant. Thus we also impose the condition

$$\left.\frac{\partial v^{i\neq t}_{ST,NN}}{\partial r}\right|_{r=0} = 0 \tag{6.0.22}$$

Lab Frame Kinematics

Before we move on, I wanted to make a note about center of mass and lab frame kinematics. The phase shifts are all given in the lab frame, but we will often work with the center of mass energy and relative momentum. The radial Schrodinger equation is written in terms of the center of mass momentum k.

$$(\nabla^2 + k^2)\psi = 2M_r V\psi \tag{6.0.23}$$

Where M_r is the usual reduced mass $M_r = \frac{m_1 m_2}{m_1+m_2}$.

The relativistic invariant CM energy is related to the individual particle energies by the standard relativistic invariant.

$$E^2_{\text{CM}} = (E_1 + E_2)^2 - |\vec{p}_1 + \vec{p}_2|^2 \tag{6.0.24}$$

In the CM frame, the energy can be calculated directly using the center of mass momentum k.

$$E_{\text{CM}} = \sqrt{m_1^2 + k^2} + \sqrt{m_2^2 + k^2} \tag{6.0.25}$$

In the lab frame, we set $\vec{p}_2 = 0$. Then the lab frame kinetic energy only comes from particle 1.

$$E_1 = m_1 + T_{\text{lab}} \tag{6.0.26}$$

In this frame, the CM energy is

$$\begin{aligned} E_{\text{CM}} &= \sqrt{(E_1 + m_2)^2 - |\vec{p}_1|^2} \\ &= \sqrt{(m_1 + m_2)^2 + 2m_2 T_{\text{lab}}} \end{aligned} \tag{6.0.27}$$

Equating these two and solving for k in terms of T_{lab}, we find

$$k^2 = \frac{m_2^2 T_{\text{lab}}(2m_1 + T_{\text{lab}})}{(m_1 + m_2)^2 + 2m_2 T_{\text{lab}}} \tag{6.0.28}$$

For np scattering with $m_1 = M_n$ and $m_2 = M_p$ we have

$$k^2 = \frac{M_p^2 T_{\text{lab}}(2M_n + T_{\text{lab}})}{(M_n + M_p)^2 + 2M_p T_{\text{lab}}} \tag{6.0.29}$$

and for *pp* scattering this is simply

$$k^2 = \frac{1}{2} M_p T_{\text{lab}} \tag{6.0.30}$$

Finally, in order to define the relativistic correction to the coulomb interaction, we also need the lab frame velocity v_{lab}.

$$v_{\text{lab}} = \sqrt{\frac{E_1^2 - m_1^2}{E_1^2}} = \frac{\sqrt{T_{\text{lab}}(2m_1 + T_{\text{lab}})}}{m_1 + T_{\text{lab}}} \tag{6.0.31}$$

For *pp* scattering this is

$$v_{\text{lab}} = \frac{2k}{M_p} \times \frac{\sqrt{1 + k^2/M_p^2}}{1 + 2k^2/M_p^2} \tag{6.0.32}$$

We will use this to define the so called "relativistic coulomb factor" [Bre55][Ber+88].

$$\eta' = \frac{\alpha}{v_{\text{lab}}} = \frac{\alpha M_p}{2k} \frac{1 + 2k^2/M_p^2}{\sqrt{1 + k^2/M_p^2}} \tag{6.0.33}$$

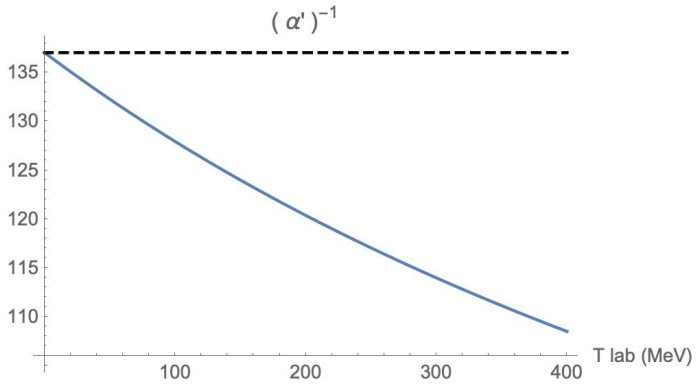

Figure 6.2: Energy dependent α' which accounts for relativistic corrections described in [Bre55] and [Ber+88]

Angular Momentum Operators

The Av18 potential depends on whether we are working in the *nn*, *np*, or *pp* channel. We pick some (s, t) and we can write the potential in terms of the coordinate functions V_{ST}^i times an operator $\mathcal{O}^i$.

$$V_{ST}^i \mathcal{O}^i \tag{6.0.34}$$

The operators will be one of the five following operators.

$$\mathcal{O}^i = \{1, L^2, S_{ij}, L \cdot S, (L \cdot S)^2\} \tag{6.0.35}$$

The action of the operators is simple to calculate, apart from the tensor term S_{ij}. Ordinary angular momentum operator algebra tells us the value of the other three operators. The all of the operators besides the tensor operator conserve orbital angular momentum.

$$\begin{aligned}\langle (l's)j|L^2|(ls)j\rangle &= l(l+1)\delta_{l,l'} \\ \langle (l's)j|L\cdot S|(ls)j\rangle &= \frac{1}{2}(j(j+1)-l(l+1)-s(s+1))\delta_{l,l'} \\ \langle (l's)j|(L\cdot S)^2|(ls)j\rangle &= \frac{1}{4}(j(j+1)-l(l+1)-s(s+1))^2\delta_{l,l'}\end{aligned} \tag{6.0.36}$$

The tensor operator mixes orbital angular momentum which differ by two units. For completeness, I will go through the derivation here. The tensor operator is defined as

$$S_{ij} = 3(\sigma_i\cdot\hat{r})(\sigma_j\cdot\hat{r}) - \sigma_i\cdot\sigma_j \tag{6.0.37}$$

This form hides the fact that it is actually the dot product of $j=2$ tensor products $[\sigma_i\otimes\sigma_j]_2$ and $[\hat{r}\otimes\hat{r}]_2$. The $j=2$ tensor product of two spin 1 vectors is given by the Clebsch-Gordan coefficients.

$$C^{2m}_{1s1r}a_s b_r = \begin{cases} a_1b_1 \\ \frac{1}{\sqrt{2}}(a_1b_0+a_0b_1) \\ \frac{1}{\sqrt{6}}(a_1b_{-1}+2a_0b_0+a_{-1}b_1) \\ \frac{1}{\sqrt{2}}(a_{-1}b_0+a_0b_{-1}) \\ a_{-1}b_{-1}\end{cases} \tag{6.0.38}$$

The $m=0$ term can be re-written using the scalar dot product $a\cdot b$

$$a_1b_{-1}+2a_0b_0+a_{-1}b_1 = 3a_0b_0 - a\cdot b \tag{6.0.39}$$

Using the form above, we can go through term by term and write down the general form of the dot product of two $j=2$ tensor products.

$$[a\otimes b]_2\cdot[c\otimes d]_2 = \frac{1}{2}(a\cdot c)(b\cdot d)+\frac{1}{2}(a\cdot d)(b\cdot c)-\frac{1}{3}(a\cdot b)(c\cdot d) \tag{6.0.40}$$

The tensor product $[\hat{r}\otimes\hat{r}]_2$ is related to the spherical harmonic Y_{2m},

$$\sqrt{\frac{4\pi}{5}}Y_{2m} = \sqrt{\frac{3}{2}}[\hat{r}\otimes\hat{r}]_{2m} \tag{6.0.41}$$

Putting this altogether, we can express the tensor operator as a dot product of a purely orbital piece and a purely spin piece.

$$S_{ij} = 3[\hat{r}\otimes\hat{r}]_2\cdot[\sigma_i\otimes\sigma_j]_2 = 3\sqrt{\frac{4\pi}{5}}\sqrt{\frac{2}{3}}Y_{2\cdot}\cdot[\sigma_i\otimes\sigma_j]_2 \tag{6.0.42}$$

The tensor product of the spin matrices can be computed using the standard tensor product formula from Edmonds.

$$\langle s'||[\sigma_1 \otimes \sigma_2]_2||s\rangle = \sqrt{5(2s'+1)(2s+1)} \begin{Bmatrix} 1/2 & 1/2 & 1 \\ 1/2 & 1/2 & 1 \\ s' & s & 2 \end{Bmatrix} \langle 1/2||\sigma||1/2\rangle^2 \tag{6.0.43}$$

This is only non-zero for $s = s' = 1$. Evaluate the $9-j$ symbol and use the fact that $\langle 1/2||\sigma||1/2\rangle = \sqrt{6}$ and we find

$$\langle 1||[\sigma_1 \otimes \sigma_2]_2||1\rangle = 2\sqrt{5} \tag{6.0.44}$$

The reduced matrix element of the spherical harmonic is a well known formula.

$$\langle l'||Y_k||l\rangle = (-1)^{l'} \sqrt{\frac{(2l+1)(2k+1)(2l'+1)}{4\pi}} \begin{pmatrix} l' & k & l \\ 0 & 0 & 0 \end{pmatrix} \tag{6.0.45}$$

Again use the standard formula for the tensor product of two operators from Edmonds, and we find

$$\begin{aligned} \langle (l's')j|S_{ij}|(ls)j\rangle &= 3\sqrt{\frac{4\pi}{5}}\sqrt{\frac{2}{3}}(-1)^{l+s'+j} \begin{Bmatrix} l' & l & 2 \\ s & s' & j \end{Bmatrix} \langle l'||Y_2||l\rangle \langle s'||[\sigma_i \otimes \sigma_j]_2||s\rangle \\ &= (-1)^{1+j} 2\sqrt{30}\sqrt{(2l+1)(2l'+1)} \begin{Bmatrix} l' & l & 2 \\ 1 & 1 & j \end{Bmatrix} \begin{pmatrix} l' & 2 & l \\ 0 & 0 & 0 \end{pmatrix} \end{aligned} \tag{6.0.46}$$

if $s = s' = 1$, and it is zero otherwise.

We will also need the matrix element of $\sigma_1 \cdot \sigma_2$

$$\langle s|\sigma_1 \cdot \sigma_2|s\rangle = 4s - 3 \tag{6.0.47}$$

And similarly for $\tau_1 \cdot \tau_2$.

6.1 Solving the Schrodinger Equation

Now that we have the coordinate form of the potential, we need a method for solving it. We are interested in scattering solutions with $E > 0$ and bound states with $E < 0$, in particular the deuteron. For the following sections, we will work with the spherical wavefunction. This is equal to the ordinary radial wavefunction times r.

$$u(r) = rR(r) \tag{6.1.1}$$

The advantage is that the kinetic energy looks like the one-dimensional kinetic energy, but with an extra term for the centrifugal potential. In the single-channel case, the radial Schrodinger equation can be written as

$$\left[-\frac{d^2}{dr^2} + \frac{l(l+1)}{r^2} + U(r)\right] u(r) = p^2 u(r) \tag{6.1.2}$$

The center-of-mass energy is related to p by $E = \frac{p^2}{2M_r}$. Here $U(r)$ is the reduced potential

$$U(r) = \frac{2M_r}{\hbar^2} V(r) \tag{6.1.3}$$

where M_r is the reduced mass.

The inner solution is subject to a regularity condition at the origin.

$$u(0) = 0 \tag{6.1.4}$$

More specifically, the inner wavefunction should obey the stronger condition.

$$u(r) \propto r^{l+1} \tag{6.1.5}$$

This is so that the centrifugal potential term does not cause problems at the origin.

In the region where $r \to \infty$ and $U(r) \to 0$, we know that the wavefunction is some linear combination of the spherical Bessel functions. It will be more convenient to work with spherical Hankel functions, which are simply related by a linear combination.

$$\begin{aligned} h_n^{(1)}(z) &= j_n(z) + iy_n(z) \\ h_n^{(2)}(z) &= j_n(z) - iy_n(z) \end{aligned} \tag{6.1.6}$$

One of the most important properties we will need is the asymptotic form of these functions. For large r, we have

$$\begin{aligned} j_l(pr) &= \frac{1}{pr} \sin\left(pr - \frac{l\pi}{2}\right) \\ y_l(pr) &= -\frac{1}{pr} \cos\left(pr - \frac{l\pi}{2}\right) \end{aligned} \tag{6.1.7}$$

and

$$\begin{aligned} h_l^{(1)}(pr) &= (-i)^{l+1} \frac{1}{pr} e^{ipr} \\ h_l^{(2)}(pr) &= (i)^{l+1} \frac{1}{pr} e^{-ipr} \end{aligned} \tag{6.1.8}$$

For scattering states, we know that this linear combination is related to the phase shift.

$$\begin{aligned} u(r) &\sim \sin\left(pr - l\frac{\pi}{2} + \delta_l\right) \\ &\sim \frac{1}{2} e^{i\delta_l} pr h_l^{(1)}(pr) + \frac{1}{2} e^{-i\delta_l} pr h_l^{(2)}(pr) \end{aligned} \tag{6.1.9}$$

Taking a look at the asymptotic behaviour of the spherical Hankel functions, we can identify the $h^{(1)}$ part with the outgoing wave and the $h^{(2)}$ part as the incoming wave. The way

we have written it here, the wavefunction is manifestly real. Alternatively, we can write the wavefunction in a way which demonstrates the relation between incoming and outgoing waves. This relationship is governed by the S-matrix.

$$u(r) \sim \frac{1}{2} S p r h_l^{(1)}(pr) + \frac{1}{2} p r h_l^{(2)}(pr) \tag{6.1.10}$$

In the single channel case, the S-matrix is simply related to the phase shift by

$$S = e^{2i\delta_l} \tag{6.1.11}$$

Now the question is this: how do we actually go about finding the S-matrix and solving the Schrodinger equation? Our first guess might be to start from the origin and integrate out as far as we would like in r. However, this becomes problematic since we want our wavefunctions to be normalized at large r according to Equation 6.1.9. It would be more convenient to start with the asymptotic form of the wavefunction at some large R where the potential is small, and then integrate in to small r. This requires knowing the S-matrix or, equivalently, the phase shift. We will do this using the *variable S-matrix formalism*, described below.

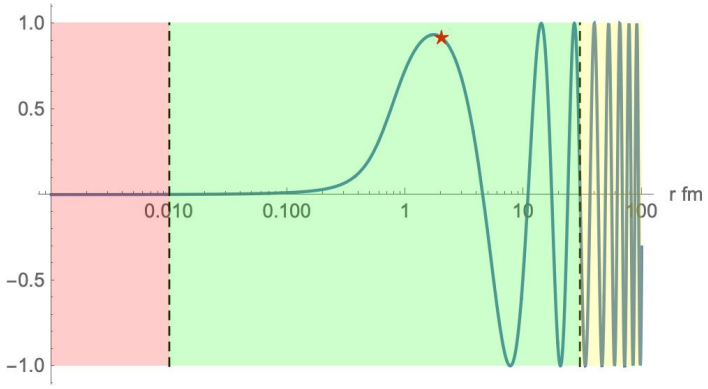

Figure 6.3: Numerical solution to the Schrodinger equation, highlighting the three regions described in the text. This example is in the $np\ ^1S_0$ channel at $T_{\text{lab}} = 30$ MeV.

One snag we will always run into when we integrate in is that we will numerical noise is guaranteed to generate some small contribution from the inner solution at small r. This is a problem because the inner solution has the wrong behaviour at the origin, so our regularity condition for inner solutions cannot be met. In practice, this only effects the very small r behaviour. We will deal with this by only integrating in to some minimum r_{min}, and then for $r < r_{\text{min}}$ we can use a polynomial form which obeys the regularity condition at $r = 0$. Our matching condition at r_{min} is that the wavefunction and its first derivative are continuous.

A typical example is shown in Figure 6.3. In this example, we find the S-matrix at $R = 10$ fm. Past 10 fm, we use the asymptotic form of the wavefunction. We then use a

numerical solution from 10 fm down to 0.1 fm. Below 0.1 fm, we use a polynomial which matches the numerical solution at 0.1 such that the wavefunction and its first derivative are continuous. We find that we can typically take $R = 15$ fm and $r_{\min} = 0.1$ and we get a good wavefunction.

Variable S-Matrix Formulation

As described in the paragraphs above, it is advantageous to calculate $u(R)$ and $u'(R)$ at some point R and integrate in toward $r = 0$. Then all we need to do is find boundary condition at a point R. We will now go over a simple method for calculating the boundary condition, which is presented in [VA05], called the *variable S-matrix* method.

The trick is to introduce a "masking radius" R, after which we artificially set the potential to zero.

$$U(r, R) = U(r)\theta(R - r) \tag{6.1.12}$$

The wavefunction $u(r, R)$ satisfies a modified Schrodinger equation.

$$\left[-\frac{d^2}{dr^2} + \frac{l(l+1)}{r^2} + U(r, R)\right] u(r, R) = p^2 u(r, R) \tag{6.1.13}$$

When $r > R$, the wavefunction has an asymptotic form given by $S(R)$. This variable S-matrix now depends on our choice of masking radius.

$$u(r, R) = \frac{1}{2} S(R) prh_l^{(1)}(pr) + \frac{1}{2} prh_l^{(2)}(pr), \quad r > R \tag{6.1.14}$$

When $r < R$, $u(r, R)$ is a solution to the second order differential equation which is regular at the origin. The only possibility is that $u(r, R)$ is proportional to the inner solution we are after.

$$u(r, R) = c(R)u(r), \quad r < R \tag{6.1.15}$$

Here $c(R)$ is some undetermined constant, which will drop out in this calculation.

The crux of this derivation hinges on the properties of the Wronskian. Recall that the Wronskian of two solutions of a second order linear differential equation is given by

$$W(f, g) = f(r)\frac{dg(r)}{dr} - \frac{df(r)}{dr} g(r) \tag{6.1.16}$$

We will not need all of the properties of the Wronskian in full generality. All we need to know is that it is anti-symmetric and, if f, g are two solutions of the radial Schrodinger equation, then the Wronskian of the two solutions is constant - independent of r. We also need to know the Wronskian of the spherical Hankel functions.

$$W(prh^{(1)}(pr), prh^{(2)}(pr)) = -2ip \tag{6.1.17}$$

Now consider the Wronskian of two solutions with slightly different masking radii.

$$W(u(r, R), u(r, R + \Delta R)) \tag{6.1.18}$$

By anti-symmetry, the Wronskian of the inner solution with itself vanishes

$$W(u(r), u(r)) = 0 \tag{6.1.19}$$

So this vanishes when $r < R$. When $r > R + \Delta R$, when we can calculate the Wronskian from the asymptotic form.

$$W(u(r,R), u(r,R+\Delta R)) = \begin{cases} 0 & r < R \\ \frac{ip}{2}\left(S(R+\Delta R) - S(R)\right) & R + \Delta R < r \end{cases} \tag{6.1.20}$$

Taking the limit $\Delta R \to 0$, we have

$$W(u(r,R), u(r,R+\Delta R)) = \begin{cases} 0 & r < R \\ \frac{ip}{2}\frac{dS}{dR}\Delta R & R + \Delta R < r \end{cases} \tag{6.1.21}$$

When $R < r < R + \Delta R$ the Wronskian will not be constant. Indeed, we have

$$\begin{aligned} \frac{d}{dr}W(u(r,R), u(r,R+\Delta R)) &= u(r,R)\left[\frac{d^2}{dr^2}u(r,R+\Delta R)\right] - \left[\frac{d^2}{dr^2}u(r,R)\right]u(r,R+\Delta R) \\ &= u(r,R)\left[U(r,R+\Delta R) - U(r,R)\right]u(r,R+\Delta R) \end{aligned} \tag{6.1.22}$$

Integrating over the region $R < r < R + \Delta R$, we have

$$W(u(r,R), u(r,R+\Delta R)) = \begin{cases} 0 & r < R \\ u(R)^2 U(R)\Delta R & R + \Delta R < r \end{cases} \tag{6.1.23}$$

Equating these two expressions, we find

$$2ip\frac{dS(r)}{dr} = U(r)\left(S(r)prh_l^{(1)}(pr) + prh_l^{(2)}(pr)\right)^2 \tag{6.1.24}$$

Subject to the boundary condition

$$S(0) = 1 \tag{6.1.25}$$

It is simple to show that S always has absolute value $|S|^2 = 1$. First multiply through by S^* and use the fact that $S^*S = 1$ at the initial value.

$$2ipS^*(r)\frac{dS(r)}{dr} = \left(prh_l^{(1)}(pr) + S(r)^* prh_l^{(2)}(pr)\right)U(r)\left(S(r)prh_l^{(1)}(pr) + prh_l^{(2)}(pr)\right) \tag{6.1.26}$$

when $p \in \mathbb{R}$, the RHS is manifestly real. Taking the complex conjugate gives us

$$-2ipS(r)\frac{dS(r)^*}{dr} = \left(prh_l^{(1)}(pr) + S(r)^* prh_l^{(2)}(pr)\right)U(r)\left(S(r)prh_l^{(1)}(pr) + prh_l^{(2)}(pr)\right) \tag{6.1.27}$$

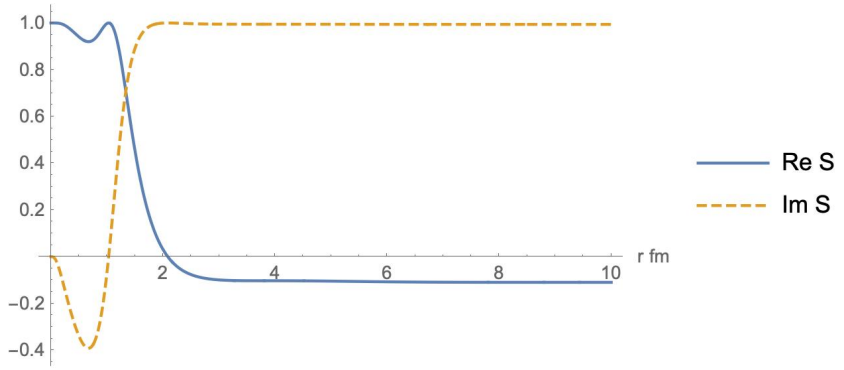

Figure 6.4: S-matrix as a function of masking radius using the variable S-matrix formalism. This example is in the np $^1S_0$ channel at $T_{\text{lab}} = 30$ MeV.

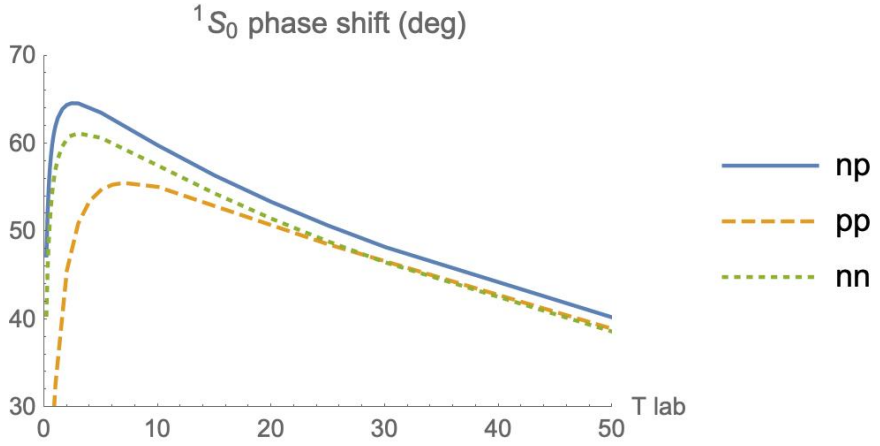

Figure 6.5: Phase shifts in the $^1S_0$ channel for np, pp, and nn scattering using the Av18 potential. Phase shifts for np and nn scattering are calculated relative to the spherical Bessel functions, while those for pp scattering are calculated relative to the Coulomb wavefunctions.

Subtracting these gives

$$\frac{d}{dr}|S(r)|^2 = S(r)^* \frac{dS(r)}{dr} + S(r)\frac{dS(r)^*}{dr} = 0 \tag{6.1.28}$$

Note that when p is complex, this argument no longer works.

Coulomb Phase Shifts

The analysis above can be immediately extended to include the Coulomb interaction. First we need to define the Coulomb functions. These functions satisfy the Schrodinger

equation with a point particle Coulomb interaction.

$$\left[\nabla^2 + k^2 - 2M_r \frac{Z_1 Z_2 \alpha}{r}\right] \psi = 0 \tag{6.1.29}$$

where M_r is the reduced mass, and $Z_{1,2}$ are the charges of the scattering particles. We define the Coulomb parameter η as

$$\eta = \frac{Z_1 Z_2 \alpha M_r}{k} = \frac{Z_1 Z_2 \alpha}{v_{\text{rel}}} \tag{6.1.30}$$

The regular solution is given in terms of Kummer's hypergeometric function M

$$F_{\eta l}(\rho) = C_{\eta l} \rho^{l+1} e^{\pm i\rho} M(l + 1 \pm i\eta, 2l + 2, \mp 2i\rho) \tag{6.1.31}$$

The sign we take makes no difference. The normalization $C_{\eta l}$ is given by

$$C_{\eta l} = \frac{2^l |\Gamma(l + 1 + i\eta)|}{\Gamma(2l + 2) e^{\eta\pi/2}} \tag{6.1.32}$$

In the limit $\eta \to 0$, this is related to the spherical bessel function by

$$\lim_{\eta \to 0} F_{\eta l}(pr) = pr j_l(pr) \tag{6.1.33}$$

The irregular solutions $H^{\pm}_{\eta l}$ can be defined in terms of the other Kummer hypergeometric function U.

$$H^{\pm}_{\eta l}(\rho) = D^{\pm}_{\eta l} \rho^{l+1} e^{\pm i\rho} U(l + 1 \pm i\eta, 2l + 2, \mp 2i\rho) \tag{6.1.34}$$

where the normalization $D^{\pm}_{\eta l}$ is given by

$$D^{\pm}_{\eta l} = (\mp 2i)^{2l+1} \frac{\Gamma(l + 1 \pm i\eta)}{C_{\eta l} \Gamma(2l + 2)} \tag{6.1.35}$$

Alternatively, they can be defined using Whittaker functions.

$$H^{\pm}_{\eta l}(\rho) = (\mp i)^l e^{\pi\eta/2} e^{\pm i\sigma_l(\eta)} W_{\mp i\eta, l+1/2}(\mp 2i\rho) \tag{6.1.36}$$

Here $\sigma_l(\eta)$ is the Coulomb phase shift

$$\sigma_l(\eta) = \arg\Gamma(l + 1 + i\eta) \tag{6.1.37}$$

At large r, the irregular solutions go asymptotically like

$$H^{\pm}_{\eta l} \to e^{\pm\theta_{\eta l}} \tag{6.1.38}$$

with

$$\theta_{\eta l}(\rho) = \rho - l\frac{\pi}{2} - \eta \log(2\rho) + \sigma_l(\eta) \tag{6.1.39}$$

In the limit $\eta \to 0$, these are related to the spherical Hankel functions by

$$\begin{aligned} \lim_{\eta\to 0} H^+_{\eta l}(pr) &= ipr h^{(1)}_l(pr) \\ \lim_{\eta\to 0} H^-_{\eta l}(pr) &= -ipr h^{(2)}_l(pr) \end{aligned} \tag{6.1.40}$$

In analogy with the irregular spherical Bessel function $y_l(x)$, we have the irregular Coulomb function $G_{\eta l}(x)$.

$$\begin{aligned} H^+_{\eta l}(x) &= G_{\eta l}(x) + iF_{\eta l}(x) \\ H^-_{\eta l}(x) &= G_{\eta l}(x) - iF_{\eta l}(x) \end{aligned} \tag{6.1.41}$$

The entire analysis presented above for the phase shifts goes through if we replace the full potential U by the non-Coulomb part of the potential, ΔU.

$$U(r) \to \Delta U = U - 2M_r V_C \tag{6.1.42}$$

where $2M_r V_C = 2\eta k/r$ is the Coulomb potential. In particular, the Schrodinger equation becomes

$$\left[-\frac{d^2}{dr^2} + \frac{l(l+1)}{r^2} + \frac{2\eta k}{r} + \Delta U(r)\right] u(r) = p^2 u(r) \tag{6.1.43}$$

The asymptotic region where $r \to \infty$ and $\Delta U \to 0$, the solution can be written in terms of the regular and irregular Coulomb functions.

$$u \sim \cos(\delta_l) F_{\eta l}(pr) + \sin(\delta_l) G_{\eta l}(pr) \tag{6.1.44}$$

In the variable S-matrix formalism, it will instead be convenient to use the incoming and outgoing coulomb functions.

$$u \sim -\frac{i}{2} e^{i\delta_l} H^+_{\eta l}(pr) + \frac{i}{2} e^{i\delta_l} H^-_{\eta l}(pr) \tag{6.1.45}$$

In the variable S-matrix differential equation, Equation 6.1.24, we replace the spherical Hankel functions with the Coulomb functions.

$$-2ip\frac{dS(r)}{dr} = \Delta U(r)\left(S(r)H^+_{\eta l}(pr) - H^-_{\eta l}(pr)\right)^2 \tag{6.1.46}$$

Note that in the Av18 potential, we instead take a modified form of the Coulomb parameter called the *relativistic coulomb parameter* [Bre55][Ber+88].

$$\eta' = \frac{\alpha}{v_{\text{lab}}} = \frac{\alpha M_p}{2k}\frac{1 + 2k^2/M_p^2}{\sqrt{1 + k^2/M_p^2}} \quad pp\text{-scattering} \tag{6.1.47}$$

Making the replacement $\eta \to \eta'$ introduces energy dependence in the pp-channel potential.

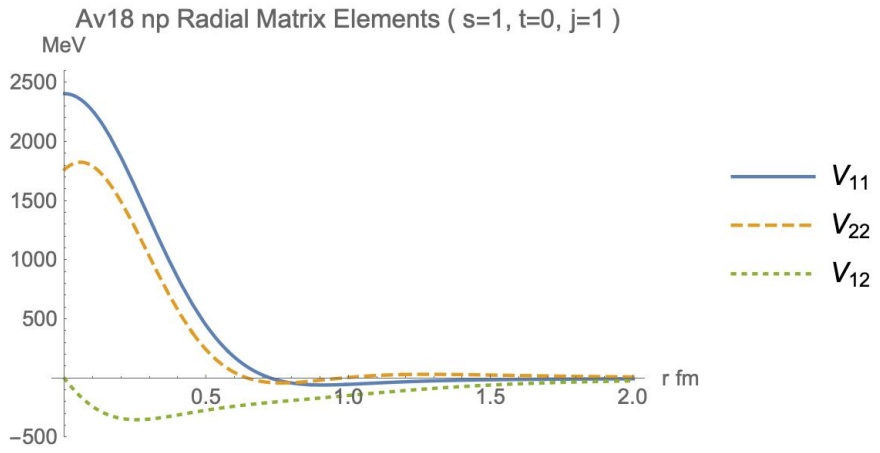

Figure 6.6: The three components of the Av18 potential in the deuteron channel $s = 1$, $t = 0$, and $j = 1$.

Coupled Channels

In coupled channels, the wavefunction is a combination of the two different orbital angular momentum. In coordinate space, this is

$$\psi(\vec{r}) = u(r)\mathbf{\Psi}^{jm}_{j-1,1}(\hat{r}) + w(r)\mathbf{\Psi}^{jm}_{j+1,1}(\hat{r}) \tag{6.1.48}$$

Where we have defined the coupled spherical spin harmonic.

$$\mathbf{\Psi}^{jm}_{l,s} = \sum_{m_l,m_s} C^{jm}_{lm_l,sm_s} Y_{lm_l}(\hat{r})\chi_{s,m_s} \tag{6.1.49}$$

We have a radial wavefunction for each orbital angular momentum channel. These satisfy two coupled differential equations.

$$\begin{aligned} [-\frac{d^2}{dr^2} + \frac{(j-1)j}{r^2} + U^{11}]u + U^{12}w &= p^2 u \\ [-\frac{d^2}{dr^2} + \frac{(j+1)(j+2)}{r^2} + U^{22}]w + U^{21}u &= p^2 w \end{aligned} \tag{6.1.50}$$

with $U^{12} = U^{21}$.

There are now two linearly independent inner solutions, not just one. Using the eigenphase parameterization, the asymptotic form of the two orthogonal inner solutions is

$$\begin{aligned} u_1 &\sim \cos(\varepsilon_j)\sin\left(kr - \frac{(J-1)\pi}{2} + \delta_1\right), \quad w_1 \sim \sin(\varepsilon_j)\sin\left(kr - \frac{(J+1)\pi}{2} + \delta_1\right) \\ u_2 &\sim -\sin(\varepsilon_j)\sin\left(kr - \frac{(J-1)\pi}{2} + \delta_2\right), \quad w_2 \sim \cos(\varepsilon_j)\sin\left(kr - \frac{(J+1)\pi}{2} + \delta_2\right) \end{aligned} \tag{6.1.51}$$

We can express this as a matrix where each column represents a linearly independent solution.

$$\mathbf{u} = \begin{pmatrix} u_1 & u_2 \\ w_1 & w_2 \end{pmatrix} \tag{6.1.52}$$

We can write the radial hamiltonian in matrix form

$$\mathbf{H} = \begin{pmatrix} -\frac{d^2}{dr^2} + \frac{(j-1)j}{r^2} + U^{11} & U^{12} \\ U^{21} & -\frac{d^2}{dr^2} + \frac{(j+1)(j+2)}{r^2} + U^{22} \end{pmatrix} \tag{6.1.53}$$

And write the differential equation as a matrix equation

$$\mathbf{Hu} = p^2\mathbf{u} \tag{6.1.54}$$

We can also write the solution in coordinate space in terms of our matrix.

$$\begin{pmatrix} \psi_1(\vec{r}) \\ \psi_2(\vec{r}) \end{pmatrix} = \mathbf{u}^T \begin{pmatrix} \mathbf{\Psi}^{jm}_{j-1,1} \\ \mathbf{\Psi}^{jm}_{j+1,1} \end{pmatrix} \tag{6.1.55}$$

In order to express the asymptotic wavefunction, write

$$\mathbf{h}^{(1)}(pr) = \begin{pmatrix} prh^{(1)}_{j-1}(pr) & 0 \\ 0 & prh^{(1)}_{j+1}(pr) \end{pmatrix}, \quad \mathbf{h}^{(2)}(pr) = \begin{pmatrix} prh^{(2)}_{j-1}(pr) & 0 \\ 0 & prh^{(2)}_{j+1}(pr) \end{pmatrix} \tag{6.1.56}$$

Instead of simple exponentials of the phase shift $e^{\pm i\delta_l}$, we now have coefficients of $\mathbf{h}^{(1,2)}$ which are themselves matrices. Let those coefficient matrices be $\mathbf{A}$, $\mathbf{B}$.

$$\mathbf{u} \sim \frac{1}{2}\mathbf{h}^{(1)}\mathbf{A} + \frac{1}{2}\mathbf{h}^{(2)}\mathbf{B} \tag{6.1.57}$$

The coefficient matrices $\mathbf{A}$ and $\mathbf{B}$ can be read off from the asymptotic form of the wavefunction.

$$\mathbf{A} = \begin{pmatrix} \cos(\varepsilon_j) & -\sin(\varepsilon_j) \\ \sin(\varepsilon_j) & \cos(\varepsilon_j) \end{pmatrix} \begin{pmatrix} e^{i\delta_1} & 0 \\ 0 & e^{i\delta_2} \end{pmatrix}, \quad \mathbf{B} = \begin{pmatrix} \cos(\varepsilon_j) & -\sin(\varepsilon_j) \\ \sin(\varepsilon_j) & \cos(\varepsilon_j) \end{pmatrix} \begin{pmatrix} e^{-i\delta_1} & 0 \\ 0 & e^{-i\delta_2} \end{pmatrix} \tag{6.1.58}$$

The $\mathbf{S}$ matrix is identified with the combination which cancels out the coefficient of the incoming $h^{(2)}$ term, $\mathbf{S} = \mathbf{AB}^{-1}$

$$\mathbf{u} \sim \frac{1}{2}\mathbf{h}^{(1)}\mathbf{S} + \frac{1}{2}\mathbf{h}^{(2)} \tag{6.1.59}$$

By simple matrix multiplication, we find the so-called eigenphase parameterization of the S-matrix.

$$\mathbf{S} = \begin{pmatrix} \cos(\varepsilon_j) & -\sin(\varepsilon_j) \\ \sin(\varepsilon_j) & \cos(\varepsilon_j) \end{pmatrix} \begin{pmatrix} e^{2i\delta_1} & 0 \\ 0 & e^{2i\delta_2} \end{pmatrix} \begin{pmatrix} \cos(\varepsilon_j) & \sin(\varepsilon_j) \\ -\sin(\varepsilon_j) & \cos(\varepsilon_j) \end{pmatrix} \tag{6.1.60}$$

Compare this to the nuclear bar parameterization, which is the one more often quoted in the experimental data [Sto+93].

$$\mathbf{S} = \begin{pmatrix} \exp(2i\bar{\delta}_{j-1})\cos 2\bar{\varepsilon}_j & i\exp(i(\bar{\delta}_{j-1}+\bar{\delta}_{j+1}))\sin 2\bar{\varepsilon}_j \\ i\exp(i(\bar{\delta}_{j-1}+\bar{\delta}_{j+1}))\sin 2\bar{\varepsilon}_j & \exp(2i\bar{\delta}_{j+1})\cos 2\bar{\varepsilon}_j \end{pmatrix} \tag{6.1.61}$$

When comparing to data, note that this parameterization is not unique. For example, it has a symmetry $\bar{\varepsilon}_j \to -\bar{\varepsilon}_j$ and $\bar{\delta}_{j-1} \to \bar{\delta}_{j-1} + \pi$.

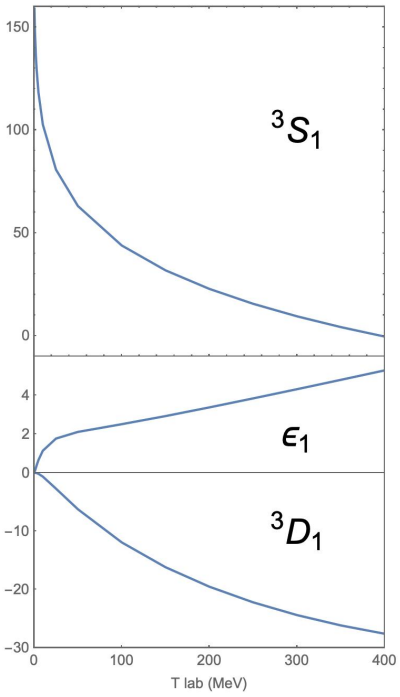

Figure 6.7: Phase shifts in the coupled channels $^3S_1$ and $^3D_1$ using the nuclear bar parameterization, Equation 6.1.61. Phase shifts and mixing angles are all in degrees.

We want to now adapt the variable S-matrix formalism to the coupled channel case. We define a matrix Wronskian.

$$W(\mathbf{f}^T, \mathbf{g}) = \mathbf{f}^T \left(\frac{d}{dr}\mathbf{g}\right) - \left(\frac{d}{dr}\mathbf{f}^T\right)\mathbf{g} \tag{6.1.62}$$

Under the assumption that the potential is symmetric $\mathbf{U}^T = \mathbf{U}$, it is simple to see that this has the correct properties of a Wronskian. Namely, the Wronskian of two solutions to the Schrodinger equation is constant. We can use the Wronskian of the Hankel functions

$$W(\mathbf{h}^{(1)}(pr), \mathbf{h}^{(2)}(pr)) = -2ip \tag{6.1.63}$$

Now introduce the masking radius just as before. When $r < R$, the solution $\mathbf{u}(R)$ is some linear combination of the inner solutions we are after. Since the Wronskian of the inner solutions with themselves is zero, we have as before

$$W(\mathbf{u}^T(r,R), \mathbf{u}(r, R+\Delta R)) = \begin{cases} 0 & r < R \\ \frac{ip}{2}(\mathbf{S}(R+\Delta R) - \mathbf{S}(R)) & R + \Delta R < r \end{cases} \tag{6.1.64}$$

Note here we needed to use $\mathbf{S}^T = \mathbf{S}$. Also in just the same way as before, we can relate the derivative of the Wronskian to the potential

$$\frac{d}{dr} W(\mathbf{u}^T(r,R), \mathbf{u}(r, R+\Delta R)) = \mathbf{u}^T(r,R) \left[\mathbf{U}(r, R+\Delta R) - \mathbf{U}(r,R)\right] \mathbf{u}(r, R+\Delta R) \tag{6.1.65}$$

Where we used the fact that $\mathbf{U}^T = \mathbf{U}$.

In analogy with the single channel result, the coupled channel result is (remember $\mathbf{S}^T = \mathbf{S}$).

$$2ip\frac{d}{dr}\mathbf{S}(r) = \left(\mathbf{S}(r)\mathbf{h}^{(1)}(pr) + \mathbf{h}^{(2)}(pr)\right) \mathbf{U}(r) \left(\mathbf{h}^{(1)}(pr)\mathbf{S}(r) + \mathbf{h}^{(2)}(pr)\right) \tag{6.1.66}$$

The differential equation for the S-matrix is a set of three coupled, first order differential equations for S_{11}, S_{12} and S_{22}. The initial condition at $r = 0$ is

$$\mathbf{S}(0) = 1 \tag{6.1.67}$$

And $\mathbf{S}$ is guaranteed to be a unitary matrix when $p \in \mathbb{R}$

$$\frac{d}{dr}(\mathbf{S}^\dagger \mathbf{S}) = 0 \tag{6.1.68}$$

Extending the Formalism to Bound States

The case of bound states is quite different from the case of scattering states. We do not have any unknown phase shift parameter. The asymptotic behaviour of bound state wavefunctions is known - it is a decaying exponential.

$$u \sim e^{-\kappa r} \tag{6.1.69}$$

where $p = i\kappa$ and $E = -\kappa^2/2M_r$. However, we do not necessarily know what the bound state energy is. In coupled channels, we will also need to know the ratio of the two parts of the wavefunction - which we call the *asymptotic ratio*, η.

$$u \sim e^{-\kappa r}, \quad w \sim \eta e^{-\kappa r} \tag{6.1.70}$$

In general, we need to go through some numerical procedure to find the binding energy and asymptotic ratio. There are many approaches we can take here. There are iterative integral solutions, which are rapidly convergent but are numerically quite costly. There are

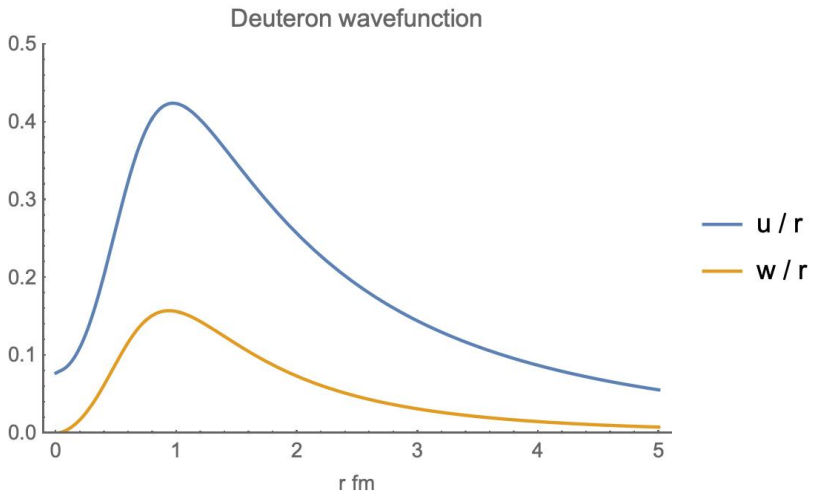

Figure 6.8: Two components of the deuteron wavefunction calculated using the $Av18$ potential and the modified variable S-matrix formalism.

more straightforward methods such as the shooting method, where we start with test values of the parameters and adjust them until we have a solution which is regular at the origin.

For the sake of consistency, we make a minor tweak to the variable S-matrix formalism so that it works for bound states. Like the shooting method, this will also involve adjusting the binding energy until we find a bound state. The one benefit of this method over the simple shooting method is that we will get the asymptotic ratio for free. This reduction in the space of parameters we need to check from a two-dimensional space of (κ, η) down to just κ is a significant improvement.

When p is pure imaginary, as it is for bound states, the functions $h^{(1)}$ and $h^{(2)}$ become exponential rather than oscillatory. This can create major issues when we try to solve the Schrodinger equation numerically, since going out to large r is always guaranteed to blow up at some point. The results we present here should be taken with a grain of salt, and integrals should only ever be done up to intermediate r.

We let $p = i\kappa$ where $\kappa \in \mathbb{R}$. The asymptotic form of the wavefunction for a bound state is a decaying exponential. In particular, it has no component of $h^{(2)}$.

$$u(r) \sim r h_l^{(1)}(i\kappa r) \tag{6.1.71}$$

Clearly the asymptotic form we used before will not suffice, since the coefficient of the incoming wave $h^{(2)}$ was equal to 1. For this generalized case, we simply write the asymptotic form in terms of unknown complex coefficients A and B.

$$u \sim \frac{1}{2} A p r h_l^{(1)}(i\kappa r) + \frac{1}{2} B p r h_l^{(2)}(i\kappa r) \tag{6.1.72}$$

The boundary condition for a bound state is that $B = 0$, which means we cannot set $B = 1$ as we would like to do. Instead, we parameterize the asymptotic solution as

$$A = \frac{1}{2}\left(\tilde{A} + 1\right), \quad B = -\frac{i}{2}\left(\tilde{A} - 1\right) \tag{6.1.73}$$

This might seem like an odd choice, but it has some nice properties we will come to later. Then we have

$$A\frac{dB}{dr} - B\frac{dA}{dr} = -\frac{i}{2}\frac{d\tilde{A}}{dr} \tag{6.1.74}$$

And the function $\tilde{A}(r)$ can be found using the first order differential equation as before.

$$\frac{4i}{\kappa}\frac{d\tilde{A}}{dr} = U(r)\left(\left(\tilde{A} + 1\right) r h_l^{(1)}(i\kappa r) - i\left(\tilde{A} - 1\right) r h_l^{(2)}(i\kappa r)\right)^2 \tag{6.1.75}$$

However, there is an obvious problem. The function $h^{(2)}(i\kappa r)$ is an increasing exponential. Despite this, we can still use this up to intermediate r.

The boundary condition at $r = 0$ is

$$\tilde{A}(0) = i \tag{6.1.76}$$

When $\kappa \in \mathbb{R}$, we have

$$\left(h_n^{(1,2)}(i\kappa r)\right)^* = (-1)^n h_n^{(1,2)}(i\kappa r) \tag{6.1.77}$$

Using the same reasoning as before, when $\kappa \in \mathbb{R}$ we can show that

$$|\tilde{A}(r)|^2 = 1 \tag{6.1.78}$$

If we have a bound state, then at large r we have

$$\tilde{A}(\infty) \to 1 \quad \text{bound state} \tag{6.1.79}$$

This looks right, but in practice does not work. The term $h^{(2)}(i\kappa r)$ blows up, and so there is no stable large r behaviour unless $U(r)$ goes to zero faster than an exponential. We cannot actually integrate this up to large r, but we can integrate this up to intermediate r and integrate in to find the inner solution.

The same analysis works just as well for coupled channels. Write the asymptotic behaviour in terms of unknown matrix coefficients $\mathbf{A}$ and $\mathbf{B}$.

$$\mathbf{u} \sim \frac{1}{2}\mathbf{h}^{(1)}\mathbf{A} + \frac{1}{2}\mathbf{h}^{(2)}\mathbf{B} \tag{6.1.80}$$

We have a bound sate if $\mathbf{B}$ has a zero eigenvalue. Therefore we will have a bound state when

$$\det \mathbf{B} = 0 \tag{6.1.81}$$

This means $\mathbf{B}$ will not be inevitable, so we need to change our approach as before.

In analogy with the single-channel case, we make the following redefinition

$$\mathbf{A} = \frac{1}{2}\left(\tilde{\mathbf{A}} + 1\right), \quad \mathbf{B} = -\frac{i}{2}\left(\tilde{\mathbf{A}} - 1\right) \tag{6.1.82}$$

with $\tilde{\mathbf{A}}^T = \tilde{\mathbf{A}}$. Then the differential equation for $\tilde{\mathbf{A}}$ becomes

$$\begin{aligned} &\frac{4i}{\kappa}\frac{d}{dr}\tilde{\mathbf{A}}(r) \\ &= \left(\tilde{\mathbf{A}}\left(\mathbf{h}^{(1)} - i\mathbf{h}^{(2)}\right) + \left(\mathbf{h}^{(1)} + i\mathbf{h}^{(2)}\right)\right)\mathbf{U}\left(\left(\mathbf{h}^{(1)} - i\mathbf{h}^{(2)}\right)\tilde{\mathbf{A}} + \left(\mathbf{h}^{(1)} + i\mathbf{h}^{(2)}\right)\right) \end{aligned} \tag{6.1.83}$$

As before, this is always unitary.

$$\tilde{\mathbf{A}}^\dagger(r)\tilde{\mathbf{A}}(r) = 1 \tag{6.1.84}$$

The initial condition is $\tilde{\mathbf{A}}(0) = i$, and we have a bound state if

$$\det(\tilde{\mathbf{A}}(\infty) - 1) = 0 \tag{6.1.85}$$

Then the bound state will be the eigenvecvtor for which $\tilde{\mathbf{A}}$ has eigenvalue 1. We can use this technique to find the deuteron binding energy, asymptotic normalization, and wavefunction. This is indeed how we find the deuteron wavefunction shown in Figure 6.8.

In order to calculate the deuteron wavefunction, we solve the first order differential equation for $\tilde{\mathbf{A}}$ out to some large r and adjust κ until $\det(\tilde{\mathbf{A}}(\infty) - 1) = 0$. I did this using the ParametricNDSolve function in Mathematica. This gives us the binding energy, and we can read off the asymptotic ratio from the eigenvector with eigenvalue 1.

$$\mathbf{A}\begin{pmatrix} 1 \\ \eta \end{pmatrix} = \begin{pmatrix} 1 \\ \eta \end{pmatrix} \tag{6.1.86}$$

With the binding energy and asymptotic ratio in hand, we use the boundary condition at large R and numerically solve the differential equation down to $r = 0$. As in the case of scattering states, we are guaranteed to run into problems at very small r. Once again, we integrate in only to some very small $r_{\min}$ and match onto a polynomial which obeys the regularity condition at $r = 0$, and is continuous at $r_{\min}$ with continuous first derivative.

Chapter 7

Radiative Correction to pp-Fusion

We now wish to use the formula we derived in Section 5.3 to calculate the two-body correction to $C_{\rm NS}^{\rm GT}$ in the case of proton-proton fusion. As we discussed at the end of Section 3.3, the pp-fusion cross section is given by

$$\sigma(E) = \frac{1}{(2\pi)^3}\frac{G_V^2}{v_{\rm rel}} m_e^5 f_R(E)(1+\Delta_R^V)(1+\frac{\alpha}{\pi}C_{\rm NS}^{\rm GT})\sum_M |\,\langle d, M|\mathbf{A}^-|pp\rangle\,|^2 \tag{7.0.1}$$

Here, $\mathbf{A}^-$ is the space-like part of the axial-vector weak current. At small momentum transfer, this is simply given by the Gamow-Teller operator in Equation 1.3.5.

The phase space factor f was defined in Equation 1.3.13. It includes the Fermi function and the outer radiative corrections, Equation 2.1.25.

$$f_R(E) = \int_1^{W_0} dW\, W\sqrt{W^2-1}(W_0-W)^2 F(Z,W)\left(1+\frac{\alpha}{2\pi}g(W,W_0)\right) \tag{7.0.2}$$

The maximum energy is $W_0 = (E+\Delta M)/m_e$ with $\Delta M = 2M_p - M_d$. Near $E=0$ we can approximate this using a third order polynomial.

$$f_R(E) \approx 0.14446 + 1.307E + 4.375E^2 + 7.776E^3 \quad E < 0.1 \text{ MeV} \tag{7.0.3}$$

where E is measured in MeV. The most important term here is the value at $E=0$. Without the Fermi function and radiative corrections, this gives $f(E=0) = 0.148$.

Note that, since g_A is defined in neutron decay, the outer correction Δ_R^V for the Fermi matrix element appears here. This is the same correction we discussed in the case of super allowed Fermi beta decay in Section 3.1. Keep in mind this really comes from the definition of g_A, not from some box diagram for pp-fusion.

The radiative correction specific to pp-fusion is the term

$$\frac{\alpha}{\pi}C_{\rm NS}^{\rm GT} \tag{7.0.4}$$

Note that the Born contribution does not appear here, since it is again absorbed into the definition of g_A. We only pick up the part of the box diagram which is different from the neutron decay box diagram. Hence we get the nuclear structure dependent part.

In practice, we do not use the cross section presented here in actual calculations. In solar physics applications, we are really interested in the thermally averaged cross section.

$$\langle \sigma v \rangle = \sqrt{\frac{8}{\pi \mu (kT)^3}} \int_0^\infty E\sigma(E) \exp\left(-\frac{E}{kT}\right) dE \tag{7.0.5}$$

This is then converted into the *astrophysical S-factor*.

$$\sigma(E) = \frac{S(E)}{E} \exp(-2\pi\eta) \tag{7.0.6}$$

This is the value quoted in [Ade+11], which is used in solar models. The core of the sun reaches temperatures around 10^7 K. Compared to nuclear energy scales, this corresponds to small energies $E \approx 0$. Therefore, we take the limit of zero energy when we calculate the cross section and the radiative correction.

7.1 Radial Overlap Integral

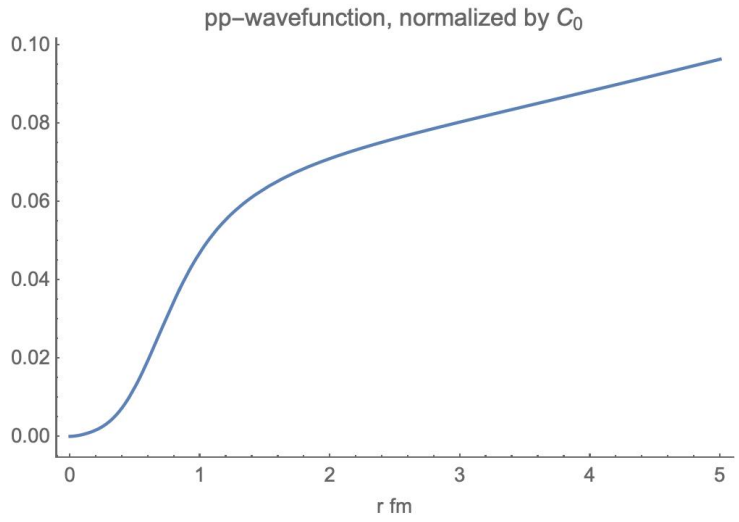

Figure 7.1: Proton-proton scattering wavefunction $u_0(p, r)$, divided by the Coulomb normalization C_0. The *pp*-wavefunction is calculated a center-of-mass energy $E = 3.3$ keV.

We now want to discuss how we calculate the nuclear matrix element for the cross section. The deuteron wavefunction has two components - an $l = 0$ and an $l = 2$ component.

$$\psi_d = \frac{1}{r}\left[u_d(r)\Psi_{01}^{1M}(\hat{r}) + w_d(r)\Psi_{21}^{1M}(\hat{r})\right]\zeta_{00} \tag{7.1.1}$$

Where ζ_{00} represents the $T = 0$ and $M_T = 0$ isospin eigenstate. The functions u and w are plotted in Figure 6.8.

The part of the *pp*-wavefunction which contributes to the fusion reaction is the $l = 0$ state. In particular, it has spin $S = 0$. Of course the isospin state is $T = 1$ $M_T = 1$. For a *pp*-scattering state, we write the wavefunction as

$$\psi_{pp}^{(+)} = 4\pi\sqrt{2}\sum_{l\text{ even}}\sum_{m_l} i^l Y_{lm_l}(\hat{p})^* \frac{e^{i\delta_l}}{pr} u_l(p,r) Y_{lm_l}(\hat{r})\chi_{00}\zeta_{11} \tag{7.1.2}$$

Here $p = \sqrt{2M_r E}$ is the usual center of mass momentum. Apologies for the use of p to mean both "proton" and center of mass momentum. We use p here to distinguish it from the loop momentum, which we will call k. The wavefunction $u_l(p,r)$ is normalized asymptotically using the Coulomb functions, Equation 6.1.31.

$$u_l(p,r) \sim \cos\delta_l F_{\eta l}(pr) + \sin\delta_l G_{\eta l}(pr) \tag{7.1.3}$$

The *pp*-fusion reaction involves a change in the spin state from $S = 0$ to $S = 1$, which means it goes through the Gamow-Teller operator.

$$\mathbf{GT} = \sum_a \vec{\sigma}_a \tau_a^- \tag{7.1.4}$$

This can also be written using the operators with proper exchange symmetry, Equation 5.2.10.

$$\mathbf{GT} = 2\vec{\Sigma}_{(+)}\Xi_{(+)}^- + 2\vec{\Sigma}_{(-)}\Xi_{(-)}^- \tag{7.1.5}$$

Only the second term contributes to *pp*-fusion, since it is the one which generates transitions from $S = 0$ to $S = 1$ and from $T = 1$ to $T = 0$.

Following [Sch+98], we write the matrix element of the Gamow-Teller operator in terms of a dimensionless radial matrix element, $\Lambda(E)$.

$$\begin{aligned}\langle d, M|\mathbf{GT}_{1,q}|pp\rangle = \delta_{M,q}\sqrt{16\pi}g_A\frac{e^{i\delta_0}}{p}\int_0^\infty dr u_d(r)u_0(p,r) \\ = \sqrt{\frac{32\pi}{\gamma^3}}g_A C_0\Lambda(E)\end{aligned} \tag{7.1.6}$$

Here $\mathbf{GT}_{1,q}$ are the angular momentum components of the Gamow-Teller operator. We factor out the deuteron binding momentum $\gamma = \sqrt{2M_r E_d}$ so that $\Lambda(E)$ is dimensionless. We also factor out the Coulomb normalization factor C_0 which we defined in Equation 6.1.32. For $l = 0$, this is equal to

$$C_0 = \frac{2\pi\eta}{e^{2\pi\eta} - 1} \tag{7.1.7}$$

In this context, this is known as the *Gamow penetration factor*. This definition allows us to calculate the limit $E \to 0$ of the overlap integral $\Lambda(E)$.

$$\Lambda(E) = (\gamma^3/2)^{1/2}\frac{e^{i\delta_0}}{C_0 p}\int_0^\infty dr u(r)u_0(p,r) \tag{7.1.8}$$

In other calculations such as [KB94], they chose to write this in terms of the scattering length.

$$-\frac{1}{a_{pp}} = \lim_{p\to 0} C_0^2 p \cot \delta_0 \tag{7.1.9}$$

However, we follow [Sch+98] and do not use this form.

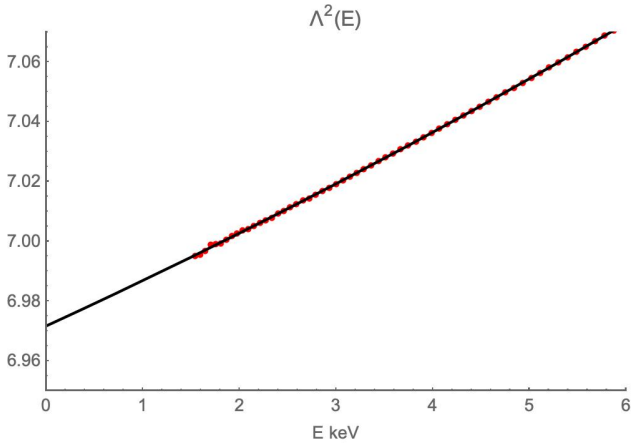

Figure 7.2: Radial overlap integral used in the definition of the proton-proton fusion cross section, extrapolated to zero energy. Calculated values are in red, and the extrapolation is in black.

Using Av18 deuteron and proton-proton wavefunctions, we can calculate the overlap integral directly at various energies and extrapolate to $E = 0$. By extrapolating the data using a simple polynomial fit, we find an extrapolated value at $E = 0$.

$$\Lambda^2(E = 0) = 6.9716(2) \tag{7.1.10}$$

The uncertainty quoted here only includes the uncertainty from the energy extrapolation, and does not include systematic uncertainties. This is in good agreement with the result given in [Sch+98], who consider the average over a range of nuclear models. They also perform this calculation down to 2 keV. This is good enough of a proof of concept to give us confidence in calculating the radiative correction.

7.2 Radiative Correction - 2-Body

Before we discuss the details of the calculation, lets begin with the simple estimates which have been put forward in the literature so far. In [KRV03], they give a simple scaling argument for the estimated size of the correction based on the correction to Fermi transitions. They argue that the correction should roughly scale with the average nucleon momentum

in the nucleus. Given that the deuteron binding momentum is about $\gamma = 45$ MeV, and the typical Fermi momentum of a larger nucleus is about 300 MeV, we expect the correction for proton-proton fusion to be reduced by about 45/300. In [TH02], they give the nuclear structure corrections for different nuclei. Taking the correction they quote for ^{10}C, we expect the rough size of the correction to be

$$|C_{\rm GT}^{\rm NS}| \sim \frac{45}{300} 1.3 \sim 0.2 \tag{7.2.1}$$

Now we will be able to calculate it directly to check if this is accurate.

In Section 5.3, we derived a formula for the two-body contribution to $C_{\rm NS}^{\rm GT}$. The result is broken up into an orbital angular momentum, a spin, and a tensor operator. The orbital angular momentum operator does not contribute. The only operators which contribute are the ones which flip the spin from $S = 0$ to $S = 1$ and the isospin from $T = 1$ to $T = 0$. This leaves us with only the spin operator and tensor operator.

$$\begin{aligned} C_{\rm NS}^{\rm GT}(\sigma) &= \frac{(\mu_v - \mu_s)}{g_A \langle |\mathbf{GT}| \rangle} \frac{2\pi}{3M_N} \left(\langle f || \sum_{a<b} \frac{f_\sigma(\Lambda r)}{r} \vec{\Sigma}_{(-)} \Xi_{(-)}^- \, || i \rangle \right) \\ C_{\rm NS}^{\rm GT}(t) &= \frac{(\mu_v - \mu_s)}{g_A \langle |\mathbf{GT}| \rangle} \frac{\pi}{2M_N} \left(\langle f || \sum_{a<b} \frac{f_t(\Lambda r)}{r} \Big[\Big(\hat{r} (\hat{r} \cdot \vec{\Sigma}_{(-)}) - \frac{1}{3} \vec{\Sigma}_{(-)} \Big) \Xi_{(-)}^- \Big] \, || i \rangle \right) \end{aligned} \tag{7.2.2}$$

The spin operator is directly proportional to the tree level Gamow-Teller operator, and so it is trivial to calculate. The correction is simply the ratio of the overlap integral with $f_\sigma(\Lambda r)/r$ to the tree-level overlap integral.

$$C_{\rm NS}^{\rm GT}(\sigma) = \frac{(\mu_v - \mu_s)}{g_A} \frac{\pi}{3M_N} \frac{1}{[\int_0^\infty dr \, u(r) u_0(p,r)]} \int_0^\infty dr \frac{f_\sigma(\Lambda r)}{r} u(r) u_0(p,r) \tag{7.2.3}$$

For the tensor operator, we need to do a bit more work. We know that the tensor operator will connect the $l = 0$ proton-proton wavefunction to the $l = 2$ component of the deuteron wavefunction. In order to compare this to the tree-level matrix element, we need to calculate a reduced matrix element. First, we expand out the tensor operator in terms of the spherical harmonic Y_2.

$$e_q \cdot (\hat{r}(\hat{r} \cdot \Sigma) - \frac{1}{3}\Sigma) = -\sqrt{\frac{2}{3}} \sqrt{\frac{4\pi}{3}} [Y_2(\hat{r}) \otimes \Sigma]_{1q} \tag{7.2.4}$$

Now we need to compute the $(ls)j$ coupled reduced matrix elements. For details, see Appendix E. For the tree-level spin operator, this is

$$\langle (01)1 || \Sigma || (00)0 \rangle = \sqrt{3} \begin{Bmatrix} 0 & 1 & 1 \\ 1 & 0 & 0 \end{Bmatrix} \langle 1 || \Sigma || 0 \rangle = \langle 1 || \Sigma || 0 \rangle \tag{7.2.5}$$

For the tensor operator, we have

$$\langle (21)1 || [Y_2(\hat{r}) \otimes \Sigma]_1 || (00)0 \rangle = 3 \begin{Bmatrix} 2 & 0 & 2 \\ 1 & 0 & 1 \\ 1 & 0 & 1 \end{Bmatrix} \langle 2 || Y_2(\hat{r}) || 0 \rangle \langle 1 || \Sigma || 0 \rangle = \sqrt{\frac{1}{4\pi}} \langle 1 || \Sigma || 0 \rangle \tag{7.2.6}$$

The reduced matrix element of the spin operator shows up in both places, and cancels out. The reduced matrix element of the spherical harmonic is a standard formula, which we give in Appendix E. The end result is again a ratio of overlap integrals, except now the tensor operator involves the $l = 2$ part of the deuteron wavefunction.

$$C_{\rm NS}^{\rm GT}(t) = -\frac{(\mu_v - \mu_s)}{g_A}\frac{\pi}{6\sqrt{2}M_N}\frac{1}{[\int_0^\infty dr\, u(r)u_0(p,r)]}\int_0^\infty dr\frac{f_t(\Lambda r)}{r}w(r)u_0(p,r) \tag{7.2.7}$$

This contribution has the opposite sign from the spin operator, but it is also about 20 times smaller.

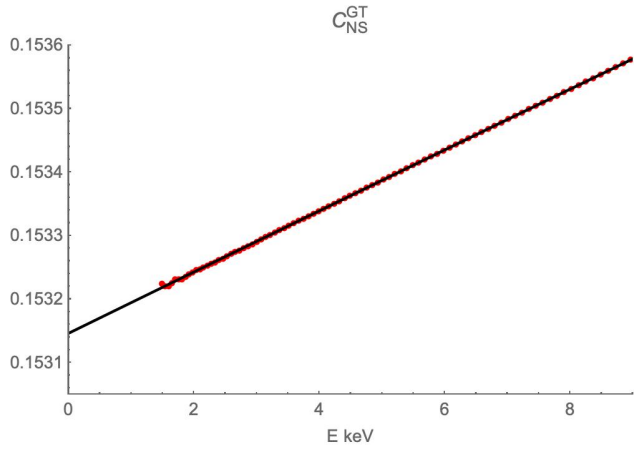

Figure 7.3: Two-body nuclear structure radiative correction for proton-proton fusion, extrapolated to zero energy.

By once again extrapolating to zero energy, we find the nuclear structure correction for proton-proton fusion.

$$\begin{aligned} C_{\rm NS}^{\rm GT} &= 0.162 - 0.008 \\ &= 0.153 \end{aligned} \tag{7.2.8}$$

In the first line, we separate out the contributions due to the spin term $C_{\rm NS}^{\rm GT}(\sigma)$ and the tensor term $C_{\rm NS}^{\rm GT}(t)$. The tensor term comes with the opposite sign and causes a partial cancellation, however it is quite small. This is due to the relative size of the deuteron D-wavefunction, which is reduced relative to the S-wavefunction by a factor 0.025. Also the tensor form factor $f_t(\Lambda r)$ causes a much more drastic reduction than the spin form factor $f_\sigma(\Lambda r)$, as shown in Figure 5.8.

Comparing this calculated result to the estimated result in Equation 7.2.1, we see very good agreement with the naive momentum scaling argument. This confirms the analysis given in [KRV03], with no enhancement. In fact, we see that the presence of the tensor term

$C_{\rm NS}^{\rm GT}(t)$ actually slightly reduces the result. Also, as we discuss below, we need to take into account the momentum space wavefunction of the proton-proton scattering state as well. The momentum we need to plug into the scaling argument is even smaller than what we would expect just by considering the deuteron alone.

The correction coming from $C_{\rm NS}^{\rm GT}$ results in an increase in the proton-proton fusion cross section by about

$$\frac{\alpha}{\pi} C_{\rm NS}^{\rm GT} \approx 0.036\% \tag{7.2.9}$$

This is about 25 times smaller than the current quoted uncertainty in the overall cross section [Ade+11]. You will also notice that I have not listed any uncertainty estimation. It is not clear how to evaluate the uncertainty related to the assumptions we made in deriving the formula for the two-body part $C_{\rm NS}^{\rm GT}$. I would recommend an uncertainty of 100% for this calculation in order to account for the systematic uncertainties in the assumptions which led to it.

The real benefit of having this result is that we can confirm that the two-body radiative correction is indeed small. Knowing the size of this correction is important, because it was always possible that there was some enhancement which made it larger than one would expect. Having directly calculated it, we now know that is not the case. This should be reflected in higher confidence and reduced uncertainty for the proton-proton fusion cross section.

7.3 Two-Body Part as a Function of Loop Momentum

Going back to Section 5.3, we see that this formula resulted from an integral over loop momentum, $\vec{k}$. It is also instructive to calculate the result as a function of loop momentum. Based on the arguments we made in Section 5.1, we know that the two-body part should die off past momentum transfer $2k_F$.

We begin by going back to the representation of $C_{\rm NS}^{\rm GT}$ in momentum space, Equation 5.3.7.

$$\vec{\mathcal{J}} = \frac{8\pi^2}{2M_N} \int \frac{d^3k}{(2\pi)^3} \frac{1}{(|\vec{k}|^2 - i\epsilon)^2} \Bigg(\langle f| \sum_{a\neq b} e^{-i\vec{k}\cdot\vec{r}} \Big[-i4\vec{k} \times \vec{p}_r \hat{e}_a + \mu_v \left(\vec{k}(\vec{k}\cdot\vec{\sigma}_b) - |\vec{k}|^2 \vec{\sigma}_b \right) \hat{e}_a \\ + \hat{\mu}_a \left(\vec{k}(\vec{k}\cdot\vec{\sigma}_a) - |\vec{k}|^2 \vec{\sigma}_a \right) \Big] \tau_b^+ |i\rangle \Bigg) \tag{7.3.1}$$

Split apart the spin terms into an ordinary spin and a tensor term. We also separate out

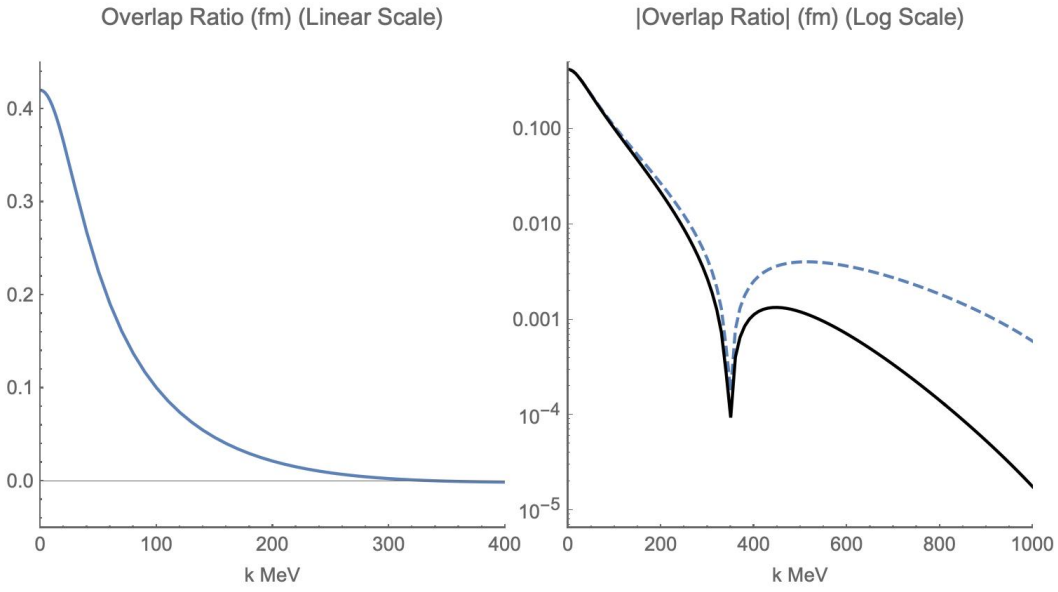

Figure 7.4: Contribution to $C_{\rm NS}^{\rm GT}$ as a function of the loop momentum $|\vec{k}|$ with nucleon form factors (solid) and without nucleon form factors (dashed). The *pp*-wavefunction is calculated at 3.3 keV.

the angular part of the integration measure and simplify.

$$\begin{aligned}\vec{\mathcal{J}} = \frac{2}{M_N}\int_0^\infty d|\vec{k}| \int \frac{d\Omega_k}{4\pi}\Bigg(\langle f| \sum_{a\neq b} e^{-i\vec{k}\cdot\vec{r}}\Big[-\frac{i4}{|\vec{k}|}\hat{k}\times\vec{p}_r\hat{e}_a - \frac{2}{3}\left(\mu_v\hat{e}_a\vec{\sigma}_b + \hat{\mu}_a\vec{\sigma}_a\right) \\ +\mu_v\left(\hat{k}(\hat{k}\cdot\vec{\sigma}_b) - \frac{1}{3}\vec{\sigma}_b\right)\hat{e}_a + \hat{\mu}_a\left(\hat{k}(\hat{k}\cdot\vec{\sigma}_a) - \frac{1}{3}\vec{\sigma}_a\right)\Big]\tau_b^+ |i\rangle\Bigg)\end{aligned} \tag{7.3.2}$$

Perform a multipole expansion on the exponential

$$e^{-i\vec{k}\cdot\vec{r}} = 4\pi\sum_{LM}(-i)^L j_L(|\vec{k}|r)Y_{LM}(\hat{r})Y_{LM}(\hat{k})^* \tag{7.3.3}$$

Now we integrate over angles, but leave the integral over loop momentum. The integrals we need are

$$\begin{aligned}\int\frac{d\Omega_k}{4\pi}e^{-i\vec{k}\cdot r} &= j_0(|\vec{k}|r) \\ \int\frac{d\Omega_k}{4\pi}e^{-i\vec{k}\cdot\vec{r}}\hat{k} &= (-i)j_1(|\vec{k}|r)\hat{r} \\ \int\frac{d\Omega_k}{4\pi}e^{-i\vec{k}\cdot\vec{r}}(\hat{k}(\hat{k}\cdot\sigma) - \frac{1}{3}\sigma) &= -j_2(|\vec{k}|r)(\hat{r}(\hat{r}\cdot\sigma) - \frac{1}{3}\sigma)\end{aligned} \tag{7.3.4}$$

This gives us an expression in terms of an integral over the loop momentum magnitude $|\vec{k}|$.

$$\begin{aligned}\vec{\mathcal{J}} = -\frac{2}{M_N}\int_0^\infty d|\vec{k}|\Bigg(\langle f|\sum_{a\neq b}\Big[4\hat{e}_a\frac{j_1(|\vec{k}|r)}{|\vec{k}|r}\vec{r}\times\vec{p}_r + \frac{2}{3}j_0(|\vec{k}|r)\left(\mu_v\hat{e}_a\vec{\sigma}_b + \hat{\mu}_a\vec{\sigma}_a\right) \\ +\mu_v\hat{e}_a j_2(|\vec{k}|r)\left(\hat{r}(\hat{r}\cdot\vec{\sigma}_b) - \frac{1}{3}\vec{\sigma}_b\right) + \hat{\mu}_a j_2(|\vec{k}|r)\left(\hat{r}(\hat{r}\cdot\vec{\sigma}_a) - \frac{1}{3}\vec{\sigma}_a\right)\Big]\tau_b^+\,|i\rangle\Bigg)\end{aligned} \tag{7.3.5}$$

Of course, this must give us the same answer if we integrate over $|\vec{k}|$. Indeed, the integrals over the spherical Bessel functions with the nucleon form factors give rise to the functions we found in Equation 5.3.15.

$$\begin{aligned}\frac{2}{\pi}\int_0^\infty d|\vec{k}|\left(\frac{1}{1+|\vec{k}|^2/\Lambda^2}\right)^4 j_0(|\vec{k}|r) &= \frac{1}{r}f_\sigma(\Lambda r) \\ \frac{4}{\pi}\int_0^\infty d|\vec{k}|\left(\frac{1}{1+|\vec{k}|^2/\Lambda^2}\right)^4 \frac{j_1(|\vec{k}|r)}{|\vec{k}|r} &= \frac{1}{r}f_l(\Lambda r) \\ \frac{4}{\pi}\int_0^\infty d|\vec{k}|\left(\frac{1}{1+|\vec{k}|^2/\Lambda^2}\right)^4 j_2(|\vec{k}|r) &= \frac{1}{r}f_t(\Lambda r)\end{aligned} \tag{7.3.6}$$

As before, we want to write this in terms of operators which have explicit symmetry properties under particle exchange. We can also express the result in terms of multipoles, defined in Equation D.2.11. The term which contributes to *pp*-fusion only involves the electric multipole $E1$.

$$\frac{2}{3}j_0(|\vec{k}|r)\vec{\sigma} + j_2(|\vec{k}|r)(\hat{r}(\hat{r}\cdot\sigma) - \frac{1}{3}\sigma) = (-i)\sqrt{2}\sqrt{\frac{4\pi}{3}}\mathbf{X}^{(e)}_{1q}(|\vec{k}|\vec{r})\cdot\vec{\sigma}e^*_q \tag{7.3.7}$$

Keeping only the part which contributes to *pp*-fusion, we have

$$\vec{\mathcal{J}} = -(-i)\sqrt{2}\sqrt{\frac{4\pi}{3}}e^*_q\frac{2(\mu_v-\mu_s)}{M_N}\int d|\vec{k}|\left(\frac{1}{1+|\vec{k}|^2/\Lambda^2}\right)^4\langle f|\sum_{a<b}\mathbf{X}^{(e)}_{1q}(|\vec{k}|\vec{r})\cdot\Sigma_{(-)}\Xi^+_{(-)}\,|i\rangle \tag{7.3.8}$$

The reduced matrix element of the $E1$ operator can be expressed in terms of radial integrals as before. The radial integrals involve the spherical Bessel functions, which depend on the loop momentum.

$$\langle d||\mathbf{X}^{(e)}_1\cdot\Sigma_{(-)}||pp\rangle = i\frac{1}{\sqrt{4\pi}}\left[\sqrt{2}\int_0^\infty dr\,u(r)j_0(|\vec{k}|r)u_0(p,r) - \int_0^\infty dr\,w(r)j_2(|\vec{k}|r)u_0(p,r)\right] \tag{7.3.9}$$

By comparing this to the tree-level Gamow-Teller operator, we find the correction $C^{\rm GT}_{\rm NS}$ as a function of momentum transfer.

$$C^{\rm GT}_{\rm NS}(\sigma) = \frac{2(\mu_v-\mu_s)}{3g_AM_N}\int_0^\infty d|\vec{k}|\left(\frac{\Lambda^2}{|\vec{k}|^2+\Lambda^2}\right)^4\frac{1}{[\int_0^\infty dr\,u(r)u_0(p,r)]}\int_0^\infty dr\,u(r)j_0(|\vec{k}|r)u_0(p,r) \tag{7.3.10}$$

and for the tensor term

$$C_{\rm NS}^{\rm GT}(t) = -\frac{\sqrt{2}(\mu_v - \mu_s)}{3 g_A M_N} \int_0^\infty d|\vec{k}| \left(\frac{\Lambda^2}{|\vec{k}|^2 + \Lambda^2}\right)^4 \frac{1}{[\int_0^\infty dr\, u(r) u_0(p,r)]} \int_0^\infty dr\, w(r) j_2(|\vec{k}|r) u_0(p,r) \tag{7.3.11}$$

This is analogous to the formula which we used in the Coulomb sum rule in Equation 5.1.16.

The result for *pp*-fusion is shown in Figure 7.4. The benefit of doing the calculation in terms of momentum transfer is that we can see how the two-body part drops off at high momentum. The nucleon form factors cause an even faster drop off at high momentum transfer, which can be seen in the plot on the right. This can be compared to the Coulomb sum rule example we did in Figure 5.7.

By comparing the two plots, we can see that the two-body part of $C_{\rm NS}^{\rm GT}$ for *pp*-fusion drops off before $2k_F$ of the deuteron. This is because *pp*-fusion involves both the deuteron wavefunction and the *pp*-scattering wavefunction. This partly explains why the correction $C_{\rm NS}^{\rm GT}$ we calculated is slightly smaller than the expected result based on the momentum scaling argument, Equation 7.2.1.

Chapter 8

Completeness Relation

In the previous section, we discussed how the low energy nuclear structure correction $C_{\rm NS}^{\rm GT}$ is calculated from the box diagram. We started from the anti-symmetric part of the box diagram, which we can write in terms of the effective hadronic current.

$$\mathcal{M}_{\rm box} = \frac{\alpha}{2\pi}\frac{G_V}{\sqrt{2}} L_\beta \mathcal{J}^\beta \tag{8.0.1}$$

The effective hadronic current for the box diagram (ignoring recoil corrections) is given by Equation 4.0.7.

$$\mathcal{J}^\beta = 8\pi^2 \int \frac{d^4k}{(2\pi)^4} \frac{\varepsilon^{\mu\lambda\alpha\beta} k_\alpha}{(k^2+i\epsilon)^2} T_{\mu\lambda}(p_f, p_i, k) \tag{8.0.2}$$

Here $T^{\mu\lambda}$ is the generalized Compton tensor we defined in Equation 2.1.4.

$$T^{\mu\lambda}(p_f, p_i, k) = -i \int d^4x e^{ikx} \langle p_f | T J^\mu_{em}(x) J^\lambda_W(0) | p_i \rangle \tag{8.0.3}$$

Using the integral form of the theta function Equation 2.2.10, we can write this in terms of a nuclear Green's function.

$$\begin{aligned} T^{\mu\lambda}(p_f, p_i, k) = &\int d^3x e^{-i\vec{k}\cdot\vec{x}} \langle p_f | J^\mu_{em}(\vec{x}) \frac{1}{E_f + k^0 - H + i\epsilon} J^\lambda_W(0) | p_i \rangle \\ &+ \int d^3x e^{-i\vec{k}\cdot\vec{x}} \langle p_f | J^\lambda_W(0) \frac{1}{E_i - k^0 - H + i\epsilon} J^\mu_{em}(\vec{x}) | p_i \rangle \end{aligned} \tag{8.0.4}$$

Since only the vector currents are involved, the space-like part of the currents are order $1/M_N$ while the time-like part is order 1. With this in mind, we only keep terms of order $1/M_N$.

$$\mathcal{J}^i = 8\pi^2 \int \frac{d^4k}{(2\pi)^4} \frac{1}{(k^2+i\epsilon)^2} \epsilon^{ijk} k^j \left(T^{k0}(p_f, p_i, k) - T^{0k}(p_f, p_i, k) \right) \tag{8.0.5}$$

In Section 5, we discussed how the correction is calculated in practice. The full nuclear Green's function is never calculated. For the one-body Born contribution $C_{\rm Born}$, we replace

the nuclear Green's function by free-nucleon propagators in Equation 4.0.9. For the two-body nuclear structure contribution C_{NS}, we made an argument that the momentum transfer had to be small and that we could ignore the energy denominators. Then we ended up with a product of the currents in Equation 5.0.6, which allowed us to separate out the two-body part.

However, in Section 5.4 we pointed out that there was disagreement about how the one-body part should be handled. In [Tow94], they argued that we should use quenched nuclear currents to account for the effect of the nuclear environment. In [SGR19], they argue that the Born term went beyond the low-lying nuclear states where quenching was relevant. Instead, they identified the Born term with the quasi-elastic response and found a reduction in the Born term due to Pauli-blocking and the nucleon removal energy.

The goal of this work is to calculate the nuclear structure correction to both the one-body and two-body parts using the full nuclear Green's function. Of course, this is impractical for larger nuclei which is why this is not typically done. This is why we restrict ourselves to small nuclei, such as the two and three nucleon systems, where the nuclear Green's function can be calculated reliably.

Before moving on to calculate the full nuclear Green's function, we start with a simpler warm-up problem - verifying the completeness relation.

$$1 = \sum_n |n\rangle \langle n| \tag{8.0.6}$$

In particular, we choose the states to be eigenstates of the nuclear Hamiltonian. We can then express the nuclear Green's function in terms of a sum over energy eigenstates.

$$\begin{aligned} T^{\mu\lambda}(p_f, p_i, k) = &\sum_n \frac{1}{E_f + k^0 - E_n + i\epsilon} \int d^3x e^{-i\vec{k}\cdot\vec{x}} \langle p_f | J^\mu_{em}(\vec{x}) | n \rangle \langle n | J^\lambda_W(0) | p_i \rangle \\ &+ \sum_n \frac{1}{E_i - k^0 - E_n + i\epsilon} \int d^3x e^{-i\vec{k}\cdot\vec{x}} \langle p_f | J^\lambda_W(0) | n \rangle \langle n | J^\mu_{em}(\vec{x}) | p_i \rangle \end{aligned} \tag{8.0.7}$$

In Section 5, we then let the nuclear energy ΔE_n in the denominators go to zero. We then used the completeness relatoin to remove the intermediate states entirely. In this section, we will calculate the result by explicitly summing over intermediate states. We can then compare the two results and verify that they are identical. This should give us confidence to then calculate the result using the full nuclear Green's function.

This new method presents one major new challenge - it is no longer clear how to separate out the one-body and two-body parts. Instead, we use the separation of scales given by the Fermi momentum, k_F. In Section 5.1, we argued that the one-body part should take over when the momentum transferred by the currents is larger than $2k_F$. This leads us to the guiding principle for how we will calculate the nuclear structure corrections. We will calculate the full nuclear Green's function below $|\vec{k}| < 2k_F$, and then match this onto the one-body Born term for $|\vec{k}| > 2k_F$. This way, we can capture the nuclear structure effects on both the one-body and two-body parts simultaneously.

8.1 Separation of Scales

It is instructive to go back to the example we used in Section 5.1 to show how this works. Recall that we looked at the isoscalar Coulomb sum rule for the deuteron. We wrote this in terms of a sum over states as

$$S(|\vec{k}|) = \sum_n |\langle n|\tilde{\rho}(\vec{k})|\psi\rangle|^2 \tag{8.1.1}$$

Using the completeness relation, this becomes a product of the charge operators.

$$S(|\vec{k}|) = \langle\psi|\tilde{\rho}(-\vec{k})\tilde{\rho}(\vec{k})|\psi\rangle \tag{8.1.2}$$

Consider a pure iso-scalar part of the charge operator.

$$\tilde{\rho}(\vec{k}) = \sum_a e^{i\vec{k}\cdot\vec{x}_a} \tag{8.1.3}$$

When we are dealing with the product of current operators, we get a sum over each nucleon that the currents can act on. The sum separates out into a one-body part where $a = b$, and a two-body part where $a \neq b$.

$$\sum_{a,b} \rightarrow \sum_{a=b} + \sum_{a\neq b} \tag{8.1.4}$$

In this case, the one-body part is trivial - it simply counts the number of nucleons. The two-body part involves a function of the relative coordinate $\vec{r}$, and must be evaluated between the initial and final wavefunctions.

$$S(|\vec{k}|) = 2 + \langle\psi|(e^{-i\vec{k}\cdot\vec{r}} + e^{i\vec{k}\cdot\vec{r}})|\psi\rangle \tag{8.1.5}$$

As we saw in Figure 5.7, the one-body part persists to all $|\vec{k}|$ while the two-body part dies off past $|\vec{k}| > 2k_F$.

If we want to verify the completeness relation, we also need to calculate this in terms of the sum over intermediate states. The intermediate states have good angular momentum, so it is useful to do a multipole decomposition of the current operators.

$$\begin{aligned}\tilde{\rho}(\vec{k}) = e^{i\vec{k}\cdot\vec{x}_1} + e^{i\vec{k}\cdot\vec{x}_2} = e^{i\vec{k}\cdot\vec{X}} \sum_{L \text{ even},M} 4\pi i^L \left[2j_L(|\vec{k}||\vec{r}|/2)Y_{LM}(\hat{r})\right] Y_{LM}(\hat{k})^* \\ = e^{i\vec{k}\cdot\vec{X}} \sum_{LM} 4\pi i^L C_{LM}(|\vec{k}|)Y_{LM}(\hat{k})^*\end{aligned} \tag{8.1.6}$$

The exponential out in front of the sum deals with the center of mass motion, and the multipole decomposition is only done in the relative space. Similarly, the sum over states involves an integral over center of mass momentum and a sum over relative states.

$$\sum_n |n\rangle\langle n| \rightarrow \int \frac{d^3p}{(2\pi)^3} \sum_{\alpha_r} |\vec{p},\alpha_r\rangle\langle\vec{p},\alpha_r| \tag{8.1.7}$$

The relative intermediate states α_r are angular momentum eigenstates, and that means we can express the result in terms of reduced matrix elements. Doing a bit of angular momentum algebra gives us a result in terms of reduced matrix elements.

$$S(|\vec{k}|) = \sum\!\!\!\!\!\!\int_{\alpha_r} \sum_L \frac{4\pi}{2j_i+1} |\langle \alpha_r || C_L(|\vec{k}|) || \psi_r \rangle|^2 \tag{8.1.8}$$

where $j_i = 1$ is the total angular momentum of the deuteron. This now involves a sum over all intermediate states, α_r, as well as a sum over the angular momentum of the operator, L. Verifying the completeness relation means checking that this expression matches the simple expression we found by removing the intermediate states.

It is possible to do this in coordinate space. However, this involves solving the Schrodinger equation at every energy to calculate the intermediate state wavefunctions. This would also need to be done in every angular momentum channel. Then we would need to calculate the matrix element $\langle \alpha_r || C_L(|\vec{k}|) || \psi_r \rangle$ at each value of $|\vec{k}|$. This is tedious to do in practice.

It is much simpler to do this calculation in a discrete basis. Then, the integral over continuum intermediate state energies becomes an ordinary sum over the discrete energy eigenstates.

$$\int dE_\alpha \rho(E_\alpha) |E_\alpha\rangle \langle E_\alpha| \to \sum_{\alpha_r} |\alpha_r\rangle \langle \alpha_r| \tag{8.1.9}$$

We will carry out this calculation in the simple harmonic oscillator basis. This basis has another added benefit that the current operator matrix elements can be expressed as polynomials in $|\vec{k}|$, times an exponential.

$$\langle \alpha_r || C_L(|\vec{k}|) || \psi_r \rangle \to (\text{polynomial in } |\vec{k}|) \times e^{-|\vec{k}|^2 b^2/8} \tag{8.1.10}$$

For details, see Appendix F.2. This way, we automatically get a result which is a function of $|\vec{k}|$ and we do not need to repeat the calculation at each value of $|\vec{k}|$. The result is shown in Figure 8.1. We can see that adding more intermediate states gives a result which converges to the simple result we found by removing intermediate states.

Note that the separation of scales into $|\vec{k}| < 2k_F$ and $|\vec{k}| > 2k_F$ is <u>not</u> equivalent to the separation into a one-and two-body part. When $|\vec{k}| < 2k_F$, the sum rule Equation 5.1.14 gets contributions from both the one-body and two-body parts. However, when $|\vec{k}| > 2k_F$, then the only term that remains is the one-body part. We can show the relation between the two using a simple diagram.

Without using the completeness relation to remove the intermediate states, we can no longer separate out the one-body and two-body parts. The result we find will automatically contain both. Similarly, consider the Green's function which we need to compute the box diagram. The Hamiltonian in the Green's function is an operator, and we cannot simply move the currents past it. The Hamiltonian is at least two-body, so it generates additional many-body terms which represent a modification by the nuclear environment.

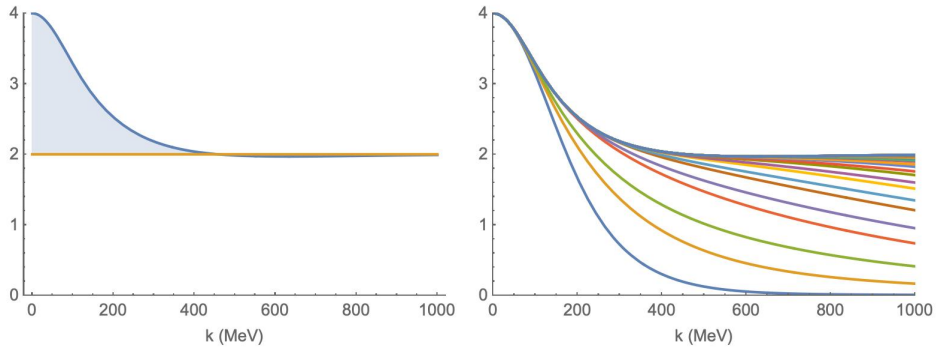

Figure 8.1: Deuteron isoscalar Coulomb sum rule $S(|\vec{k}|)$ showing the one-body and two-body parts (left), and the contribution from each intermediate state angular momentum channel in Equation 8.1.8 (right).

$$|\vec{k}| < 2k_F \longrightarrow \text{2-Body}$$
$$|\vec{k}| > 2k_F \longrightarrow \text{1-Body}$$

8.2 Completeness Relation for $C^{\mathbf{GT}}$ in pp-Fusion

In Section 5, we then argued that we could ignore the nuclear energy difference in the denominator because it should be of order $1/M_N$. Plugging this into the generalized Compton tensor, we get

$$\begin{aligned} T^{\mu\lambda}(p_f, p_i, k) = &\sum_n \frac{1}{k^0 + i\epsilon} \int d^3x e^{-i\vec{k}\cdot\vec{x}} \langle p_f | J^\mu_{em}(\vec{x}) | n \rangle \langle n | J^\lambda_W(0) | p_i \rangle \\ &+ \sum_n \frac{1}{-k^0 + i\epsilon} \int d^3x e^{-i\vec{k}\cdot\vec{x}} \langle p_f | J^\lambda_W(0) | n \rangle \langle n | J^\mu_{em}(\vec{x}) | p_i \rangle \end{aligned} \tag{8.2.1}$$

Then we can do the k^0 integral very easily.

$$\int \frac{dk^0}{2\pi} \frac{1}{(k^2 + i\epsilon)^2 (k^0 + i\epsilon)} = -\frac{i}{2|\vec{k}|^4} \tag{8.2.2}$$

Plugging this back into the effective hadronic current, we are left with an integral over d^3k. Expanding out the Levi-Civita symbol and only keeping terms of order $1/M_N$ gives us four

terms.

$$\begin{aligned}\vec{\mathcal{J}} = -\frac{i}{2}(8\pi^2)\int \frac{d^3k}{(2\pi)^3}\frac{1}{|\vec{k}|^4}\int d^3x\, e^{-i\vec{k}\cdot\vec{x}}\sum_n \Big(&\langle f|\vec{k}\times\vec{J}_{em}(\vec{x})|n\rangle\,\langle n|\rho_W(\vec{0})|i\rangle \\ &+\langle f|\rho_W(\vec{0})|n\rangle\,\langle n|\vec{k}\times\vec{J}_{em}(\vec{x})|i\rangle \\ &-\langle f|\rho_{em}(\vec{x})|n\rangle\,\langle n|\vec{k}\times\vec{J}_W(\vec{0})|i\rangle \\ &-\langle f|\vec{k}\times\vec{J}_W(\vec{0})|n\rangle\,\langle n|\rho_{em}(\vec{x})|i\rangle\Big)\end{aligned} \tag{8.2.3}$$

where $\rho = J^0$ is the time-like component of the current. These four terms are also shown pictorially in Figure 8.2. In the following section, we will go through the multipole decomposition and angular momentum algebra to calculate each of the terms.

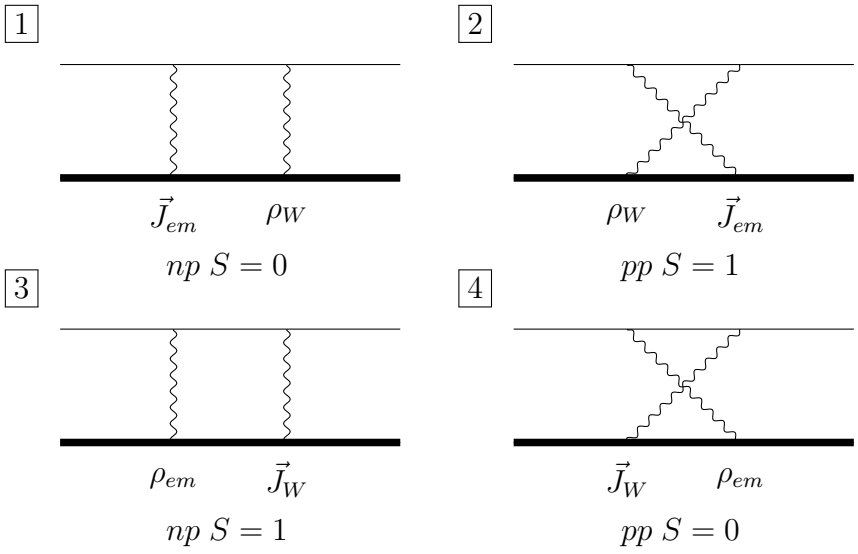

Figure 8.2: Diagramatic representation of the four terms in Equation 8.2.3. The thick line represents the nucleus, and the thin line represents the leptonic part.

Applying the completeness relation allows us to remove the sum over intermediate states. The expression above must then be equal to this simpler expression without the sum over intermediate states.

$$\begin{aligned}\vec{\mathcal{J}} = -\frac{i}{2}(8\pi^2)\int \frac{d^3k}{(2\pi)^3}\frac{1}{|\vec{k}|^4}\int d^3x\, e^{-i\vec{k}\cdot\vec{x}}\Big(&\langle f|\vec{k}\times\vec{J}_{em}(\vec{x})\rho_W(\vec{0})|i\rangle + \langle f|\rho_W(\vec{0})\vec{k}\times\vec{J}_{em}(\vec{x})|i\rangle \\ &-\langle f|\rho_{em}(\vec{x})\vec{k}\times\vec{J}_W(\vec{0})|i\rangle - \langle f|\vec{k}\times\vec{J}_W(\vec{0})\rho_{em}(\vec{x})|i\rangle\Big)\end{aligned} \tag{8.2.4}$$

This form involves the product of current operators, which is exactly what we dealt with in Section 5. Each term here has both a one-body and two-body part which can be separated out by normal ordering the current operators.

As we did in Section 5, we keep the current operators to order $1/M_N$. This is not valid for the high-momentum part of the loop integral, which requires us to use the full relativistic form as was done in Section 4. In this section, we will only be concerned with the low-momentum behaviour where the two-body part of the box diagram should be important.

With this in mind, we can write the electromagnetic current as

$$\begin{aligned} \rho_{em}(\vec{x}) &= \sum_a \hat{e}_a \delta^3(\vec{x}-\vec{x}_a) \\ J^i_{em}(\vec{x}) &= \frac{1}{2M_N}\sum_a \hat{e}_a\{p^i_a, \delta^3(\vec{x}-\vec{x}_a)\} - i\hat{\mu}_a\epsilon^{ilm}[p^l_a, \delta^3(\vec{x}-\vec{x}_a)]\sigma^m_a \end{aligned} \tag{8.2.5}$$

For the weak current, we only want to keep the vector part. As before, we write

$$\begin{aligned} \rho_W(\vec{x}) &= \sum_a \delta^3(\vec{x}-\vec{x}_a)\tau^+_a \\ J^i_W(\vec{x}) &= \frac{1}{2M_N}\sum_a \left[\{p^i_a, \delta^3(\vec{x}-\vec{x}_a)\} - i\mu_v\epsilon^{ilm}[p^l_a, \delta^3(\vec{x}-\vec{x}_a)]\sigma^m_a\right]\tau^+_a \end{aligned} \tag{8.2.6}$$

The details of the separation of the center of mass and the multipole decomposition are given in Section D. For brevity, we will simply state the results here.

For C_J with J even

$$C_{JM}(em) = [Q_s + Q_v\Xi^z_{(+)}]X_{JM}(q\vec{r}/2) \tag{8.2.7}$$

$$C_{JM}(W) = 2Q_v\Xi^-_{(+)}X_{JM}(q\vec{r}/2) \tag{8.2.8}$$

For C_J with J odd

$$C_{JM}(em) = Q_v\Xi^z_{(-)}X_{JM}(q\vec{r}/2) \tag{8.2.9}$$

$$C_{JM}(W) = 2Q_v\Xi^-_{(-)}X_{JM}(q\vec{r}/2) \tag{8.2.10}$$

For M_J with J even

$$\begin{aligned} M_{JM}(em) &= Q_v\Xi^z_{(-)}\frac{\bar{p}_r}{M}\cdot\mathbf{X}^{(m)}_{JM}(q\vec{r}/2) \\ &+\frac{q}{2M}[\mu_s\Sigma_{(-)} + \mu_v\Xi^z_{(+)}\Sigma_{(-)} + \mu_v\Xi^z_{(-)}\Sigma_{(+)}]\cdot\mathbf{X}^{(e)}_{JM}(q\vec{r}/2) \end{aligned} \tag{8.2.11}$$

$$\begin{aligned} M_{JM}(W) &= 2Q_v\Xi^z_{(-)}\frac{\bar{p}_r}{M}\cdot\mathbf{X}^{(m)}_{JM}(q\vec{r}/2) \\ &+\frac{q}{2M}[2\mu_v\Xi^-_{(+)}\Sigma_{(-)} + 2\mu_v\Xi^-_{(-)}\Sigma_{(+)}]\cdot\mathbf{X}^{(e)}_{JM}(q\vec{r}/2) \end{aligned} \tag{8.2.12}$$

For M_J with J odd

$$\begin{aligned} M_{JM}(em) &= \left[Q_s + Q_v \Xi^z_{(+)}\right] \frac{\bar{p}_r}{M} \cdot \mathbf{X}^{(m)}_{JM}(q\vec{r}/2) \\ &+ \frac{q}{2M}[\mu_s \Sigma_{(+)} + \mu_v \Xi^z_{(+)} \Sigma_{(+)} + \mu_v \Xi^z_{(-)} \Sigma_{(-)}] \cdot \mathbf{X}^{(e)}_{JM}(q\vec{r}/2) \end{aligned} \tag{8.2.13}$$

$$\begin{aligned} M_{JM}(W) &= 2Q_v \Xi^-_{(+)} \frac{\bar{p}_r}{M} \cdot \mathbf{X}^{(m)}_{JM}(q\vec{r}/2) \\ &+ \frac{q}{2M}[2\mu_v \Xi^-_{(+)} \Sigma_{(+)} + 2\mu_v \Xi^-_{(-)} \Sigma_{(-)}] \cdot \mathbf{X}^{(e)}_{JM}(q\vec{r}/2) \end{aligned} \tag{8.2.14}$$

For E_J with J even

$$\begin{aligned} E_{JM}(em) &= \left[Q_s + Q_v \Xi^z_{(+)}\right] \frac{\bar{p}_r}{M} \cdot \mathbf{X}^{(e)}_{JM}(q\vec{r}/2) \\ &+ \frac{q}{2M}[\mu_s \Sigma_{(+)} + \mu_v \Xi^z_{(+)} \Sigma_{(+)} + \mu_v \Xi^z_{(-)} \Sigma_{(-)}] \cdot \mathbf{X}^{(m)}_{JM}(q\vec{r}/2) \end{aligned} \tag{8.2.15}$$

$$\begin{aligned} E_{JM}(W) &= 2Q_v \Xi^-_{(+)} \frac{\bar{p}_r}{M} \cdot \mathbf{X}^{(e)}_{JM}(q\vec{r}/2) \\ &+ \frac{q}{2M}[2\mu_v \Xi^-_{(+)} \Sigma_{(+)} + 2\mu_v \Xi^-_{(-)} \Sigma_{(-)}] \cdot \mathbf{X}^{(m)}_{JM}(q\vec{r}/2) \end{aligned} \tag{8.2.16}$$

And finally for E_J with J odd

$$\begin{aligned} E_{JM}(em) &= Q_v \Xi_{(-)} \frac{\bar{p}_r}{M} \cdot \mathbf{X}^{(e)}_{JM}(q\vec{r}/2) \\ &+ \frac{q}{2M}[\mu_s \Sigma_{(-)} + \mu_v \Xi^z_{(+)} \Sigma_{(-)} + \mu_v \Xi^z_{(-)} \Sigma_{(+)}] \cdot \mathbf{X}^{(m)}_{JM}(q\vec{r}/2) \end{aligned} \tag{8.2.17}$$

$$\begin{aligned} E_{JM}(W) &= 2Q_v \Xi_{(-)} \frac{\bar{p}_r}{M} \cdot \mathbf{X}^{(e)}_{JM}(q\vec{r}/2) \\ &+ \frac{q}{2M}[2\mu_v \Xi^-_{(+)} \Sigma_{(-)} + 2\mu_v \Xi^-_{(-)} \Sigma_{(+)}] \cdot \mathbf{X}^{(m)}_{JM}(q\vec{r}/2) \end{aligned} \tag{8.2.18}$$

The operator $\Xi^z_{(+)}$ conserves isospin and gives the value M_T.

$$\Xi^z_{(+)} |TM_T\rangle = M_T |TM_T\rangle \tag{8.2.19}$$

On the other hand, the operator $\Xi^z_{(-)}$ changes the isospin. It is only non-zero for $M_T = 0$.

$$\Xi^z_{(-)} |T = 1, M_T = 0\rangle = |T = 0, M_T = 0\rangle , \quad \Xi^z_{(-)} |T = 0, M_T = 0\rangle = |T = 1, M_T = 0\rangle \tag{8.2.20}$$

The isospin lowering operator we need is

$$\Xi^-_{(+)} |1, 1\rangle = \frac{1}{\sqrt{2}} |1, 0\rangle , \quad \Xi^-_{(-)} |1, 1\rangle = -\frac{1}{\sqrt{2}} |0, 0\rangle \tag{8.2.21}$$

Some of the terms will also involve an iso-tensor

$$T_{1,-1} = -\frac{1}{2}(\tau_a^- \tau_b^z - \tau_a^z \tau_b^-) \tag{8.2.22}$$

And we will need the matrix element

$$T_{1,-1}\,|1,1\rangle = \frac{1}{\sqrt{2}}\,|0,0\rangle \tag{8.2.23}$$

The initial, final, and intermediate states will be product states of center of mass motion and a relative wavefunction. As before, we ignore nuclear recoil and go to the target frame.

$$\begin{aligned} |i\rangle &\to |\vec{0}, \psi_{ir}\rangle \\ |f\rangle &\to |\vec{0}, \psi_{fr}\rangle \end{aligned} \tag{8.2.24}$$

The sum over intermediate states is an integral over center of mass momentum and a sum/integral over intermediate relative wavefunctions.

$$\sum_n |n\rangle\langle n| \to \int \frac{d^3p}{(2\pi)^3} \sum\!\!\!\!\!\!\int_{\alpha_r} |\vec{p}, \alpha_r\rangle\langle \vec{p}, \alpha_r| \tag{8.2.25}$$

Then use translation invariance for the current operators

$$\langle \vec{p}_2 \psi_r' | J^\mu(\vec{x}) | \vec{p}_1 \psi\rangle = \langle \vec{p}_2 \psi_r' | J^\mu(\vec{0}) | \vec{p}_1 \psi\rangle\, e^{-i(\vec{p}_2 - \vec{p}_1)\cdot\vec{x}} \tag{8.2.26}$$

This gives us a delta function which eliminates the integral over center of mass momentum for the intermediate states. All that remains is a sum over intermediate relative states.

$$\begin{aligned} \vec{\mathcal{J}} = -\frac{i}{2}(8\pi^2) \int \frac{d^3k}{(2\pi)^3} \frac{1}{|\vec{k}|^4} \sum\!\!\!\!\!\!\int_{\alpha_r} \Big(& \langle \vec{0}, \psi_{fr} | \vec{k} \times \vec{J}_{em}(\vec{0}) | \vec{k}, \alpha_r\rangle \langle \vec{k}, \alpha_r | \rho_W(\vec{0}) | \vec{0}, \psi_{ir}\rangle \\ & + \langle \vec{0}, \psi_{fr} | \rho_W(\vec{0}) | -\vec{k}, \alpha_r\rangle \langle -\vec{k}, \alpha_r | \vec{k} \times \vec{J}_{em}(\vec{0}) | \vec{0}, \psi_{ir}\rangle \\ & - \langle \vec{0}, \psi_{fr} | \rho_{em}(\vec{0}) | \vec{k}, \alpha_r\rangle \langle \vec{k}, \alpha_r | \vec{k} \times \vec{J}_W(\vec{0}) | \vec{0}, \psi_{ir}\rangle \\ & - \langle \vec{0}, \psi_{fr} | \vec{k} \times \vec{J}_W(\vec{0}) | -\vec{k}, \alpha_r\rangle \langle -\vec{k}, \alpha_r | \rho_{em}(\vec{0}) | \vec{0}, \psi_{ir}\rangle \Big) \end{aligned} \tag{8.2.27}$$

Because we take a cross product with $\vec{k}$, the center of mass current terms don't contribute. Therefore we can write this only in terms of the relative current matrix operators and matrix elements. We also rearrange the integrals to reflect the way we are going to evaluate it.

$$\begin{aligned} \vec{\mathcal{J}} = -2i \int_0^\infty \frac{d|\vec{k}|}{|\vec{k}|} \sum\!\!\!\!\!\!\int_{\alpha_r} \int \frac{d\Omega_k}{4\pi} \Big(& \langle \psi_{fr} | \hat{k} \times \vec{\tilde{J}}_{em,r}(-\vec{k}) | \alpha_r\rangle \langle \alpha_r | \tilde{\rho}_{W,r}(\vec{k}) | \psi_{ir}\rangle \\ & + \langle \psi_{fr} | \tilde{\rho}_{W,r}(\vec{k}) | \alpha_r\rangle \langle \alpha_r | \hat{k} \times \vec{\tilde{J}}_{em,r}(-\vec{k}) | \psi_{ir}\rangle \\ & - \langle \psi_{fr} | \tilde{\rho}_{em,r}(-\vec{k}) | \alpha_r\rangle \langle \alpha_r | \hat{k} \times \vec{\tilde{J}}_{W,r}(\vec{k}) | \psi_{ir}\rangle \\ & - \langle \psi_{fr} | \hat{k} \times \vec{\tilde{J}}_{W,r}(\vec{k}) | \alpha_r\rangle \langle \alpha_r | \tilde{\rho}_{em,r}(-\vec{k}) | \psi_{ir}\rangle \Big) \end{aligned} \tag{8.2.28}$$

Of course this looks very similar to the result we had earlier, but now we have been careful to remove the center of mass and write everything only in terms of relative matrix elements.

The charge operator can be written in terms of a multipole decomposition.

$$\tilde{\rho}(\vec{q}) = 4\pi \sum_{JM} i^J C_{JM} Y_{JM}(\hat{q})^* \tag{8.2.29}$$

Since we take a cross product with $\vec{k}$ in both the Fermi and Gamow-Teller case, we do not need to consider the longitudinal part of the currents. We can write the magnetic and electric multipoles of the current using the vector spherical harmonics, defined in Equation D.2.8.

$$\tilde{J}(\vec{q}) = 4\pi \sum_{JM} \left\{ i^J M_{JM} \mathbf{\Phi}_{JM}(\hat{q})^* - i^J E_{JM} \mathbf{\Psi}_{JM}(\hat{q})^* \right\} \tag{8.2.30}$$

When we take the cross product with the momentum transfer, we need to use the cross product identity for the vector spherical harmonics.

$$\begin{aligned} \hat{q} \times \mathbf{\Psi}_{JM} &= i\mathbf{\Phi}_{JM} \\ \hat{q} \times \mathbf{\Phi}_{JM} &= i\mathbf{\Psi}_{JM} \end{aligned} \tag{8.2.31}$$

And we need the integral identities

$$\begin{aligned} \int d\Omega_k Y_{LM_L}(\hat{k}) \mathbf{\Phi}_{JM_J}(\hat{k})^* &= C^{JM_J}_{LM_L 1q} \delta_{J,L} e_q^* \\ \int d\Omega_k Y_{LM_L}(\hat{k}) \mathbf{\Psi}_{JM_J}(\hat{k})^* &= C^{JM_J}_{LM_L 1q} \left(\delta_{L,J-1} \sqrt{\frac{J+1}{2J+1}} + \delta_{L,J+1} \sqrt{\frac{J}{2J+1}} \right) e_q^* \end{aligned} \tag{8.2.32}$$

Now we can go through term-by-term and evaluate the result in terms of reduced matrix elements. Each term involves an integral over angles $d\Omega_k$. We eliminate the sums over angular momentum quantum number m by expressing the result in terms of reduced matrix elements. The final results are all functions of the loop momentum $|\vec{k}|$. Then we can compare to the result using the completeness relation, which consists of both a one-body and two-body part.

First Term

We will go through the first term in more detail, and then the other three terms proceed in exactly the same way. Term 1 in Figure 8.2 is given by the expression

$$-2i \int_0^\infty \frac{d|\vec{k}|}{|\vec{k}|} \sum\!\!\!\!\!\!\int_{\alpha_r} \frac{d\Omega_k}{4\pi} \left\langle \psi_{fr} | \hat{k} \times \vec{\tilde{J}}_{em,r}(-\vec{k}) | \alpha_r \right\rangle \left\langle \alpha_r | \tilde{\rho}_{W,r}(\vec{k}) | \psi_{ir} \right\rangle \tag{8.2.33}$$

Using the completeness relation to remove intermediate states, we have an expression involving the sum over one-body currents. Plugging in the one-body currents, we have

$$\begin{aligned} &-2i\frac{1}{|\vec{k}|}\int\frac{d\Omega_k}{4\pi}\,\langle\psi_{fr}|\hat{k}\times\vec{\tilde{J}}_{em,r}(-\vec{k})\tilde{\rho}_{W,r}(\vec{k})|\psi_{ir}\rangle \\ =\frac{1}{M_N}\int\frac{d\Omega_k}{4\pi}\,\langle\psi_{fr}|\sum_{a,b}e^{-i\vec{k}\cdot(\vec{x}_a-\vec{x}_b)}\Big(&-\frac{2i}{|\vec{k}|}\hat{e}_a\hat{k}\times\vec{p}_a+\hat{\mu}_a(\hat{k}(\hat{k}\cdot\vec{\sigma}_a)-\vec{\sigma}_a)\Big)\tau_b^-|\psi_{ir}\rangle \end{aligned} \tag{8.2.34}$$

The sum over nucleons splits up into a one-body part with $a=b$ and a two-body part with $a\neq b$. When $a=b$ we use $\hat{e}\tau^-=0$ and $\hat{\mu}\tau^-=\mu_n\tau^-$. The exponential goes to 1 and the integral over angles $d\Omega_k$ becomes spherically symmetric, so we can use $k^ik^j\to\frac{1}{3}|\vec{k}|^2\delta^{ij}$. The result is that the one-body term is independent of $|\vec{k}|$, and proportional to the tree-level Gamow-Teller matrix element.

$$-\frac{2\mu_n}{3M_N}\,\langle\psi_{fr}|\sum_a\vec{\sigma}_a\tau_a^-|\psi_{ir}\rangle \tag{8.2.35}$$

It is easy to understand why this term is proportional to the neutron magnetic moment, μ_n. In the one-body part of term 1, the the weak charge operator converts one proton into a neutron. Then, the electromagnetic current $\vec{J}_{em}$ latches onto the same neutron and flips the spin. The strength of this interaction is proportional to the neutron magnetic moment, μ_n.

For the two-body part when $a\neq b$, use the identities in Equation 7.3.4 to integrate over angles.

$$\begin{aligned} -\frac{1}{M_N}\,\langle\psi_{fr}|\sum_{a\neq b}\Bigg(&2\frac{j_1(|\vec{k}|r)}{|\vec{k}|r}\hat{e}_a\vec{r}\times\vec{p}_a+\frac{2}{3}j_0(|\vec{k}|r)\hat{\mu}_a\vec{\sigma}_a \\ &+\hat{\mu}_a j_2(|\vec{k}|r)(\hat{r}(\hat{r}\cdot\vec{\sigma}_a)-\frac{1}{3}\vec{\sigma}_a)\Bigg)\tau_b^-\,|\psi_{ir}\rangle \end{aligned} \tag{8.2.36}$$

Write this in terms of symmetric operators and convert the sum into a sum over $a<b$. Just as we did in Section 5.3, we get terms involving spin, orbital angular momentum, and a tensor operator. This time, the result also involves the center of mass momentum $\vec{P}$.

$$\begin{aligned} -\frac{1}{M_N}\,\langle\psi_{fr}|\sum_{a<b}\Bigg(&\frac{j_1(|\vec{k}|r)}{|\vec{k}|r}\vec{r}\times\vec{P}(-\Xi^-_{(-)}+T_{1,-1})+2\frac{j_1(|\vec{k}|r)}{|\vec{k}|r}\vec{r}\times\vec{p}_r(\Xi^-_{(+)}+T_{2,-1}) \\ &+\left[\frac{2}{3}j_0(|\vec{k}|r)\Sigma_{(+)}+j_2(|\vec{k}|r)\left(\hat{r}(\hat{r}\cdot\Sigma_{(+)})-\Sigma_{(+)}\right)\right](\mu_s\Xi^-_{(+)}+\mu_vT_{2,-1}) \\ &+\left[\frac{2}{3}j_0(|\vec{k}|r)\Sigma_{(-)}+j_2(|\vec{k}|r)\left(\hat{r}(\hat{r}\cdot\Sigma_{(-)})-\Sigma_{(-)}\right)\right](-\mu_s\Xi^-_{(-)}+\mu_vT_{1,-1})\Bigg)\,|\psi_{ir}\rangle \end{aligned} \tag{8.2.37}$$

This greatly simplifies when we keep only the terms which contribute to pp-fusion, which must involve the spin-flip, $\Sigma_{(-)}$. The isospin matrix element we need to compute is

$$\langle 0,0|(-\mu_s\Xi^-_{(-)}+\mu_vT_{1,-1})|1,1\rangle=\frac{1}{\sqrt{2}}(\mu_s+\mu_v)=\sqrt{2}\mu_p \tag{8.2.38}$$

Expressing the result in terms of multipoles, we find the two-body part for term 1. Again this only involves the electric multipole $E1$.

$$-\frac{2\mu_p}{M_N}\sqrt{\frac{4\pi}{3}}\,\langle\psi_{fr}|\sum_{a<b}(-i)\mathbf{X}^{(e)}_{1q}(|\vec{k}|\vec{r})\cdot\Sigma_{(-)}\,|\psi_{ir}\rangle\,e^*_q \tag{8.2.39}$$

Just as we did for the one-body part, we can understand why the two-body part must be proportional to the proton magnetic moment, μ_p. In this case, the weak current converts one proton into a neutron and the electromagnetic current flips the spin of the remaining proton. This interaction strength is proportional to μ_p.

Now suppose we do not use the completeness relation, and we instead calculate the result using intermediate states. We plug in the multipole decomposition of the currents and use the integral identities for the vector spherical harmonics to integrate over angles $d\Omega_k$.

$$\begin{aligned}
&\int\frac{d\Omega_k}{4\pi}\,\langle\psi_{fr}|\hat{k}\times\vec{\tilde{J}}_{em,r}(-\vec{k})|\alpha_r\rangle\,\langle\alpha_r|\tilde{\rho}_{W,r}(\vec{k})|\psi_{ir}\rangle\\
&= e^*_q 4\pi(-1)^{M_L}C^{JM_J}_{L-M_L,1q}\Bigg(-\delta_{L,J-1}\sqrt{\frac{J+1}{2J+1}}\,\langle\psi_{fr}|M_{JM_J}(em)|\alpha_r\rangle\,\langle\alpha_r|C_{J-1,M_L}(W)|\psi_{ir}\rangle\\
&\qquad -i\delta_{L,J}\,\langle\psi_{fr}|E_{JM_J}(em)|\alpha_r\rangle\,\langle\alpha_r|C_{J,M_L}(W)|\psi_{ir}\rangle\\
&\qquad +\delta_{L,J+1}\sqrt{\frac{J}{2J+1}}\,\langle\psi_{fr}|M_{JM_J}(em)|\alpha_r\rangle\,\langle\alpha_r|C_{J+1,M_L}(W)|\psi_{ir}\rangle\Bigg)
\end{aligned} \tag{8.2.40}$$

This expression can be greatly simplified by writing the result in terms of reduced matrix elements. This allows us to isolate the dependence on the angular momentum quantum number m and do the sums over m explicitly. We write the current matrix elements in terms of the reduced matrix elements, and this gives us two additional Clebsh-Gordon coefficients. In order to sum over m's, we need to use the following identity for the six-J symbol.

$$\begin{aligned}
&\sum_{M_J,M_L,m_\alpha}(-1)^{M_L}C^{JM_J}_{L-M_L,1q}\frac{C^{j_fm_f}_{j_\alpha m_\alpha,JM_J}}{\sqrt{2j_f+1}}\frac{C^{j_\alpha m_\alpha}_{j_i m_i,LM_L}}{\sqrt{2j_\alpha+1}}\\
&= (-1)^{L+1+j_i+j_f}\sqrt{2J+1}\begin{Bmatrix} j_i & j_f & 1\\ J & L & j_\alpha\end{Bmatrix}\frac{C^{j_fm_f}_{j_i m_i,1q}}{\sqrt{2j_f+1}}
\end{aligned} \tag{8.2.41}$$

The remaining Clebsh-Gordon symbol is the same one that shows up in the tree-level matrix element of the Gamow-Teller operator, which also has spin 1. The six-J symbol we need in this case evaluates to

$$\begin{Bmatrix} 0 & 1 & 1\\ J & L & L\end{Bmatrix} = \frac{(-1)^{J+L+1}}{\sqrt{3(2L+1)}} \tag{8.2.42}$$

Applying this identity allows us to write the contribution from term 1 in terms of reduced matrix elements.

$$\begin{aligned}
&\int \frac{d\Omega_k}{4\pi} \langle \psi_{fr}|\hat{k}\times\vec{\tilde{J}}_{em,r}(-\vec{k})|\alpha_r\rangle \langle \alpha_r|\tilde{\rho}_{W,r}(\vec{k})|\psi_{ir}\rangle \\
&\quad = 4\pi(-1)^{J+j_i+j_f} \left\{ \begin{array}{ccc} j_i & j_f & 1 \\ J & L & j_\alpha \end{array} \right\} \frac{C^{j_f m_f}_{j_i m_i,1q}}{\sqrt{2j_f+1}} e^*_q \\
\times\Bigg(&- \delta_{L,J-1}\sqrt{J+1}\,\langle \psi_{fr}||M_J(em)||\alpha_r\rangle \langle \alpha_r||C_{J-1}(W)||\psi_{ir}\rangle \\
&+ i\delta_{L,J}\sqrt{2J+1}\,\langle \psi_{fr}||E_J(em)||\alpha_r\rangle \langle \alpha_r||C_J(W)||\psi_{ir}\rangle \\
&+ \delta_{L,J+1}\sqrt{J}\,\langle \psi_{fr}||M_J(em)||\alpha_r\rangle \langle \alpha_r||C_{J+1}(W)||\psi_{ir}\rangle \Bigg)
\end{aligned} \tag{8.2.43}$$

Note that the weak charge operator does not cause a spin flip at lowest order in $1/M_N$, so the spin flip must come from the electromagnetic current. Therefore the intermediate states we need to consider are np spin singlet states with $S = 0$. This leaves us with two options for the total isospin. We can go through even parity states with $S = 0$ and $T = 1$.

$$np: \quad {}^1S_0, \quad {}^1D_2, ... \tag{8.2.44}$$

This picks out unique operator structures for each of the multipole operators.

$$\begin{aligned}
C_{JM}(W) &\to 2Q_v \Xi^-_{(+)} X_{JM}(k\vec{r}/2), \quad (J \text{ even}) \\
M_{JM}(em) &\to \mu_v \frac{|\vec{k}|}{2M_N} \mathbf{X}^{(e)}_{JM}(k\vec{r}/2)\cdot\Sigma_{(-)}\Xi^z_{(-)}, \quad (J \text{ odd}) \\
E_{JM}(em) &\to \mu_v \frac{|\vec{k}|}{2M_N} \mathbf{X}^{(m)}_{JM}(k\vec{r}/2)\cdot\Sigma_{(-)}\Xi^z_{(-)}, \quad (J \text{ even})
\end{aligned} \tag{8.2.45}$$

The isospin matrix elements we need are

$$\langle 0,0|\Xi^z_{(-)}|1,0\rangle \langle 1,0|\Xi^-_{(+)}|1,1\rangle = 1/\sqrt{2} \tag{8.2.46}$$

Since $j_i = 0$, it is helpful to rearrange the terms using L instead of J. We only need to sum

over even values of L. We also plug in the result for the six-J symbol.

$$\begin{aligned}(-2i)\frac{1}{|\vec{k}|}\int\frac{d\Omega_k}{4\pi}\langle\psi_{fr}|\hat{k}\times\vec{\tilde{J}}_{em,r}(-\vec{k})|\alpha_r\rangle\langle\alpha_r|\tilde{\rho}_{W,r}(\vec{k})|\psi_{ir}\rangle\\ =(2)2\mu_v\frac{1}{\sqrt{2}}\frac{1}{2M_N}4\pi\frac{1}{\sqrt{3(2L+1)}}\frac{C^{j_fm_f}_{j_im_i,1q}}{\sqrt{2j_f+1}}e^*_q\\ \times\Bigg(-\delta_{L+1,J}\sqrt{L+2}\,\langle\psi_{fr}||(-i)\mathbf{X}^{(e)}_{L+1}(q\vec{r}/2)\cdot\Sigma_{(-)}||\alpha_r\rangle\langle\alpha_r||X_L(k\vec{r}/2)||\psi_{ir}\rangle\quad(L\text{ even})\\ +\delta_{L,J}\sqrt{2L+1}\,\langle\psi_{fr}||\mathbf{X}^{(m)}_{L}(q\vec{r}/2)\cdot\Sigma_{(-)}||\alpha_r\rangle\langle\alpha_r||X_L(k\vec{r}/2)||\psi_{ir}\rangle\quad(L\text{ even})\\ +\delta_{L-1,J}\sqrt{L-1}\,\langle\psi_{fr}||(-i)\mathbf{X}^{(e)}_{L-1}(q\vec{r}/2)\cdot\Sigma_{(-)}||\alpha_r\rangle\langle\alpha_r||X_L(k\vec{r}/2)||\psi_{ir}\rangle\quad(L\text{ even})\Bigg)\end{aligned}\tag{8.2.47}$$

Alternatively, we can go through odd parity np intermediate states with $S=0$ and $T=0$.

$$np:\quad {}^1P_1,\quad {}^1F_3,...\tag{8.2.48}$$

This again picks out unique operator structures for each of the multipole operators.

$$\begin{aligned}C_{JM}(W)&\to 2Q_v\Xi^-_{(-)}X_{JM}(k\vec{r}/2),\quad (J\text{ odd})\\ M_{JM}(em)&\to\mu_s\frac{|\vec{k}|}{2M_N}\mathbf{X}^{(e)}_{JM}(k\vec{r}/2)\cdot\Sigma_{(-)},\quad (J\text{ even})\\ E_{JM}(em)&\to\mu_s\frac{|\vec{k}|}{2M_N}\mathbf{X}^{(m)}_{JM}(k\vec{r}/2)\cdot\Sigma_{(-)},\quad (J\text{ odd})\end{aligned}\tag{8.2.49}$$

The isospin matrix elements we need are

$$\langle 0,0|1|0,0\rangle\langle 0,0|\Xi^-_{(-)}|1,1\rangle=-1/\sqrt{2}\tag{8.2.50}$$

Again it is helpful to rewrite this in terms of L, which is always odd in this case. Plug in the six-J symbol.

$$\begin{aligned}(-2i)\frac{1}{|\vec{k}|}\int\frac{d\Omega_k}{4\pi}\langle\psi_{fr}|\hat{k}\times\vec{\tilde{J}}_{em,r}(-\vec{k})|\alpha_r\rangle\langle\alpha_r|\tilde{\rho}_{W,r}(\vec{k})|\psi_{ir}\rangle\\ =(2)2\mu_s\left(\frac{1}{\sqrt{2}}\right)\frac{1}{2M_N}4\pi\frac{1}{\sqrt{3(2L+1)}}\frac{C^{j_fm_f}_{j_im_i,1q}}{\sqrt{2j_f+1}}e^*_q\\ \times\Bigg(-\delta_{L+1,J}\sqrt{L+2}\,\langle\psi_{fr}||(-i)\mathbf{X}^{(e)}_{L+1}(q\vec{r}/2)\cdot\Sigma_{(-)}||\alpha_r\rangle\langle\alpha_r||X_L(k\vec{r}/2)||\psi_{ir}\rangle\quad(L\text{ odd})\\ +\delta_{L,J}\sqrt{2L+1}\,\langle\psi_{fr}||\mathbf{X}^{(m)}_{L}(q\vec{r}/2)\cdot\Sigma_{(-)}||\alpha_r\rangle\langle\alpha_r||X_L(k\vec{r}/2)||\psi_{ir}\rangle\quad(L\text{ odd})\\ +\delta_{L-1,J}\sqrt{L-1}\,\langle\psi_{fr}||(-i)\mathbf{X}^{(e)}_{L-1}(q\vec{r}/2)\cdot\Sigma_{(-)}||\alpha_r\rangle\langle\alpha_r||X_L(k\vec{r}/2)||\psi_{ir}\rangle\quad(L\text{ odd})\Bigg)\end{aligned}\tag{8.2.51}$$

Second Term

The second term in Figure 8.2 corresponds to the expression

$$-2i\int_0^\infty \frac{d|\vec{k}|}{|\vec{k}|}\sum\!\!\!\!\!\!\int_{\alpha_r}\frac{d\Omega_k}{4\pi}\,\langle\psi_{fr}|\tilde{\rho}_{W,r}(\vec{k})|\alpha_r\rangle\,\langle\alpha_r|\hat{k}\times\vec{\tilde{J}}_{em,r}(-\vec{k})|\psi_{ir}\rangle \tag{8.2.52}$$

When we use the completeness relation to sum over states, we find the same thing as in term 1, except with the order of the operators flipped

$$\begin{aligned}&(-2i)\frac{1}{|\vec{k}|}\int\frac{d\Omega_k}{4\pi}\,\langle\psi_{fr}|\tilde{\rho}_{W,r}(\vec{k})\hat{k}\times\vec{\tilde{J}}_{em,r}(-\vec{k})|\psi_{ir}\rangle\\ =\frac{1}{M_N}\int\frac{d\Omega_k}{4\pi}\,\langle\psi_{fr}|\sum_{a,b}e^{-i\vec{k}\cdot(\vec{x}_a-\vec{x}_b)}\tau_b^-\bigg(&-\frac{2i}{|\vec{k}|}\hat{e}_a\hat{k}\times\vec{p}_a+\hat{\mu}_a(\hat{k}(\hat{k}\cdot\vec{\sigma}_a)-\vec{\sigma}_a)\bigg)|\psi_{ir}\rangle\end{aligned} \tag{8.2.53}$$

The two-body part doesn't change when we swap the order of the operators, so the two-body part is the same as in the first term. When $a=b$ we use $\tau^-\hat{e}=\tau^-$ and $\tau^-\hat{\mu}=\mu_p\tau^-$. We can also use $k^ik^j\to\frac{1}{3}|\vec{k}|^2\delta^{ij}$.

$$-\frac{2\mu_p}{3M_N}\,\langle\psi_{fr}|\sum_a\vec{\sigma}_a\tau_a^-|\psi_{ir}\rangle \tag{8.2.54}$$

Now calculate the result with explicit intermediate states. We do the same multipole decomposition and angular momentum algebra as we did in the first term, and we find

$$\begin{aligned}&\int\frac{d\Omega_k}{4\pi}\,\langle\psi_{fr}|\tilde{\rho}_{W,r}(\vec{k})|\alpha_r\rangle\,\langle\alpha_r|\hat{k}\times\vec{\tilde{J}}_{em,r}(-\vec{k})|\psi_{ir}\rangle\\ &\qquad=4\pi(-1)^{J+j_i+j_f}\left\{\begin{array}{ccc}j_i&j_f&1\\L&J&j_\alpha\end{array}\right\}\frac{C^{j_fm_f}_{j_im_i,1q}}{\sqrt{2j_f+1}}e_q^*\\ \times\bigg(&-\delta_{L,J-1}\sqrt{J+1}\,\langle\psi_{fr}||C_{J-1}(W)||\alpha_r\rangle\,\langle\alpha_r||M_J(em)||\psi_{ir}\rangle\\ &-i\delta_{L,J}\sqrt{2J+1}\,\langle\psi_{fr}||C_J(W)||\alpha_r\rangle\,\langle\alpha_r||E_J(em)||\psi_{ir}\rangle\\ &+\delta_{L,J+1}\sqrt{J}\,\langle\psi_{fr}||C_{J+1}(W)||\alpha_r\rangle\,\langle\alpha_r||M_J(em)||\psi_{ir}\rangle\bigg)\end{aligned} \tag{8.2.55}$$

This goes through odd parity pp intermediate states with $S=1$ and $T=1$.

$$pp:\ \ {}^3P_0,\ \ {}^3P_1,\ \ {}^3P_2-{}^3F_2,\ \ {}^3F_3,... \tag{8.2.56}$$

This selects out the following operator structures from each of the multipole operators.

$$\begin{aligned}C_{JM}(W)&\to 2Q_v\Xi^-_{(-)}X_{JM}(k\vec{r}/2),\quad (J\text{ odd})\\ M_{JM}(em)&\to\frac{|\vec{k}|}{2M_N}\mathbf{X}^{(e)}_{JM}(k\vec{r}/2)\cdot\Sigma_{(-)}(\mu_s+\mu_v\Xi^z_{(+)}),\quad (J\text{ even})\\ E_{JM}(em)&\to\frac{|\vec{k}|}{2M_N}\mathbf{X}^{(m)}_{JM}(k\vec{r}/2)\cdot\Sigma_{(-)}(\mu_s+\mu_v\Xi^z_{(+)}),\quad (J\text{ odd})\end{aligned} \tag{8.2.57}$$

The isospin matrix element we need to compute is

$$\langle 0,0|\Xi^{-}_{(-)}|1,1\rangle \langle 1,1|(\mu_s+\mu_v\Xi^{z}_{(+)})|1,1\rangle = -\frac{1}{\sqrt{2}}(\mu_s+\mu_v) \tag{8.2.58}$$

Plug in for the six-J symbol and we find

$$\begin{aligned}
&(-2i)\frac{1}{|\vec{k}|}\int \frac{d\Omega_k}{4\pi}\langle\psi_{fr}|\tilde{\rho}_{W,r}(\vec{k})|\alpha_r\rangle\langle\alpha_r|\hat{k}\times\vec{\tilde{J}}_{em,r}(-\vec{k})|\psi_{ir}\rangle \\
&\quad = (2)2\left(-\frac{(\mu_s+\mu_v)}{\sqrt{2}}\right)\frac{1}{2M_N}4\pi\frac{1}{\sqrt{3(2J+1)}}\frac{C^{j_f m_f}_{j_i m_i,1q}}{\sqrt{2j_f+1}}e^*_q \\
\times\Bigg(&\delta_{L,J-1}\sqrt{J+1}\,\langle\psi_{fr}||X_{J-1}(k\vec{r}/2)||\alpha_r\rangle\langle\alpha_r||(-i)\mathbf{X}^{(e)}_J(k\vec{r}/2)\cdot\Sigma_{(-)}||\psi_{ir}\rangle \quad (J \text{ even}) \\
&+\delta_{L,J}\sqrt{2J+1}\,\langle\psi_{fr}||X_J(k\vec{r}/2)||\alpha_r\rangle\langle\alpha_r||\mathbf{X}^{(m)}_J(k\vec{r}/2)\cdot\Sigma_{(-)}||\psi_{ir}\rangle \quad (J \text{ odd}) \\
&-\delta_{L,J+1}\sqrt{J}\,\langle\psi_{fr}||X_{J+1}(k\vec{r}/2)||\alpha_r\rangle\langle\alpha_r||(-i)\mathbf{X}^{(e)}_J(k\vec{r}/2)\cdot\Sigma_{(-)}||\psi_{ir}\rangle \quad (J \text{ even})\Bigg)
\end{aligned} \tag{8.2.59}$$

Third Term

The third term in Figure 8.2 corresponds to the expression

$$+2i\int_0^\infty \frac{d|\vec{k}|}{|\vec{k}|}\sum\!\!\!\!\!\!\int_{\alpha_r}\frac{d\Omega_k}{4\pi}\langle\psi_{fr}|\tilde{\rho}_{em,r}(-\vec{k})|\alpha_r\rangle\langle\alpha_r|\hat{k}\times\vec{\tilde{J}}_{W,r}(\vec{k})|\psi_{ir}\rangle \tag{8.2.60}$$

Using the completeness relation to sum over intermediate states, we find

$$\begin{aligned}
&+2i\frac{1}{|\vec{k}|}\int\frac{d\Omega_k}{4\pi}\langle\psi_{fr}|\tilde{\rho}_{em,r}(-\vec{k})\hat{k}\times\vec{\tilde{J}}_{W,r}(\vec{k})|\psi_{ir}\rangle \\
&= \frac{1}{M_N}\int\frac{d\Omega_k}{4\pi}\langle\psi_{fr}|\sum_{a,b}e^{-i\vec{k}\cdot(\vec{x}_a-\vec{x}_b)}\hat{e}_a\left(\frac{2i}{|\vec{k}|}\hat{k}\times\vec{p}_b+\mu_v(\hat{k}(\hat{k}\cdot\vec{\sigma}_b)-\vec{\sigma}_b)\right)\tau^-_b|\psi_{ir}\rangle
\end{aligned} \tag{8.2.61}$$

When $a=b$ we use $\hat{e}\tau^-=0$, and we simply get zero for the one-body part. For the two-body part with $a\neq b$ we integrate over angles as before.

$$\begin{aligned}
-\frac{1}{M_N}\langle\psi_{fr}|\sum_{a\neq b}\hat{e}_a\Bigg(&-2\frac{j_1(|\vec{k}|r)}{|\vec{k}|r}\vec{r}\times\vec{p}_b+\frac{2}{3}j_0(|\vec{k}|r)\mu_v\vec{\sigma}_b \\
&+j_2(|\vec{k}|r)\mu_v(\hat{r}(\hat{r}\cdot\vec{\sigma}_b)-\frac{1}{3}\vec{\sigma}_b)\Bigg)\tau^-_b\,|\psi_{ir}\rangle
\end{aligned} \tag{8.2.62}$$

We can once again convert this to a sum over $a < b$, and write this in terms of operators which respect the exchange symmetry.

$$\begin{aligned}-\frac{1}{M_N}\langle\psi_{fr}|\sum_{a<b}\Bigg(&\frac{j_1(|\vec{k}|r)}{|\vec{k}|r}\vec{r}\times\vec{P}(\Xi^-_{(-)}-T_{1,-1})+2\frac{j_1(|\vec{k}|r)}{|\vec{k}|r}\vec{r}\times\vec{p}_r(\Xi^-_{(+)}+T_{2,-1})\\&+\left[\frac{2}{3}j_0(|\vec{k}|r)\vec{\Sigma}_{(+)}+j_2(|\vec{k}|r)(\hat{r}(\hat{r}\cdot\vec{\Sigma}_{(+)})-\frac{1}{3}\vec{\Sigma}_{(+)})\right]\mu_v(\Xi^-_{(+)}+T_{2,-1})\\&+\left[\frac{2}{3}j_0(|\vec{k}|r)\vec{\Sigma}_{(-)}+j_2(|\vec{k}|r)(\hat{r}(\hat{r}\cdot\vec{\Sigma}_{(-)})-\frac{1}{3}\vec{\Sigma}_{(-)})\right]\mu_v(\Xi^-_{(-)}-T_{1,-1})\Bigg)|\psi_{ir}\rangle\end{aligned} \tag{8.2.63}$$

The isospin matrix element we need to calculate is

$$\langle 0,0|(\mu_v\Xi^-_{(-)}-\mu_vT_{1,-1})|1,1\rangle=-\frac{2\mu_v}{\sqrt{2}} \tag{8.2.64}$$

The term which contributes to *pp*-fusion is

$$-(-i)\sqrt{2}\sqrt{\frac{4\pi}{3}}\left(-\frac{2\mu_v}{\sqrt{2}}\right)\frac{1}{M_N}e^*_q\langle\psi_{fr}|\sum_{a<b}\mathbf{X}^{(e)}_{1q}(|\vec{k}|\vec{r})\cdot\Sigma^-_{(-)}|\psi_{ir}\rangle \tag{8.2.65}$$

On the other hand, keeping intermediate states we find

$$\begin{aligned}&-\int\frac{d\Omega_k}{4\pi}\langle\psi_{fr}|\tilde{\rho}_{em,r}(-\vec{k})|\alpha_r\rangle\langle\alpha_r|\hat{k}\times\vec{\tilde{J}}_{W,r}(\vec{k})|\psi_{ir}\rangle\\&\quad=4\pi(-1)^{J+j_i+j_f}\left\{\begin{array}{ccc}j_i&j_f&1\\L&J&j_\alpha\end{array}\right\}\frac{C^{j_fm_f}_{j_im_i,1q}}{\sqrt{2j_f+1}}e^*_q\\\times\Bigg(&-\delta_{L,J-1}\sqrt{J+1}\langle\psi_{fr}||C_{J-1}(em)||\alpha_r\rangle\langle\alpha_r||M_J(W)||\psi_{ir}\rangle\\&-i\delta_{J,L}\sqrt{2J+1}\langle\psi_{fr}||C_J(em)||\alpha_r\rangle\langle\alpha_r||E_J(W)||\psi_{ir}\rangle\\&+\delta_{L,J+1}\sqrt{J}\langle\psi_{fr}||C_{J+1}(em)||\alpha_r\rangle\langle\alpha_r||M_J(W)||\psi_{ir}\rangle\Bigg)\end{aligned} \tag{8.2.66}$$

This goes through np intermediate states with $S=1$. We can have even parity states with $S=1$ and $T=0$.

$$np:\ \ {}^3S_1-{}^3D_1,\ \ {}^3D_2,... \tag{8.2.67}$$

This selects out the following operator structures for the multipole operators.

$$\begin{aligned}C_{JM}(em)&\to Q_sX_{JM}(k\vec{r}/2),\quad (J\text{ even})\\M_{JM}(W)&\to 2\mu_v\frac{|\vec{k}|}{2M_N}\mathbf{X}^{(e)}_{JM}(k\vec{r}/2)\cdot\Sigma_{(-)}\Xi^-_{(-)},\quad (J\text{ odd})\\E_{JM}(W)&\to 2\mu_v\frac{|\vec{k}|}{2M_N}\mathbf{X}^{(m)}_{JM}(k\vec{r}/2)\cdot\Sigma_{(-)}\Xi^-_{(-)},\quad (J\text{ even})\end{aligned} \tag{8.2.68}$$

The isospin matrix element we need to calculate is

$$\langle 0,0|1|0,0\rangle \langle 0,0|\Xi^-_{(-)}|1,1\rangle = -1/\sqrt{2} \tag{8.2.69}$$

Plug in for the six-J symbol, we find

$$\begin{aligned}
&(-2i)\frac{1}{|\vec{k}|}(-1)\int \frac{d\Omega_k}{4\pi}\langle\psi_{fr}|\tilde{\rho}_{em,r}(-\vec{k})|\alpha_r\rangle\langle\alpha_r|\hat{k}\times\vec{\tilde{J}}_{W,r}(\vec{k})|\psi_{ir}\rangle \\
&\qquad = (2)2\mu_v\left(-\frac{1}{\sqrt{2}}\right)\frac{1}{2M_N}4\pi\frac{1}{\sqrt{3(2J+1)}}\frac{C^{j_f m_f}_{j_i m_i,1q}}{\sqrt{2j_f+1}}e^*_q \\
\times\Bigg(&-\delta_{L,J-1}\sqrt{J+1}\,\langle\psi_{fr}||X_{J-1}(k\vec{r}/2)||\alpha_r\rangle\langle\alpha_r||(-i)\mathbf{X}^{(e)}_{JM}(k\vec{r}/2)\cdot\Sigma_{(-)}||\psi_{ir}\rangle \quad (J \text{ odd}) \\
&-\delta_{J,L}\sqrt{2J+1}\,\langle\psi_{fr}||X_J(k\vec{r}/2)||\alpha_r\rangle\langle\alpha_r||\mathbf{X}^{(m)}_{JM}(k\vec{r}/2)\cdot\Sigma_{(-)}||\psi_{ir}\rangle \quad (J \text{ even}) \\
&+\delta_{L,J+1}\sqrt{J}\,\langle\psi_{fr}||X_{J+1}(k\vec{r}/2)||\alpha_r\rangle\langle\alpha_r||(-i)\mathbf{X}^{(e)}_{JM}(k\vec{r}/2)\cdot\Sigma_{(-)}||\psi_{ir}\rangle \quad (J \text{ odd})\Bigg)
\end{aligned} \tag{8.2.70}$$

Alternatively, we can go through odd parity states with $S = 1$ and $T = 1$.

$$np: \;\; {}^3P_0, \;\; {}^3P_1, \;\; {}^3P_2 - {}^3F_2, \;\; {}^3F_3, ... \tag{8.2.71}$$

This selects out the following operator structures.

$$\begin{aligned}
C_{JM}(em) &\to Q_v\Xi^z_{(-)}X_{JM}(k\vec{r}/2), \quad (J \text{ odd}) \\
M_{JM}(W) &\to 2\mu_v\frac{|\vec{k}|}{2M_N}\mathbf{X}^{(e)}_{JM}(k\vec{r}/2)\cdot\Sigma_{(-)}\Xi^-_{(+)}, \quad (J \text{ even}) \\
E_{JM}(W) &\to 2\mu_v\frac{|\vec{k}|}{2M_N}\mathbf{X}^{(m)}_{JM}(k\vec{r}/2)\cdot\Sigma_{(-)}\Xi^-_{(+)}, \quad (J \text{ odd})
\end{aligned} \tag{8.2.72}$$

The isospin matrix element we need in this case is

$$\langle 0,0|\Xi^z_{(-)}|1,0\rangle\langle 1,0|\Xi^-_{(+)}|1,1\rangle = 1/\sqrt{2} \tag{8.2.73}$$

Plug in for the six-J symbol and we find

$$(-2i)\frac{1}{|\vec{k}|}(-1)\int\frac{d\Omega_k}{4\pi}\langle\psi_{fr}|\tilde{\rho}_{em,r}(-\vec{k})|\alpha_r\rangle\langle\alpha_r|\hat{k}\times\vec{\tilde{J}}_{W,r}(\vec{k})|\psi_{ir}\rangle$$
$$=(2)2\mu_v\left(\frac{1}{\sqrt{2}}\right)\frac{1}{2M_N}4\pi\frac{1}{\sqrt{3(2J+1)}}\frac{C^{j_fm_f}_{j_im_i,1q}}{\sqrt{2j_f+1}}e^*_q$$
$$\times\Bigg(+\delta_{L,J-1}\sqrt{J+1}\,\langle\psi_{fr}||X_{J-1}(k\vec{r}/2)||\alpha_r\rangle\langle\alpha_r||(-i)\mathbf{X}^{(e)}_{JM}(k\vec{r}/2)\cdot\Sigma_{(-)}||\psi_{ir}\rangle\quad(J\text{ even})$$
$$+\delta_{J,L}\sqrt{2J+1}\,\langle\psi_{fr}||X_J(k\vec{r}/2)||\alpha_r\rangle\langle\alpha_r||\mathbf{X}^{(m)}_{JM}(k\vec{r}/2)\cdot\Sigma_{(-)}||\psi_{ir}\rangle\quad(J\text{ odd})$$
$$-\delta_{L,J+1}\sqrt{J}\,\langle\psi_{fr}||X_{J+1}(k\vec{r}/2)||\alpha_r\rangle\langle\alpha_r||(-i)\mathbf{X}^{(e)}_{JM}(k\vec{r}/2)\cdot\Sigma_{(-)}||\psi_{ir}\rangle\quad(J\text{ even})\Bigg)\tag{8.2.74}$$

Fourth Term

The fourth term in Figure 8.2 corresponds to the expression

$$+2i\int_0^\infty\frac{d|\vec{k}|}{|\vec{k}|}\sum\!\!\!\!\!\!\int_{\alpha_r}\frac{d\Omega_k}{4\pi}\langle\psi_{fr}|\hat{k}\times\vec{\tilde{J}}_{W,r}(\vec{k})|\alpha_r\rangle\langle\alpha_r|\tilde{\rho}_{em,r}(-\vec{k})|\psi_{ir}\rangle\tag{8.2.75}$$

Using the completeness relation to sum over intermediate states, we find

$$(-2i)\frac{1}{|\vec{k}|}\int\frac{d\Omega_k}{4\pi}(-1)\langle\psi_{fr}|\tilde{\rho}_{em,r}(-\vec{k})\hat{k}\times\vec{\tilde{J}}_{W,r}(\vec{k})|\psi_{ir}\rangle$$
$$=\frac{1}{M_N}\int\frac{d\Omega_k}{4\pi}\langle\psi_{fr}|\sum_{a,b}e^{-i\vec{k}\cdot(\vec{x}_a-\vec{x}_b)}\left(\frac{2i}{|\vec{k}|}\hat{k}\times\vec{p}_b+\mu_v(\hat{k}(\hat{k}\cdot\vec{\sigma}_b)-\vec{\sigma}_b)\right)\tau^-_b\hat{e}_a|\psi_{ir}\rangle\tag{8.2.76}$$

This has the same two-body term as the previous term. For the one-body term when $a=b$, we use the fact that $\tau^-\hat{e}=\tau^-$ and once again use rotational symmetry of the integral.

$$(-2i)\frac{1}{|\vec{k}|}\int\frac{d\Omega_k}{4\pi}(-1)\langle\psi_{fr}|\tilde{\rho}_{em,r}(-\vec{k})\hat{k}\times\vec{\tilde{J}}_{W,r}(\vec{k})|\psi_{ir}\rangle$$
$$=-\frac{2\mu_v}{3M_N}\langle\psi_{fr}|\sum_a\vec{\sigma}_a\tau^-_a|\psi_{ir}\rangle\tag{8.2.77}$$

On the other hand, keeping intermediate states explicit

$$\begin{aligned}
&-\int \frac{d\Omega_k}{4\pi} \langle\psi_{fr}|\hat{k}\times\vec{\tilde{J}}_{W,r}(\vec{k})|\alpha_r\rangle\langle\alpha_r|\tilde{\rho}_{em,r}(-\vec{k})|\psi_{ir}\rangle \\
&\quad = 4\pi(-1)^{J+j_i+j_f}\left\{\begin{array}{ccc} j_i & j_f & 1 \\ J & L & j_\alpha \end{array}\right\}\frac{C^{j_f m_f}_{j_i m_i,1q}}{\sqrt{2j_f+1}}e^*_q \\
\times\Bigg(&-\delta_{L,J-1}\sqrt{J+1}\,\langle\psi_{fr}||M_J(W)||\alpha_r\rangle\langle\alpha_r||C_{J-1}(em)||\psi_{ir}\rangle \\
&+i\delta_{J,L}\sqrt{2J+1}\,\langle\psi_{fr}||E_J(W)||\alpha_r\rangle\langle\alpha_r||C_J(em)||\psi_{ir}\rangle \\
&+\delta_{L,J+1}\sqrt{J}\,\langle\psi_{fr}||M_J(W)||\alpha_r\rangle\langle\alpha_r||C_{J+1}(em)||\psi_{ir}\rangle\Bigg)
\end{aligned} \tag{8.2.78}$$

This goes through even parity pp intermediate states with $S=0$ and $T=1$.

$$pp: \quad {}^1S_0, \quad {}^1D_2, ... \tag{8.2.79}$$

This selects out the following operator structures from the multipoles.

$$\begin{aligned}
C_{JM}(em) &\to (Q_s + Q_v\Xi^z_{(+)})X_{JM}(k\vec{r}/2), \quad (J \text{ even}) \\
M_{JM}(W) &\to 2\mu_v\frac{|\vec{k}|}{2M_N}\mathbf{X}^{(e)}_{JM}(k\vec{r}/2)\cdot\Sigma_{(-)}\Xi^-_{(-)}, \quad (J \text{ odd}) \\
E_{JM}(W) &\to 2\mu_v\frac{|\vec{k}|}{2M_N}\mathbf{X}^{(m)}_{JM}(k\vec{r}/2)\cdot\Sigma_{(-)}\Xi^-_{(-)}, \quad (J \text{ even})
\end{aligned} \tag{8.2.80}$$

The isospin matrix element we need is

$$\langle 0,0|\Xi^-_{(-)}|1,1\rangle\langle 1,1|(Q_s+Q_v\Xi^z_{(+)})|1,1\rangle = -\frac{2}{\sqrt{2}} \tag{8.2.81}$$

It is helpful to rewrite this in terms of L, which is always even in this case. Also plug in the six-J symbol.

$$\begin{aligned}
&(-2i)\frac{1}{|\vec{k}|}(-1)\int\frac{d\Omega_k}{4\pi}\langle\psi_{fr}|\hat{k}\times\vec{\tilde{J}}_{W,r}(\vec{k})|\alpha_r\rangle\langle\alpha_r|\tilde{\rho}_{em,r}(-\vec{k})|\psi_{ir}\rangle \\
&\quad = (2)2\mu_v\left(-\frac{2}{\sqrt{2}}\right)\frac{1}{2M_N}4\pi\frac{1}{\sqrt{3(2L+1)}}\frac{C^{j_f m_f}_{j_i m_i,1q}}{\sqrt{2j_f+1}}e^*_q \\
\times\Bigg(&-\delta_{L+1,J}\sqrt{L+2}\,\langle\psi_{fr}||(-i)\mathbf{X}^{(e)}_{L+1}(k\vec{r}/2)\cdot\Sigma_{(-)}||\alpha_r\rangle\langle\alpha_r||X_L(k\vec{r}/2)||\psi_{ir}\rangle \quad (L \text{ even}) \\
&+\delta_{J,L}\sqrt{2L+1}\,\langle\psi_{fr}||\mathbf{X}^{(m)}_L(k\vec{r}/2)\cdot\Sigma_{(-)}||\alpha_r\rangle\langle\alpha_r||X_L(k\vec{r}/2)||\psi_{ir}\rangle \quad (L \text{ even}) \\
&+\delta_{L-1,J}\sqrt{L-1}\,\langle\psi_{fr}||(-i)\mathbf{X}^{(e)}_{L-1}(k\vec{r}/2)\cdot\Sigma_{(-)}||\alpha_r\rangle\langle\alpha_r||X_L(k\vec{r}/2)||\psi_{ir}\rangle \quad (L \text{ even})\Bigg)
\end{aligned} \tag{8.2.82}$$

8.3 Simple Harmonic Oscillator Basis Results

It is possible to do the calculation in terms of intermediate states in the coordinate space formulation. The sum over intermediate states would require us to solve the Schrodinger equation at every energy, and in every angular momentum channel. We would then need to re-calculate the matrix elements of the current operator for every value of $|\vec{k}|$. It is much more convenient to use the discrete simple harmonic oscillator (SHO) basis.

The SHO basis is a discrete basis, which makes it very convenient for computer calculation. All of the details are discussed in Appendix F. The basis is defined by picking a length scale, b, and a maximum number of oscillator quanta, Λ. States in the SHO basis are linear combinations of simple basis states.

$$|\psi\rangle = \sum_{nl}^{\Lambda} \psi_{nl} \, |(nl)stj\rangle \tag{8.3.1}$$

The basis wavefunctions are the usual SHO states with the length scale by b. The larger b we choose means that our wavefunctions will be more spread out. However, we need a smaller b in order to resolve the short-range core of the Av18 potential. It is good to choose a value of b similar to the size of the Av18 core. For these calculations, we choose a value of $b = 0.7$ fm.

The initial, final, and intermediate states are all calculated by diagonalizing the Av18 nuclear Hamiltonian in the SHO basis. This is made much easier by using the Talmi integrals, as described in Appendix F.1. Matrix elements of the current operators can be expressed as polynomials in $|\vec{k}|$, multiplied by a decaying exponential. This means we can do the calculation once, and we get an answer which is a function of $|\vec{k}|$. The current operator matrix elements we need are calculated in Appendix F.2.

The results for each of the four terms is given in Figure 8.3. The two-body part is the shaded region. We can see that the two-body part dies off past $|\vec{k}| > 2k_F$, and the result converges to the one-body part. At small $|\vec{k}|$, we only need to consider a few angular momentum channels to converge the result. At larger $|\vec{k}|$, the multipole description breaks down and we require more and more angular momentum channels to converge the result.

The SHO basis is a good tool for this problem, but it has some serious drawbacks. Ideally, we would choose a very large Λ so that our deuteron wavefunction converges to the true wavefunction. However, it will never be possible to adequately represent the initial *pp*-wavefunction due to its infinite extent. Our best hope is to reproduce the correct *pp*-wavefunction at small r, so that it gives the correct overlap with the compact deuteron wavefunction. A larger value of Λ means our *pp*-wavefunction is more spread out, and thus closer to $E_{pp} = 0$. However, a larger value of Λ means we need to work to higher precision, and the calculation becomes more and more challenging. The current operator matrix elements give very high order polynomials in $|\vec{k}|$, which begin to break down without very high precision. These calculations are done at the modest value of $\Lambda = 60$.

Because the basis is compact, we cannot go down to arbitrarily small energy for the initial *pp*-state. Using the values $b = 0.7$ and $\Lambda = 60$, the lowest energy we can get the

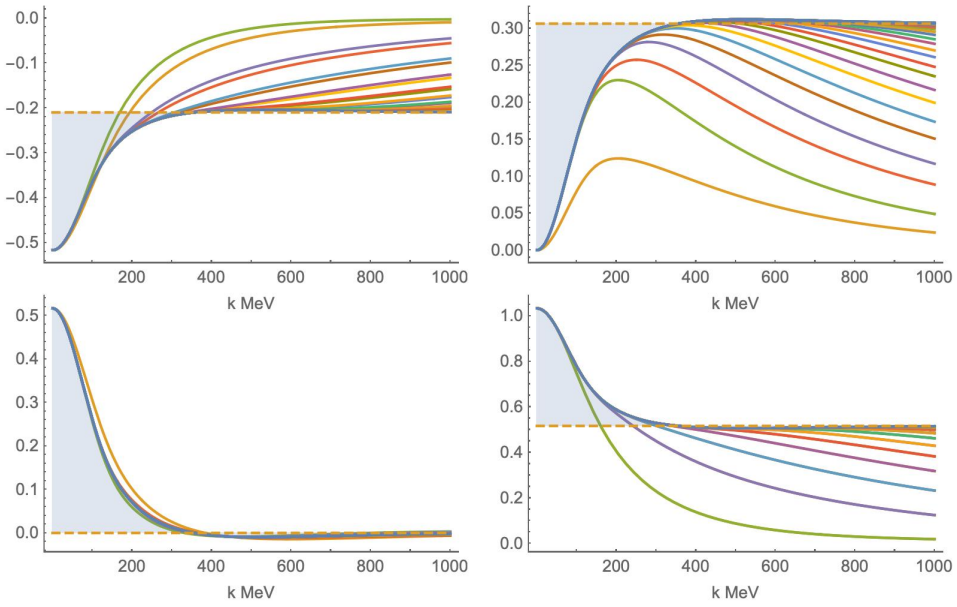

Figure 8.3: Completeness relation for the four terms described in Section 8. The shaded region represents the two-body part, and the orange dotted line represents the one-body part.

initial pp-state is at $E_{pp} = 1.3$ MeV. Thus the SHO basis cannot be used to extrapolate the result and calculate the radiative correction down to $E_{pp} \to 0$. The SHO basis is only used to analyze how intermediate states contribute to the overall result. In the next section, we will use the results of this section to analyze how the intermediate state energies effect the result when we go beyond the $\Delta E = 0$ approximation.

Chapter 9

Nuclear Energy Corrections

We want to compute the box diagram which, after factoring out the coupling constant and the lepton part, is given by an effective hadronic current.

$$\mathcal{J}^\beta = 8\pi^2 \int \frac{d^4k}{(2\pi)^4} \frac{\varepsilon^{\mu\lambda\alpha\beta} k_\alpha}{(k^2 + i\epsilon)^2} T_{\mu\lambda}(p,k) \tag{9.0.1}$$

and for a Gamow-Teller transition, we take $\beta = i$. As we did in Sections 5.3 and 8, we ignore the current-current terms which are higher order in the $1/M_N$ expansion.

$$\mathcal{J}^i = 8\pi^2 \int \frac{d^4k}{(2\pi)^4} \frac{1}{(k^2 + i\epsilon)^2} \epsilon^{ijk} k^j \left(T^{k0}(p_f, p_i, k) - T^{0k}(p_f, p_i, k) \right) \tag{9.0.2}$$

This involves the generalized Compton tensor for the $W\gamma$-box diagram. Using the integral form of the theta function, we can express this in terms of the full nuclear Hamiltonian (including the center of mass energy). Ignoring nuclear recoil and setting $p_i = p_f$, we have

$$\begin{aligned} T^{\mu\lambda}(p,k) = &\int d^3x\, e^{-i\vec{k}\cdot\vec{x}} \langle f | J^\mu_{em}(\vec{x}) \frac{1}{E_f + k^0 - H + i\epsilon} J^\lambda_W(\vec{0}) | i \rangle \\ &+ \int d^3x\, e^{-i\vec{k}\cdot\vec{x}} \langle f | J^\lambda_W(\vec{0}) \frac{1}{E_i - k^0 - H + i\epsilon} J^\mu_{em}(\vec{x}) | i \rangle \end{aligned} \tag{9.0.3}$$

The first term represents the so-called "direct" contribution, and the second term is the "cross" term. The full nuclear Hamiltonian consists of both a center of mass piece and a relative piece. In the non-relativistic formulation, we can write this as

$$H = \frac{P^2_{\text{cm}}}{2M_T} + H_r \tag{9.0.4}$$

Throughout this section, we will be making use of the Av18 nuclear Hamiltonian which we described in Section 6.

There are now two different approaches we can take in evaluating this expression. The first method involves calculating the nuclear Green's function, and the other approach involves plugging in intermediate states. The latter is a natural extension of what we did with

the completeness relation in Section 8, and this is the approach we will focus on. The Green's function approach will be discussed more when we discuss the coordinate space approach in Section 9.5.

With that in mind, we plug in a complete set of intermediate energy eigenstates and let the Hamiltonian hit the intermediate states. Then we have an expansion in terms of intermediate states.

$$\begin{aligned} T^{\mu\lambda}(p,k) = &\sum\!\!\!\!\!\!\int_{\alpha_r} \left(k^0 - \frac{|\vec{k}|^2}{2M_T} + E_{fr} - E_{\alpha r}\right)^{-1} \langle \vec{0}, \psi_{fr}|J^\mu_{em}(\vec{0})|\vec{k},\alpha_r\rangle \langle \vec{k},\alpha_r|J^\lambda_W(\vec{0})|\vec{0},\psi_{ir}\rangle \\ &+ \sum\!\!\!\!\!\!\int_{\alpha_r} \left(-k^0 - \frac{|\vec{k}|^2}{2M_T} + E_{ir} - E_{\alpha r}\right)^{-1} \langle \vec{0}, \psi_{fr}|J^\lambda_W(\vec{0})|-\vec{k},\alpha_r\rangle \langle -\vec{k},\alpha_r|J^\mu_{em}(\vec{0})|\vec{0},\psi_{ir}\rangle \end{aligned} \tag{9.0.5}$$

We need to plug this into the formula for the effective hadronic current and integrate over d^4k. Now we swap the order of the integrals and do the integral over k^0 first. The integral over k^0 gives us

$$\begin{aligned} \int \frac{dk^0}{2\pi} \frac{1}{(k^2+i\epsilon)^2} \frac{1}{k^0 - \Delta E + i\epsilon} &= -i \frac{(2|\vec{k}| + \Delta E - 3i\epsilon)}{4(|\vec{k}| - i\epsilon)^3(|\vec{k}| + \Delta E - 2i\epsilon)^2} \\ &\to -\frac{i}{2}\frac{1}{|\vec{k}|^4}\left(\frac{|\vec{k}|(2|\vec{k}| + \Delta E)}{2(|\vec{k}| + \Delta E)^2}\right) \end{aligned} \tag{9.0.6}$$

We then have the same decomposition into four terms as we did before.

$$\begin{aligned} \vec{\mathcal{J}} = &(-2i)\int_0^\infty \frac{d|\vec{k}|}{|\vec{k}|} \sum\!\!\!\!\!\!\int_{\alpha_r} \left[\frac{|\vec{k}|(2|\vec{k}| + \Delta E_d)}{2(|\vec{k}| + \Delta E_d)^2}\right] \int \frac{d\Omega_k}{4\pi} \langle \psi_{fr}|\hat{k} \times \vec{\tilde{J}}_{em,r}(-\vec{k})|\alpha_r\rangle \langle \alpha_r|\tilde{J}^0_{W,r}(\vec{k})|\psi_{ir}\rangle \\ &+(-2i)\int_0^\infty \frac{d|\vec{k}|}{|\vec{k}|} \sum\!\!\!\!\!\!\int_{\alpha_r} \left[\frac{|\vec{k}|(2|\vec{k}| + \Delta E_c)}{2(|\vec{k}| + \Delta E_c)^2}\right] \int \frac{d\Omega_k}{4\pi} \langle \psi_{fr}|\tilde{J}^0_{W,r}(\vec{k})|\alpha_r\rangle \langle \alpha_r|\hat{k} \times \vec{\tilde{J}}_{em,r}(-\vec{k})|\psi_{ir}\rangle \\ &-(-2i)\int_0^\infty \frac{d|\vec{k}|}{|\vec{k}|} \sum\!\!\!\!\!\!\int_{\alpha_r} \left[\frac{|\vec{k}|(2|\vec{k}| + \Delta E_d)}{2(|\vec{k}| + \Delta E_d)^2}\right] \int \frac{d\Omega_k}{4\pi} \langle \psi_{fr}|\tilde{J}^0_{em,r}(-\vec{k})|\alpha_r\rangle \langle \alpha_r|\hat{k} \times \vec{\tilde{J}}_{W,r}(\vec{k})|\psi_{ir}\rangle \\ &-(-2i)\int_0^\infty \frac{d|\vec{k}|}{|\vec{k}|} \sum\!\!\!\!\!\!\int_{\alpha_r} \left[\frac{|\vec{k}|(2|\vec{k}| + \Delta E_c)}{2(|\vec{k}| + \Delta E_c)^2}\right] \int \frac{d\Omega_k}{4\pi} \langle \psi_{fr}|\hat{k} \times \vec{\tilde{J}}_{W,r}(\vec{k})|\alpha_r\rangle \langle \alpha_r|\tilde{J}^0_{em,r}(-\vec{k})|\psi_{ir}\rangle \end{aligned} \tag{9.0.7}$$

These are the same four terms we calculated in the Section 8. The only difference is now they are modified by the nuclear energy ΔE, which depends on the energy of the intermediate state.

$$\frac{|\vec{k}|(2|\vec{k}| + \Delta E)}{2(|\vec{k}| + \Delta E)^2} \tag{9.0.8}$$

For the direct terms, we have

$$\Delta E_d = \frac{|\vec{k}|^2}{2M_T} - E_{fr} + E_{\alpha r} \tag{9.0.9}$$

and for the cross terms this is

$$\Delta E_c = \frac{|\vec{k}|^2}{2M_T} - E_{ir} + E_{\alpha r} \tag{9.0.10}$$

In the limit where we ignore the energy transferred to the nucleus, we have $\Delta E \to 0$ and we have

$$\frac{|\vec{k}|(2|\vec{k}| + \Delta E)}{2(|\vec{k}| + \Delta E)^2} \to 1 \tag{9.0.11}$$

This is then independent of the intermediate nuclear energy, and we recover the result we found before.

9.1 Modified Normal Ordering Approach

When we insert intermediate states, the result is a function of the energy transferred to the nucleus, ΔE_n, for a given intermediate state $|n\rangle$. In Section 5, we made an approximation that $\Delta E_n \to 0$ in order to normal order the currents and extract the two-body part. However, this is not the only choice which allows us to normal order the currents. We could replace ΔE_n with some realistic value.

$$\Delta E_n \to \langle \Delta E \rangle \tag{9.1.1}$$

In fact, this is allowed to be a function of the loop momentum, $|\vec{k}|$. The key is that $\langle \Delta E \rangle$ no longer depends on the intermediate state, and we can once again collapse the sum over intermediate states and use the completeness relation. Applying this to the four terms, this would give us

$$\begin{aligned}
\vec{\mathcal{J}} = &(-2i)\int_0^\infty \frac{d|\vec{k}|}{|\vec{k}|}\left[\frac{|\vec{k}|(2|\vec{k}| + \langle \Delta E_d\rangle)}{2(|\vec{k}| + \langle \Delta E_d\rangle)^2}\right]\int \frac{d\Omega_k}{4\pi}\,\langle \psi_{fr}|\hat{k}\times \vec{\tilde{J}}_{em,r}(-\vec{k})\tilde{J}^0_{W,r}(\vec{k})|\psi_{ir}\rangle \\
&+(-2i)\int_0^\infty \frac{d|\vec{k}|}{|\vec{k}|}\left[\frac{|\vec{k}|(2|\vec{k}| + \langle \Delta E_c\rangle)}{2(|\vec{k}| + \langle \Delta E_c\rangle)^2}\right]\int \frac{d\Omega_k}{4\pi}\,\langle \psi_{fr}|\tilde{J}^0_{W,r}(\vec{k})\hat{k}\times \vec{\tilde{J}}_{em,r}(-\vec{k})|\psi_{ir}\rangle \\
&-(-2i)\int_0^\infty \frac{d|\vec{k}|}{|\vec{k}|}\left[\frac{|\vec{k}|(2|\vec{k}| + \langle \Delta E_d\rangle)}{2(|\vec{k}| + \langle \Delta E_d\rangle)^2}\right]\int \frac{d\Omega_k}{4\pi}\,\langle \psi_{fr}|\tilde{J}^0_{em,r}(-\vec{k})\hat{k}\times \vec{\tilde{J}}_{W,r}(\vec{k})|\psi_{ir}\rangle \\
&-(-2i)\int_0^\infty \frac{d|\vec{k}|}{|\vec{k}|}\left[\frac{|\vec{k}|(2|\vec{k}| + \langle \Delta E_c\rangle)}{2(|\vec{k}| + \langle \Delta E_c\rangle)^2}\right]\int \frac{d\Omega_k}{4\pi}\,\langle \psi_{fr}|\hat{k}\times \vec{\tilde{J}}_{W,r}(\vec{k})\tilde{J}^0_{em,r}(-\vec{k})|\psi_{ir}\rangle
\end{aligned} \tag{9.1.2}$$

Note that these are the same terms in Equation 8.2.3 that we computed using the $\Delta E = 0$ approximation. The difference here is that these are now modified by an energy correction which can depend on the loop momentum $|\vec{k}|$.

We now want to discuss reasonable approximations to the average value $\langle \Delta E \rangle$ we could choose. First, consider the case where there is no internal excitation of the nucleus. In that case, the only energy transfer is associated with the center of mass energy.

$$\langle \Delta E \rangle \to \frac{|\vec{k}|^2}{2M_T}, \quad \text{(no internal excitations)} \tag{9.1.3}$$

where M_T is the target mass, or the total mass of the nucleus. Next, consider the quasi-elastic limit in which the currents act on a single nucleon and the energy transferred is equal to the non-relativistic free particle energy.

$$\langle \Delta E \rangle \to \frac{|\vec{k}|^2}{2M_N}, \quad \text{(quasi-elastic)} \tag{9.1.4}$$

These approximate forms are modified by the nuclear interactions and their contribution to the energy. Quantifying this effect requires us to enumerate over all nuclear eigenstates, as we did in the previous section, and weight their contributions by the energy. Before we do that, we can start with the simpler case of the limit $|\vec{k}| \to 0$. In particular, suppose we have an energy gap $\Delta E \neq 0$ as $|\vec{k}| \to 0$, then this factor goes to

$$\frac{|\vec{k}|(2|\vec{k}| + \langle \Delta E \rangle)}{2(|\vec{k}| + \langle \Delta E \rangle)^2} \to \frac{|\vec{k}|}{2\langle \Delta E \rangle} \to 0 \tag{9.1.5}$$

This is potentially relevant in the case of a spin-flip, which can cause a transition at $|\vec{k}| \to 0$ and produce an energy gap $\Delta E \neq 0$. As we will see, this is the cause of the biggest qualitative shift in the result.

9.2 Limit $k \to 0$

Now lets consider the case where $|\vec{k}| \to 0$ while keeping the dependence on nuclear energies. We get a huge simplification due to the fact that the spherical Bessel functions which depend on $|\vec{k}|$ go to

$$j_L(|\vec{k}|r/2) \to \begin{cases} 1 & L = 0 \\ 0 & L \neq 0 \end{cases} \tag{9.2.1}$$

Going back to the analysis we did in Section 8, the only multipoles which contribute are the even parity operators C_0 and M_1. In the $|\vec{k}| \to 0$ limit, we only need to consider intermediate states which are accessible through these operators.

We will go through and check the $|\vec{k}| \to 0$ limit of each of the four terms in Figure 8.2. Term 1 is the interesting case. Schematically, we have

$$\langle d||\vec{J}_{em}||\alpha\rangle \, \langle \alpha||\rho_W||pp\rangle \tag{9.2.2}$$

This goes through np intermediate states with $S = 0$. The energy denominator in this case is

$$\Delta E = \frac{|\vec{k}|^2}{2M_T} + BE(d) + E(np, S = 0) \tag{9.2.3}$$

In the limit $|\vec{k}| \to 0$, we have a superposition of intermediate np states with orbital angular momentum $l_\alpha = 0$. There is no bound state in this channel, so the energy is greater than or equal to zero. Thus there is a remaining energy gap at $|\vec{k}| \to 0$.

$$\Delta E \to BE(d) + E(np, S = 0) \tag{9.2.4}$$

Term 2 does not contribute in the limit $|\vec{k}| \to 0$. Schematically, term 2 has the form

$$\langle d||\rho_W||\alpha\rangle \langle\alpha||\vec{J}_{em}||pp\rangle \tag{9.2.5}$$

This goes through pp states with $S = 1$. Only odd parity states contribute, and we have no contribution at $|\vec{k}| \to 0$.

Term 3 has the form

$$\langle d||\rho_{em}||\alpha\rangle \langle\alpha||\vec{J}_W||pp\rangle \tag{9.2.6}$$

This goes through np states with $S = 1$. The energy difference is

$$\Delta E = \frac{|\vec{k}|^2}{2M_T} + BE(d) + E(np, S = 1) \tag{9.2.7}$$

At $|\vec{k}| \to 0$, the intermediate state matches onto the deuteron ground state. Therefore there is no energy gap, and we have

$$\Delta E \to 0 \tag{9.2.8}$$

Therefore there is no change to the small $|\vec{k}|$ behaviour of term 3.

The same thing happens to term 4. Term 4 has the form

$$\langle d||\vec{J}_W||\alpha\rangle \langle\alpha||\rho_{em}||pp\rangle \tag{9.2.9}$$

This goes through pp intermeidate states with $S = 0$.

$$\Delta E \to \frac{|\vec{k}|^2}{2M_T} - E(pp) + E(pp, S = 0) \tag{9.2.10}$$

As $|\vec{k}| \to 0$, the intermeidate pp state matches the initial state and we have

$$\Delta E \to 0 \tag{9.2.11}$$

Thus there is no change to the fourth term in the limit $|\vec{k}| \to 0$. This analysis shows that including nuclear energy effects only change the first term as $|\vec{k}| \to 0$.

The results for the SHO basis calculation for each term is shown in Figure 9.2. The only change due to the nuclear energy at $|\vec{k}| = 0$ is in the first term, as expected. This is important since the two-body contribution is all in the low $|\vec{k}|$ region. This leads us to expect that this could be the largest effect.

9.3 Approximate Form of the Green's Function

We would now like to come up with an approximate form for the nuclear Green's function using the modified normal ordering approach. We use the normal ordering result with an average value $\langle \Delta E \rangle$ which depends on $|\vec{k}|$. Given what we know from the previous discussion, we would like to come up with a reasonable value of $\langle \Delta E \rangle$ for each of the four terms.

Since we are using the completeness relation, we can normal order and separate out the one-body and two-body contributions. For the one-body part, we assume that the energy transfer is equal to the usual one body non-relativist energy $\langle \Delta E \rangle = \frac{|\vec{k}|^2}{2M_N}$. The two-body part is all at low momentum, so we suppose there is no change in the internal nuclear energy. Thus all the energy transfer is due to the center of mass motion $\langle \Delta E \rangle = \frac{|\vec{k}|^2}{2M_T}$.

The important exception to this general rule is the first term, which has an extra energy contribution as $|\vec{k}| \to 0$. Using the results from the previous section, our approximation for the effective hadronic current can be written as follows.

$$\mathcal{J} = \frac{|\vec{k}|(2|\vec{k}| + \frac{|\vec{k}|^2}{2M_N} + BE(d) + E(np))}{2(|\vec{k}| + \frac{|\vec{k}|^2}{2M_N} + BE(d) + E(np))^2}\mathcal{J}_1(\text{1b}) + \frac{|\vec{k}|(2|\vec{k}| + \frac{|\vec{k}|^2}{2M_T} + BE(d) + E(np))}{2(|\vec{k}| + \frac{|\vec{k}|^2}{2M_T} + BE(d) + E(np))^2}\mathcal{J}_1(\text{2b})$$
$$+\frac{|\vec{k}|(2|\vec{k}| + \frac{|\vec{k}|^2}{2M_N})}{2(|\vec{k}| + \frac{|\vec{k}|^2}{2M_N})^2}[\mathcal{J}_2(\text{1b}) + \mathcal{J}_3(\text{1b}) + \mathcal{J}_4(\text{1b})] + \frac{|\vec{k}|(2|\vec{k}| + \frac{|\vec{k}|^2}{2M_T})}{2(|\vec{k}| + \frac{|\vec{k}|^2}{2M_T})^2}[\mathcal{J}_2(\text{2b}) + \mathcal{J}_3(\text{2b}) + \mathcal{J}_4(\text{2b})] \tag{9.3.1}$$

From this expression, we need to subtract out the free, single-nucleon contribution. This was already calculated in the Born contribution in Section 4, and should not be included twice. By definition, the nuclear structure correction is the difference between the full answer and the free, one-body part.

$$\mathcal{J}(\text{NS}) = \left[\frac{|\vec{k}|(2|\vec{k}| + \frac{|\vec{k}|^2}{2M_N} + BE(d) + E(np))}{2(|\vec{k}| + \frac{|\vec{k}|^2}{2M_N} + BE(d) + E(np))^2} - \frac{|\vec{k}|(2|\vec{k}| + \frac{|\vec{k}|^2}{2M_N})}{2(|\vec{k}| + \frac{|\vec{k}|^2}{2M_N})^2}\right]\mathcal{J}_1(\text{1b})$$
$$+\frac{|\vec{k}|(2|\vec{k}| + \frac{|\vec{k}|^2}{2M_T} + BE(d) + E(np))}{2(|\vec{k}| + \frac{|\vec{k}|^2}{2M_T} + BE(d) + E(np))^2}\mathcal{J}_1(\text{2b}) + \frac{|\vec{k}|(2|\vec{k}| + \frac{|\vec{k}|^2}{2M_T})}{2(|\vec{k}| + \frac{|\vec{k}|^2}{2M_T})^2}[\mathcal{J}_2(\text{2b}) + \mathcal{J}_3(\text{2b}) + \mathcal{J}_4(\text{2b})] \tag{9.3.2}$$

The first term represents a shift in the one-body part due to the change in the nuclear energy at low momentum. The other terms represent the two-body part, with a correction due to the nuclear energy.

The result using the modified normal ordering approximation is shown in Figure 9.1. The one-body and two-body parts for each of the four terms was calculated in Section 8. The calculation is basically the same as the one we did in Section 7.3, except we have an additional factor which depends on $|\vec{k}|$ due to the nuclear energy correction. We do not attempt to do

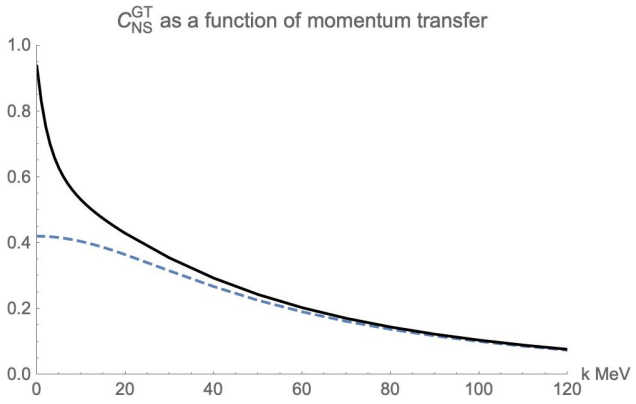

Figure 9.1: Nuclear structure correction to *pp*-fusion using the modified normal ordering approximation (solid), compared to the $\Delta E = 0$ approximation (dashed).

the integral over loop momentum analytically. Instead, we calculate the overlaps at many different values of $|\vec{k}|$ and interpolate the result in order to integrate over $d|\vec{k}|$. The result we find is

$$C_{\rm NS}^{\rm GT} = 0.180 \quad \text{Modified Normal Ordering} \tag{9.3.3}$$

This is a 18% increase over the result we found using the $\Delta E = 0$ approximation in Section 7. The discrepancy is much larger than one would expect using a simple $1/M_N$ power counting. This is entirely due to a non-zero energy gap as $|\vec{k}| \to 0$ in the first term in Figure 8.2.

9.4 Simple Harmonic Oscillator Basis Results

In Section 8, we used the simple harmonic oscillator (SHO) basis to check the completeness relation. This involved enumerating over all intermediate states in the discrete SHO basis, and summing over intermediate states. Comparing Equation 8.2.28 to Equation 9.1.2, we need to again do the same thing. Now, we want to weight the sum over intermediate states by an energy dependent factor. We can then compare the result in the SHO basis to the result we expect from the modified normal ordering approximation outlined above.

The results from the SHO basis calculation for each of the four terms in Equation 9.1.2 are shown in Figure 9.2. This confirms that the largest effect is due to the energy gap as $|\vec{k}| \to 0$. The result from the SHO basis takes into account the entire Av18 nuclear interaction. The modified normal ordering approximation ignores additional effects from the nuclear interaction, and so they don't agree completely. However, the main effect at $|\vec{k}| \to 0$ is captured well by the approximation. The remaining correction is a small effect - an additional order $1/M_N$ correction - as expected.

Note that each term in Figure 9.2 converges to the free, one-body part at large $|\vec{k}|$. The free, one-body part was calculated in Section 4 using the full relativistic set up. When we

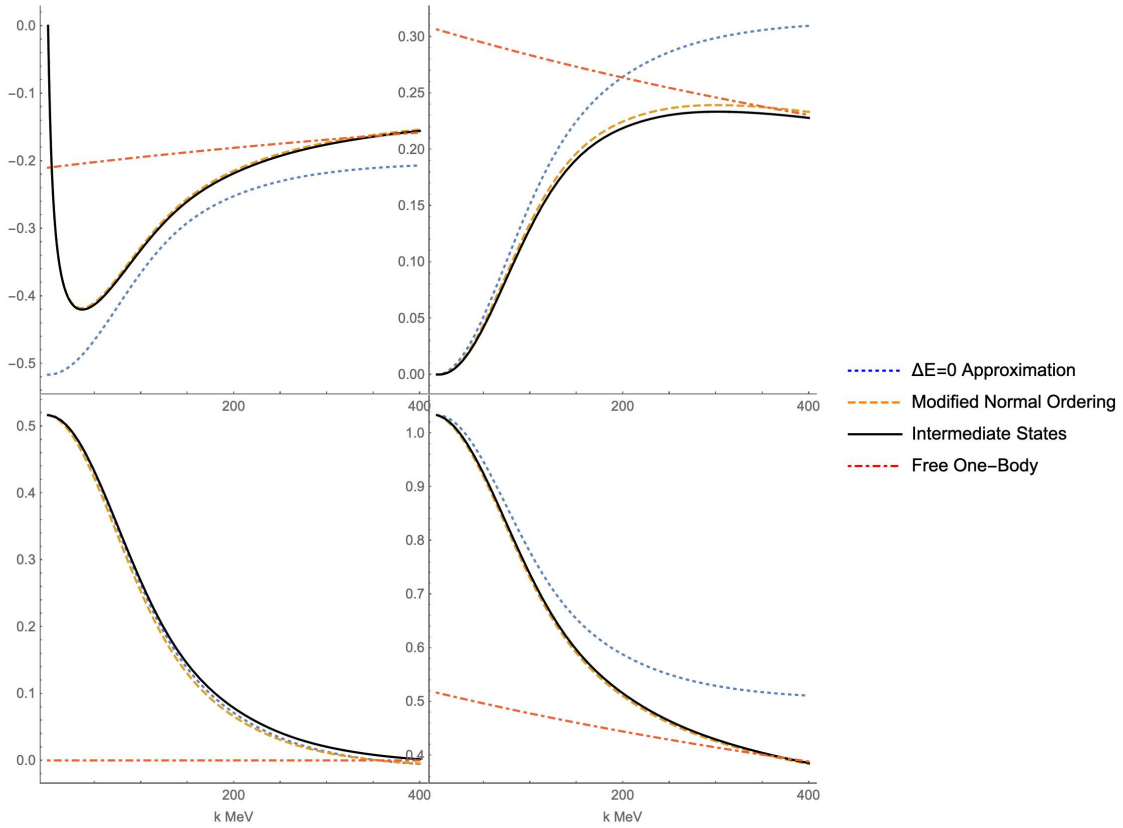

Figure 9.2: Calculation of each of the four terms in Equation 9.1.2 using the SHO basis.

calculate the nuclear structure correction $C_{\mathrm{NS}}^{\mathrm{GT}}$, the free one-body part is subtracted out. The result for the nuclear structure correction is shown in Figure 9.3.

One big caveat to this result is that the SHO basis is compact. We cannot accurately represent extended, continuum wavefunctions. In particular, we want to calculate the correction at solar energy scales. Using the parameters $b = 0.7$ fm and $\Lambda = 60$, the SHO basis can only get down to energies of about 1.5 MeV. On the other hand, the coordinate space calculations we did were able to go all the way down to 2 keV - three orders of magnitude smaller. In order to address this discrepancy, we accompany this SHO basis result by a calculation in coordinate space where we focus on the biggest effect as $|\vec{k}| \to 0$.

9.5 Coordinate Space Form

We would now like to supplement the SHO basis results above with a calculation done in coordinate space. We have two options for how we can proceed. The first option is to calculate the nuclear Green's function. In coordinate space, this is a function of two

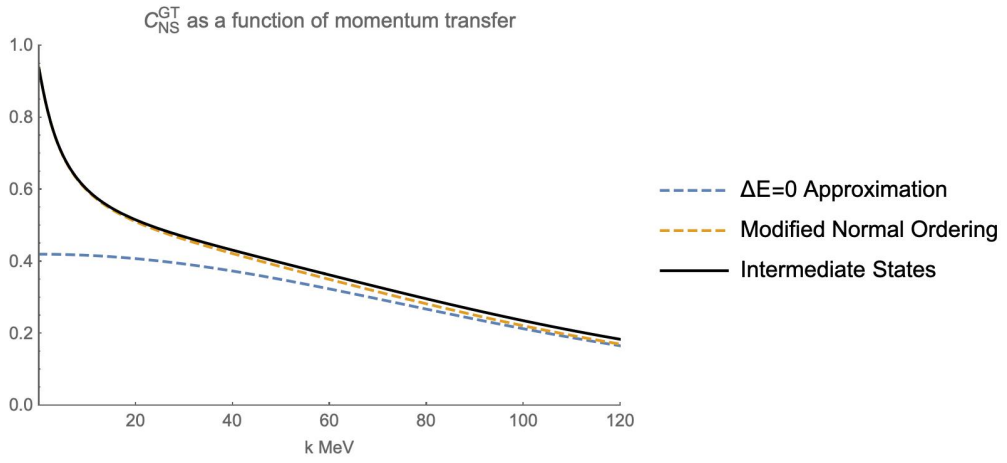

Figure 9.3: Nuclear energy correction to $C_{\mathrm{NS}}^{\mathrm{GT}}$ in pp-fusion. Comparison between the $\Delta E = 0$ approximation, the modified normal ordering scheme, and the SHO basis results using intermediate states.

coordinates r, r' which can be calculated in each angular momentum channel. In the case of a single channel, it obeys the radial Schrodinger equation

$$\left[p^2 + \frac{d^2}{dr^2} - \frac{l(l+1)}{r^2} - U(r)\right] g(p, r, r') = \delta(r - r') \tag{9.5.1}$$

where $U = 2M_r V$. When $r < r'$ or $r > r'$, the Green's function is a solution of the usual Schrodinger equation. At $r = r'$ it is continuous, and has a unit discontinuity in its first derivative.

$$\lim_{\epsilon \to 0} \left(\frac{d}{dr} g(p, r, r') \bigg|_{r=r'+\epsilon} - \frac{d}{dr} g(p, r, r') \bigg|_{r=r'-\epsilon} \right) = 1 \tag{9.5.2}$$

More details on how to calculate this, including in coupled channels, are given in Appendix G. Here we will focus on how this could be used to calculate the correction from the loop diagram.

Going back to Equation 9.0.3, we note that the operator $(\omega - H_r)^{-1}$ can be expanded in coordinate space using the coordinate space Green's function.

$$\frac{1}{\omega - H_r} |\psi\rangle = 2M_r \int_0^\infty dr dr' g_l(p, r, r') u(r') |rl\rangle \tag{9.5.3}$$

where $\omega = p^2/2M_r$. This formula can be extended to the case of coupled channels, as is described in Appendix G. When we apply this to the generalized Compton tensor Equation 9.0.3, we get different Green's functions for the direct and cross term. For the direct term, we have

$$\omega_d = k^0 - \frac{|\vec{k}|^2}{2M_T} + E_{fr} \tag{9.5.4}$$

In the cross term, k^0 comes with the opposite sign.

$$\omega_c = -k^0 - \frac{|\vec{k}|^2}{2M_T} + E_{ir} \tag{9.5.5}$$

Since the coordinate space Green's function is calculated in each individual angular momentum channel, we need to do the same multipole decomposition as we did in Section 8. Now, all of the radial integrals we need to do are double integrals of the form

$$\int_0^\infty dr \int_0^\infty dr'\, u(d,r) j_L(|\vec{k}|r/2) g_L(p,r,r') j_L(|\vec{k}|r'/2) u(pp,r') \tag{9.5.6}$$

The spherical Bessel functions come from the multipole decompositions of the current operators. These are difficult integrals for two reasons.

1. At continuum energies where $\omega > 0$, both the Green's function and the initial pp-wavefunction have infinite range. This must be regulated by keeping ϵ finite, which provides a small exponential damping at large r, r'.

2. At negative energies where $\omega < 0$, the Green's function is the product of two exponentials. These can be numerically difficult to handle, especially at large $-\omega$.

Both of these issues are explored further in Appendix G. However, these are not the only difficulties we face. Even if we are able to calculate the nuclear Green's function and do this double integral, we still need to remember that ω is a function of k^0 and we still need to integrate over all k^0 from $-\infty$ to $+\infty$. This means repeating the calculation at many different values of k^0, and interpolating the result. This must also be done in every angular momentum channel, and at each value of $|\vec{k}|$.

Given the difficulties outlined above, we do not make use of the coordinate space Green's function method. Instead, we continue with the theme of expanding over intermediate states. However, we will not be using a discrete basis like the SHO basis. Working in coordinate space means we need to deal with a continuum of intermediate state energies, E_α, which we need to integrate over.

$$\int dE_\alpha\, \rho(E_\alpha)\, |E_\alpha\rangle\, \langle E_\alpha| \tag{9.5.7}$$

Here, $\rho(E_\alpha)$ is the density of states which we get using the box normalization approach outlined in Appendix H. The difficulty here is that we need to solve the Schrodinger equation to find the wavefunction at each E_α. The main challenge here is that we need to pick a set of E_α and interpolate the result in order to do this integral.

As we have seen, the largest deviation from the $\Delta E \to 0$ approximation occurs in the first term of Equation 9.1.2 as $|\vec{k}| \to 0$. We will not do the full calculation of all four terms in each angular momentum channel, but we will focus on the biggest effect in the first term. As $|\vec{k}| \to 0$, the only intermediate state which contributes is at ${}^1S_0$.

$$\langle d|M1(em)|{}^1S_0(np)\rangle\, \langle {}^1S_0(np)|C_0(W)|pp\rangle \tag{9.5.8}$$

Using the multipole expansion of the currents outlined in Section 8, we can write the contribution to the first term in the ${}^1S_0$ channel as

$$\begin{aligned}(-2i)\frac{1}{|\vec{k}|}\int\frac{d\Omega_k}{4\pi}\langle\psi_{fr}|\hat{k}\times\vec{\tilde{J}}_{em,r}(-\vec{k})|\alpha_r\rangle\langle\alpha_r|\tilde{J}^0_{W,r}(\vec{k})|\psi_{ir}\rangle\\ \to -4\pi\frac{2\mu_v}{\sqrt{3}M_N}\langle\psi_{fr}||(-i)\mathbf{X}_1^{(e)}(q\vec{r}/2)\cdot\Sigma_{(-)}||\alpha_r\rangle\langle\alpha_r||X_0(k\vec{r}/2)||\psi_{ir}\rangle\frac{C^{j_fm_f}_{j_im_i,1q}}{\sqrt{2j_f+1}}e^*_q\end{aligned} \tag{9.5.9}$$

The first matrix element results in a radial integral between the deuteron wavefunction and the intermediate state.

$$\begin{aligned}\langle d||(-i)\mathbf{X}_1^{(e)}(q\vec{r}/2)\cdot\Sigma_{(-)}||{}^1S_0(np)\rangle\\ =\frac{1}{\sqrt{4\pi}}\left[\sqrt{2}\int_0^\infty dr\,u(r)j_0(|\vec{k}|r/2)u(E_{\alpha r})-\int_0^\infty dr\,w(r)j_2(|\vec{k}|r/2)u(E_{\alpha r})\right]\end{aligned} \tag{9.5.10}$$

The second matrix element involves a radial integral between the intermediate state and the initial *pp*-state.

$$\langle{}^1S_0(np)||X_0(k\vec{r}/2)||pp\rangle=\frac{1}{\sqrt{4\pi}}\int_0^\infty dr\,u(E_{\alpha r})j_0(|\vec{k}|r/2)u_0(p,r) \tag{9.5.11}$$

As is described in Appendix H, we can simplify the density of states by writing it in terms of the intermediate state wavenumber $E_\alpha=p_\alpha^2/2M_r$.

$$\int_0^\infty\frac{2}{\pi}dp_\alpha\,|E_{\alpha r}\rangle\langle E_{\alpha r}| \tag{9.5.12}$$

There is no intermediate bound state to worry about, so we just have continuum intermediate states. The intermediate states are normalized asymptotically as usual.

$$u(E_{\alpha r})\sim\sin\left(p_\alpha r-\frac{\pi l}{2}+\delta_l\right) \tag{9.5.13}$$

Combining all of this together, we arrive at the result for the first term in the ${}^1S_0$ channel in terms of a product of radial integrals.

$$\begin{aligned}-\frac{2\mu_v}{\sqrt{3}M_N}\int_0^\infty\frac{2}{\pi}dp_\alpha\left[\sqrt{2}\int_0^\infty dr\,u(r)j_0(|\vec{k}|r/2)u(E_{\alpha r})-\int_0^\infty dr\,w(r)j_2(|\vec{k}|r/2)u(E_{\alpha r})\right]\\ \times\left[\int_0^\infty dr\,u(E_{\alpha r})j_0(|\vec{k}|r/2)u_0(p,r)\right]\end{aligned} \tag{9.5.14}$$

This is formally correct, but turns out to be problematic in practice. The first term in brackets is fine because the integrals are regulated by the decaying exponential associated with the Deuteron bound state, $e^{-\kappa r}$. However, the last term in brackets has no decaying

exponential to regulate it. Both the initial pp-state and the intermediate np-state wavefunctions are continuum states, and behave like a sine wave at large r. In order to calculate the result more reliably, one can include a small decaying exponential, $e^{-\lambda r}$, in order to render the numerical computation more tractable. This won't effect the result significantly, as long as the decay is much slower than the deuteron bound state, $\lambda \ll \kappa$.

This is the result using the $\Delta E \to 0$ approximation. This is then modified by the function of the intermediate state energy, according to Equation 9.1.2. In this form, we can use the completeness relation in the ${}^1S_0$ channel.

$$\begin{aligned} -\frac{2\mu_v}{\sqrt{3}M_N}\Bigg[\sqrt{2}\int_0^\infty dr\, u(r) j_0(|\vec{k}|r/2) j_0(|\vec{k}|r/2) u_0(p,r) \\ -\int_0^\infty dr\, w(r) j_2(|\vec{k}|r/2) j_0(|\vec{k}|r/2) u_0(p,r)\Bigg] \end{aligned} \tag{9.5.15}$$

This should be the result we get by integrating over intermediate state continuum energies. The calculation using intermediate states must be repeated for many values of intermediate state energy $E_{\alpha r}$. We then need to interpolate between those energy values in order to do approximate the integral over continuum intermediate state energies. We can use the completeness relation to double check our result, and make sure we have done these steps correctly.

Ignoring the small initial pp-energy, the full nuclear Green's function result for the first term in the ${}^1S_0$ channel is given by the integral over the continuum energy of the intermediate state np.

$$\begin{aligned} -\frac{2\mu_v}{\sqrt{3}M_N}\int_0^\infty \frac{2}{\pi} dp_\alpha \left(\frac{|\vec{k}|(2|\vec{k}| + \frac{|\vec{k}|^2}{2M_T} + BE(d) + E_{\alpha r})}{2(|\vec{k}| + \frac{|\vec{k}|^2}{2M_T} + BE(d) + E_{\alpha r})^2}\right) \\ \times \left[\sqrt{2}\int_0^\infty dr\, u(r) j_0(|\vec{k}|r/2) u(E_{\alpha r}) - \int_0^\infty dr\, w(r) j_2(|\vec{k}|r/2) u(E_{\alpha r})\right] \\ \times \left[\int_0^\infty dr\, u(E_{\alpha r}) j_0(|\vec{k}|r/2) u_0(p,r)\right] \end{aligned} \tag{9.5.16}$$

It is not possible to separate out the one-body and two-body contributions when we consider only a single angular momentum channel like this. However, we can try to approximate the result using either the COM energy $\frac{|\vec{k}|^2}{2M_T}$ or the free single particle energy $\frac{|\vec{k}|^2}{2M_N}$.

$$\begin{aligned} -\frac{2\mu_v}{\sqrt{3}M_N}\frac{|\vec{k}|(2|\vec{k}| + \frac{|\vec{k}|^2}{2M_T} + BE(d))}{2(|\vec{k}| + \frac{|\vec{k}|^2}{2M_T} + BE(d))^2}\Bigg[\sqrt{2}\int_0^\infty dr\, u(r) j_0(|\vec{k}|r/2) j_0(|\vec{k}|r/2) u_0(p,r) \\ -\int_0^\infty dr\, w(r) j_2(|\vec{k}|r/2) j_0(|\vec{k}|r/2) u_0(p,r)\Bigg] \end{aligned} \tag{9.5.17}$$

The full nuclear Green's function result will contain more corrections from the full nuclar Hamiltonian, but the largest effect is at small $|\vec{k}|$ due to the bound state energy gap. This is confirmed by looking at the results in Figure 9.4

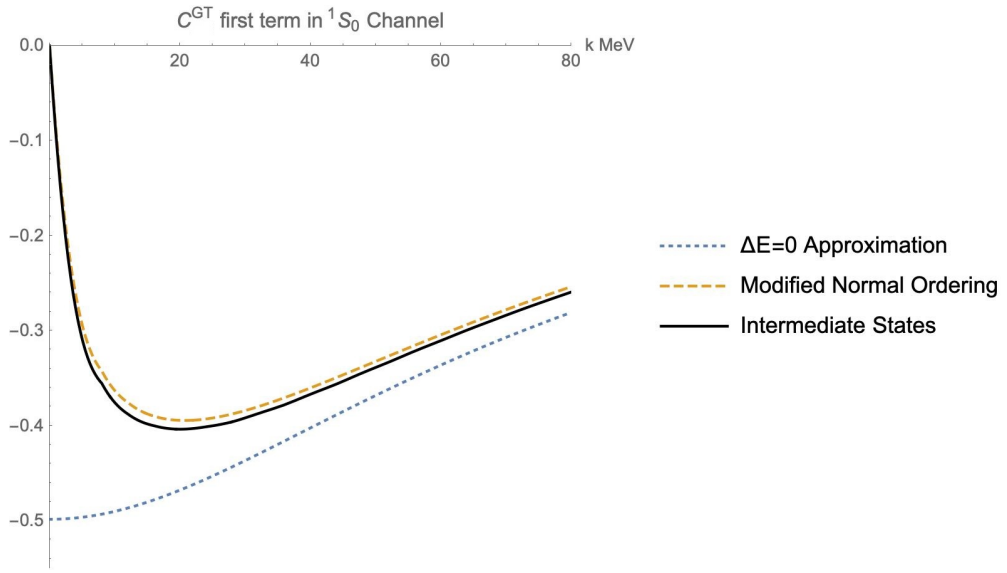

Figure 9.4: Contribution to C^{GT} from the first term in Figure 8.2 in the $^1S_0$ channel using the sum over continuum intermediate states in coordinate space, Equation 9.5.16.

9.6 Current-Current Terms

The one thing we have not calculated is the contribution from current-current terms. To see why we have neglected this contribution, go back to the effective hadronic current for the box diagram.

$$\mathcal{J}^\beta = 8\pi^2 \int \frac{d^4k}{(2\pi)^4} \frac{\varepsilon^{\mu\lambda\alpha\beta} k_\alpha}{(k^2 + i\epsilon)^2} T_{\mu\lambda}(p_f, p_i, k) \tag{9.6.1}$$

In Section 5, we ignored the nuclear energies in the denominator and set $\Delta E = 0$. Then, since we were only looking at the two-body part, we were able to ignore the commutator of the currents and we got an overall delta function $\delta(k^0)$. Thus we were allowed to set α to be a space-like index, and that meant one of the current operators had to be time-like. Thus all the terms we considered thus far have involved one current and one charge operator.

Consider the case where α is time-like. This gives us the aforementioned current-current terms, which involve the cross product of the currents $\epsilon^{ijk} T^{ij}$.

$$\mathcal{J}^i = 8\pi^2 \int \frac{d^4k}{(2\pi)^4} \frac{k^0}{(k^2 + i\epsilon)^2} \epsilon^{ijk} T^{jk}(p, k) \tag{9.6.2}$$

Since we are only dealing with the vector current, the space-like part of the current is order $1/M_N$. Thus these current-current terms should be order $1/M_N^2$, compared to the charge-current terms we have considered up to this point which are order $1/M_N$. However, the nuclear energy ΔE should also be order $1/M_N$, so the nuclear energy corrections would be

order $1/M_N^2$ as well. In order to be consistent in the power counting, we should consider the potential impact of these current-current terms.

If we assume $\Delta E \sim 1/M_N$, then we can set $\Delta E \to 0$ in the current-current terms. This should lead to an error of order $1/M_N^3$, which can be safely ignored. The generalized compton tensor becomes

$$\begin{aligned} T^{\mu\lambda}(p_f, p_i, k) = &\sum_n \frac{1}{k^0 + i\epsilon} \int d^3x e^{-i\vec{k}\cdot\vec{x}} \langle p_f | J^\mu_{em}(\vec{x}) | n \rangle \langle n | J^\lambda_W(0) | p_i \rangle \\ &+ \sum_n \frac{1}{-k^0 + i\epsilon} \int d^3x e^{-i\vec{k}\cdot\vec{x}} \langle p_f | J^\lambda_W(0) | n \rangle \langle n | J^\mu_{em}(\vec{x}) | p_i \rangle \end{aligned} \tag{9.6.3}$$

We then need to multiply by k^0, which cancels out the k^0 in the denominators. We can then combine the direct and cross terms into a current commutator.

$$k^0 T^{jk}(p, k) \sim \int d^3x \, e^{-i\vec{k}\cdot\vec{x}} \langle f | [J^j_{em}(\vec{x}), J^k_W(\vec{0})] | i \rangle \tag{9.6.4}$$

The commutator of the currents is purely one-body. This term does not contribute to the two-body part in the $\Delta E \to 0$ approximation, so we have thus far neglected it. The one-body part of this term is already included in the relativistic Born term we computed earlier.

According to the above reasoning, we shouldn't have to worry about these terms impacting the nuclear structure correction. The one way in which this argument can fail is in the case we have persistent energy gap $\Delta E \neq 0$ as $|\vec{k}| \to 0$. In particular, as we found in Section 9.3 the direct term can have a persistent energy gap due to the deuteron binding energy.

$$\int d^3x e^{-i\vec{k}\cdot\vec{x}} \langle f | J^j_{em}(\vec{x}) \frac{k^0}{k^0 - \Delta E_d + i\epsilon} J^k_W(\vec{0}) | i \rangle \tag{9.6.5}$$

If the intermediate state we go through is not the deuteron, then there will be a minimum energy gap due to the deuteron binding energy $\Delta E_d \geq BE(d)$. This energy gap can persist down to $|\vec{k}| \to 0$, and can thus change the behaviour of the box diagram contribution at small momentum transfer.

In this case as $|\vec{k}| \to 0$, the energy gap is simply the deuteron binding energy. Thus we replace ΔE with $\langle \Delta E \rangle \to BE(d)$. Plugging this in, we can again remove the dependence on intermediate state energy.

$$\frac{k^0}{k^0 - \langle \Delta E \rangle + i\epsilon} \int d^3x e^{-i\vec{k}\cdot\vec{x}} \langle f | J^j_{em}(\vec{x}) J^k_W(\vec{0}) | i \rangle \tag{9.6.6}$$

Now the k^0 integral we need is given by

$$\int \frac{dk^0}{2\pi} \frac{1}{(k^2 + i\epsilon)^2} \frac{k^0}{k^0 - \Delta E + i\epsilon} = \frac{i}{4|\vec{k}|(|\vec{k}| + \Delta E)^2} \tag{9.6.7}$$

Plugging in a value for $\langle \Delta E \rangle$ into the direct term, we get

$$\mathcal{J}^i = i \int \frac{|\vec{k}| d |\vec{k}|}{(|\vec{k}| + \langle \Delta E \rangle)^2} \frac{d\Omega_k}{4\pi} \epsilon^{ijk} \int d^3x e^{-i\vec{k}\cdot\vec{x}} \langle f | J^j_{em}(\vec{x}) J^k_W(\vec{0}) | i \rangle \tag{9.6.8}$$

Here $\langle \Delta E \rangle \to 0$ if the intermediate state is the deuteron, and $\langle \Delta E \rangle \to BE(d)$ if the intermediate state is anything other than the deuteron. Having an energy gap as $|\vec{k}| \to 0$ suppresses the contribution by $|\vec{k}|^2/\langle \Delta E \rangle^2$. This is similar to what we found before, where the contribution was suppressed at small $|\vec{k}|$.

We might be worried this could lead to an enhancement, like the one we saw in Section 9.3. There, we found that term 1 in Equation 9.1.2 was suppressed at small $|\vec{k}|$. Instead of going to a constant, it went to zero at small $|\vec{k}|$. This term came with the opposite sign from the rest of the terms, so the suppression actually led to an enhancement of the overall result. It looks like the same thing can happen here - and we might even worry that the current-current term could cancel out the enhancement effect we found in Section 9.3.

However, a power counting analysis in $|\vec{k}|$ shows that this is not the case. The current matrix elements always contribute at least $|\vec{k}|^2$, so this contribution always goes to zero at small momentum transfer. The additional suppression due to the non-zero ΔE at small momentum transfer thus doesn't have a significant impact on the result for the current-current terms.

For example, we will look at a term very similar to the $M_1 \times C_0$ term we focused on in Section 9.5. In this case, we expand the current operator in terms of multipoles and keep the longitudinal component. As we describe in Appendix D, the longitudinal current involves a term due to the center of mass motion which is proportional to the charge multipole.

$$\begin{aligned}\vec{\tilde{J}}(\vec{q}) = 4\pi \sum_{JM} \Bigg\{ & i^{J-1} \left[L_{JM} + i \frac{|\vec{q}|}{2M_T} C_{JM} \right] \mathbf{Y}^*_{JM}(\hat{q}) \\ & + i^J M_{JM} \mathbf{\Phi}^*_{JM}(\hat{q}) - i^J E_{JM} \mathbf{\Psi}^*_{JM}(\hat{q}) \Bigg\}\end{aligned} \tag{9.6.9}$$

Plugging this in and doing the integral over angles $d\Omega_k$, we get a term which looks very similar to the one we found previously.

$$\begin{aligned}& \int \frac{d\Omega_k}{4\pi} \epsilon^{ijk} \int d^3x e^{-i\vec{k}\cdot\vec{x}} \langle f | J^j_{em}(\vec{x}) J^k_W(\vec{0}) | i \rangle \\ \to & \, 4\pi \langle f | i M_{1M}(em) \left(-i L_{00}(W) + \frac{|\vec{k}|}{2M_T} C_{00}(W) \right) | i \rangle \, e^*_M\end{aligned} \tag{9.6.10}$$

As before, the M_1 is required in order to provide the necessary spin-flip. The matrix element of the M_1 operator gives one power of $|\vec{k}|$. Similarly, both the center of mass and the L_0 operator contribute one power of $|\vec{k}|$. Thus this contribution always goes to zero for small loop momentum. The further suppression due to the inclusion of the non-zero ΔE does not have a significant impact, as claimed.

We can look at all of the other combinations of multipole operators and we find the same result. For example, we can look at the $E_1 \times E_1$ term. Since this must produce a spin-flip, this must also go like $|\vec{k}|^2$. This argument should be convincing, but it is still somewhat hand-wavey. It would be good to double check that these terms are not important by direct computation.

Chapter 10

Conclusions

In analogy with the work which has been done on Fermi transitions, we extended the analysis to cover Gamow-Teller transitions and pp-fusion in particular. The free, single-nucleon Born contribution was re-calculated for Gamow-Teller transitions. We found a slightly different result from the analysis done by [Hay21]. Similarly, the two-body nuclear structure correction was calculated for Gamow-Teller transitions following the work in [Tow92] on Fermi transitions.

Our new formulas for the two-body nuclear structure correction were applied to the case of pp-fusion. This allowed us to directly calculate the contribution from the term in Figure 1b of [KRV03]. We were able to confirm that their approximate result for the two-body part is of the correct size.

Then we moved on to tackle the question of how the nuclear environment affects the result for both the one-body and two-body parts. In particular, our goal was to calculate the effect of the nuclear energies in the nuclear Green's function. In the case of pp-fusion, we were able to calculate these corrections by summing over all intermediate states and weighting them by the energy. This simple harmonic oscillator basis was particularly convenient for this, as the basis is discrete and it allowed us to get a result which was a function of the loop momentum.

We found a large deviation in the result, much larger than one would expect from simple power counting in $1/M_N$. This was due to the deuteron binding energy creating a persistent energy gap at zero loop momentum. When we calculated the result using this method, we found a significant increase in the result over what we found without considering the nuclear energies. This new result was confirmed by repeating the calculation in coordinate space, where we could avoid any drawbacks of the simple harmonic oscillator basis.

The analysis in terms of intermediate states meant we could not use the usual normal ordering trick to separate out the one-body and the two-body parts. Instead, we had to use the fact that the two-body part dies off past $|\vec{k}| > 2k_F$. This allowed us to match onto the one-body part at high momentum, and subtract out the free one-body part. The free-one body part is then calculated separately using the full relativistic formulation, and goes into the Born contribution.

Using our knowledge of the physics, we were also able to come up with an approximate result called the "modified normal ordering" scheme. In this set up, we replace the nuclear energies with an average value which is allowed to depend on the loop momentum. The benefit of this is that we can again use the normal ordering trick to separate out the one-body and the two-body part. Using this, we were able to capture the largest effects from the nuclear environment. While this method requires some guesswork, it has the highest chance of being successful in the calculation of the nuclear energy effects in larger nuclei where normal ordering is critical.

With the increased precision in the measurement of g_A and interest in the precision measurements of the neutron lifetime and solar physics applications of Gamow-Teller transitions, my hope is that more of the research focus in this field can be directed toward Gamow-Teller transitions as well as the superallowed Fermi transitions which have been the main focus thus far. The formulas derived in Section 5.3 could immediately be implemented in larger nuclei for Gamow-Teller beta decays. However, this is only warranted in the case in which the tree-level nuclear matrix element is known with enough precision.

The research done in this thesis leaves open the door to many opportunities for further work. Here, I would like to outline my ideas for the logical next steps when it comes to this research.

In addition to the anti-symmetric part of the box diagram, which was the focus of this thesis, there is also the contribution from the axial divergence. We had previously called this term M^μ in Equation 2.2.7. In [Hay21], it was argued that this contribution should be small. However, it should be checked specifically for the case of pp-fusion.

In addition to that, there were also the current-current terms which we ignored. In Section 9.6, we gave an argument for why the nuclear structure correction from these terms should be small. However, again this should be checked by direct calculation. The calculation would be very similar to what was done here in terms of the multipole decomposition and nuclear energy correction from intermediate states.

Throughout this work, we have focused specifically on the one-body currents. In this context, two-body refers to the part of the box diagram in which the two one-body currents latch onto different nucleons in the nucleus. We did not consider the effect of intrinsic two-body currents, which would naturally also give rise to an additional two-body nuclear structure correction. These additional corrections should be included as well.

Finally, there is the natural extension of this work to larger systems. It would be nice to extend this work to large enough systems so that the double quenching effect we discussed in Section 5.4, which is used in the analysis of superallowed Fermi decays, could be checked directly. However, in order to use the methods presented here, we would like to be able to include enough intermediate states so that the completeness relation we discussed in Section 8 is satisfied. If the completeness relation cannot be satisfied, then we cannot use intermediate states to calculate the corrections due to the nuclear environment.

The methods used in this work could naturally be extended to other small nuclear systems, such as the three-nucleon or four-nucleon system. Again these are interesting appli-

cations to solar physics and the pp-chain. However, those other reactions are not known to as much precision as the *pp*-fusion reaction. A full calculation of the nuclear structure correction to those reaction is not yet warranted.

Bibliography

[Fer34] E. Fermi. "Versuch einer Theorie der β-Strahlen. I". In: *Zeitschrift für Physik* 88 (Mar. 1934), pp. 161–177. ISSN: 0044-3328. DOI: 10.1007/BF01351864.

[GT36] G. Gamow and E. Teller. "Selection Rules for the β-Disintegration". In: *Phys. Rev.* 49 (12 June 1936), pp. 895–899. DOI: 10.1103/PhysRev.49.895.

[BC38] H. A. Bethe and C. L. Critchfield. "The Formation of Deuterons by Proton Combination". In: *Phys. Rev.* 54 (4 Aug. 1938), pp. 248–254. DOI: 10.1103/PhysRev.54.248.

[Mic52] Louis Michel. "μ-Meson Decay and β-Radioactivity". In: *Phys. Rev.* 86 (5 June 1952), pp. 814–815. DOI: 10.1103/PhysRev.86.814.

[Bre55] G. Breit. "Relativistic Corrections for High-Energy $p-p$ Scattering". In: *Phys. Rev.* 99 (5 Sept. 1955), pp. 1581–1596. DOI: 10.1103/PhysRev.99.1581.

[BFS56] R. E. Behrends, R. J. Finkelstein, and A. Sirlin. "Radiative Corrections to Decay Processes". In: *Phys. Rev.* 101 (2 Jan. 1956), pp. 866–873. DOI: 10.1103/PhysRev.101.866.

[LY56a] T. D. Lee and C. N. Yang. "Charge conjugation, a new quantum numberG, and selection rules concerning a nucleon-antinucleon system". In: *Il Nuovo Cimento (1955-1965)* 3 (4 Apr. 1956), pp. 749–753. DOI: 10.1007/BF02744530.

[LY56b] T. D. Lee and C. N. Yang. "Question of Parity Conservation in Weak Interactions". In: *Phys. Rev.* 104 (1 Oct. 1956), pp. 254–258. DOI: 10.1103/PhysRev.104.254.

[Edm57] A. R. Edmonds. *Angular Momentum in Quantum Mechanics*. Princeton: Princeton University Press, 1957. ISBN: 9781400884186. DOI: doi:10.1515/9781400884186.

[Wu+57] C. S. Wu et al. "Experimental Test of Parity Conservation in Beta Decay". In: *Phys. Rev.* 105 (4 Feb. 1957), pp. 1413–1415. DOI: 10.1103/PhysRev.105.1413.

[Ber58] S. M. Berman. "Radiative Corrections to Muon and Neutron Decay". In: *Phys. Rev.* 112 (1 Oct. 1958), pp. 267–270. DOI: 10.1103/PhysRev.112.267.

[FG58] R. P. Feynman and M. Gell-Mann. "Theory of the Fermi Interaction". In: *Phys. Rev.* 109 (1 Jan. 1958), pp. 193–198. DOI: 10.1103/PhysRev.109.193.

[Wei58] Steven Weinberg. "Charge Symmetry of Weak Interactions". In: *Phys. Rev.* 112 (4 Nov. 1958), pp. 1375–1379. DOI: 10.1103/PhysRev.112.1375.

[KS59] Toichiro Kinoshita and Alberto Sirlin. "Radiative Corrections to Fermi Interactions". In: *Phys. Rev.* 113 (6 Mar. 1959), pp. 1652–1660. DOI: 10.1103/PhysRev.113.1652.

[BS62] S.M Berman and A Sirlin. "Some considerations on the radiative corrections to muon and neutron decay". In: *Annals of Physics* 20.1 (1962), pp. 20–43. ISSN: 0003-4916. DOI: 10.1016/0003-4916(62)90114-8.

[Lee62] T. D. Lee. "Application of ξ-Limiting Process to Intermediate Bosons". In: *Phys. Rev.* 128 (2 Oct. 1962), pp. 899–910. DOI: 10.1103/PhysRev.128.899.

[Cab63] Nicola Cabibbo. "Unitary Symmetry and Leptonic Decays". In: *Phys. Rev. Lett.* 10 (12 June 1963), pp. 531–533. DOI: 10.1103/PhysRevLett.10.531.

[Bjo66] J. D. Bjorken. "Applications of the Chiral $U(6) \bigotimes U(6)$ Algebra of Current Densities". In: *Phys. Rev.* 148 (4 Aug. 1966), pp. 1467–1478. DOI: 10.1103/PhysRev.148.1467.

[FW66] T. de Forest Jr. and J.D. Walecka. "Electron scattering and nuclear structure". In: *Advances in Physics* 15.57 (1966), pp. 1–109. DOI: 10.1080/00018736600101254.

[AND67] Ernest S. Abers, Richard E. Norton, and Duane A. Dicus. "Electromagnetic Corrections to the Weak $\Delta S = 0$ Vector Coupling Constant". In: *Phys. Rev. Lett.* 18 (16 Apr. 1967), pp. 676–680. DOI: 10.1103/PhysRevLett.18.676.

[Sir67] A. Sirlin. "General Properties of the Electromagnetic Corrections to the Beta Decay of a Physical Nucleon". In: *Phys. Rev.* 164 (5 Dec. 1967), pp. 1767–1775. DOI: 10.1103/PhysRev.164.1767.

[Abe+68] Ernest S. Abers et al. "Radiative Corrections to the Fermi Part of Strangeness-Conserving β Decay". In: *Phys. Rev.* 167 (5 Mar. 1968), pp. 1461–1478. DOI: 10.1103/PhysRev.167.1461.

[Wil68] Fred L. Wilson. "Fermi's Theory of Beta Decay". In: *American Journal of Physics* 36.12 (Dec. 1968), pp. 1150–1160. ISSN: 0002-9505. DOI: 10.1119/1.1974382.

[WAL75] J.D. WALECKA. "Section 4 - SEMILEPTONIC WEAK INTERACTIONS IN NUCLEI**Research sponsored by the Air Force Office of Scientific Research, Office of Aerospace Research, U.S. Air Force, under AFOSR Contract No. F44620-71-C-0044." In: *Muon Physics*. Ed. by VERNON W. HUGHES and C.S. WU. Academic Press, 1975, pp. 113–218. ISBN: 978-0-12-360602-0. DOI: 10.1016/B978-0-12-360602-0.50010-5.

[MS76] Gerald A Miller and James E Spencer. "A survey of pion charge-exchange reactions with nuclei". In: *Annals of Physics* 100.1 (1976), pp. 562–606. ISSN: 0003-4916. DOI: 10.1016/0003-4916(76)90073-7.

[Sir78] A. Sirlin. "Current algebra formulation of radiative corrections in gauge theories and the universality of the weak interactions". In: *Rev. Mod. Phys.* 50 (3 July 1978), pp. 573–605. DOI: 10.1103/RevModPhys.50.573.

[New82] Roger G. Newton. *Scattering Theory of Waves and Particles*. Theoretical and Mathematical Physics. Springer Berlin, Heidelberg, 1982. ISBN: 978-3-642-88130-5. DOI: 10.1007/978-3-642-88128-2.

[HS84] W.C. Haxton and G.J. Stephenson. "Double beta decay". In: *Progress in Particle and Nuclear Physics* 12 (1984), pp. 409–479. ISSN: 0146-6410. DOI: 10.1016/0146-6410(84)90006-1.

[WSA84] R. B. Wiringa, R. A. Smith, and T. L. Ainsworth. "Nucleon-nucleon potentials with and without $\Delta(1232)$ degrees of freedom". In: *Phys. Rev. C* 29 (4 Apr. 1984), pp. 1207–1221. DOI: 10.1103/PhysRevC.29.1207.

[MS86] W. J. Marciano and A. Sirlin. "Radiative corrections to β decay and the possibility of a fourth generation". In: *Phys. Rev. Lett.* 56 (1 Jan. 1986), pp. 22–25. DOI: 10.1103/PhysRevLett.56.22.

[JR87] W. Jaus and G. Rasche. "Radiative corrections to 0^+-0^+ β transitions". In: *Phys. Rev. D* 35 (11 June 1987), pp. 3420–3422. DOI: 10.1103/PhysRevD.35.3420.

[Tow87] I.S. Towner. "Quenching of spin matrix elements in nuclei". In: *Physics Reports* 155.5 (1987), pp. 263–377. ISSN: 0370-1573. DOI: 10.1016/0370-1573(87)90138-4.

[BU88] John N. Bahcall and Roger K. Ulrich. "Solar models, neutrino experiments, and helioseismology". In: *Rev. Mod. Phys.* 60 (2 Apr. 1988), pp. 297–372. DOI: 10.1103/RevModPhys.60.297.

[Ber+88] J. R. Bergervoet et al. "Phase shift analysis of 0–30 MeV pp scattering data". In: *Phys. Rev. C* 38 (1 July 1988), pp. 15–50. DOI: 10.1103/PhysRevC.38.15.

[BW88] B. A. Brown and B. H. Wildenthal. "Status of the Nuclear Shell Model". In: *Ann. Rev. Nucl. Part. Sci.* 38 (Dec. 1988), pp. 29–66. DOI: 10.1146/annurev.ns.38.120188.000333.

[Kra88] Kenneth S Krane. *Introductory nuclear physics*. New York, NY: Wiley, 1988. ISBN: 9780471805533.

[JR90] W. Jaus and G. Rasche. "Nuclear-structure dependence of $O(\alpha)$ corrections to Fermi decays and the value of the Kobayashi-Maskawa matrix element V_{ud}". In: *Phys. Rev. D* 41 (1 Jan. 1990), pp. 166–176. DOI: 10.1103/PhysRevD.41.166.

[SV90] M. Spiro and D. Vignaud. "Solar model independent neutrino oscillatiion signals in the forthcoming solar neutrino experiments?" In: *Physics Letters B* 242.2 (1990), pp. 279–284. ISSN: 0370-2693. DOI: 10.1016/0370-2693(90)91471-M.

[Tow92] I.S. Towner. "The nuclear-structure dependence of radiative corrections in superallowed Fermi beta-decay". In: *Nuclear Physics A* 540.3 (1992), pp. 478–500. ISSN: 0375-9474. DOI: 10.1016/0375-9474(92)90170-O.

[Sto+93] V. G. J. Stoks et al. "Partial-wave analysis of all nucleon-nucleon scattering data below 350 MeV". In: *Phys. Rev. C* 48 (2 Aug. 1993), pp. 792–815. DOI: 10.1103/PhysRevC.48.792.

[KB94] Marc Kamionkowski and John N. Bahcall. "The Rate of the Proton-Proton Reaction". In: *The Astrophysical Journal* 420 (Jan. 1994), p. 884. DOI: 10.1086/173612. arXiv: astro-ph/9305020 [astro-ph].

[Tow94] I.S. Towner. "Quenching of spin operators in the calculation of radiative corrections for nuclear beta decay". In: *Physics Letters B* 333.1 (1994), pp. 13–16. ISSN: 0370-2693. DOI: 10.1016/0370-2693(94)91000-6.

[PS95] Michael E. Peskin and Daniel V. Schroeder. *An Introduction to quantum field theory*. Reading, USA: Addison-Wesley, 1995. ISBN: 978-0-201-50397-5.

[Wei95] Steven Weinberg. *The Quantum Theory of Fields. Volume 1: Foundations*. Cambridge University Press, 1995. ISBN: 9781139644167. DOI: 10.1017/CBO9781139644167.

[WSS95] R. B. Wiringa, V. G. J. Stoks, and R. Schiavilla. "Accurate nucleon-nucleon potential with charge-independence breaking". In: *Phys. Rev. C* 51 (1 Jan. 1995), pp. 38–51. DOI: 10.1103/PhysRevC.51.38.

[Wei96] Steven Weinberg. *The Quantum Theory of Fields. Volume 2: Modern Applications*. Cambridge University Press, 1996. ISBN: 9781139644174. DOI: 10.1017/CBO9781139644174.

[Sch+98] R. Schiavilla et al. "Weak capture of protons by protons". In: *Phys. Rev. C* 58 (2 Aug. 1998), pp. 1263–1277. DOI: 10.1103/PhysRevC.58.1263.

[Bah02] John N. Bahcall. "The luminosity constraint on solar neutrino fluxes". In: *Phys. Rev. C* 65 (2 Jan. 2002), p. 025801. DOI: 10.1103/PhysRevC.65.025801.

[Poo02] A. W. P. Poon. "Neutrino observations from the Sudbury Neutrino Observatory". In: *AIP Conference Proceedings* 610.1 (Apr. 2002), pp. 218–230. ISSN: 0094-243X. DOI: 10.1063/1.1469931.

[TH02] I. S. Towner and J. C. Hardy. "Calculated corrections to superallowed Fermi β decay: New evaluation of the nuclear-structure-dependent terms". In: *Phys. Rev. C* 66 (3 Sept. 2002), p. 035501. DOI: 10.1103/PhysRevC.66.035501.

[KRV03] A. Kurylov, M. J. Ramsey-Musolf, and P. Vogel. "Radiative corrections to low-energy neutrino reactions". In: *Phys. Rev. C* 67 (3 Mar. 2003), p. 035502. DOI: 10.1103/PhysRevC.67.035502.

[FK04] M. Fukugita and T. Kubota. "Radiative Corrections to Neutrino–Nucleon Quasielastic Scattering". In: *Acta Physica Polonica B* 35.5 (May 2004), p. 1687. DOI: 10.48550/arXiv.hep-ph/0403149. arXiv: hep-ph/0403149 [hep-ph].

[Wal04] John Dirk Walecka. *Theoretical Nuclear and Subnuclear Physics*. 2nd. CO-PUBLISHED WITH IMPERIAL COLLEGE PRESS, 2004. DOI: 10.1142/5500. eprint: https://www.worldscientific.com/doi/pdf/10.1142/5500.

[VA05] M. Pavón Valderrama and E. Ruiz Arriola. "Low-energy NN scattering at next-to-next-to-next-to-next-to-leading order for partial waves with $j \leq 5$". In: *Phys. Rev. C* 72 (4 Oct. 2005), p. 044007. DOI: 10.1103/PhysRevC.72.044007.

[MS06] William J. Marciano and Alberto Sirlin. "Improved Calculation of Electroweak Radiative Corrections and the Value of V_{ud}". In: *Phys. Rev. Lett.* 96 (3 Jan. 2006), p. 032002. DOI: 10.1103/PhysRevLett.96.032002.

[Pau09] Stephan Paul. "The puzzle of neutron lifetime". In: *Nuclear Instruments and Methods in Physics Research Section A: Accelerators, Spectrometers, Detectors and Associated Equipment* 611.2 (2009). Particle Physics with Slow Neutrons, pp. 157–166. ISSN: 0168-9002. DOI: 10.1016/j.nima.2009.07.095.

[HP10] Richard J. Hill and Gil Paz. "Model-independent extraction of the proton charge radius from electron scattering". In: *Phys. Rev. D* 82 (11 Dec. 2010), p. 113005. DOI: 10.1103/PhysRevD.82.113005.

[Ade+11] E. G. Adelberger et al. "Solar fusion cross sections. II. The *pp* chain and CNO cycles". In: *Rev. Mod. Phys.* 83 (1 Apr. 2011), pp. 195–245. DOI: 10.1103/RevModPhys.83.195.

[SF13] Alberto Sirlin and Andrea Ferroglia. "Radiative corrections in precision electroweak physics: A historical perspective". In: *Rev. Mod. Phys.* 85 (1 Feb. 2013), pp. 263–297. DOI: 10.1103/RevModPhys.85.263.

[HT15] J. C. Hardy and I. S. Towner. "Superallowed $0^+ \to 0^+$ nuclear β decays: 2014 critical survey, with precise results for V_{ud} and CKM unitarity". In: *Phys. Rev. C* 91 (2 Feb. 2015), p. 025501. DOI: 10.1103/PhysRevC.91.025501.

[Mam+15] E. E. Mamajek et al. *IAU 2015 Resolution B3 on Recommended Nominal Conversion Constants for Selected Solar and Planetary Properties*. Feb. 2015. arXiv: 1510.07674 [astro-ph.SR].

[Pat+16] C Patrignani et al. "Review of Particle Physics, 2016-2017". In: *Chin. Phys. C* 40.10 (2016), p. 100001. DOI: 10.1088/1674-1137/40/10/100001.

[Vin+17] Núria Vinyoles et al. "A New Generation of Standard Solar Models". In: *ApJ* 835 (2 Jan. 2017). DOI: 10.3847/1538-4357/835/2/202.

[Hay+18] Leendert Hayen et al. "High precision analytical description of the allowed β spectrum shape". In: *Rev. Mod. Phys.* 90 (1 Mar. 2018), p. 015008. DOI: 10.1103/RevModPhys.90.015008.

[Ye+18] Zhihong Ye et al. "Proton and neutron electromagnetic form factors and uncertainties". In: *Physics Letters B* 777 (2018), pp. 8–15. ISSN: 0370-2693. DOI: 10.1016/j.physletb.2017.11.023.

[Ago+19] M. Agostini et al. "Simultaneous precision spectroscopy of *pp*, ^{7}Be, and *pep* solar neutrinos with Borexino Phase-II". In: *Phys. Rev. D* 100 (8 Oct. 2019), p. 082004. DOI: 10.1103/PhysRevD.100.082004.

[CMS19] Andrzej Czarnecki, William J. Marciano, and Alberto Sirlin. "Radiative corrections to neutron and nuclear beta decays revisited". In: *Phys. Rev. D* 100 (7 Oct. 2019), p. 073008. DOI: 10.1103/PhysRevD.100.073008.

[Mär+19] B. Märkisch et al. "Measurement of the Weak Axial-Vector Coupling Constant in the Decay of Free Neutrons Using a Pulsed Cold Neutron Beam". In: *Phys. Rev. Lett.* 122 (24 June 2019), p. 242501. DOI: 10.1103/PhysRevLett.122.242501.

[SGR19] Chien-Yeah Seng, Mikhail Gorchtein, and Michael J. Ramsey-Musolf. "Dispersive evaluation of the inner radiative correction in neutron and nuclear β decay". In: *Phys. Rev. D* 100 (1 July 2019), p. 013001. DOI: 10.1103/PhysRevD.100.013001.

[Ves+20] Diego Vescovi et al. "The luminosity constraint in the era of precision solar physics". In: *Journal of Physics G: Nuclear and Particle Physics* 48.1 (Nov. 2020), p. 015201. DOI: 10.1088/1361-6471/abb784.

[Wal+20] André Walker-Loud et al. "Lattice QCD determination of the nucleon axial charge". In: *PoS* CD2018 (2020), p. 020. DOI: 10.22323/1.317.0020.

[Hay21] Leendert Hayen. "Standard model $\mathcal{O}(\alpha)$ renormalization of g_A and its impact on new physics searches". In: *Phys. Rev. D* 103 (11 June 2021), p. 113001. DOI: 10.1103/PhysRevD.103.113001.

[Gro+22] Particle Data Group et al. "Review of Particle Physics". In: *Progress of Theoretical and Experimental Physics* 2022.8 (Aug. 2022), p. 083C01. ISSN: 2050-3911. DOI: 10.1093/ptep/ptac097.

[Cai+23] T Cai et al. "Measurement of the axial vector form factor from antineutrino–proton scattering". In: *Nature* 614 (7946 Feb. 2023), pp. 48–53. DOI: 10.1038/s41586-022-05478-3.

Appendix A

Numerical Evaluation of Nucleon Form Factors

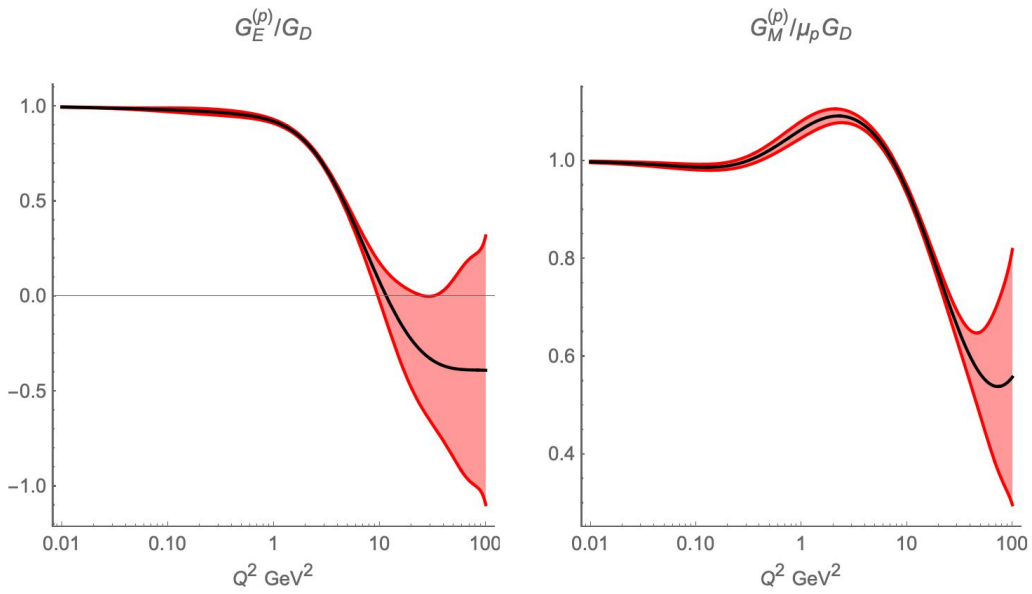

Figure A.1: Sachs electric and magnetic form factors for the proton, divided by the dipole form factor $G_D = (1 + Q^2/\Lambda_V^2)^{-2}$ with dipole mass $\Lambda_V^2 = 0.71$ GeV^2. The black curve shows the central value, while the red region shows the uncertainty.

Instead of working directly with the form factors F_1 and F_2 in the vector current in

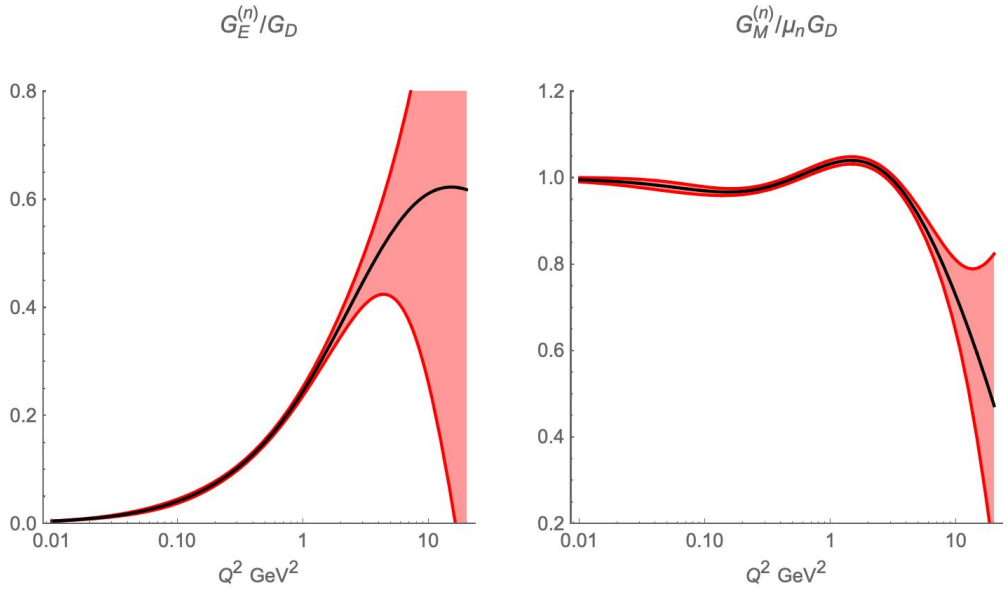

Figure A.2: Sachs electric and magnetic form factors for the neutron, divided by the dipole form factor $G_D = (1 + Q^2/\Lambda_V^2)^{-2}$ with dipole mass $\Lambda_V^2 = 0.71$ GeV^2. The black curve shows the central value, while the red region shows the uncertainty.

Equation 1.2.23, we instead use data for the Sachs form factors G_E and G_M.

$$\begin{aligned} G_E &= F_1 - \tau F_2 \\ G_M &= F_1 + F_2 \end{aligned} \tag{A.0.1}$$

where $\tau = Q^2/4M_N^2$. These values of these form factors at zero momentum transfer is related to the nucleon charge and magnetic moment.

$$\begin{aligned} G_E^{(p)}(0) &= 1, \quad & G_M^{(p)}(0) &= \mu_p \\ G_E^{(n)}(0) &= 0, \quad & G_M^{(n)}(0) &= \mu_n \end{aligned} \tag{A.0.2}$$

The benefit of using Sachs form factors is that they can be directly related to experiment. For example, they appear in the Rosenbluth formula for unpolarized electron-nucleon scattering in the one-photon exchange approximation.

$$\frac{d\sigma}{d\Omega_{\text{lab}}} = \frac{\alpha^2 \cos^2(\theta/2)}{4\varepsilon_i^2 \sin^4(\theta/2)} \frac{\epsilon G_E^2 + \tau G_M^2}{\epsilon(1+\tau)} r \tag{A.0.3}$$

where $\varepsilon_{i,f}$ are the initial and final lepton energies, and $\epsilon = [1+2(1+\tau)\tan^2(\theta/2)]^{-1}$. The recoil factor is $r = \varepsilon_f/\varepsilon_i$. Using the θ-dependence of electron-proton scattering, we can extract

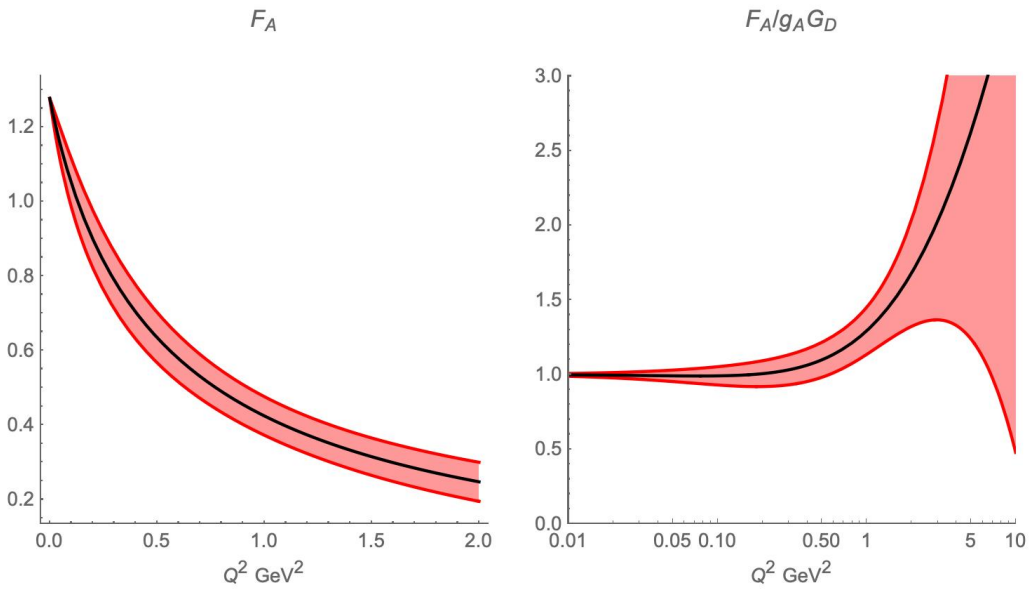

Figure A.3: Left, nucleon axial form factor with uncertainties. Right, nucleon axial form factor divided by the dipole form factor $G_D = (1 + Q^2/\Lambda_A^2)^{-2}$ with dipole mass $\Lambda_A = 1.014$ GeV.

$G_E^{(p)}$ and $G_M^{(p)}$ as a function of Q^2. Measuring the neutron form factor $G_E^{(n)}$ is typically done using quasi-elastic electron-deuteron scattering, which introduces some model dependence. Then the ratio $G_E^{(n)}/G_M^{(n)}$ is determined using polarization observables.

We can also define charge radii, which captures the momentum dependence at small Q.

$$G(Q^2) = G(0)\left[1 - \frac{r^2}{6}Q^2 + \dots\right] \tag{A.0.4}$$

The neutron electric radius is measured in neutron-electron scattering length measurements, which give $(r_E^n)^2 = -0.1161(22)$ fm^2. The proton electric radius can be measured directly from electron-proton scattering data with $r_E^p = 0.879$ fm For the magnetic radii we have the PDG averages $r_M^n = 0.864$ fm and $r_M^p = 0.851$ fm.

Typically, the form factors are described using the *dipole form factor* approximation. The functional form of the form factor is assumed to be a constant times the dipole form factor.

$$G_D = (1 + Q^2/\Lambda^2)^{-2} \tag{A.0.5}$$

The benefit of this form is that it has the correct $1/Q^4$ behaviour at large Q^2, and it only depends on one parameter Λ. This parameter is usually called the "dipole mass". Another advantage of this form is that it can be used to give simple analytic results.

We could try to capture the Q^2 dependence more accurately by doing a taylor expansion in Q^2. However, then we run into problems at high Q^2. A better approach is the so-called *z-expansion* [HP10]. We use the fact that the form factor $G(Q^2)$ is an analytic function of Q^2, aside from the branch cut at time-like $-Q^2_{\text{cut}} = t_{\text{cut}} = 4m_\pi^2$ where we can create two pion states. We then perform a conformal mapping from Q^2 to a new parameter z.

$$z = \frac{\sqrt{t_{\text{cut}} + Q^2} - \sqrt{t_{\text{cut}} - t_0}}{\sqrt{t_{\text{cut}} + Q^2} + \sqrt{t_{\text{cut}} - t_0}} \tag{A.0.6}$$

Here t_0 is a free parameter which maps onto the point $z = 0$. This is now well behaved as $Q^2 \to \infty$, so we can perform a taylor expansion in z.

$$G(Q^2) = \sum_{k=0}^{\infty} a_k z^k \tag{A.0.7}$$

In practice, we truncate the sum at some k_{max}. Then the values of a_k can be fit from data. Not all of the a_k are independent, however. They must reproduce the correct value at $Q^2 = 0$. Also we require that the form factor goes at $1/Q^4$ for large Q, which implies the following sum rules.

$$\sum_{k=n}^{\infty} \frac{k!}{(k-n)!} a_k = 0, \quad n = 0, 1, 2, 3 \tag{A.0.8}$$

In practice, we use the sum rules to fix a_0 and the highest four a_k. The remaining a_k which are not determined by the sum rules are then fit to data. For the electromagnetic nucleon form factors we use the fits and uncertainties from [Ye+18]. These are plotted in Figure A.1 and A.2. Then we derive the form factors $F_{1,2}$ using the definition of the Sachs form factors Equation A.0.1.

On the other hand, the axial form factor F_A is much less well known. As we mentioned in Section 3.2, the value at zero momentum transfer g_A has been determined to much higher accuracy using the new PERKEO III experiment. For the full form factor $F_A(Q^2)$, we use a determination performed by [Cai+23] using antineutrino-proton scattering data. The fitted z-expansion with uncertainties are shown in Figure A.3.

Appendix B

Dirac Algebra for $C_{\mathbf{Born}}^{\mathbf{GT}}$

In what follows, we repeatedly make the following simplifications. The Levi-Civita symbol kills off any terms which are symmetric under the exchange $\mu \leftrightarrow \lambda$. Also any term proportional to k^μ or k^λ vanishes. We use the static nucleon approximation, where the GT matrix element has no time component.

$$\bar{u}\gamma^\mu\gamma^5 u \to 2M_N\chi^\dagger\vec{\sigma}\chi \tag{B.0.1}$$

In the static-nucleon limit, we also have an axial-vector Gordon identity for $\sigma^{\mu\nu}\gamma^5$.

$$\bar{u}(\sigma^{\mu\nu}\gamma^5 p_\nu)u \to -iM_N\bar{u}\gamma^\mu\gamma^5 u \tag{B.0.2}$$

We also use rotational symmetry of the integral with respect to the space components of k.

We define an effective hadronic current for the box diagram.

$$\mathcal{J}^\beta = 8\pi^2\int\frac{d^4k}{(2\pi)^4}\frac{\varepsilon^{\mu\lambda\alpha\beta}k_\alpha}{(k^2+i\epsilon)^2}T_{\mu\lambda}(p,k) \tag{B.0.3}$$

For the Born term, we take $T^{\mu\lambda}$ from Equation 4.0.9. And we will now go through the algebra term-by-term, inserting the various currents into the electromagnetic vertex Γ^μ and the weak vertex W^λ. We start with the diagram where the photon latches onto the proton line. The $F_1^{(p)}F_1$ term gives us

$$8\pi^2\int\frac{d^4k}{(2\pi)^4}\frac{\varepsilon_{\mu\lambda\alpha\beta}k^\alpha}{(k^2+i\epsilon)^2}\frac{\bar{u}\gamma^\mu(\not{p}+\not{k}+M)\gamma^\lambda u}{k^2+2p\cdot k+i\epsilon}F_1^{(p)}F_1 \tag{B.0.4}$$

The term with $\not{p}+M$ vanishes, which can be seen by writing it in a symmetric form.

$$\bar{u}\gamma^\mu(\not{p}+M)\gamma^\lambda u = \bar{u}(p^\mu\gamma^\lambda+\gamma^\mu p^\lambda)u \tag{B.0.5}$$

The term which survives is

$$\begin{aligned}
&8\pi^2 \int \frac{d^4k}{(2\pi)^4} \frac{\varepsilon_{\mu\lambda\alpha\beta}k^\alpha}{(k^2+i\epsilon)^2} \frac{\bar{u}\gamma^\mu(\not{p}+\not{k}+M)\gamma^\lambda u}{k^2+2p\cdot k+i\epsilon} F_1^{(p)}F_1 \\
&= 8\pi^2 \int \frac{d^4k}{(2\pi)^4} \frac{\varepsilon_{\mu\lambda\alpha\beta}k^\alpha}{(k^2+i\epsilon)^2} \frac{\bar{u}[-i\varepsilon^{\mu\lambda\nu\rho}k_\nu\gamma_\rho\gamma^5]u}{k^2+2p\cdot k+i\epsilon} F_1^{(p)}F_1 \\
&= 16i\pi^2 \int \frac{d^4k}{(2\pi)^4} \frac{1}{(k^2+i\epsilon)^2} \frac{\bar{u}[k^2\gamma_\beta - \not{k}k_\beta]\gamma^5 u}{k^2+2p\cdot k+i\epsilon} F_1^{(p)}F_1
\end{aligned} \tag{B.0.6}$$

In the static nucleon approximation, the matrix element of $\gamma^\mu\gamma^5$ only has space components. We also use rotational symmetry to rewrite the space components of k using $k^ik^j \to \frac{1}{3}\delta^{ij}|\vec{k}|^2$.

$$\mathcal{J}_\beta = 16i\pi^2[\bar{u}\gamma_\beta\gamma^5 u]\int \frac{d^4k}{(2\pi)^4} \frac{(k^2+\frac{1}{3}|\vec{k}|^2)}{(k^2+i\epsilon)^2} \frac{1}{k^2+2p\cdot k+i\epsilon} F_1^{(p)}F_1 \tag{B.0.7}$$

Performing a Wick rotation as before, we find

$$\begin{aligned}
\mathcal{J}_\beta &= -\frac{2}{3\pi}[\bar{u}\gamma_\beta\gamma^5 u]\int_0^\infty dQ^2 \int_{-1}^1 du \frac{\sqrt{1-u^2}(2+u^2)}{Q^2+4M^2u^2} F_1^{(p)}(Q^2)F_1(Q^2) \\
&= -\frac{2}{3}[\bar{u}\gamma_\beta\gamma^5 u]\int_0^\infty \frac{dQ}{Q}\frac{(5+4r)}{(1+r)^2} F_1^{(p)}(Q^2)F_1(Q^2)
\end{aligned} \tag{B.0.8}$$

For the $F_2^{(p)}F_1$ term, we use the on-shell identity $(\not{p}+M)\gamma^\lambda u = (2p^\lambda)u$. The rest is simple (but tedious) Dirac matrix algebra.

$$\begin{aligned}
&8\pi^2 \int \frac{d^4k}{(2\pi)^4} \frac{\varepsilon_{\mu\lambda\alpha\beta}k^\alpha}{(k^2+i\epsilon)^2} \frac{\bar{u}(-i\sigma^{\mu\nu}k_\nu)(\not{p}+\not{k}+M)\gamma^\lambda u}{k^2+2p\cdot k+i\epsilon} \frac{F_2^{(p)}F_1}{2M} \\
&= 8\pi^2 \int \frac{d^4k}{(2\pi)^4} \frac{\varepsilon_{\mu\lambda\alpha\beta}k^\alpha}{(k^2+i\epsilon)^2} \frac{\bar{u}(-i\sigma^{\mu\nu}k_\nu)(2p^\lambda+i\sigma^{\lambda\rho}k_\rho)u}{k^2+2p\cdot k+i\epsilon} \frac{F_2^{(p)}F_1}{2M} \\
&= 8\pi^2 \int \frac{d^4k}{(2\pi)^4} \frac{\varepsilon_{\mu\lambda\alpha\beta}k^\alpha}{(k^2+i\epsilon)^2} \frac{\bar{u}(-2i\sigma^{\mu\nu}k_\nu p^\lambda - ik^2\sigma^{\mu\lambda})u}{k^2+2p\cdot k+i\epsilon} \frac{F_2^{(p)}F_1}{2M} \\
&= 8\pi^2 \int \frac{d^4k}{(2\pi)^4} \frac{1}{(k^2+i\epsilon)^2} \frac{\bar{u}(-2i\varepsilon_{\mu\lambda\alpha\beta}k^\alpha\sigma^{\mu\nu}k_\nu p^\lambda - 2k^2\sigma_{\alpha\beta}\gamma^5 k^\alpha)u}{k^2+2p\cdot k+i\epsilon} \frac{F_2^{(p)}F_1}{2M}
\end{aligned} \tag{B.0.9}$$

In the first term, we only get the space components and the rotational symmetry of the integral allows us to make the replacement $k^ik^j \to \frac{1}{3}\delta^{ij}|\vec{k}|^2$. In the second term, the k^α must be in the time direction, and we make the replacement $k^\alpha \to p^\alpha(p\cdot k)/M^2$. Then we can use

the axial-vector Gordon Identity to reduce the $\sigma_{\alpha\beta}$.

$$\begin{aligned}
&8\pi^2 \int \frac{d^4k}{(2\pi)^4} \frac{\varepsilon_{\mu\lambda\alpha\beta}k^\alpha}{(k^2+i\epsilon)^2} \frac{\bar{u}(-i\sigma^{\mu\nu}k_\nu)(\not{p}+\not{k}+M)\gamma^\lambda u}{k^2+2p\cdot k+i\epsilon} \frac{F_2^{(p)}F_1}{2M} \\
&= 8\pi^2 \int \frac{d^4k}{(2\pi)^4} \frac{1}{(k^2+i\epsilon)^2} \frac{\bar{u}(\frac{2}{3}i|\vec{k}|^2\varepsilon_{\mu\lambda\alpha\beta}\sigma^{\mu\alpha}p^\lambda - 2k^2\sigma_{\alpha\beta}\gamma^5 p^\alpha (p\cdot k)/M^2)u}{k^2+2p\cdot k+i\epsilon} \frac{F_2^{(p)}F_1}{2M} \\
&= -i8\pi^2[\bar{u}\gamma_\beta\gamma^5 u]\int \frac{d^4k}{(2\pi)^4} \frac{(\frac{2}{3}|\vec{k}|^2 + k^2(p\cdot k)/M^2)}{(k^2+i\epsilon)^2} \frac{F_2^{(p)}F_1}{k^2+2p\cdot k+i\epsilon}
\end{aligned} \tag{B.0.10}$$

Wick rotating and doing the integral, we have

$$\begin{aligned}
&-[\bar{u}\gamma_\beta\gamma^5 u]\frac{2}{3\pi}\int_0^\infty dQ^2 \int_{-1}^1 du \frac{\sqrt{1-u^2}(1+2u^2)}{Q^2+4M^2u^2} F_2^{(p)}(Q^2)F_1(Q^2) \\
&= -[\bar{u}\gamma_\beta\gamma^5 u]\frac{4}{3}\int_0^\infty \frac{dQ}{Q}\frac{(2+r)}{(1+r)^2}F_2^{(p)}(Q^2)F_1(Q^2)
\end{aligned} \tag{B.0.11}$$

Similarly for the weak magnetism term $F_1^{(p)}F_2$ we have

$$\begin{aligned}
&8\pi^2 \int \frac{d^4k}{(2\pi)^4} \frac{\varepsilon_{\mu\lambda\alpha\beta}k^\alpha}{(k^2+i\epsilon)^2} \frac{\bar{u}\gamma^\mu(\not{p}+\not{k}+M)(i\sigma^{\lambda\rho}k_\rho)u}{k^2+2p\cdot k+i\epsilon} \frac{F_1^{(p)}F_2}{2M} \\
&= 8\pi^2 \int \frac{d^4k}{(2\pi)^4} \frac{\varepsilon_{\mu\lambda\alpha\beta}k^\alpha}{(k^2+i\epsilon)^2} \frac{\bar{u}(2p^\mu - i\sigma^{\mu\nu}k_\nu)(i\sigma^{\lambda\rho}k_\rho)u}{k^2+2p\cdot k+i\epsilon} \frac{F_1^{(p)}F_2}{2M} \\
&= 8\pi^2 \int \frac{d^4k}{(2\pi)^4} \frac{\varepsilon_{\mu\lambda\alpha\beta}k^\alpha}{(k^2+i\epsilon)^2} \frac{\bar{u}(2ip^\mu\sigma^{\lambda\rho}k_\rho - ik^2\sigma^{\mu\lambda})u}{k^2+2p\cdot k+i\epsilon} \frac{F_1^{(p)}F_2}{2M} \\
&= 8\pi^2 \int \frac{d^4k}{(2\pi)^4} \frac{1}{(k^2+i\epsilon)^2} \frac{\bar{u}(2ip^\mu\varepsilon_{\mu\lambda\alpha\beta}k^\alpha\sigma^{\lambda\rho}k_\rho - 2k^2k^\alpha\sigma_{\alpha\beta}\gamma^5)u}{k^2+2p\cdot k+i\epsilon} \frac{F_1^{(p)}F_2}{2M} \\
&= 8\pi^2 \int \frac{d^4k}{(2\pi)^4} \frac{1}{(k^2+i\epsilon)^2} \frac{\bar{u}(-i\frac{2}{3}|\vec{k}|^2p^\mu\varepsilon_{\mu\lambda\alpha\beta}\sigma^{\lambda\alpha} - 2k^2p^\alpha\sigma_{\alpha\beta}\gamma^5(p\cdot k)/M^2)u}{k^2+2p\cdot k+i\epsilon} \frac{F_1^{(p)}F_2}{2M} \\
&= 8\pi^2 \int \frac{d^4k}{(2\pi)^4} \frac{(-\frac{4}{3}|\vec{k}|^2 - 2k^2(p\cdot k)/M^2)}{(k^2+i\epsilon)^2} \frac{\bar{u}(p^\alpha\sigma_{\alpha\beta}\gamma^5)u}{k^2+2p\cdot k+i\epsilon} \frac{F_1^{(p)}F_2}{2M} \\
&= -i8\pi^2[\bar{u}\gamma_\beta\gamma^5 u]\int \frac{d^4k}{(2\pi)^4} \frac{(\frac{2}{3}|\vec{k}|^2 + k^2(p\cdot k)/M^2)}{(k^2+i\epsilon)^2} \frac{F_1^{(p)}F_2}{k^2+2p\cdot k+i\epsilon}
\end{aligned} \tag{B.0.12}$$

The integration is the same as for the previous term

$$-[\bar{u}\gamma_\beta\gamma^5 u]\frac{4}{3}\int_0^\infty \frac{dQ}{Q}\frac{(2+r)}{(1+r)^2}F_1^{(p)}(Q^2)F_2(Q^2) \tag{B.0.13}$$

And finally the weak magnetism term $F_2^{(p)}F_2$.

$$
\begin{aligned}
&8\pi^2 \int \frac{d^4k}{(2\pi)^4} \frac{\varepsilon_{\mu\lambda\alpha\beta}k^\alpha}{(k^2+i\epsilon)^2} \frac{\bar{u}(-i\sigma^{\mu\nu}k_\nu)(\not{p}+\not{k}+M)(i\sigma^{\lambda\rho}k_\rho)u}{k^2+2p\cdot k+i\epsilon} \frac{F_2^{(p)}F_2}{4M^2} \\
&= 8\pi^2 \int \frac{d^4k}{(2\pi)^4} \frac{1}{(k^2+i\epsilon)^2} \frac{\bar{u}(2i(k^2+2p\cdot k)[k^2\gamma_\beta - k_\beta \not{k}]\gamma^5 - 2iMk^2\varepsilon_{\mu\lambda\alpha\beta}k^\alpha\sigma^{\mu\lambda})u}{k^2+2p\cdot k+i\epsilon} \frac{F_2^{(p)}F_2}{4M^2} \\
&= 8\pi^2 \int \frac{d^4k}{(2\pi)^4} \frac{1}{(k^2+i\epsilon)^2} \frac{\bar{u}(2i(k^2+2p\cdot k)(k^2+\frac{1}{3}|\vec{k}|^2)\gamma_\beta\gamma^5 - 4k^2(p\cdot k)/Mp^\alpha\sigma_{\alpha\beta}\gamma^5)u}{k^2+2p\cdot k+i\epsilon} \frac{F_2^{(p)}F_2}{4M^2} \\
&= 16i\pi^2[\bar{u}\gamma_\beta\gamma^5 u] \int \frac{d^4k}{(2\pi)^4} \frac{1}{(k^2+i\epsilon)^2} \left((k^2+\frac{1}{3}|\vec{k}|^2) - \frac{2k^2(p\cdot k)}{k^2+2p\cdot k+i\epsilon} \right) \frac{F_2^{(p)}F_2}{4M^2}
\end{aligned}
\tag{B.0.14}
$$

Wick rotating and doing the integral, we find that the weak magnetism term $F_2^{(p)}F_2$ is suppressed by Q^2/M^2

$$
\begin{aligned}
&-\frac{2}{3\pi}[\bar{u}\gamma_\beta\gamma^5 u] \int_0^\infty dQ^2 \int_{-1}^1 \sqrt{1-u^2}du \left(-\frac{(2+u^2)}{4M^2} + \frac{3u^2}{Q^2+4M^2u^2} \right) F_2^{(p)}F_2 \\
&\qquad = -[\bar{u}\gamma_\beta\gamma^5 u] \int_0^\infty \frac{dQ}{Q} \left(-\frac{3Q^2}{8M^2} + \frac{2}{(1+r)^2} \right) F_2^{(p)}F_2 \\
&\qquad = -[\bar{u}\gamma_\beta\gamma^5 u] \int_0^\infty \frac{dQ}{Q} \left(\frac{2Q^4(1-r)+M^2Q^2}{8M^4} \right) F_2^{(p)}F_2
\end{aligned}
\tag{B.0.15}
$$

In order to calculate the result for the term where the photon latches onto the neutron line, we can use symmetry to relate it back to the results above. The end result is that we can replace all of the form factors $F_{1,2}^{(p)}$ by the isoscalar form factors $F_{1,2}^{(0)}$.

Appendix C

Non-Relativistic Reduction of One-Body Currents

We want to evaluate the matrix elements of the single-nucleon current operators in the nuclear setting. For small nucleon velocities, we make the non-relativistic reduction. This amounts to expanding out the current operators to order $\mathcal{O}(1/M_N)$ or $\mathcal{O}(1/M_N^2)$. We also want to expand out the Dirac spinors in terms of the two component Pauli spinors.

The Dirac algebra identities we need can all be found by looking at the action of boosts on spinors. A simple boost takes us from a particle at rest $p_0 = (m, \vec{0})$ to a particle with arbitrary momentum $p^\mu = \Lambda^\mu{}_\nu (p_0)^\nu$. It is convenient to express this in terms of the rapidity angle η (not to be confused with the Coulomb parameter).

The rapidity is given by the hyperbolic trigonometic relation

$$\tanh \eta = \frac{|\vec{p}|}{E} = v \tag{C.0.1}$$

For convenience, we also write $\vec{\eta}$ as a vector where the direction is given by the direction of the momentum. Then the boost can be written in as a 4x4 matrix.

$$\Lambda(\vec{\eta}) = \begin{pmatrix} \cosh(\eta) & \hat{\eta} \sinh(\eta) \\ \hat{\eta} \sinh(\eta) & (\delta^{ij} - \hat{\eta}^i \hat{\eta}^j) + \hat{\eta}^i \hat{\eta}^j \cosh(\eta) \end{pmatrix} \tag{C.0.2}$$

Here $\hat{\eta}$ is a unit vector in the direction of the momentum. The boost matrix takes a particle at rest to a particle of momentum $\vec{p} = m\hat{\eta} \sinh(\eta)$

$$\Lambda(\vec{\eta}) \cdot (m, \vec{0}) = (m \cosh(\eta), \hat{\eta} m \sinh(\eta)) \tag{C.0.3}$$

Now let's look at how the boost acts on Dirac spinors. This will allow us to then expand in powers of $1/M_N$. Recall that the Dirac equation for spinors is

$$\not{p} u(p) = m u(p) \tag{C.0.4}$$

And the spinors are normalized by

$$\bar{u}(p)u(p) = 2m\xi^\dagger\xi \tag{C.0.5}$$

Where ξ is a two-component Pauli spinor. We define a spinor at rest as $u_0 = u(p_0)$. Boosts act on Dirac spinors in the spinor representation

$$u(\vec{p}) = D(\vec{\eta})u_0 \tag{C.0.6}$$

It is not hard to check that the spinor Boost can be represented using a typical half-angle formula - analogous to the half-angle rotation formulae for spin 1/2.

$$\begin{aligned} D(\vec{\eta}) &= \exp\left(\frac{\vec{\eta}\cdot\vec{\alpha}}{2}\right) \\ &= \cosh(\eta/2) + \hat{\eta}\cdot\vec{\alpha}\sinh(\eta/2) \end{aligned} \tag{C.0.7}$$

Where $\vec{\alpha} = \gamma^0\vec{\gamma}$ are standard notation for Diracs original matrices. They are hermitian matrices which obey the following relation

$$\vec{\alpha}^\dagger = \vec{\alpha}, \quad \gamma^0\vec{\alpha}\gamma^0 = -\vec{\alpha} \tag{C.0.8}$$

The boosts themselves are hermitian - not unitary!

$$D(\vec{\eta})^\dagger = D(\vec{\eta}) \tag{C.0.9}$$

However, we can use this to show explicitly that boosts preserve the normalization.

$$\overline{D(\vec{\eta})} = \gamma^0 D(\vec{\eta})^\dagger\gamma^0 = D(\vec{\eta})^{-1} \tag{C.0.10}$$

We also have the following identity

$$\not{p} = mD(\vec{\eta})\gamma^0 D(\vec{\eta})^{-1} \tag{C.0.11}$$

This allows us to prove that $u(\vec{p})$ satisfies the Dirac equation

$$\not{p}u(\vec{p}) = mD(\vec{\eta})\gamma^0 D(\vec{\eta})^{-1}D(\vec{\eta})u_0 = mD(\vec{\eta})u_0 = mu(\vec{p}) \tag{C.0.12}$$

As desired.

Use the fact that $\eta = \text{arcsinh}(|\vec{p}|/m)$ and we can expand the half angle hyperbolic trig functions to order $\mathcal{O}(1/m^2)$.

$$\cosh(\eta/2) \approx 1 + \frac{|\vec{p}|^2}{8m^2} \quad \sinh(\eta/2) \approx \frac{|\vec{p}|}{2m} \tag{C.0.13}$$

Then we can expand out the boost to order $\mathcal{O}(1/m^2)$.

$$u(p) = D(\vec{p})u_0 = \left(1 + \frac{\vec{\alpha}\cdot\vec{p}}{2m} + \frac{|\vec{p}|^2}{8m^2}\right)u_0 \tag{C.0.14}$$

And we use the inverse for the $\bar{u}(p)$ term.

$$\bar{u}(p) = \bar{u}_0 D(\vec{p})^{-1} = \bar{u}_0 \left(1 - \frac{\vec{\alpha}\cdot\vec{p}}{2m} + \frac{|\vec{p}|^2}{8m^2}\right) \tag{C.0.15}$$

However, we need to be careful about the normalization. The relativistic normalization has an energy dependence which we need to account for. We can similarly expand out the normalization to order $\mathcal{O}(1/m^2)$.

$$\frac{1}{\sqrt{2E_p}} \approx \frac{1}{\sqrt{2m}}\left(1 - \frac{|\vec{p}|^2}{4m^2}\right) \tag{C.0.16}$$

Thus the overall low-velocity expansion goes like

$$\boxed{\frac{1}{\sqrt{2E_p}}u(\vec{p}) \approx \frac{1}{\sqrt{2m}}\left(1 + \frac{\vec{\alpha}\cdot\vec{p}}{2m} - \frac{|\vec{p}|^2}{8m^2}\right)u_0} \tag{C.0.17}$$

We can now immediately use this to derive the $\mathcal{O}(1/m)$ and $\mathcal{O}(1/m^2)$ expansions for the currents. Suppose we have some operator $\mathcal{O}$ made up of gamma matrices. Then we can expand this out in terms of spinors at rest u_0 as. To order $\mathcal{O}(1/m)$, we have

$$\begin{aligned}\frac{1}{\sqrt{2E_{p'}}\sqrt{2E_p}}\bar{u}(p')\mathcal{O}u(p) &= \frac{1}{2m}\bar{u}_0\left(1 - \frac{\vec{p}'\cdot\vec{\alpha}}{2m}\right)\mathcal{O}\left(1 + \frac{\vec{p}\cdot\vec{\alpha}}{2m}\right)u_0 \\ &= \frac{1}{2m}\bar{u}_0\left[\mathcal{O} + \mathcal{O}\frac{\vec{p}\cdot\vec{\alpha}}{2m} - \frac{\vec{p}'\cdot\vec{\alpha}}{2m}\mathcal{O}\right]u_0 \\ &= \frac{1}{2m}\bar{u}_0\left[\mathcal{O} + \frac{\bar{\mathbf{p}}}{2m}\cdot[\mathcal{O},\vec{\alpha}] - \frac{\mathbf{q}}{4m}\cdot\{\mathcal{O},\vec{\alpha}\}\right]u_0\end{aligned} \tag{C.0.18}$$

where $\bar{p} = \frac{1}{2}(p' + p), \quad q = p' - p$. The order $\mathcal{O}(1/m^2)$ expansion involves expanding the particle energy, which introduces model dependence from the nuclear interaction. Using the free nucleon energies, we get

$$\begin{aligned}\frac{1}{\sqrt{2E_{p'}}\sqrt{2E_p}}\bar{u}(p')\mathcal{O}u(p) = \frac{1}{2m}\bar{u}_0\left[\mathcal{O}\left(1 - \frac{|\mathbf{q}|^2}{16m^2} - \frac{|\bar{\mathbf{p}}|^2}{4m^2}\right) + \frac{\bar{\mathbf{p}}}{2m}\cdot[\mathcal{O},\vec{\alpha}] - \frac{\mathbf{q}}{4m}\cdot\{\mathcal{O},\vec{\alpha}\}\right]u_0 \\ + \bar{u}_0\left[\left(\frac{q^i q^j}{16m^2} - \frac{\overline{p}^i\overline{p}^j}{4m^2}\right)\alpha^i\mathcal{O}\alpha^j + \frac{\overline{p}^i q^j - \overline{p}^j q^i}{8m^2}\alpha^i\mathcal{O}\alpha^j\right]u_0\end{aligned} \tag{C.0.19}$$

Then all we need to do is use dirac matrix algebra to calculate the matrix elements of

$$\mathcal{O}, \quad [\mathcal{O},\vec{\alpha}], \quad \{\mathcal{O},\vec{\alpha}\}, \quad \alpha^i\mathcal{O}\alpha^j \tag{C.0.20}$$

between the spinors at rest u_0.

Many possible matrix elements vanish when we use the fact that $u_0 = \gamma^0 u_0$.

$$\bar{u}_0\gamma^i u_0 = \bar{u}_0\alpha^i u_0 = \bar{u}_0\gamma^5 u_0 = \bar{u}_0\gamma^0\gamma^5 u_0 = \bar{u}_0\sigma^{ij}\gamma^5 u_0 = 0 \tag{C.0.21}$$

The matrix elements of 1 and γ^0 give us a scalar operator.

$$\frac{1}{2m}\bar{u}_0 u_0 = \frac{1}{2m}\bar{u}_0\gamma^0 u_0 = \xi^\dagger\xi \tag{C.0.22}$$

The matrix elements of the spin operator σ^{ij} naturally give us a spin operator.

$$\frac{1}{2m}\bar{u}_0\sigma^{ij}u_0 = \epsilon^{ijk}\xi^\dagger\Sigma^k\xi \tag{C.0.23}$$

The matrix element of $\gamma^i\gamma^5$ gives us the Gamow-Teller operator.

$$\frac{1}{2m}\bar{u}_0\gamma^i\gamma^5 u_0 = \frac{1}{2m}\bar{u}_0\alpha^i\gamma^5 u_0 = \xi^\dagger\Sigma^i\xi \tag{C.0.24}$$

We now want to apply this to the vertex functions for the weak and electromagnetic interactions. With the relativistic normalization factor, the non-relativistic limit of the vertex function can be defined as

$$\frac{1}{\sqrt{2E_{p'}2E_p}}\bar{u}(p')\Gamma^\mu(p',p)u(p) = \xi^\dagger\Sigma^\mu(p',p)\xi \tag{C.0.25}$$

For the vector current, we get the standard formula to order $\mathcal{O}(1/m^2)$ which you can find in [Wal04] Chapter 8.3 for example. The time-like part gives the usual charge term, plus corrections of order $\mathbf{O}(1/M_N^2)$.

$$\begin{aligned}&\frac{1}{\sqrt{2E_{p'}}\sqrt{2E_p}}\bar{u}(p')\left[\gamma^0 F_1(q^2) + \frac{i\sigma^{0j}q_j}{2M_N}F_2(q^2)\right]u(p)\\ &\to \xi^\dagger\left[F_1 - \left(\frac{|\mathbf{q}|^2}{8M_N^2} - i\frac{(\bar{p}\times\Sigma)\cdot q}{4M_N^2}\right)(F_1+2F_2)\right]\xi\end{aligned} \tag{C.0.26}$$

Note the standard $\mathcal{O}(1/M_N^2)$ correction, which depends on the expansion of the energy denominator. The space-like part only contributes to $\mathcal{O}(1/M_N)$, and it doesn't require expanding out the energy denominators.

$$\begin{aligned}&\frac{1}{\sqrt{2E_{p'}}\sqrt{2E_p}}\bar{u}(p')\left[\gamma^i F_1(q^2) + \frac{i\sigma^{ij}q_j}{2M_N}F_2(q^2)\right]u(p)\\ &\to \xi^\dagger\left[\frac{\bar{p}}{M_N}F_1 - i\frac{q\times\Sigma}{2M_N}(F_1+F_2)\right]\xi\end{aligned} \tag{C.0.27}$$

The axial-vector term has a time-like part which depends on momentum.

$$\begin{aligned}\frac{1}{\sqrt{2E_{p'}}\sqrt{2E_p}}\bar{u}(p')\left[\gamma^0\gamma^5 F_A(q^2)+\frac{q^0\gamma^5}{M_N}F_P(q^2)\right]u(p)\\ \rightarrow \xi^\dagger\left[\frac{\bar{p}\cdot\Sigma}{M_N}F_A(q^2)\right]\xi\end{aligned} \tag{C.0.28}$$

The space-like part has the usual Gamow-Teller operator, plus a term which contributes at order $\mathcal{O}(1/M_N^2)$.

$$\begin{aligned}\frac{1}{\sqrt{2E_{p'}}\sqrt{2E_p}}\bar{u}(p')\left[\gamma^i\gamma^5 F_A(q^2)+\frac{q^i\gamma^5}{M_N}F_P(q^2)\right]u(p)\\ \rightarrow F_A\xi^\dagger\Sigma^i\xi\\ +\xi^\dagger\left[(\frac{(\overline{p}^i\overline{p}^j-\delta^{ij}|\overline{p}|^2)}{2M_N^2}\Sigma^j+i\frac{\overline{p}\times q}{4M_N^2})F_A+(-\frac{q^iq^j}{8M_N^2}\Sigma^j)(F_A+4F_P)\right]\xi\end{aligned} \tag{C.0.29}$$

Appendix D

Separating Center of Mass Currents and Multipole Decomposition

In the non-relativistic setting, we can separate out the center of mass energy using relative Jacobi coordinates. The center of mass part of the Hamiltonian is given by

$$H = \frac{P_{\rm cm}^2}{2M_T} + H_r \tag{D.0.1}$$

We call the remaining Hamiltonian H_r the relative Hamiltonian, indicated by the subscript r. The center of mass momentum $P_{\rm cm}$ is the generator of translations of the center of mass. It is simply equal to the sum of the individual particle momenta.

$$P_{\rm cm} = \sum_a p_a \tag{D.0.2}$$

Similarly, the total mass is the sum of the individual masses. Ignoring the mass differences between the nucleons and the binding energy, we can simply write $M_T = AM_N$.

We would now like to separate out the center of mass pieces of the one-body current operators. In the two-body system, we define a relative coordinate and a center of mass coordinates $\{r, X\}$.

$$\begin{aligned} r &= x_1 - x_2 \\ X &= \frac{1}{2}(x_1 + x_2) \end{aligned} \tag{D.0.3}$$

Similarly for the momenta

$$\begin{aligned} p_r &= \frac{1}{2}(p_1 - p_2) \\ P_{\rm cm} &= p_1 + p_2 \end{aligned} \tag{D.0.4}$$

We can use this to separate out the parts which act on the center of mass, and treat them separately. Then the result is a matrix element only in the relative coordinates. For example,

take the density operator.

$$\begin{aligned}\sum_a e^{iqx_a} &= e^{iqx_1} + e^{iqx_2} \\ &= e^{iqX}\left(e^{iqr/2} + e^{-iqr/2}\right)\end{aligned} \tag{D.0.5}$$

Each operator that comes with a momentum transfer has a piece which transfers momentum to the center of mass e^{iqX}. This can be evaluated separately with the center of mass in momentum eigenstates.

$$\langle P_f|e^{iqX}|P_i\rangle = (2\pi)^3\delta^3(P_f - q - P_i) \tag{D.0.6}$$

The standard convective current includes momentum operators, which gives us a contribution from the center of mass momentum. This can be evaluated by plugging in the p_1 and p_2.

$$\begin{aligned}\sum_i j_i(q) &= \frac{1}{2}\{p_1, e^{iqx_1}\} + \frac{1}{2}\{p_2, e^{iqx_2}\} \\ &= \frac{1}{2}\{p_r + \frac{1}{2}P_{\rm cm}, e^{iq(r/2+X)}\} + \frac{1}{2}\{-p_r + \frac{1}{2}P_{\rm cm}, e^{iq(-r/2+X)}\} \\ &= \frac{1}{2}\{p_r, e^{iqr/2} - e^{-iqr/2}\}e^{iqX} + \frac{1}{4}\{P_{\rm cm}, e^{iqX}\}(e^{iqr/2} + e^{-iqr/2})\end{aligned} \tag{D.0.7}$$

Then again the center of mass piece can be evaluated using center of mass momentum eigenstates.

$$\begin{aligned}\langle P_f|\frac{1}{2}\{P_{\rm cm}, e^{iqX}\}|P_i\rangle &= \frac{1}{2}(P_i + P_f)\langle P_f|e^{iqX}|P_i\rangle \\ &= \frac{1}{2}(P_i + P_f)(2\pi)^3\delta^3(P_f - q - P_i)\end{aligned} \tag{D.0.8}$$

We define the quantity in front of the delta function to be

$$\overline{P} = \frac{1}{2}(P_i + P_f) \tag{D.0.9}$$

D.1 Separating the Center of Mass

In general, we can consider a system of A nucleons. We can always separate out a center of mass piece from the one-body current operators using Jacobi coordinates. Consider a one-body, hermitian current operator.

$$J^\mu(\vec{x}) = \sum_a \frac{1}{2}\left(\mathcal{O}_a\delta(\vec{x} - \vec{x}_a) + \delta(\vec{x} - \vec{x}_a)\mathcal{O}_a^\dagger\right) \tag{D.1.1}$$

where $\mathcal{O}_a$ is a coefficient times one of the five following basic operators.

$$\mathcal{O}_a = \left\{1, \frac{p_a}{M}, \frac{-ip_a \times \sigma_a}{M}, \sigma_a, \frac{p_a \cdot \sigma_a}{M}\right\} \tag{D.1.2}$$

We can begin to separate out the center of mass by taking a fourier transform and wiring the current operator in momentum space.

$$\tilde{J}^{\mu}(\vec{q}) = \sum_{a} \frac{1}{2} \left(\mathcal{O}_a e^{i\vec{q}\cdot\vec{x}_a} + e^{i\vec{q}\cdot\vec{x}_a} \mathcal{O}_a^{\dagger} \right) \tag{D.1.3}$$

Now use the Jacobi coordinate transformation to isolate the center of mass and relative coordinates. It doesn't really matter exactly what form of the Jacobi coordinates we use. In any case, we can write the individual coordinates in terms of a center of mass coordinate plus a linear combination of the relative coordinates.

$$x_a = X + \Lambda_{ab} r_b \tag{D.1.4}$$

This gives

$$\tilde{J}^{\mu}(\vec{q}) = \sum_{a} \frac{1}{2} \left(\mathcal{O}_a e^{i\vec{q}\cdot\vec{X}} e^{i\Lambda_{ab}\vec{q}\cdot\vec{r}_a} + e^{i\vec{q}\cdot\vec{X}} e^{i\Lambda_{ab}\vec{q}\cdot\vec{r}_a} \mathcal{O}_a^{\dagger} \right) \tag{D.1.5}$$

We then sandwich this operator between center of mass and relative product states, and we get

$$\begin{aligned} \langle P_f \psi_{fr} | J^{\mu}(\vec{x}) | P_i \psi_{ir} \rangle = \langle \psi_{fr} | \sum_{a} \frac{1}{2} \left(\mathcal{O}'_a(\bar{P}) e^{i\Lambda_{ab}\vec{q}\cdot\vec{r}_a} + e^{i\Lambda_{ab}\vec{q}\cdot\vec{r}_a} \tilde{\mathcal{O}}'_a(\bar{P}) \right) | \psi_{ir} \rangle \, e^{-i\vec{q}\cdot\vec{x}} \\ = \langle \psi_{fr} | \tilde{J}^{\mu}(\overline{P}, \vec{q}) | \psi_{ir} \rangle \, e^{-i\vec{q}\cdot\vec{x}} \end{aligned} \tag{D.1.6}$$

where

$$\bar{P} = \frac{P_i + P_f}{2}, \quad q = P_f - P_i \tag{D.1.7}$$

The remaining current operator which acts only on the relative wavefunction.

$$\tilde{J}^{\mu}(\overline{P}, \vec{q}) = \sum_{a} \frac{1}{2} \left(\mathcal{O}'_a(\bar{P}) e^{i\Lambda_{ab}\vec{q}\cdot\vec{r}_a} + e^{i\Lambda_{ab}\vec{q}\cdot\vec{r}_a} \tilde{\mathcal{O}}'_a(\bar{P}) \right) \tag{D.1.8}$$

The coefficients of the operator now depend on the center of mass, but it is treated as a number - not an operator.

Taking the inverse fourier transform gives us a relative current operator in relative coordinate space.

$$\tilde{J}^{\mu}(\overline{P}, \vec{q}) = \int d^3x \, e^{i\vec{q}\cdot\vec{x}} J^{\mu}(\overline{P}, \vec{x}) \tag{D.1.9}$$

where

$$J^{\mu}(\bar{P}, \vec{x}) = \sum_{a} \frac{1}{2} \left(\mathcal{O}'_a(\bar{P}) \delta(\vec{x} - \Lambda_{ab}\vec{r}_a) + \delta(\vec{x} - \Lambda_{ab}\vec{r}_a) \tilde{\mathcal{O}}'_a(\bar{P}) \right) \tag{D.1.10}$$

We will then use this to define multipole operators which act only on the relative space.

WARNING: this current operator no longer transforms in the usual way under translations of the center of mass. Translating the center of mass has no effect - which is what we

want. Note also that, because this form acts in the relative coordinates, it is constrained by particle exchange symmetry.

Charge Operator

Take the usual charge operator

$$\rho(\vec{x}) = \sum_a Q_a \delta(\vec{x} - \vec{x}_a) \tag{D.1.11}$$

When we take a matrix element between the center of mass states, we get no $\bar{P}$ dependence.

$$\langle P_f \psi_{fr} | \rho(\vec{x}) | P_i \psi_{ir} \rangle = \langle \psi_{fr} | \tilde{\rho}_r(\vec{q}) | \psi_{ir} \rangle \, e^{-i\vec{q}\cdot\vec{x}} \tag{D.1.12}$$

The result is simply

$$\tilde{\rho}_r(\vec{q}) = \sum_a Q_a e^{i\Lambda_{ab}\vec{q}\cdot\vec{r}_b} \tag{D.1.13}$$

Fourier transforming back into coordinate space, we can define a relative charge operator in relative coordinate space.

$$\rho_r(\vec{x}) = \sum_a Q_a \delta(\vec{x} - \Lambda_{ab}\vec{r}_b) \tag{D.1.14}$$

Convective Current

Take the standard convective current operator

$$\mathcal{O}_a = Q_a \frac{p_a}{M} \tag{D.1.15}$$

The current associated with this is

$$\vec{J}(\vec{x}) = \sum_a Q_a \frac{1}{2} \left(\frac{p_a}{M} \delta(\vec{x} - \vec{x}_a) + \delta(\vec{x} - \vec{x}_a) \frac{p_a}{M} \right) \tag{D.1.16}$$

Convert this to momentum space

$$\tilde{J}(\vec{q}) = \sum_a Q_a \frac{1}{2} \left(\frac{p_a}{M} e^{i\vec{q}\cdot\vec{X}} e^{i\Lambda_{ab}\vec{q}\cdot\vec{r}_b} + e^{i\vec{q}\cdot\vec{X}} e^{i\Lambda_{ab}\vec{q}\cdot\vec{r}_b} \frac{p_a}{M} \right) \tag{D.1.17}$$

Now use the relative momenta in the Jacobi basis

$$p_a = \frac{P_{\text{cm}}}{A} + \Lambda'_{ac} p_{rc} \tag{D.1.18}$$

Plugging this into the momentum space current, we have a center of mass piece and a relative piece.

$$\begin{aligned} \tilde{J}(\vec{q}) = &\sum_a Q_a \frac{1}{2} \left(\frac{P_{\text{cm}}}{AM} e^{i\vec{q}\cdot\vec{X}} + e^{i\vec{q}\cdot\vec{X}} \frac{P_{\text{cm}}}{AM} \right) e^{i\Lambda_{ab}\vec{q}\cdot\vec{r}_b} \\ + &\sum_a Q_a \frac{1}{2} \left(\Lambda'_{ac} \frac{p_{rc}}{M} e^{i\Lambda_{ab}\vec{q}\cdot\vec{r}_b} + e^{i\Lambda_{ab}\vec{q}\cdot\vec{r}_b} \Lambda'_{ac} \frac{p_{rc}}{M} \right) e^{i\vec{q}\cdot\vec{X}} \end{aligned} \tag{D.1.19}$$

Taking the matrix element between product CM-rel states gives us a $\overline{P}$-dependant piece.

$$\langle P_f \psi_{fr} | J(\vec{x}) | P_i \psi_{ir} \rangle = \langle \psi_{fr} | \left[\frac{\overline{P}}{M_T} \tilde{\rho}_r(\vec{q}) + \tilde{J}_r(\vec{q}) \right] | \psi_{ir} \rangle \, e^{-i\vec{q}\cdot\vec{x}} \tag{D.1.20}$$

where $M_T = AM$ is the total mass, or the target mass. The term proportional to the CM momentum is just the relative charge piece we found previously. The remaining relative current piece involves the relative momenta in Jacobi coordinates.

$$\tilde{J}_r(q) = \sum_a Q_a \frac{1}{2} \left(\Lambda'_{ac} \frac{p_{rc}}{M} e^{i\Lambda_{ab}\vec{q}\cdot\vec{r}_b} + e^{i\Lambda_{ab}\vec{q}\cdot\vec{r}_b} \Lambda'_{ac} \frac{p_{rc}}{M} \right) \tag{D.1.21}$$

Thus we come to the general result that the convective current has a center of mass piece which is proportional to the charge term. This is true for any size nucleus.

Magnetic Moment

The magnetic moment operator is

$$\mathcal{O}_a = -i\mu_a \frac{p_a \times \sigma_a}{M} \tag{D.1.22}$$

Because of the factor of i, we get a minus sign between the two terms

$$\vec{J}(\vec{x}) = \sum_a -i\mu_a \frac{1}{2} \left(\frac{p_a \times \sigma_a}{M} \delta(\vec{x} - \vec{x}_a) - \delta(\vec{x} - \vec{x}_a) \frac{p_a \times \sigma_a}{M} \right) \tag{D.1.23}$$

This becomes a the standard commutator - which is of course just a derivative of the delta function.

$$\vec{J}(\vec{x}) = \sum_a -i\mu_a [p_a, \delta(\vec{x} - \vec{x}_a)] \times \frac{\sigma_a}{2M} \tag{D.1.24}$$

Which we can write as a derivative with respect to x.

$$\vec{J}(\vec{x}) = \sum_a \mu_a \nabla \delta(\vec{x} - \vec{x}_a) \times \frac{\sigma_a}{2M} \tag{D.1.25}$$

Going to momentum space, The commutator pulls out a factor of $\vec{q}$

$$\tilde{J}(\vec{q}) = \sum_a -i\mu_a \frac{\vec{q} \times \sigma_a}{2M} e^{i\vec{q}\cdot\vec{x}_a} \tag{D.1.26}$$

Clearly we are not going to get any center of mass terms from this. Now plugging in Jacobi coordinates.

$$\tilde{J}(\vec{q}) = \sum_a -i\mu_a \frac{\vec{q} \times \sigma_a}{2M} e^{i\Lambda_{ab}\vec{q}\cdot\vec{r}_b} e^{i\vec{q}\cdot\vec{X}} \tag{D.1.27}$$

Or in position space

$$\vec{J}_r(\vec{x}) = \sum_a \mu_a \nabla \delta(\vec{x} - \Lambda_{ab}\vec{r}_b) \times \frac{\sigma_a}{2M} \tag{D.1.28}$$

Axial Current

The axial-vector current is the usual Gamow-Teller operator.

$$\vec{J}_5(\vec{x}) = \sum_a \vec{\sigma}_a \tau_a^+ \delta(\vec{x} - \vec{x}_a) \tag{D.1.29}$$

Go to momentum space

$$\tilde{J}_5(\vec{q}) = \sum_a \vec{\sigma}_a \tau_a^+ e^{i\vec{q}\cdot\vec{x}_a} \tag{D.1.30}$$

and we see that we don't get any center of mass piece. Going back to relative coordinate space, we have

$$\vec{J}_{5r}(\vec{x}) = \sum_a \vec{\sigma}_a \tau_a^+ \delta(\vec{x} - \Lambda_{ab}\vec{r}_b) \tag{D.1.31}$$

Axial Charge

The axial charge does involve the momentum. The relevent operator is

$$\rho_5(\vec{x}) = \sum_a \frac{1}{2}\left(\frac{\vec{p}_a \cdot \vec{\sigma}_a}{M}\tau_a^+ \delta(\vec{x} - \vec{x}_a) + \delta(\vec{x} - \vec{x}_a)\frac{\vec{p}_a \cdot \vec{\sigma}_a}{M}\tau_a^+\right) \tag{D.1.32}$$

Go to momentum space

$$\tilde{\rho}_5(\vec{q}) = \sum_a \frac{1}{2}\left(\frac{\vec{p}_a \cdot \vec{\sigma}_a}{M}\tau_a^+ e^{i\vec{q}\cdot\vec{x}_a} + e^{i\vec{q}\cdot\vec{x}_a}\frac{\vec{p}_a \cdot \vec{\sigma}_a}{M}\tau_a^+\right) \tag{D.1.33}$$

And plug in Jacobi coordinates

$$\begin{aligned}\tilde{\rho}_5(\vec{q}) = \sum_a \frac{1}{2}\left(\frac{P_{\rm cm}}{AM}e^{i\vec{q}\cdot X} + e^{i\vec{q}\cdot X}\frac{P_{\rm cm}}{AM}\right)\cdot\vec{\sigma}_a\tau_a^+ e^{i\vec{q}\cdot\Lambda_{ab}\vec{r}_b} \\ + \sum_a \frac{1}{2}\left(\Lambda'_{ac}\frac{\vec{p}_{rc}\cdot\vec{\sigma}_a}{M}\tau_a^+ e^{i\vec{q}\cdot\Lambda_{ab}\vec{r}_b} + e^{i\vec{q}\cdot\Lambda_{ab}\vec{r}_b}\Lambda'_{ac}\frac{\vec{p}_{rc}\cdot\vec{\sigma}_a}{M}\tau_a^+\right)e^{i\vec{q}\cdot X}\end{aligned} \tag{D.1.34}$$

Now take a matrix element with a product of center of mass and relative states and we see that we have a term which depends on the center of mass momentum $\overline{P}$ which is proportional to the axial-vector current.

$$\langle P_f\psi_{fr}|\rho_5(\vec{x})|P_i\psi_{ir}\rangle = \langle\psi_{fr}|\left[\frac{\overline{P}}{M_T}\cdot\tilde{J}_{5r}(\vec{q}) + \tilde{\rho}_{5r}(\vec{q})\right]|\psi_{ir}\rangle\, e^{-i\vec{q}\cdot\vec{x}} \tag{D.1.35}$$

where $M_T = AM$. Again, this is a general result which is independent of the size of the nucleus. The axial charge operator which acts on relative coordinates is given by

$$\rho_{5r}(\vec{x}) = \sum_a \frac{1}{2}\Lambda'_{ac}\left(\frac{\vec{p}_{rc}}{M}\delta(\vec{x} - \Lambda_{ab}\vec{r}_b) + \delta(\vec{x} - \Lambda_{ab}\vec{r}_b)\frac{\vec{p}_{rc}}{M}\right)\cdot\vec{\sigma}_a\tau_a^+ \tag{D.1.36}$$

D.2 Multipole Formalism

We will be intersted in taking matrix elements of the current operator in momentum space. This is of course related to the coordinate space version by the fourier transform.

$$\tilde{J}^{\mu}(\vec{q}) = \int d^3x\, e^{i\vec{q}\cdot\vec{x}} J^{\mu}(\vec{x}) \tag{D.2.1}$$

It is often helpful to break this down into angular momentum components. This is where the multipole formalism comes in. We expand out the exponential inside the fourier transform in terms of multipoles using the standard formula.

$$e^{i\vec{q}\cdot\vec{x}} = 4\pi \sum_{lm} i^l j_l(|\vec{q}||\vec{x}|) Y_{lm}(\hat{x}) Y_{lm}(\hat{q})^* \tag{D.2.2}$$

We use this to write the charge operator in terms of multipoles as follows

$$\tilde{J}^0(\vec{q}) = 4\pi \sum_{JM} i^J \left[\int d^3x\, J^0(\vec{x}) X_{JM}(q\vec{x}) \right] Y_{JM}(\hat{q})^* \tag{D.2.3}$$

where we have packaged together the spherical bessel function and the spherical harmonic into a new function.

$$X_{JM}(q\vec{x}) = j_J(qx) Y_{JM}(\hat{x}) \tag{D.2.4}$$

The fundamental property of this function is that it is a definite eigenstate of the laplacian operator.

$$\nabla^2 X_{JM}(q\vec{x}) = -q^2 X_{JM}(q\vec{x}) \tag{D.2.5}$$

Similarly, we can play the same game with the current. Using the definitions and expanding and rearranging the different terms, we can show that the current can be written in terms of a longitudinal (l), transverse electric (e), and transverse magnetic (m) multipoles.

$$\begin{aligned} \vec{\tilde{J}}(\vec{q}) = 4\pi \sum_{JM} \Bigg\{ & i^{J-1} \left[\int d^3x\, \vec{J}(\vec{x}) \cdot \mathbf{X}^{(l)}_{JM}(|\vec{q}|, \vec{x}) \right] \mathbf{Y}^*_{JM}(\hat{q}) \\ & i^J \left[\int d^3x\, \vec{J}(\vec{x}) \cdot \mathbf{X}^{(m)}_{JM}(|\vec{q}|, \vec{x}) \right] \mathbf{\Phi}^*_{JM}(\hat{q}) \\ & -i^J \left[\int d^3x\, \vec{J}(\vec{x}) \cdot \mathbf{X}^{(e)}_{JM}(|\vec{q}|, \vec{x}) \right] \mathbf{\Psi}^*_{JM}(\hat{q}) \Bigg\} \end{aligned} \tag{D.2.6}$$

The functions can be defined in terms of vector spherical harmonics. The standard basis for vector spherical harmonics is defined as

$$\mathbf{Y}_{JLM} = \sum_{q,m} C^{JM}_{Lm,1q} Y_{L,m}(\hat{r}) \vec{e}_q \tag{D.2.7}$$

where e_q is the spherical vector. The vector spherical harmonics $\mathbf{Y}$, $\mathbf{\Psi}$, and $\mathbf{\Phi}$ are just another choice of basis. They can be defined as

$$\begin{aligned} \mathbf{Y}_{JM}(\hat{r}) &= \hat{r}Y_{JM}(\hat{r}) \\ \mathbf{\Psi}_{JM}(\hat{r}) &= \frac{1}{\sqrt{J(J+1)}} r\nabla Y_{JM}(\hat{r}) \\ \mathbf{\Phi}_{JM}(\hat{r}) &= \frac{1}{\sqrt{J(J+1)}} \vec{L}Y_{JM}(\hat{r}) \end{aligned} \tag{D.2.8}$$

or, equivalently,

$$\begin{aligned} \mathbf{Y}_{JM} &= \sqrt{\frac{J}{2J+1}}\mathbf{Y}_{JJ-1M} - \sqrt{\frac{J+1}{2J+1}}\mathbf{Y}_{JJ+1M} \\ \mathbf{\Psi}_{JM} &= \sqrt{\frac{J+1}{2J+1}}\mathbf{Y}_{JJ-1M} + \sqrt{\frac{J}{2J+1}}\mathbf{Y}_{JJ+1M} \\ \mathbf{\Phi}_{JM} &= \mathbf{Y}_{JJM} \end{aligned} \tag{D.2.9}$$

Wherever possible, it is usually convenient to pick $\vec{q}$ to lie in the $\hat{z}$-direction. In that case, these simplify to the following forms.

$$\begin{aligned} \mathbf{Y}_{J,0}(\hat{z}) &= \sqrt{\frac{2J+1}{4\pi}}e_0 \\ \mathbf{\Psi}_{J,\pm1}(\hat{z}) &= \sqrt{\frac{2J+1}{4\pi}}\frac{1}{\sqrt{2}}e_{\pm1} \\ \mathbf{\Phi}_{J,\pm1}(\hat{z}) &= (\mp1)\sqrt{\frac{2J+1}{4\pi}}\frac{1}{\sqrt{2}}e_{\pm1} \end{aligned} \tag{D.2.10}$$

The multipoles $\mathbf{X}^{(\alpha)}_{JM}$ can be defined similarly to the scalar multipole X_{JM}.

$$\begin{aligned} \mathbf{X}^{(l)}_{JM}(q\vec{x}) &= \frac{1}{q}\nabla[j_J(qx)Y_{JM}(\hat{x})] \\ \mathbf{X}^{(m)}_{JM}(q\vec{x}) &= j_J(qx)\mathbf{Y}_{JJM}(\hat{x}) \\ \mathbf{X}^{(e)}_{JM}(q\vec{x}) &= \frac{1}{q}\nabla\times[j_J(qx)\mathbf{Y}_{JJM}(\hat{x})] \end{aligned} \tag{D.2.11}$$

alternatively, we can define $\mathbf{X}_{JLM}(q\vec{x}) = j_L(qx)\mathbf{Y}_{JLM}(\hat{x})$ and we have

$$\begin{aligned} \mathbf{X}^{(l)}_{JM}(q\vec{x}) &= \sqrt{\frac{J}{2J+1}}\mathbf{X}_{JJ-1M}(q\vec{x}) + \sqrt{\frac{J+1}{2J+1}}\mathbf{X}_{JJ+1M}(q\vec{x}) \\ \mathbf{X}^{(m)}_{JM}(q\vec{x}) &= \mathbf{X}_{JJM}(q\vec{x}) \\ \mathbf{X}^{(e)}_{JM}(q\vec{x}) &= i\sqrt{\frac{J+1}{2J+1}}\mathbf{X}_{JJ-1M}(q\vec{x}) - i\sqrt{\frac{J}{2J+1}}\mathbf{X}_{JJ+1M}(q\vec{x}) \end{aligned} \tag{D.2.12}$$

These satisfy a number of important relations we will use repeatedly.

$$\begin{aligned}\nabla^2 \mathbf{X}^{(\alpha)}_{JM}(q\vec{x}) &= -q^2 \mathbf{X}^{(\alpha)}_{JM}(q\vec{x}) \\ \nabla \times \mathbf{X}^{(m)}_{JM}(q\vec{x}) &= q\mathbf{X}^{(e)}_{JM}(q\vec{x}) \\ \nabla \times \mathbf{X}^{(e)}_{JM}(q\vec{x}) &= q\mathbf{X}^{(m)}_{JM}(q\vec{x}) \\ \nabla X_{JM}(q\vec{x}) &= q\mathbf{X}^{(l)}_{JM}(q\vec{x})\end{aligned} \tag{D.2.13}$$

This leads us to the definition of what I will call the "Walecka multipoles" as described in [Wal04] Chapter 45.

$$\begin{aligned}\mathcal{C}_{JM}(q) &= \int d^3x\, \rho(\vec{x}) X_{JM}(q\vec{x}) \\ \mathcal{L}_{JM}(q) &= \int d^3x\, \vec{J}(\vec{x}) \cdot \mathbf{X}^{(l)}_{JM}(q\vec{x}) \\ \mathcal{M}_{JM}(q) &= \int d^3x\, \vec{J}(\vec{x}) \cdot \mathbf{X}^{(m)}_{JM}(q\vec{x}) \\ \mathcal{E}_{JM}(q) &= \int d^3x\, \vec{J}(\vec{x}) \cdot \mathbf{X}^{(e)}_{JM}(q\vec{x})\end{aligned} \tag{D.2.14}$$

Notice that the center of mass is not separated out in these formulas. The use of these operators implicitly assumes that recoil is ignored and we do not have explicit conservation of momentum. Really, we want to be able to factor out a momentum conserving delta function from the center of mass piece. The Walecka formaism does not allow us to do that, and instead he deals with the center of mass using [FW66] Section 4.2.1. For example, the charge matrix element in the shell model gets corrected by a factor

$$\mathcal{C}_{JM}(q) = \exp\left[\frac{1}{A}\left(\frac{qb}{2}\right)^2\right]\Big(\mathcal{C}_{JM}(q)\Big)_{\text{shell model}} \tag{D.2.15}$$

where b is the simple harmonic oscillator length scale. This formula assumes that the shell model states are in the lowest simple harmonic oscillator state, $n = 0$, which is not usually enforced in a shell model with a core.

We would like to separate out the center of mass before doing the multipole decomposition. Instead of using these standard definitions, we define *relative charge and current multipoles* using the relative charge and current operators defined above.

$$\begin{aligned}C_{JM}(q) &= \int d^3x\, \rho_r(\vec{x}) X_{JM}(|\vec{q}|, \vec{x}) \\ L_{JM}(q) &= \int d^3x\, \vec{J}_r(\vec{x}) \cdot \mathbf{X}^{(l)}_{JM}(q\vec{x}) \\ M_{JM}(q) &= \int d^3x\, \vec{J}_r(\vec{x}) \cdot \mathbf{X}^{(m)}_{JM}(q\vec{x}) \\ E_{JM}(q) &= \int d^3x\, \vec{J}_r(\vec{x}) \cdot \mathbf{X}^{(e)}_{JM}(q\vec{x})\end{aligned} \tag{D.2.16}$$

Thankfully, we know exactly where the difference between these two formalism's lies. We know that the vector current gets a contribution from the center of mass using Equation D.1.20. In the lab frame where $P_i = 0$ and $P_f = \vec{q}$, we have $\overline{P} = \frac{1}{2}\vec{q}$. Using the properties of the multipoles, we see that this only gives a contribution to the longitudinal multipole. In particular, we have

$$\begin{aligned} \mathcal{C} &\to C \\ \mathcal{L} &\to L + i\frac{|\vec{q}|}{2M_T}C \\ \mathcal{M} &\to M \\ \mathcal{E} &\to E \end{aligned} \tag{D.2.17}$$

Similarly we get a center of mass contribution in the axial charge according to D.1.35. Using a bar to denote the axial-vector mulipoles, we have

$$\begin{aligned} \bar{\mathcal{C}} &\to \bar{C} - i\frac{|\vec{q}|}{2M_T}\bar{L} \\ \bar{\mathcal{L}} &\to \bar{L} \\ \bar{\mathcal{M}} &\to \bar{M} \\ \bar{\mathcal{M}} &\to \bar{E} \end{aligned} \tag{D.2.18}$$

Charge Operator

The standard charge operator is given by

$$\rho(\vec{x}) = Q_1\delta(\vec{x} - \vec{x}_1) + Q_2\delta(\vec{x} - \vec{x}_2) \tag{D.2.19}$$

Going through the argument laid out above, the relative charge operator is given by

$$\rho_r(\vec{x}) = Q_1\delta(\vec{x} - \vec{r}/2) + Q_1\delta(\vec{x} + \vec{r}/2) \tag{D.2.20}$$

We define a relative charge multipole as.

$$\begin{aligned} C_{JM}(q) &= \int d^3x\, X_{JM}(q\vec{x})\rho_r(\vec{x}) \\ &= \left[Q_1 + (-1)^J Q_2\right] X_{JM}(q\vec{r}/2) \end{aligned} \tag{D.2.21}$$

Convective Current

The convective current is

$$\begin{aligned} \vec{J}(\vec{x}) = Q_1 &\left(\frac{p_1}{2M}\delta(\vec{x} - \vec{x}_1) + \delta(\vec{x} - \vec{x}_1)\frac{p_1}{2M}\right) \\ +Q_2 &\left(\frac{p_2}{2M}\delta(\vec{x} - \vec{x}_2) + \delta(\vec{x} - \vec{x}_2)\frac{p_2}{2M}\right) \end{aligned} \tag{D.2.22}$$

As we stated previously, we get a center of mass piece which is proportional to the relative charge operator. The remaining relative current operator is

$$J_r(\vec{x}) = \frac{p_r}{2M}\left[Q_1\delta(\vec{x}-\vec{r}/2) - Q_2\delta(\vec{x}+\vec{r}/2)\right] + \left[Q_1\delta(\vec{x}-\vec{r}/2) - Q_2\delta(\vec{x}+\vec{r}/2)\right]\frac{p_r}{2M} \quad \text{(D.2.23)}$$

We can define a symmetrized relative current operator $\bar{p}_r$ and we have

$$J_r(\vec{x}) = \frac{\bar{p}_r}{M}\left[Q_1\delta(\vec{x}-\vec{r}/2) - Q_2\delta(\vec{x}+\vec{r}/2)\right] \quad \text{(D.2.24)}$$

We use this to define a longitudinal, magnetic, and electric current multipole operators.

$$\begin{aligned} L_{JM}(q) &= [Q_1 + (-1)^J Q_2]\frac{\bar{p}_r}{M}\cdot\mathbf{X}^{(l)}_{JM}(q\vec{r}/2) \\ M_{JM}(q) &= [Q_1 + (-1)^{J+1} Q_2]\frac{\bar{p}_r}{M}\cdot\mathbf{X}^{(m)}_{JM}(q\vec{r}/2) \\ E_{JM}(q) &= [Q_1 + (-1)^J Q_2]\frac{\bar{p}_r}{M}\cdot\mathbf{X}^{(e)}_{JM}(q\vec{r}/2) \end{aligned} \quad \text{(D.2.25)}$$

Magnetic Moment

The relative magnetic moment operator is

$$J_r(\vec{x}) = \mu_1\nabla\delta(\vec{x}-\vec{r}/2)\times\frac{\sigma_1}{2M} + \mu_2\nabla\delta(\vec{x}+\vec{r}/2)\times\frac{\sigma_2}{2M} \quad \text{(D.2.26)}$$

When we take the multipoles of the magnetic current, we can move the derivative to the multipole and we get the curl of the multipoles.

$$\begin{aligned} &\int d^3x\, \mathbf{X}^{(\alpha)}_{JM}(q\vec{x})\cdot J_r(\vec{x}) \\ &= \int d^3x \left(\mu_1\delta(\vec{x}-\vec{r}/2)\frac{\sigma_1}{2M} + \mu_2\delta(\vec{x}+\vec{r}/2)\frac{\sigma_2}{2M}\right)\cdot\nabla\times\mathbf{X}^{(\alpha)}_{JM}(q\vec{x}) \end{aligned} \quad \text{(D.2.27)}$$

The curl of the longitudinal multipole vanishes, and the curl of the electric and magnetic multipoles cause them to swap. The result is

$$\begin{aligned} M_{JM}(q) &= \frac{q}{2M}[\mu_1\sigma_1 + (-1)^{J+1}\mu_2\sigma_2]\cdot\mathbf{X}^{(e)}_{JM}(q\vec{r}/2) \\ E_{JM}(q) &= \frac{q}{2M}[\mu_1\sigma_1 + (-1)^{J}\mu_2\sigma_2]\cdot\mathbf{X}^{(m)}_{JM}(q\vec{r}/2) \end{aligned} \quad \text{(D.2.28)}$$

Axial Current

The axial vector current is

$$\vec{J}_{5r}(\vec{x}) = g_A\vec{\sigma}_1\tau_1^+\delta(\vec{x}-\vec{r}/2) + g_A\vec{\sigma}_2\tau_2^+\delta(\vec{x}+\vec{r}/2) \quad \text{(D.2.29)}$$

It is straightforward to take the multipoles of the axial current. We write bars over the multipole operators to indicate that they have the opposite parity.

$$\begin{aligned}\bar{L}_{JM} &= g_A(\vec{\sigma}_1\tau_1^+ + (-1)^{J+1}\vec{\sigma}_2\tau_2^+)\cdot\mathbf{X}^{(l)}_{JM}(q\vec{r}/2)\\ \bar{M}_{JM} &= g_A(\vec{\sigma}_1\tau_1^+ + (-1)^{J}\vec{\sigma}_2\tau_2^+)\cdot\mathbf{X}^{(m)}_{JM}(q\vec{r}/2)\\ \bar{E}_{JM} &= g_A(\vec{\sigma}_1\tau_1^+ + (-1)^{J+1}\vec{\sigma}_2\tau_2^+)\cdot\mathbf{X}^{(e)}_{JM}(q\vec{r}/2)\end{aligned} \tag{D.2.30}$$

Axial Charge

The axial charge operator is

$$\begin{aligned}\rho_{5r}(\vec{x}) = g_A\frac{1}{2}\left(\frac{\vec{p}_r}{M}\delta(\vec{x}-\vec{r}/2)+\delta(\vec{x}-\vec{r}/2)\frac{\vec{p}_r}{M}\right)\cdot\vec{\sigma}_1\tau_1^+\\ -g_A\frac{1}{2}\left(\frac{\vec{p}_r}{M}\delta(\vec{x}+\vec{r}/2)+\delta(\vec{x}+\vec{r}/2)\frac{\vec{p}_r}{M}\right)\cdot\vec{\sigma}_2\tau_2^+\end{aligned} \tag{D.2.31}$$

As was mentioned before, we get a term which involves the center of mass momentum which is proportional to the axial-vector current. The remaining relative axial charge multipole is

$$\bar{C}_{JM}(q) = g_A(\vec{\sigma}_1\tau_1^+ + (-1)^{J+1}\vec{\sigma}_2\tau_2^+)\cdot\frac{\bar{p}_r}{M}X_{JM}(q\vec{r}/2) \tag{D.2.32}$$

Isospin Form of the Charge and Current Multipoles

In order to better exhibit the exchange symmetry between the nucleons, we can write the charge and magnetic moment in terms of an isoscalar and isovector part.

$$Q_i = \frac{1}{2}(Q_s + Q_v\tau_{iz}) \tag{D.2.33}$$

where $Q_s = Q_v = 1$. Similarly for the magnetic moment.

$$\mu_i = \frac{1}{2}(\mu_s + \mu_v\tau_{iz}) \tag{D.2.34}$$

We define spin and isospin operators which have explicit exchange symmetry.

$$\begin{aligned}\Sigma_{(\pm)} &= \frac{1}{2}(\sigma_1 \pm \sigma_2)\\ \Xi_{(\pm)} &= \frac{1}{2}(\tau_1 \pm \tau_2)\end{aligned} \tag{D.2.35}$$

We can evaluate the isospin operators using the isospin of the initial and final state. For example, the operator $\Xi^z_{(+)}$ conserves isospin and gives the value M_T.

$$\Xi^z_{(+)}\left|TM_T\right\rangle = M_T\left|TM_T\right\rangle \tag{D.2.36}$$

On the other hand, the operator $\Xi^z_{(-)}$ changes the isospin. It is only non-zero for $M_T = 0$.

$$\Xi^z_{(-)} |T = 1, M_T = 0\rangle = |T = 0, M_T = 0\rangle , \quad \Xi^z_{(-)} |T = 0, M_T = 0\rangle = |T = 1, M_T = 0\rangle \tag{D.2.37}$$

Finally we can expand out products of spin and isospin as follows. The combination which is symmetric under particle exchange is

$$\frac{1}{2}(\tau_1\sigma_1 + \tau_2\sigma_2) = \Xi_{(+)}\Sigma_{(+)} + \Xi_{(-)}\Sigma_{(-)} \tag{D.2.38}$$

and the antisymmetric combination is

$$\frac{1}{2}(\tau_1\sigma_1 - \tau_2\sigma_2) = \Xi_{(+)}\Sigma_{(-)} + \Xi_{(-)}\Sigma_{(+)} \tag{D.2.39}$$

We can now rewrite all of the charge and current multipoles in terms of these operators with explicit exchange symmetry. Due to the presence of $(-1)^J$ terms, we get different operators depending on whether J is even or odd. We summarize all of the results here.

C_J, J even

$$C_{JM}(q) = \left[Q_s + Q_v\Xi^z_{(+)}\right] X_{JM}(q\vec{r}/2) \tag{D.2.40}$$

C_J, J odd

$$C_{JM}(q) = Q_v\Xi^z_{(-)} X_{JM}(q\vec{r}/2) \tag{D.2.41}$$

L_J, J even

$$L_{JM}(q) = \left[Q_s + Q_v\Xi^z_{(+)}\right] \frac{\bar{p}_r}{M} \cdot \mathbf{X}^{(l)}_{JM}(q\vec{r}/2) \tag{D.2.42}$$

L_J, J odd

$$L_{JM}(q) = Q_v\Xi^z_{(-)} \frac{\bar{p}_r}{M} \cdot \mathbf{X}^{(l)}_{JM}(q\vec{r}/2) \tag{D.2.43}$$

M_J, J even

$$\begin{aligned} M_{JM}(q) = Q_v\Xi^z_{(-)} \frac{\bar{p}_r}{M} \cdot \mathbf{X}^{(m)}_{JM}(q\vec{r}/2) \\ + \frac{q}{2M}[\mu_s\Sigma_{(-)} + \mu_v\Xi_{(+)}\Sigma_{(-)} + \mu_v\Xi_{(-)}\Sigma_{(+)}] \cdot \mathbf{X}^{(e)}_{JM}(q\vec{r}/2) \end{aligned} \tag{D.2.44}$$

M_J, J odd

$$\begin{aligned} M_{JM}(q) = \left[Q_s + Q_v\Xi^z_{(+)}\right] \frac{\bar{p}_r}{M} \cdot \mathbf{X}^{(m)}_{JM}(q\vec{r}/2) \\ + \frac{q}{2M}[\mu_s\Sigma_{(+)} + \mu_v\Xi^z_{(+)}\Sigma_{(+)} + \mu_v\Xi_{(-)}\Sigma_{(-)}] \cdot \mathbf{X}^{(e)}_{JM}(q\vec{r}/2) \end{aligned} \tag{D.2.45}$$

E_J, J even

$$\begin{aligned} E_{JM}(q) = \left[Q_s + Q_v\Xi^z_{(+)}\right] \frac{\bar{p}_r}{M} \cdot \mathbf{X}^{(e)}_{JM}(q\vec{r}/2) \\ + \frac{q}{2M}[\mu_s\Sigma_{(+)} + \mu_v\Xi^z_{(+)}\Sigma_{(+)} + \mu_v\Xi_{(-)}\Sigma_{(-)}] \cdot \mathbf{X}^{(m)}_{JM}(q\vec{r}/2) \end{aligned} \tag{D.2.46}$$

E_J, J odd

$$\begin{aligned} E_{JM}(q) &= Q_v \Xi_{(-)} \frac{\bar{p}_r}{M} \cdot \mathbf{X}^{(e)}_{JM}(q\vec{r}/2) \\ &+ \frac{q}{2M}[\mu_s \Sigma_{(-)} + \mu_v \Xi_{(+)}\Sigma_{(-)} + \mu_v \Xi_{(-)}\Sigma_{(+)}] \cdot \mathbf{X}^{(m)}_{JM}(q\vec{r}/2) \end{aligned} \tag{D.2.47}$$

Similarly, we can write the axial charge and current operators in this form. However, the axial terms are pure isovector.

$\bar{C}_J$, J even

$$\bar{C}_{JM}(q) = g_A \left(2\Xi^+_{(+)}\Sigma_{(-)} + 2\Xi^+_{(-)}\Sigma_{(+)}\right) \cdot \frac{\bar{p}_r}{M} X_{JM}(q\vec{r}/2) \tag{D.2.48}$$

$\bar{C}_J$, J odd

$$\bar{C}_{JM}(q) = g_A \left(2\Xi^+_{(+)}\Sigma_{(+)} + 2\Xi^+_{(-)}\Sigma_{(-)}\right) \cdot \frac{\bar{p}_r}{M} X_{JM}(q\vec{r}/2) \tag{D.2.49}$$

$\bar{L}_J$, J even

$$\bar{L}_{JM}(q) = g_A \left(2\Xi^+_{(+)}\Sigma_{(-)} + 2\Xi^+_{(-)}\Sigma_{(+)}\right) \cdot \mathbf{X}^{(l)}_{JM}(q\vec{r}/2) \tag{D.2.50}$$

$\bar{L}_J$, J odd

$$\bar{L}_{JM}(q) = g_A \left(2\Xi^+_{(+)}\Sigma_{(+)} + 2\Xi^+_{(-)}\Sigma_{(-)}\right) \cdot \mathbf{X}^{(l)}_{JM}(q\vec{r}/2) \tag{D.2.51}$$

$\bar{M}_J$, J even

$$\bar{M}_{JM}(q) = g_A \left(2\Xi^+_{(+)}\Sigma_{(+)} + 2\Xi^+_{(-)}\Sigma_{(-)}\right) \cdot \mathbf{X}^{(m)}_{JM}(q\vec{r}/2) \tag{D.2.52}$$

$\bar{M}_J$, J odd

$$\bar{M}_{JM}(q) = g_A \left(2\Xi^+_{(+)}\Sigma_{(-)} + 2\Xi^+_{(-)}\Sigma_{(+)}\right) \cdot \mathbf{X}^{(m)}_{JM}(q\vec{r}/2) \tag{D.2.53}$$

$\bar{E}_J$, J even

$$\bar{E}_{JM}(q) = g_A \left(2\Xi^+_{(+)}\Sigma_{(-)} + 2\Xi^+_{(-)}\Sigma_{(+)}\right) \cdot \mathbf{X}^{(e)}_{JM}(q\vec{r}/2) \tag{D.2.54}$$

$\bar{E}_J$, J odd

$$\bar{E}_{JM}(q) = g_A \left(2\Xi^+_{(+)}\Sigma_{(+)} + 2\Xi^+_{(-)}\Sigma_{(-)}\right) \cdot \mathbf{X}^{(e)}_{JM}(q\vec{r}/2) \tag{D.2.55}$$

Current Conservation

Consider the 1-body vector current to order $1/M$.

$$\vec{J}(\vec{x}) = \sum_a \frac{Q_a}{2M}\{\vec{p}_a, \delta(\vec{x} - \vec{x}_a)\} + \nabla\delta(\vec{x} - \vec{x}_a) \times \frac{\sigma_a}{2M} \tag{D.2.56}$$

The magnetic moment part does not contribute to the divergence of the current. The divergence of the current is then

$$\nabla \cdot \vec{J}(\vec{x}) = \sum_a \frac{Q_a}{2M} \left(p_a \cdot \nabla\delta(\vec{x} - \vec{x}_a) + \nabla\delta(\vec{x} - \vec{x}_a) \cdot p_a\right) \tag{D.2.57}$$

Swapping the derivative of x to a derivative of x_a, and writing the derivative in terms of a commutator with the momentum p_a, we have

$$\nabla \cdot \vec{J}(\vec{x}) = -i \sum_a \left[\frac{|\vec{p}_a|^2}{2M}, Q_a \delta(\vec{x} - \vec{x}_a) \right] = -i[T, \rho(\vec{x})] \tag{D.2.58}$$

This is, of course, a standard result.

A fundamental fact about Jacobi coordinates is that the non-relativistic kinetic energy is separable. We know we can write the kinetic energy as a sum of a center of mass part and a relative part.

$$\begin{aligned} T &= \frac{P_{\text{cm}}^2}{2M_T} + \sum_{i=1}^{A-1} \frac{p_{ri}^2}{2M_{ri}} \\ &= \frac{P_{\text{cm}}^2}{2M_T} + T_r \end{aligned} \tag{D.2.59}$$

On the other hand, we know from Equation D.1.20 that the vector current comes with a center of mass contribution. Taking the matrix element between product states of a center of mass momentum eigenstate and a relative wavefunction, we find

$$\langle P_f \psi_{fr} | \nabla \cdot J(\vec{x}) | P_i \psi_{ir} \rangle = -i \langle \psi_{fr} | \left[\frac{\vec{q} \cdot \overline{P}}{M_T} \tilde{\rho}_r(\vec{q}) + \vec{q} \cdot \tilde{J}_r(\vec{q}) \right] | \psi_{ir} \rangle \, e^{-i\vec{q}\cdot\vec{x}} \tag{D.2.60}$$

Here $q = P_f - P_i$ and $\overline{P} = \frac{1}{2}(P_i + P_f)$. Therefore we have the following identity.

$$\frac{q \cdot \overline{P}}{M_T} = \frac{P_f^2}{2M_T} - \frac{P_i^2}{2M_T} \tag{D.2.61}$$

This is the commutator of the center of mass kinetic energy operator with the charge operator. Comparing these two equations, we find a current conservation relation for the relative current operator.

$$\vec{q} \cdot \tilde{J}_r(\vec{q}) = [T_r, \tilde{\rho}_r(\vec{q})] \tag{D.2.62}$$

Transforming back to relative coordinate space, we can write this as

$$\nabla \cdot J_r(\vec{x}) = -i[T_r, \rho_r(\vec{x})] \tag{D.2.63}$$

This also gives us a relation for the multipoles if we use the identity for the longitudinal multipole.

$$\mathbf{X}_{JM}^{(l)}(q\vec{x}) = \frac{1}{q} \nabla X_{JM}(q\vec{x}) \tag{D.2.64}$$

Doing integration by parts, we have

$$\begin{aligned} L_{JM}(q) &= \int d^3x\, \mathbf{X}^{(l)}_{JM}(q\vec{x}) \cdot \vec{J}_r(\vec{x}) \\ &= -\frac{1}{q}\int d^3x\, X_{JM}(q\vec{x}) \nabla \cdot \vec{J}_r(\vec{x}) \\ &= i\frac{1}{q}\int d^3x\, X_{JM}(q\vec{x})[T_r, \rho_r(\vec{x})] \\ &= i\frac{1}{q}[T_r, C_{JM}(q)] \end{aligned} \tag{D.2.65}$$

Clearly this is not quite right. In order to have proper current conservation, we want the divergence of the current to equal the commutator of the full Hamiltonian with the charge. Suppose that the Hamiltonian is of the form kinetic plus potential energy.

$$H_r = T_r + V(r) \tag{D.2.66}$$

If the potential energy commutes with the charge operator, then we have proper current conservation.

$$\nabla \cdot J_r(\vec{x}) = -i[H_r, \rho_r(\vec{x})] \qquad (\text{if } [V, \rho] = 0) \tag{D.2.67}$$

However, this will not be the case for the Av18 potential. In particular, the charge operator has terms which depend on isospin. These do not commute with the Av18 Hamiltonian, and they generate two-body currents. Schematically, we can write

$$\nabla \cdot J_r^{\text{one-body}}(\vec{x}) + \nabla \cdot J_r^{\text{two-body}}(\vec{x}) = -i[H_r, \rho_r(\vec{x})] \tag{D.2.68}$$

In this thesis, we do not include the two-body terms explicitly. However, we can use this relation to reduce their impact using Seigert's theorem.

Appendix E

Current Operator Reduced Matrix Elements

In the previous section, we defined the multipole operators for the one-body currents. These operators have definite angular momentum, and we can express the matrix elements in terms of the *reduced matrix elements*. We can then express all the various matrix elements with different J_z using Clebsh-Gordon coefficients.

We define reduced matrix elements in accordance with Edmonds convention [Edm57]

$$\begin{aligned}\langle J'M'|T_{kq}|JM\rangle &= \frac{(-1)^{k-J+J'}}{\sqrt{2J'+1}} C^{J'M'}_{kq,JM} \langle J'||T_k||J\rangle \\ &= \frac{(-1)^{2k}}{\sqrt{2J'+1}} C^{J'M'}_{JM,kq} \langle J'||T_k||J\rangle\end{aligned} \tag{E.0.1}$$

Where we make use of properties of Clebsh Gordon coefficients

$$C^{JM}_{J_1M_1,J_2M_2} = (-1)^{J_1+J_2-J} C^{JM}_{J_2M_2,J_1M_1} \tag{E.0.2}$$

For scalar operators, the difference is just a factor of $\sqrt{2J+1}$

$$\langle J||T_0||J\rangle = \sqrt{2J+1}\,\langle JM|T_{00}|JM\rangle \tag{E.0.3}$$

E.1 Coupled Reduced Matrix Elements

The current operators involve a coupled product of an orbital part and a spin part. Coupled angular momentum operators are defined using Clebsh Gordon coefficients

$$[A_{k_1} \otimes B_{k_2}]_{KQ} = \sum_{q_1,q_2} C^{KQ}_{k_1q_1,k_2q_2} A_{k_1q_1} B_{k_2q_2} \tag{E.1.1}$$

The scalar product is a special case of this. The dot product generalizes the scalar product of vectors.

$$A_k \cdot B_k = \sum_q (-1)^q A_{kq} B_{k-q} = (-1)^k \sqrt{2k+1} [A_k \otimes B_k]_{0,0} \tag{E.1.2}$$

In order to calculate reduced matrix elements of coupled operators, we use the recoupling symbol. This is the highly symmetric six-J-symbol

$$\left\{ \begin{array}{ccc} j_1 & j_2 & j_{12} \\ j_3 & J & j_{23} \end{array} \right\} = \frac{(-1)^{j_1+j_2+j_3+J}}{\sqrt{(2j_{12}+1)(2j_{23}+1)}} \langle (j_1 j_2) j_{12}, j_3, J | j_1, (j_2 j_3) j_{23}, J \rangle \tag{E.1.3}$$

Reduced matrix elements of coupled operators are given in Edmonds

$$\langle j' || [T_{k_1} \otimes T_{k_2}]_K || j \rangle = \sqrt{2K+1}(-1)^{K+j+j'} \sum_{\gamma, j''} \left\{ \begin{array}{ccc} k_1 & k_2 & K \\ j & j' & j'' \end{array} \right\} \langle j' || T_{k_1} || j'' \rangle \langle j'' || T_{k_2} || j \rangle \tag{E.1.4}$$

A special case is the dot product

$$\langle j || T_k \cdot U_k || j \rangle = \sum_{\gamma, j''} \frac{(-1)^{j-j''}}{\sqrt{2j+1}} \langle j' || T_k || j'' \rangle \langle j'' || U_k || j \rangle \tag{E.1.5}$$

When we have coupled operators acting on different angular momenta

$$\begin{aligned} \langle (j_1' j_2') j' || [T_{k_1} \otimes U_{k_2}]_K || (j_1 j_2) j \rangle = \sqrt{(2K+1)(2j'+1)(2j+1)} \left\{ \begin{array}{ccc} j_1' & j_1 & k_1 \\ j_2' & j_2 & k_2 \\ j' & j & K \end{array} \right\} \\ \langle j_1' || T_{k_1} || j_1 \rangle \langle j_2' || U_{k_2} || j_2 \rangle \end{aligned} \tag{E.1.6}$$

A special case is the dot product

$$\begin{aligned} \langle (j_1' j_2') j' || T_k \cdot U_k || (j_1 j_2) j \rangle &= (-1)^k \sqrt{2k+1} \langle (j_1' j_2') j' || [T_k \otimes U_k]_0 || (j_1 j_2) j \rangle \\ &= \sqrt{2j+1}(-1)^{2k+j_1+j_2'+j} \left\{ \begin{array}{ccc} j_1' & j_1 & k \\ j_2 & j_2' & j \end{array} \right\} \langle j_1' || T_k || j_1 \rangle \langle j_2' || U_k || j_2 \rangle \end{aligned} \tag{E.1.7}$$

Or when one of the operators is the identity

$$\langle (j_1' j_2) j' || [T_{k_1} \otimes 1]_{k_1} || (j_1 j_2) j \rangle = (-1)^{j_1'+j_2+j+k} \sqrt{(2j'+1)(2j+1)} \left\{ \begin{array}{ccc} j_1 & j_1' & k_1 \\ j' & j & j_2 \end{array} \right\} \langle j_1' || T_{k_1} || j_1 \rangle \tag{E.1.8}$$

Or the other way

$$\langle (j_1 j_2') j' || [1 \otimes T_{k_2}]_{k_2} || (j_1 j_2) j \rangle = (-1)^{j_1+j_2+j'+k} \sqrt{(2j'+1)(2j+1)} \left\{ \begin{array}{ccc} j_2 & j_2' & k_2 \\ j' & j & j_1 \end{array} \right\} \langle j_2' || T_{k_2} || j_2 \rangle \tag{E.1.9}$$

For example, consider two spin 1/2 particles coupled together to form a state with spin S which could either be 0 or 1. This case will come up repeatedly throughout the thesis.

We can use the formula above to calculate the reduced matrix element of the spin operator which acts only on the first spin.

$$\langle S'||\sigma_1||S\rangle = (-1)^S\sqrt{(2S'+1)(2S+1)}\left\{\begin{array}{ccc} 1/2 & 1/2 & 1 \\ S' & S & 1/2 \end{array}\right\}\sqrt{6} \tag{E.1.10}$$

Likewise, we can calculate the reduced matrix element for the operator which acts only on the second spin.

$$\langle S'||\sigma_2||S\rangle = (-1)^{S'}\sqrt{(2S'+1)(2S+1)}\left\{\begin{array}{ccc} 1/2 & 1/2 & 1 \\ S' & S & 1/2 \end{array}\right\}\sqrt{6} \tag{E.1.11}$$

In the thesis, we combine these into the symmetric combinations $\Sigma_{(\pm)} \equiv \frac{1}{2}(\sigma_1 \pm \sigma_2)$. Taking the plus sign, we have

$$\langle S'||(\sigma_1+\sigma_2)||S\rangle = [(-1)^S + (-1)^{S'}]\sqrt{(2S'+1)(2S+1)}\left\{\begin{array}{ccc} 1/2 & 1/2 & 1 \\ S' & S & 1/2 \end{array}\right\}\sqrt{6} \tag{E.1.12}$$

This is non-zero only when $S = S'$.

$$\begin{aligned} \langle 0||(\sigma_1+\sigma_2)||0\rangle &= 0 \\ \langle 1||(\sigma_1+\sigma_2)||1\rangle &= 2\sqrt{6} \end{aligned} \tag{E.1.13}$$

Conversely, taking the minus sign results in a spin flip.

$$\langle S'||(\sigma_1-\sigma_2)||S\rangle = [(-1)^S - (-1)^{S'}]\sqrt{(2S'+1)(2S+1)}\left\{\begin{array}{ccc} 1/2 & 1/2 & 1 \\ S' & S & 1/2 \end{array}\right\}\sqrt{6} \tag{E.1.14}$$

This is only non-zero when $S \neq S'$.

$$\langle 1||(\sigma_1-\sigma_2)||0\rangle = -\langle 0||(\sigma_1-\sigma_2)||1\rangle = 2\sqrt{3} \tag{E.1.15}$$

Charge Operator

The orbital part of the charge operator is simply given by the charge multipole.

$$X_{LM}(q\vec{r}/2) = j_L(qr/2)Y_{LM}(\hat{r}) \tag{E.1.16}$$

First, lets calculate the reduced matrix element of this operator between states with orbital angular momentum l_f, l_i

$$\langle \psi_{fr} m_f|X_{LM}(q\vec{r}/2)|\psi_{ir}m_i\rangle = \int r^2 dr\, R_{fr}(r)^* j_L(|\vec{q}|r/2)R_{ir}(r)\int d\Omega\, Y_{l_f m_f}Y^*_{LM}Y_{l_i m_i} \tag{E.1.17}$$

The radial integral becomes the integral over the radial wavefunctions $u = rR$.

$$\int_0^\infty dr\, u_{fr}(r)^* j_L(|\vec{q}|r/2)u_{ir}(r) \tag{E.1.18}$$

The angular part of the integral can be cast in terms of the reduced matrix element of the spherical harmonic.

$$\int d\Omega\, Y^*_{l_f m_f} Y_{LM} Y_{l_i m_i} = \frac{1}{\sqrt{2l_f+1}} C^{l_f m_f}_{l_i m_i, LM} \langle l_f || Y_L || l_i \rangle \tag{E.1.19}$$

We will need to know the reduced matrix element of the spherical harmonics. The result is a standard formula.

$$\langle l' || Y_L || l \rangle = (-1)^{l'} \sqrt{\frac{(2l+1)(2L+1)(2l'+1)}{4\pi}} \begin{pmatrix} l' & L & l \\ 0 & 0 & 0 \end{pmatrix} \tag{E.1.20}$$

The reduced matrix element of the charge operator is the reduced matrix element of the spherical harmonic, times the radial integral with the spherical Bessel function

$$\langle \psi_{fr} l_f || X_{LM}(q\vec{r}/2) || \psi_{ir} l_i \rangle = \langle l_f || Y_L || l_i \rangle \int_0^\infty dr\, u_{fr}(r)^* j_L(qr/2) u_{ir}(r) \tag{E.1.21}$$

Convective Current

The convective current is the most complicated reduced matrix element we need to calculated. The orbital part is proportional to the symmetrized combination of p_r and the multipole function.

$$\overline{p}_r \cdot \mathbf{X}_{JLM}(q\vec{r}/2) \tag{E.1.22}$$

Since p_r does not commute with r, the notation $\overline{p}_r$ tells us we form the symmetric combination.

$$\overline{p}_r \cdot \mathbf{X}_{JLM}(q\vec{r}/2) = \frac{1}{2} C^{JM}_{LM'1q} \left(\vec{p}_r \cdot e_q\, X_{LM'}(q\vec{r}/2) + X_{LM'}(q\vec{r}/2) \vec{p}_r \cdot e_q \right) \tag{E.1.23}$$

Here the implicit sum over M', q is implied.

We now let the momentum hit the initial wavefunction, which gives us a derivative. We use the following gradient formula in terms of vector spherical harmonics.

$$\nabla\, f(r) Y_{JM}(\hat{r}) = \frac{df}{dr} \mathbf{Y}_{JM} + \sqrt{J(J+1)} \frac{f}{r} \mathbf{\Psi}_{JM} \tag{E.1.24}$$

Plug in and simplify.

$$\begin{aligned} \vec{p}_r \cdot e_q (R_{ir}(r) Y_{l_i m_i}) &= -i \nabla \cdot e_q (R_{ir}(r) Y_{l_i m_i}) \\ &= -i e_q \cdot \left(\frac{dR_{ir}}{dr} \mathbf{Y}_{l_i m_i} + \frac{\sqrt{l_i(l_i+1)}}{r} R_{ir} \mathbf{\Psi}_{l_i m_i} \right) \\ = -i \sqrt{\frac{l_i}{2l_i+1}} \left(\frac{dR_{ir}}{dr} + \frac{l_i+1}{r} R_{ir} \right) (-1)^q C^{l_i m_i}_{l_i - 1 m'_i, 1-q} Y_{l_i - 1 m'_i} \\ + i \sqrt{\frac{l_i+1}{2l_i+1}} \left(\frac{dR_{ir}}{dr} - \frac{l_i}{r} R_{ir} \right) (-1)^q C^{l_i m_i}_{l_i + 1 m'_i, 1-q} Y_{l_i + 1 m'_i} \end{aligned} \tag{E.1.25}$$

We now do another simplification to eliminate the phase $(-1)^q$ using a standard symmetry of the Clebsh-Gordon coefficients.

$$C^{j_3 m_3}_{j_1 m_1, j_2 m_2} = (-1)^{m_2}(-1)^{-j_3+j_1}\sqrt{\frac{2j_3+1}{2j_1+1}}C^{j_1 m_1}_{j_3 m_3, j_2 -m_2} \tag{E.1.26}$$

The result is

$$\begin{aligned}\vec{p}_r \cdot e_q(R_{ir}(r)Y_{l_i m_i}) = i\sqrt{\frac{l_i}{2l_i-1}}C^{l_i-1 m_i'}_{l_i m_i, 1q}\left(\frac{dR_{ir}}{dr}+\frac{l_i+1}{r}R_{ir}\right)Y_{l_i-1 m_i'} \\ -i\sqrt{\frac{l_i+1}{2l_i+3}}C^{l_i+1 m_i'}_{l_i m_i, 1q}\left(\frac{dR_{ir}}{dr}-\frac{l_i}{r}R_{ir}\right)Y_{l_i+1 m_i'}\end{aligned} \tag{E.1.27}$$

For the final state, p_r acts to the left. The result is the complex conjugate of what we got for the initial state, except we have to take the complex conjugate of $e_q^* = (-1)^q e_{-q}$.

$$\begin{aligned}\Big((-1)^q\vec{p}_r \cdot e_{-q}(R_{fr}(r)Y_{l_f m_f})\Big)^* = i\sqrt{\frac{l_f}{2l_f+1}}C^{l_f m_f}_{l_f-1 m_f', 1q}\left(\frac{dR_{fr}}{dr}+\frac{l_f+1}{r}R_{fr}\right)Y^*_{l_f-1 m_f'} \\ -i\sqrt{\frac{l_f+1}{2l_f+1}}C^{l_f m_f}_{l_f+1 m_f', 1q}\left(\frac{dR_{fr}}{dr}-\frac{l_f}{r}R_{fr}\right)Y^*_{l_f+1 m_f'}\end{aligned} \tag{E.1.28}$$

Acting with $\vec{p}_r$ on the initial and final state wavefunctions gives us four terms

$$\begin{aligned}&\langle\psi_{fr} m_f|\overline{p}_r \cdot \mathbf{X}_{JLM}(q\vec{r}/2)|\psi_{ir} m_i\rangle \\ &= i\frac{1}{2}\sqrt{\frac{l_i}{2l_i-1}}C^{JM}_{LM'1q}C^{l_i-1 m_i'}_{l_i m_i, 1q}\int_0^\infty r^2 dr\, R_{fr} j_L(qr/2)\left(\frac{dR_{ir}}{dr}+\frac{l_i+1}{r}R_{ir}\right) \\ &\qquad\times\int d\Omega Y^*_{l_f m_f}Y_{LM'}Y_{l_i-1 m_i'} \\ &\quad -i\frac{1}{2}\sqrt{\frac{l_i+1}{2l_i+3}}C^{JM}_{LM'1q}C^{l_i+1 m_i'}_{l_i m_i, 1q}\int_0^\infty r^2 dr\, R_{fr} j_L(qr/2)\left(\frac{dR_{ir}}{dr}-\frac{l_i}{r}R_{ir}\right) \\ &\qquad\int d\Omega\, Y^*_{l_f m_f}Y_{LM'}Y_{l_i+1 m_i'} \\ &+i\frac{1}{2}\sqrt{\frac{l_f}{2l_f+1}}C^{JM}_{LM'1q}C^{l_f m_f}_{l_f-1 m_f', 1q}\int_0^\infty r^2 dr\left(\frac{dR_{fr}}{dr}+\frac{l_f+1}{r}R_{fr}\right)j_L(qr/2)R_{ir} \\ &\qquad\int d\Omega\, Y^*_{l_f-1 m_f'}Y_{LM'}Y_{l_i m_i} \\ &\quad -i\frac{1}{2}\sqrt{\frac{l_f+1}{2l_f+1}}C^{JM}_{LM'1q}C^{l_f m_f}_{l_f+1 m_f', 1q}\int_0^\infty r^2 dr\left(\frac{dR_{fr}}{dr}-\frac{l_f}{r}R_{fr}\right)j_L(qr/2)R_{ir} \\ &\qquad\int d\Omega\, Y^*_{l_f+1 m_f'}Y_{LM'}Y_{l_i m_i}\end{aligned} \tag{E.1.29}$$

Evaluate the integrals over spherical harmonics

$$\begin{aligned}
&\langle\psi_{fr}m_f|\overline{p}_r\cdot\mathbf{X}_{JLM}(q\vec{r}/2)|\psi_{ir}m_i\rangle \\
&= i\frac{1}{2}C^{JM}_{LM'1q}C^{l_im_i}_{l_im_i,1q}C^{l_fm_f}_{l_i-1m'_i,LM'}\int_0^\infty r^2dr\,R_{fr}j_L(qr/2)\left(\frac{dR_{ir}}{dr}+\frac{l_i+1}{r}R_{ir}\right) \\
&\qquad\times\sqrt{\frac{l_i}{(2l_f+1)(2l_i-1)}}\,\langle l_f||Y_L||l_i-1\rangle \\
&\quad -i\frac{1}{2}C^{JM}_{LM'1q}C^{l_im_i}_{l_im_i,1q}C^{l_fm_f}_{l_i+1m'_i,LM'}\int_0^\infty r^2dr\,R_{fr}j_L(qr/2)\left(\frac{dR_{ir}}{dr}-\frac{l_i}{r}R_{ir}\right) \\
&\qquad\times\sqrt{\frac{l_i+1}{(2l_f+1)(2l_i+3)}}\,\langle l_f||Y_L||l_i+1\rangle \\
&+i\frac{1}{2}C^{JM}_{LM'1q}C^{l_fm_f}_{l_f-1m'_f,1q}C^{l_f-1m'_f}_{l_im_i,LM'}\int_0^\infty r^2dr\left(\frac{dR_{fr}}{dr}+\frac{l_f+1}{r}R_{fr}\right)j_L(qr/2)R_{ir} \\
&\qquad\times\sqrt{\frac{l_f}{(2l_f+1)(2l_f-1)}}\,\langle l_f-1||Y_L||l_i\rangle \\
&\quad -i\frac{1}{2}C^{JM}_{LM'1q}C^{l_fm_f}_{l_f+1m'_f,1q}C^{l_f+1m'_f}_{l_im_i,LM'}\int_0^\infty r^2dr\left(\frac{dR_{fr}}{dr}-\frac{l_f}{r}R_{fr}\right)j_L(qr/2)R_{ir} \\
&\qquad\times\sqrt{\frac{l_f+1}{(2l_f+1)(2l_f+3)}}\,\langle l_f+1||Y_L||l_i\rangle
\end{aligned} \tag{E.1.30}$$

We get a major simplification by using the recoupling formulae in terms of the six-J-symbol.

$$C^{JM}_{1qLM'}C^{l_fm_f}_{l_i-1m'_i,LM'}C^{l_i-1m'_i}_{1ql_im_i}=\sqrt{(2J+1)(2l_i-1)}C^{l_fm_f}_{l_im_iJM}\left\{\begin{array}{ccc}1&L&J\\l_f&l_i&l_i-1\end{array}\right\} \tag{E.1.31}$$

The other sum we need is

$$C^{JM}_{LM'1q}C^{l_fm_f}_{l_f-1m'_f,1q}C^{l_f-1m'_f}_{LM',l_im_i}=\sqrt{(2J+1)(2l_f-1)}C^{l_fm_f}_{l_im_iJM}\left\{\begin{array}{ccc}L&1&J\\l_f&l_i&l_f-1\end{array}\right\} \tag{E.1.32}$$

Doing the clebsh gordon sums gives

$$\begin{aligned}
&\langle \psi_{fr} l_f || \overline{p}_r \cdot \mathbf{X}_{JL}(q\vec{r}/2) || \psi_{ir} l_i \rangle \\
&= i\frac{1}{2}(-1)^{J+L+1}\sqrt{l_i(2J+1)}\left\{ \begin{array}{ccc} 1 & L & J \\ l_f & l_i & l_i - 1 \end{array} \right\} \langle l_f || Y_L || l_i - 1 \rangle \\
&\quad \times \int_0^\infty r^2 dr\, R_{fr} j_L(qr/2) \left(\frac{dR_{ir}}{dr} + \frac{l_i + 1}{r} R_{ir} \right) \\
&-i\frac{1}{2}(-1)^{J+L+1}\sqrt{(l_i+1)(2J+1)}\left\{ \begin{array}{ccc} 1 & L & J \\ l_f & l_i & l_i + 1 \end{array} \right\} \langle l_f || Y_L || l_i + 1 \rangle \\
&\quad \times \int_0^\infty r^2 dr\, R_{fr} j_L(qr/2) \left(\frac{dR_{ir}}{dr} - \frac{l_i}{r} R_{ir} \right) \\
&+i\frac{1}{2}\sqrt{l_f(2J+1)}\left\{ \begin{array}{ccc} L & 1 & J \\ l_f & l_i & l_f - 1 \end{array} \right\} \langle l_f - 1 || Y_L || l_i \rangle \\
&\quad \times \int_0^\infty r^2 dr \left(\frac{dR_{fr}}{dr} + \frac{l_f + 1}{r} R_{fr} \right) j_L(qr/2) R_{ir} \\
&-i\frac{1}{2}\sqrt{(l_f+1)(2J+1)}\left\{ \begin{array}{ccc} L & 1 & J \\ l_f & l_i & l_f + 1 \end{array} \right\} \langle l_f + 1 || Y_L || l_i \rangle \\
&\quad \times \int_0^\infty r^2 dr \left(\frac{dR_{fr}}{dr} - \frac{l_f}{r} R_{fr} \right) j_L(qr/2) R_{ir}
\end{aligned} \tag{E.1.33}$$

We might also want to write this in terms of the spherical wave function $u = rR$. For simplicity, we define $u^{(\pm)}$ as the specific combination which shows up in the radial integrals.

$$\begin{aligned}
r\left(\frac{dR_l}{dr} + \frac{l+1}{r} R_l \right) &= \left(\frac{du_l}{dr} + \frac{l}{r} u_l \right) \equiv u_l^{(-)} \\
r\left(\frac{dR_l}{dr} - \frac{l}{r} R_l \right) &= \left(\frac{du_l}{dr} - \frac{l+1}{r} u_l \right) \equiv u_l^{(+)}
\end{aligned} \tag{E.1.34}$$

The final result is not too complicated.

$$\begin{aligned}
&\langle \psi_{fr} l_f || \overline{p}_r \cdot \mathbf{X}_{JL}(q\vec{r}/2) || \psi_{ir} l_i \rangle \\
&= i\frac{1}{2}(-1)^{J+L+1}\sqrt{l_i(2J+1)}\left\{ \begin{array}{ccc} 1 & L & J \\ l_f & l_i & l_i - 1 \end{array} \right\} \langle l_f || Y_L || l_i - 1 \rangle \int_0^\infty dr\, u_f j_L(qr/2) u_i^{(-)} \\
&-i\frac{1}{2}(-1)^{J+L+1}\sqrt{(l_i+1)(2J+1)}\left\{ \begin{array}{ccc} 1 & L & J \\ l_f & l_i & l_i + 1 \end{array} \right\} \langle l_f || Y_L || l_i + 1 \rangle \int_0^\infty dr\, u_f j_L(qr/2) u_i^{(+)} \\
&+i\frac{1}{2}\sqrt{l_f(2J+1)}\left\{ \begin{array}{ccc} L & 1 & J \\ l_f & l_i & l_f - 1 \end{array} \right\} \langle l_f - 1 || Y_L || l_i \rangle \int_0^\infty dr\, u_f^{(-)} j_L(qr/2) u_i \\
&-i\frac{1}{2}\sqrt{(l_f+1)(2J+1)}\left\{ \begin{array}{ccc} L & 1 & J \\ l_f & l_i & l_f + 1 \end{array} \right\} \langle l_f + 1 || Y_L || l_i \rangle \int_0^\infty dr\, u_f^{(+)} j_L(qr/2) u_i
\end{aligned} \tag{E.1.35}$$

Coupled Angular Momentum Reduced Matrix Elements

Now that we have the orbital and spin parts computed separately, it is simple to plug into the coupled angular momentum formulae. For the terms which do not act on the spin, we use the formula with the identity operator.

$$\langle (l's)j' || [T_L \otimes 1]_L || (ls)j \rangle = (-1)^{l'+s+j+L} \sqrt{(2j'+1)(2j+1)} \left\{ \begin{array}{ccc} l & l' & L \\ j' & j & s \end{array} \right\} \langle l' || T_L || l \rangle \quad \text{(E.1.36)}$$

This gives us the formula for the coupled reduced matrix element for the charge operator.

$$\langle \psi'(l's)j' || X_L || \psi(ls)j \rangle = (-1)^{l'+j+L+s} \sqrt{(2j+1)(2j'+1)} \left\{ \begin{array}{ccc} l & l' & L \\ j' & j & s \end{array} \right\} \langle \psi' l' || X_L || \psi l \rangle \quad \text{(E.1.37)}$$

It also gives us the coupled reduced matrix element of the convective current operator.

$$\begin{aligned} &\langle \psi'(l's)j' || [X_L \otimes \overline{p}]_J || \psi(ls)j \rangle = \\ &(-1)^{l'+j+J+s} \sqrt{(2j+1)(2j'+1)} \left\{ \begin{array}{ccc} l & l' & K \\ j' & j & s \end{array} \right\} \langle \psi' l' || [X_L \otimes \overline{p}]_J || \psi l \rangle \end{aligned} \quad \text{(E.1.38)}$$

For operators which do act on the spin, we get a nine-J-symbol.

$$\begin{aligned} \langle (l's')j' || [T_L \otimes U_S]_J || (ls)j \rangle = \sqrt{(2J+1)(2j'+1)(2j+1)} \left\{ \begin{array}{ccc} l' & l & L \\ s' & s & S \\ j' & j & J \end{array} \right\} \\ \langle l' || T_L || l \rangle \langle s' || U_S || s \rangle \end{aligned} \quad \text{(E.1.39)}$$

For the magnetic moment part of the current, we have

$$\begin{aligned} \langle \psi'(l's')j' || [X_L \otimes \Sigma]_J || \psi(ls)j \rangle = \sqrt{(2J+1)(2j'+1)(2j+1)} \left\{ \begin{array}{ccc} l' & l & L \\ s' & s & 1 \\ j' & j & J \end{array} \right\} \\ \langle \psi' l' || X_L || \psi l \rangle \langle s' || \Sigma || s \rangle \end{aligned} \quad \text{(E.1.40)}$$

The axial charge operator has a slightly different form. We need to do some minor recoupling in order to couple the orbital part first, and then couple the result to the spin.

$$\begin{aligned} (\Sigma \cdot \overline{p}) X_{JM}(q\vec{r}/2) &= (-1)^q \Sigma_{-q} \overline{p}_q X_{JM}(q\vec{r}/2) \\ &= \sum_L C^{LM'}_{JM1q} (-1)^q \Sigma_{-q} [X_J \otimes \overline{p}]_{LM'} \\ &= \sum_{LJ''} C^{J''M''}_{LM'1-q} C^{LM'}_{JM1q} (-1)^q [[X_J \otimes \overline{p}]_L \otimes \Sigma]_{J''M''} \\ &= \sum_L (-1)^{J+L} \sqrt{\frac{2L+1}{2J+1}} [[X_J \otimes \overline{p}]_L \otimes \Sigma]_{JM} \end{aligned} \quad \text{(E.1.41)}$$

Plugging this in, we find

$$\begin{aligned}
&\langle\psi'(l's')j'||(\Sigma\cdot\overline{p})X_J||\psi(ls)j\rangle \\
&= \sum_L (-1)^{J+L}\sqrt{\frac{2L+1}{2J+1}}\,\langle\psi'(l's')j'||[[X_J\otimes\overline{p}]_L\otimes\Sigma]_J||\psi(ls)j\rangle \\
&= \sum_L (-1)^{J+L}\sqrt{\frac{2L+1}{2J+1}}\sqrt{(2J+1)(2j'+1)(2j+1)}\begin{Bmatrix} l' & l & L \\ s' & s & 1 \\ j' & j & J \end{Bmatrix} \\
&\qquad\qquad \langle\psi'l'||[X_J\otimes\overline{p}]_L||\psi l\rangle\,\langle s'||\Sigma||s\rangle
\end{aligned} \tag{E.1.42}$$

Appendix F

Simple Harmonic Oscillator Basis Formulation

One of the most common choice of basis for representing nuclear systems is the simple harmonic oscillator (SHO) basis. This basis spans the space of wavefunctions, such that any reasonably well behaved single-particle wavefunction can be expressed as a linear combination of SHO states.

In order to define a SHO basis, we need to specify two numbers. First, we need to specify the SHO length scale, b. This will allow us to define dimensionless SHO coordinates which we call $\{\xi, p_\xi\}$.

$$\xi = \frac{x_1 - x_2}{\sqrt{2}b}, \quad p_\xi = b\frac{p_1 - p_2}{\sqrt{2}} \tag{F.0.1}$$

These are related to the usual two-body relative coordinates as follows.

$$\xi = \frac{r}{\sqrt{2}b}, \quad p_\xi = \sqrt{2}bp_r \tag{F.0.2}$$

The second number we need to specify is the number of oscillator quanta we will allow in our basis, Λ. One can think of this as a practical necessity, since we need a finite sized basis in order to use it for computation. One can also think of this as an effective theory cut-off, but we will not take that approach here.

Individual SHO states are represented by a radial quantum number n and an orbital angular momentum l with z-component m. The wavefunction for these states is given by the usual formula.

$$\begin{aligned}\langle \vec{r}|nlm\rangle &= \left(\frac{1}{\sqrt{2}b}\right)^{3/2} R_{nl}(\xi)Y_{lm}(\theta,\phi) \\ &= \left(\frac{1}{\sqrt{2}b}\right)^{3/2} \sqrt{\frac{2\Gamma(n+1)}{\Gamma(n+l+3/2)}}\xi^l L_n^{(l+1/2)}(\xi^2)Y_{lm}(\theta,\phi)e^{-\xi^2/2}\end{aligned} \tag{F.0.3}$$

Where $L_n^{(l+1/2)}(\xi^2)$ are associated Laguerre polynomials.

$$L_n^{(\alpha)}(x) = \sum_{t=0}^{n} (-1)^t \frac{\Gamma(n+\alpha+1)}{\Gamma(n-t+1)\Gamma(t+\alpha+1)} \frac{x^t}{t!} \tag{F.0.4}$$

The total oscillator quanta associated with a SHO state (nl) is equal to $N = 2n + l$.

Relative two-nucleon wavefunctions in a specific (stj) channel can be represented as a sum over states of a given (nl). We cut off the sum at the oscillator cutoff $2n + l \leq \Lambda$.

$$|\Psi, stj\rangle = \sum_{nl}^{\Lambda} \Psi_{nl} \, |nlstj\rangle \tag{F.0.5}$$

If $s = 0$ then $l = j$, and if $s = 1$ then either $l = j$ or $l = \{j - 1, j + 1\}$ depending on parity. Allowed states must obey fermionic anti-symmetry, which gives us the constraint

$$(-1) = (-1)^{l+s+t} \tag{F.0.6}$$

The Hamiltonian in the SHO basis is a block-diagonal matrix, where each block represents a single channel (stj). Within a specific channel, we can write out the elements of the SHO basis as $\{|n_1 l_1\rangle, |n_2 l_2\rangle, \dots\}$. Then we can write the blocks of the Hamiltonian within a specific channel as

$$H(stj) = \begin{pmatrix} \langle 1|H|1\rangle & \langle 1|H|2\rangle & \dots \\ \langle 2|H|1\rangle & \langle 2|H|2\rangle & \\ \vdots & & \ddots \end{pmatrix} \tag{F.0.7}$$

The Hamiltonian consists of a kinetic energy part, plus a potential energy which comes from Av18. First, we write out the kinetic energy in SHO coordinates.

$$T = \frac{p_r^2}{2M_r} = \frac{p_\xi^2}{4M_r b^2} \tag{F.0.8}$$

where M_r is the reduced mass of the two-nucleon system. The non-zero matrix elements of the kinetic energy operator p_ξ^2 are

$$\langle n, l|p_\xi^2|n, l\rangle = 2n + l + 3/2 \tag{F.0.9}$$

and

$$\langle n-1, l|p_\xi^2|n, l\rangle = \langle n, l|p_\xi^2|n-1, l\rangle = \sqrt{n(n+l+1/2)} \tag{F.0.10}$$

In particular, the kinetic energy always creates a large connection between the included space $2n + l \leq \Lambda$ and the excluded space. Note also that the kinetic energy is proportional to $1/b^2$. As we make b smaller to resolve more fine details of the short range potential, we pay a higher price for the kinetic energy mixing us into the excluded space.

F.1 SHO Matrix Elements - Talmi Integrals

The one major benefit of the SHO basis is that it is discrete. It is trivial to put it on a computer and find the eigenstates of the Hamiltonian - given adequate computing resources.

In order to calculate the Hamiltonian matrix elements, we need to compute the radial integrals of the potential between the radial SHO wavefunctions. The SHO wavefunctions are polynomials in the SHO coordinate ξ, times an exponential $e^{-\xi^2/2}$. Thus, the matrix element is a sum of integrals of the potential times a power of ξ times $e^{-\xi^2}$. These basic building blocks are the so-called *talmi-integrals*.

$$V_p = \frac{2}{\Gamma(p+3/2)} \int_0^\infty d\xi\, \xi^{2p+2} V(\sqrt{2}b\xi) e^{-\xi^2} \tag{F.1.1}$$

Note that the Talmi integrals implicitly depend on the choice of the SHO length scale b since the physical particle separation is $r = \sqrt{2}b\xi$.

The normalization out front is chosen so that the talmi integrals of the constant function 1 are simply equal to $(1)_p = 1$. Then we define the radial matrix element of V between SHO states (nl) and $(n'l')$ to be $I[V](n'l', nl)$.

$$I[V](n'l', nl) = \int_0^\infty d\xi\, \xi^2 R_{n'l'} R_{nl} V = \sum_{p=(l+l')/2}^{(l+l')/2+n+n'} B(n'l', nl, p) V_p \tag{F.1.2}$$

The Talmi-B coefficients are simple to calculate by picking out particular powers of ξ.

$$\begin{aligned} B(nl, n'l', p) &= (-1)^s \Gamma(p+3/2) \sqrt{\frac{\Gamma(n+l+3/2)\Gamma(n'+l'+3/2)}{n!(n')!}} \\ &\times \sum_{k=-s/2}^{s/2} \binom{n}{s/2+k} \binom{n'}{s/2-k} \frac{1}{\Gamma(s/2+k+l+3/2)} \frac{1}{\Gamma(s/2-k+l'+3/2)} \end{aligned} \tag{F.1.3}$$

with $p = s + (l+l')/2$. The sum over k can evaluated in terms of the regularized hypergeometric function ${}_3\tilde{F}_2$.

$$\begin{aligned} B(nl, n'l', p) &= (-1)^s \Gamma(p+3/2) \sqrt{\frac{\Gamma(n+l+3/2)\Gamma(n'+l'+3/2)}{n!(n')!}} \\ &\times \frac{(n')!}{s!} \frac{1}{\Gamma(s+l'+3/2)} {}_3\tilde{F}_2(\{-n, -s, -s-l'-1/2\}, \{l+3/2, n'-s+1\}, -1) \end{aligned} \tag{F.1.4}$$

with $p = s + (l+l')/2$.

One must be very careful when using these formula when dealing with large oscillator quanta. The values of the talmi-B coefficients become extremely large, and they alternate in sign. In order to accurately represent the matrix elements, these must be computed to very high numerical precision.

For example, take the matrix element of the operator 1. Using orthogonality of the SHO states, we must have

$$\sum_{p=(l+l')/2}^{(l+l')+n+n'} B(n'l, nl, p) = \delta_{n,n'} \tag{F.1.5}$$

for any choice of n, n', and l. In order to accurately represent matrix elements using Talmi integrals in a SHO basis with cut-off Λ, one needs numerical precision approximately equal to

$$P = P_0 + (-1.188 + 0.469\Lambda) \tag{F.1.6}$$

Here P_0 is the desired precision of the result, and P is the precision with which we need to compute the Talmi integrals and Talmi B-coefficients. For example, if one wants to compute with $\Lambda = 100$, then one needs to calculate everything to precision $P = P_0 + 45.8$. Thus, when we go to higher values of the cut-off, not only do we have more matrix elements to compute overall, but we need to compute them to higher precision.

F.2 Simple Harmonic Oscillator Current Matrix Elements

One particularly important matrix element we need to calculate are the matrix elements of the spherical bessel functions. These show up any time we want to evaluate the current operators as a function of the momentum transfer, q. First, we define a dimensionless SHO momentum transfer k.

$$k = \frac{qb}{\sqrt{2}} \tag{F.2.1}$$

This is what shows up in the argument of the spherical Bessel functions when we write it in terms of SHO coordinates.

$$j_l(qr/2) = j_l(k\xi) \tag{F.2.2}$$

In order to calculate the radial matrix elements, we calculate the Talmi integrals of the spherical Bessel function. This turns out to be expressible in terms of the confluent hypergeometric function ${}_1F_1$.

$$\begin{aligned}(j_l(k\xi))_p &= \frac{2}{\Gamma(p+3/2)} \int_0^\infty dr\, r^{2p+2} j_l(k\xi) e^{-r^2} \\ &= (k/2)^l \frac{\Gamma(3/2)\Gamma(p+\frac{l+3}{2})}{\Gamma(l+3/2)\Gamma(p+3/2)} {}_1F_1\left(p+\frac{l+3}{2}, l+\frac{3}{2}, -k^2/4\right)\end{aligned} \tag{F.2.3}$$

This is actually just an associated Laguerre polynomial in disguise.

$$(j_l(k\xi))_p = (k/2)^l \frac{\Gamma(3/2)\Gamma(p-l/2+1)}{\Gamma(p+3/2)} L_{p-l/2}^{(l+1/2)}(k^2/4) e^{-k^2/4} \tag{F.2.4}$$

The last matrix element we need to compute the current operators is the convective current. We can simply plug into our formula we found previously.

$$\begin{aligned}
&\langle n'l'||\overline{p}_\xi \cdot \mathbf{X}_{JL}(k\vec{\xi})||nl\rangle \\
&= i\frac{1}{2}(-1)^{J+L+1}\sqrt{l(2J+1)}\left\{ \begin{array}{ccc} 1 & L & J \\ l' & l & l-1 \end{array} \right\} \langle l'||Y_L||l-1\rangle \\
&\qquad \times \int_0^\infty r^2 dr\, R_{n'l'} j_L(k\xi)\left(\frac{dR_{nl}}{dr} + \frac{l+1}{r}R_{nl}\right) \\
&-i\frac{1}{2}(-1)^{J+L+1}\sqrt{(l+1)(2J+1)}\left\{ \begin{array}{ccc} 1 & L & J \\ l' & l & l+1 \end{array} \right\} \langle l'||Y_L||l+1\rangle \\
&\qquad \times \int_0^\infty r^2 dr\, R_{n'l'} j_L(k\xi)\left(\frac{dR_{nl}}{dr} - \frac{l}{r}R_{nl}\right) \\
&+i\frac{1}{2}\sqrt{l'(2J+1)}\left\{ \begin{array}{ccc} L & 1 & J \\ l' & l & l'-1 \end{array} \right\} \langle l'-1||Y_L||l\rangle \\
&\qquad \times \int_0^\infty r^2 dr \left(\frac{dR_{n'l'}}{dr} + \frac{l'+1}{r}R_{n'l'}\right) j_L(k\xi)R_{nl} \\
&-i\frac{1}{2}\sqrt{(l'+1)(2J+1)}\left\{ \begin{array}{ccc} L & 1 & J \\ l' & l & l'+1 \end{array} \right\} \langle l'+1||Y_L||l\rangle \\
&\qquad \times \int_0^\infty r^2 dr \left(\frac{dR_{n'l'}}{dr} - \frac{l'}{r}R_{n'l'}\right) j_L(k\xi)R_{nl}
\end{aligned} \tag{F.2.5}$$

It is well known that the momentum operator in the SHO basis is simply a combination of a raising and a lowering operator. This means we can evaluate the derivatives in terms of raised and lowered SHO wavefunctions. The result is

$$\left(\frac{d}{dr} + \frac{l+1}{r}\right) R_{nl} = \sqrt{n+l+1/2}R_{n,l-1} + \sqrt{n+1}R_{n+1,l-1} \tag{F.2.6}$$

and

$$\left(\frac{d}{dr} - \frac{l}{r}\right) R_{nl} = -\sqrt{n}R_{n-1,l+1} - \sqrt{n+l+3/2}R_{n,l+1} \tag{F.2.7}$$

This allows us to express the convective current matrix elements in terms of the charge

matrix elements of different n and l.

$$\begin{aligned}
&\langle n'l'||\overline{p}_\xi \cdot \mathbf{X}_{JL}(k\vec{\xi})||nl\rangle \\
&= i\frac{1}{2}(-1)^{J+L+1}\sqrt{l(2J+1)}\left\{ \begin{array}{ccc} 1 & L & J \\ l' & l & l-1 \end{array} \right\} \\
&\times \left[\sqrt{n+l+1/2}\,\langle n'l'||X_L||n,l-1\rangle + \sqrt{n+1}\,\langle n'l'||X_L||n+1,l-1\rangle\right] \\
&+i\frac{1}{2}(-1)^{J+L+1}\sqrt{(l+1)(2J+1)}\left\{ \begin{array}{ccc} 1 & L & J \\ l' & l & l+1 \end{array} \right\} \\
&\times \left[\sqrt{n}\,\langle n'l'||X_L||n-1,l+1\rangle + \sqrt{n+l+3/2}\,\langle n'l'||X_L||n,l+1\rangle\right] \\
&+i\frac{1}{2}\sqrt{l'(2J+1)}\left\{ \begin{array}{ccc} L & 1 & J \\ l' & l & l'-1 \end{array} \right\} \\
&\times \left[\sqrt{n'+l'+1/2}\,\langle n',l'-1||X_L||nl\rangle + \sqrt{n'+1}\,\langle n'+1,l'-1||X_L||nl\rangle\right] \\
&+i\frac{1}{2}\sqrt{(l'+1)(2J+1)}\left\{ \begin{array}{ccc} L & 1 & J \\ l' & l & l'+1 \end{array} \right\} \\
&\times \left[\sqrt{n'}\,\langle n'-1,l'+1||X_L||nl\rangle + \sqrt{n'+l'+3/2}\,\langle n',l'+1||X_L||nl\rangle\right]
\end{aligned} \tag{F.2.8}$$

The convective current can be greatly simplified in the case that we take the longitudinal multipole. As before, we use the fact that the gradient of the chrage multipole is equal to the longitudinal multipole.

$$[\vec{p}_\xi, X_{JM}(k\vec{\xi})] = -ik\mathbf{X}^{(l)}_{JM}(k\vec{\xi}) \tag{F.2.9}$$

Then, as before, we can write the longitudinal component of the convective current in terms of the commutator of the kinetic energy (now written in SHO coordinates).

$$\left[\frac{|\vec{p}_\xi|^2}{2}, X_{JM}(k\vec{\xi})\right] = (-ik)\frac{1}{2}\left(\vec{p}\cdot\mathbf{X}^{(l)}_{JM} + \mathbf{X}^{(l)}_{JM}\cdot\vec{p}\right) \tag{F.2.10}$$

The SHO potential is just ξ^2, and it clearly commutes with the charge operator. Thus we have no issues in including the SHO potential in the commutator.

$$\left[\frac{|\vec{\xi}|^2}{2} + \frac{|\vec{p}_\xi|^2}{2}, X_{JM}(k\vec{\xi})\right] = -ik\,\overline{p}_\xi\cdot\mathbf{X}^{(l)}_{JM}(k\vec{\xi}) \tag{F.2.11}$$

The commutator of the SHO potential simply gives the difference in total quanta $N' - N$, and we have a simple relationship for the longitudinal convective current.

$$(2n'+l'-2n-l)\,\langle n'l'||X_{JM}(k\vec{\xi})||nl\rangle = -ik\,\langle n'l'||\overline{p}_\xi\cdot\mathbf{X}^{(l)}_{JM}(k\vec{\xi})||nl\rangle \tag{F.2.12}$$

Appendix G

Calculating the Green's Function

As we have seen, without making approximations which allow us to simplify, we need to compute the full nuclear Green's function. The center-of-mass part is trivial, but the relative Hamiltonian has all of the nuclear interactions. So we focus on how to calculate the relative Green's function operator.

$$G(\omega) = \frac{1}{\omega - H_r} \tag{G.0.1}$$

Focusing on the single channel case for simplicity, we can express the result of the Green's function in coordinate space using a function of two coordinates $g(p, r, r')$, where p is the wavenumber which comes form ω.

$$\omega = \frac{p^2}{2M_r} \tag{G.0.2}$$

Let the Green's function act on an eigenstate of the Hamiltonian with definite angular momentum and radial wavefunction $u(r)$. Then the resulting wavefunction can be written as

$$G(\omega)\,|\psi\rangle = 2M_r \int_0^\infty dr dr' g(p, r, r') u(r')\,|rl\rangle \tag{G.0.3}$$

Applying $(\omega - H_r)$ to this resulting wavefunction gives us an equation for the coordinate space Green's function.

$$\left[p^2 + \frac{d^2}{dr^2} - \frac{l(l+1)}{r^2} - U(r)\right] g(p, r, r') = \delta(r - r') \tag{G.0.4}$$

where $U = 2M_r V$, as before. When $r < r'$ or $r > r'$, the Green's function is a solution of the usual Schrodinger equation. At $r = r'$ it is continuous, and has a unit discontinuity in its first derivative.

$$\lim_{\epsilon \to 0} \left(\frac{d}{dr} g(p, r, r') \bigg|_{r=r'+\epsilon} - \frac{d}{dr} g(p, r, r') \bigg|_{r=r'-\epsilon} \right) = 1 \tag{G.0.5}$$

we can accomplish this very easily by combining two solutions to the Schrodinger equation. Let $u(r)$ be an inner solution which obeys the regularity condition at the origin.

$$u(r) \propto r^{l+1} \quad \text{at} \quad r = 0 \tag{G.0.6}$$

Let $v(r)$ be some other solution, which has no such regularity condition at the origin. We will call this an "outer solution". In contrast to the inner solution, the outer solution $v(r)$ will generally go like r^{-l} at the origin. Recall that the Wronskain of two solutions to the Schrodinger equation is constant - independent of r.

$$W(u,v) = u\frac{dv}{dr} - \frac{du}{dr}v = \text{constant} \tag{G.0.7}$$

Then it is trivial to construct a function which is continuous and has a unit discontinuity at $r = r'$.

$$g(p,r,r') = \frac{u(r^<)v(r^>)}{W(u,v)} \tag{G.0.8}$$

Here we use the notation to mean $r^<$ is the small of r, r' and $r^>$ is the larger of the two.

There is at least one obvious problem with what we have done here. We can't use this to calculate anything because the outer solution $v(r)$ is under-determined. Indeed, we can add any multiple of the inner solution and get another valid outer solution without changing any of the argument.

$$v(r) \to v(r) + \lambda u(r) \tag{G.0.9}$$

This makes the results completely ambiguous. We need some additional constraint in order to determine what $v(r)$ we should use in order to get a definite result.

This problem is completely solved by the $+i\epsilon$ which is included in the Green's function. This takes us off the real axis, where there is no ambiguity. When $p \in \mathbb{C}$ with Im $p \neq 0$, the solutions to the Schrodinger equation have an exponential behaviour. This gives us a simple constraint for our outer solution - we want to pick the decaying exponential part.

To this end, we define two outer solutions. At large r where the potential goes to zero $U(r) \to 0$, these have simple behaviour which matches the free Schrodinger equation.

$$\begin{aligned} v^{(1)} &\sim prh^{(1)}(pr) \sim (-i)^{l+1}e^{ipr} \\ v^{(2)} &\sim prh^{(2)}(pr) \sim i^{l+1}e^{-ipr} \end{aligned} \tag{G.0.10}$$

where $h^{(1,2)}$ are the usual spherical Hankel functions. I have also included the large r exponential behaviour to clear up which of the two solutions obey the large r constraint. When Im $p > 0$, we must pick $v^{(1)}$, and conversely when Im $p < 0$ we must pick $v^{(2)}$. This leads to a branch cut along the positive real ω-axis. The real part of the Green's function is continuous across the positive real axis, and the imaginary part flips sign.

This already has cleared up the ambiguity. It makes no difference what inner solution we take because this is compensates for by the factor $W(u,v)$ in the denominator. However, it is still useful to fix the inner solution. When $p \in \mathbb{C}$, we do not use the boundary condition for scattering states to fix the inner solution. Instead, we define an inner solution which matches the free solution at the origin.

$$\varphi(r) \sim prj_l(pr) \quad \text{at} \quad r = 0 \tag{G.0.11}$$

In the single channel case, there are only two linearly independent solutions to the Schrodinger equation. Therefore we know we can express the inner solution as a sum of the two outer solutions.

$$\varphi(r) = \frac{1}{2}\mathcal{F}_1 v^{(1)}(r) + \frac{1}{2}\mathcal{F}_2 v^{(2)}(r) \tag{G.0.12}$$

When we are dealing with the usual scattering states, the ratio of the two functions is the S-matrix.

$$S = \mathcal{F}_1/\mathcal{F}_2 \tag{G.0.13}$$

The functions $\mathcal{F}_1$ and $\mathcal{F}_2$ can be determined by looking at the Wronskian. From the large r behaviour, we can determine the Wronskian of the two outer solutions.

$$W(v^{(1)}, v^{(2)}) = -2ip \tag{G.0.14}$$

Then the Wronskian with the inner solution can be computed in terms of the two functions $\mathcal{F}_1$ and $\mathcal{F}_2$.

$$\begin{aligned} W(\varphi, v^{(1)}) &= ip\mathcal{F}_2 \\ W(\varphi, v^{(2)}) &= -ip\mathcal{F}_1 \end{aligned} \tag{G.0.15}$$

The functions $\mathcal{F}_{1,2}$ are analytic functions for all $p \in \mathbb{C}$. The function $\mathcal{F}_2$ is known as the *Jost function*. We can see the importance of this function by considering bound states. We know that bound states decay exponentially at large r, so when $p = i\kappa$ we must have $\mathcal{F}_2 = 0$. Therefore the zeros of the Jost function give us the bound states.

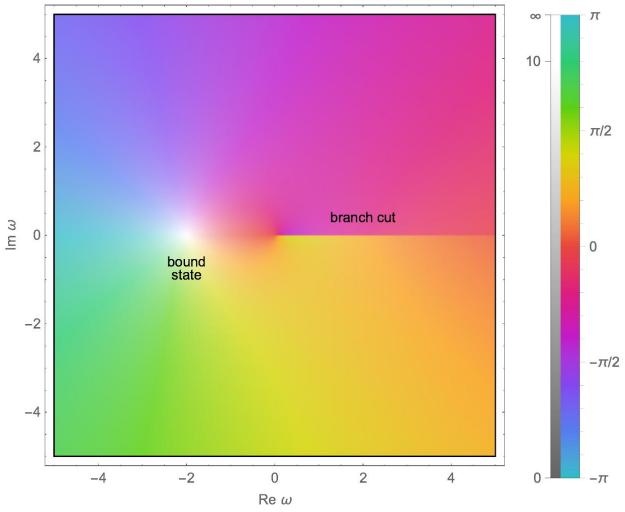

Figure G.1: Sketch of the Green's function in the complex plane, showing the bound state pole and the branch cut on the positive real axis.

Now we can define the Green's functions in the upper half plane (UHP) Im $p > 0$

$$\text{UHP: } g^+(p,r,r') = \frac{-i}{p}\frac{\varphi(r^<)v^{(1)}(r^>)}{\mathcal{F}_2}, \quad \text{Im } p > 0 \tag{G.0.16}$$

In the lower half plane (LHP) with Im $p < 0$, we have

$$\text{LHP: } g^-(p,r,r') = \frac{i}{p}\frac{\varphi(r^<)v^{(2)}(r^>)}{\mathcal{F}_1}, \quad \text{Im } p < 0 \tag{G.0.17}$$

At a bound state $p = i\kappa$, the Jost function is zero, $\mathcal{F}_2 = 0$. Therefore the Green's function has a pole at bound states. The imaginary part of the Green's function is discontinuous across the positive real axis, giving us a branch cut.

In practice, calculating the inner and outer solution needs to be done carefully. When Im $p \neq 0$, the inner solution always diverges exponentially at large r (apart from bound states), and the outer solution diverges at the origin. We calculate the inner solution by using the variable S-matrix method to find the initial conditions $\{u, u'\}$ at some intermediate r, and then numerically solve the Schrodinger equation in to $r = 0$ and out to some large R. For $r > R$, we use calculate the Wronskian with the outer solutions to find the asymptotic form. We also need to be careful when calculating the outer solution because it decays exponentially at large r, and it generally blows up at the origin. We pick some reasonably large R and integrate in to $r = 0$.

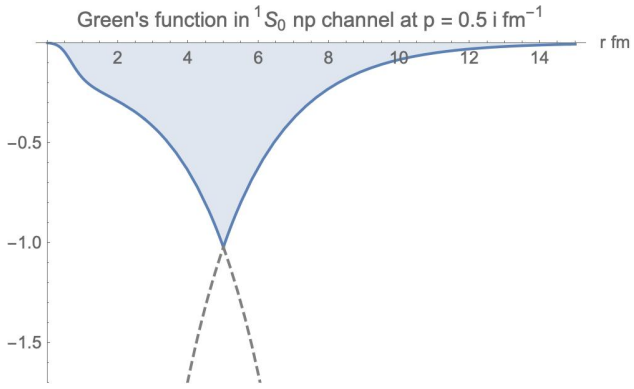

Figure G.2: Green's function at negative energy, or imaginary wavenumber. The dashed lines show the continuation of the inner/outer solutions, which both blow up.

Coupled Channel Green's Function

In coupled channels, the Green's function operator acts on states with mixed orbital angular momentum. The coordinate space Green's function can be represented as a matrix, in the same way we did in Section 6.1.

$$G(\omega)\,|\psi\rangle = 2M_r \int_0^\infty dr dr' \sum_{l,l'} g_{l,l'}(p,r,r')u_{l'}(r')\,|rl\rangle \tag{G.0.18}$$

The Green's function satisfies the matrix version of the inhomogeneous differential equation.

$$(p^2 - 2M_r\mathbf{H})\mathbf{g}(p,r,r') = \delta(r-r') \tag{G.0.19}$$

At $r = r'$ it is continuous, and has a unit discontinuity proportional to the identity matrix.

$$\lim_{\epsilon\to 0}\left(\frac{d}{dr}\mathbf{g}(p,r,r')\bigg|_{r=r'+\epsilon} - \frac{d}{dr}\mathbf{g}(p,r,r')\bigg|_{r=r'-\epsilon}\right) = \mathbf{I} \tag{G.0.20}$$

This can be seen in the example in Figure G.3.

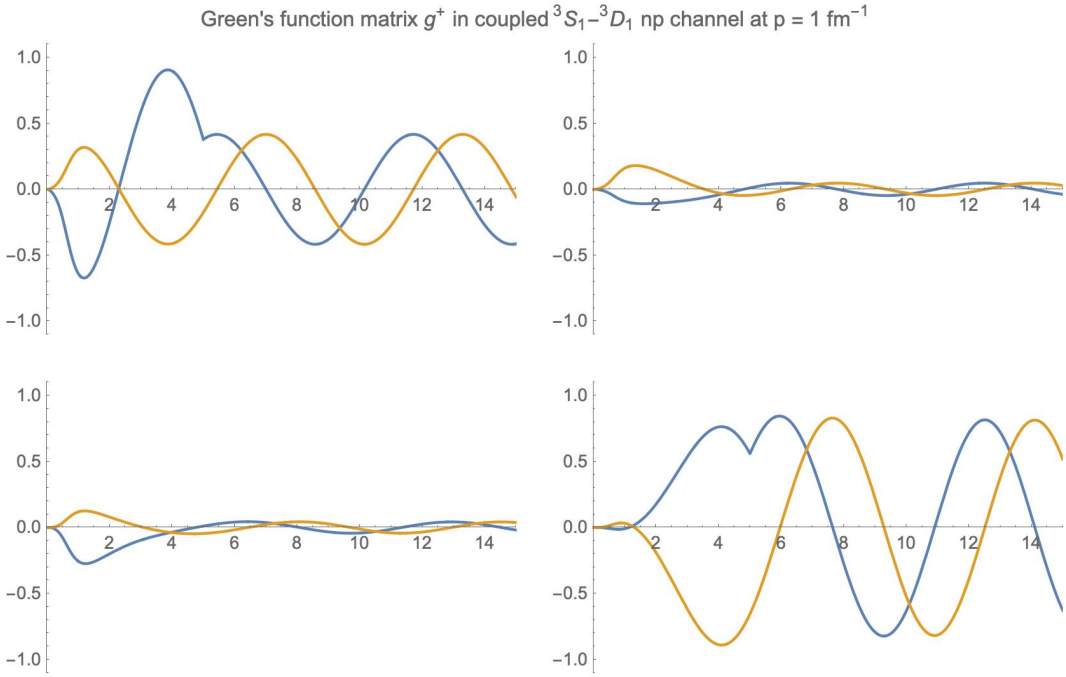

Figure G.3: Components of the Green's function matrix $\mathbf{g}^+(p,r,r')$.

For coupled channels, we again use the matrix notation we used in Section 6.1. In the UHP, we want our outer solution to have the boundary conditions

$$\mathbf{v}^{(1)} \sim \begin{pmatrix} prh^{(1)}_{j-1}(pr) & 0 \\ 0 & prh^{(1)}_{j+1}(pr) \end{pmatrix} \tag{G.0.21}$$

and similarly for $\mathbf{v}^{(2)}$. The inner solution similarly has a regularity condition at the origin, which is the natural matrix extension of the one we had in the single channel case. Again, the inner solutoin can be written as a linear combination of the outer solutions

$$\varphi(r) = \frac{1}{2}\mathbf{v}^{(1)}\mathcal{F}_1 + \frac{1}{2}\mathbf{v}^{(2)}\mathcal{F}_2 \tag{G.0.22}$$

Here the coefficients $\mathcal{F}_{1,2}$ are matrices. For scattering states $p \in \mathbb{R}$, these are again related to the S-matrix.

$$S = \mathcal{F}_1(\mathcal{F}_2)^{-1} \tag{G.0.23}$$

We want to do as we did before and define a Green's function using this and the inner solution. We can't simply write $1/\mathcal{F}_2$ since $\mathcal{F}_2$ is a matrix, so instead we use the inverse matrix $(\mathcal{F}_2)^{-1}$. We might try a matrix form like

$$\boxed{g^+(p,r,r') = \frac{-i}{p}\begin{cases} \mathbf{u}(r)(\mathcal{F}_2)^{-1}\mathbf{v}^{(1)T}(r') & r < r' \\ \mathbf{v}^{(1)}(r)((\mathcal{F}_2)^{-1})^T\mathbf{u}^T(r') & r' < r \end{cases}} \tag{G.0.24}$$

However, because we are now dealing with matrices, it is not obvious that this function is even continuous. Fortunately, It turns out this is the case! The proof is given in Newton Chapter 15.2 [New82], and we will quickly go over it here.

Following Newton Chapter 15.2, we pick an arbitrary r_0 and define an auxiliary solution $\mathbf{f}(p,r)$ such that

$$\mathbf{f}(p,r_0) = 0, \quad \frac{d}{dr}\mathbf{f}(p,r_0) = 1 \tag{G.0.25}$$

This will be some linear combination of the solutions $\mathbf{v}^{(1,2)}$

$$\mathbf{f}(p,r) = \frac{1}{2}\mathbf{v}^{(1)}(p,r)a + \frac{1}{2}\mathbf{v}^{(2)}(p,r)b \tag{G.0.26}$$

we can calculate a, b from the Wronskian

$$a = \frac{-i}{p}W(\mathbf{v}^{(2)T}(p,r), \mathbf{f}(p,r)) \tag{G.0.27}$$

and

$$b = \frac{i}{p}W(\mathbf{v}^{(1)T}(p,r), \mathbf{f}(p,r)) \tag{G.0.28}$$

Calculating the Wronskian at r_0, and using the properties of $\mathbf{f}$ outlined above, we can evaluate this directly.

$$a = \frac{-i}{p}\mathbf{v}^{(2)T}(p,r_0) \tag{G.0.29}$$

and

$$b = \frac{i}{p}\mathbf{v}^{(1)T}(p,r_0) \tag{G.0.30}$$

Plugging this in, we find

$$\mathbf{f}(p,r) = -\frac{i}{2p}\left(\mathbf{v}^{(1)}(p,r)\mathbf{v}^{(2)T}(p,r_0) - \mathbf{v}^{(2)}(p,r)\mathbf{v}^{(1)T}(p,r_0)\right) \tag{G.0.31}$$

At r_0, the properties of $\mathbf{f}$ we used now tell us that

$$\mathbf{v}^{(1)}(p,r_0)\mathbf{v}^{(2)T}(p,r_0) - \mathbf{v}^{(2)}(p,r_0)\mathbf{v}^{(1)T}(p,r_0) = 0 \tag{G.0.32}$$

and

$$\left(\frac{d}{dr}\mathbf{v}^{(1)}(p,r_0)\right)\mathbf{v}^{(2)^T}(p,r_0) - \left(\frac{d}{dr}\mathbf{v}^{(2)}(p,r_0)\right)\mathbf{v}^{(1)^T}(p,r_0) = 2ip \tag{G.0.33}$$

Since r_0 was picked arbitrarily, this is true for any r. Indeed, we find

$$(p^2 - 2M_r\mathbf{H})g^+(p,r,r') = \delta(r-r') \tag{G.0.34}$$

As desired.

Appendix H

Box Normalization

In Section 9.5, we need to know how to sum over continuum states. The solution is to use box normalization. The set up goes as follows. We consider scattering states at any energy $E > 0$. Whatever this energy is, we can choose an arbitrarily large R such that there are many oscillations of the wavefunction before it reaches the boundary. At $r = R$, we force the wavefunction to be zero. At this distance out, the wavefunction is very well represented by the sin function. Therefore, we have a condition on the wavenumber

$$pR - \frac{l\pi}{2} + \delta_l = n\pi \tag{H.0.1}$$

Where n is a natural number, $n = \{1, 2, 3, \dots\}$. At any $E > 0$, we take $R \to \infty$ and in that limit $n \to \infty$. So retaining only large terms, we can write

$$pR \approx n\pi \tag{H.0.2}$$

In the box, all states can be normalized to 1. And we choose R large enough that the integral becomes a simple integral of $\sin^2$ which averages out to $1/2$.

$$u_n(r) \sim N \sin\left(pr - \frac{l\pi}{2} + \delta_l\right) \tag{H.0.3}$$

$$N^2 \int_0^R |u(n)|^2 dr \approx N^2 \frac{R}{2} \tag{H.0.4}$$

Any corrections to this can be made arbitrarily small by picking a larger R. This tells us the normalization constant

$$N \approx \sqrt{\frac{2}{R}} \tag{H.0.5}$$

The energy is related to the wavenumber by $E = \frac{p^2}{2m}$

$$2mE = p^2 = \frac{1}{R^2}\left(n\pi + \frac{l\pi}{2} - \delta_l\right)^2 \tag{H.0.6}$$

Taking an implicit derivative gives us

$$2mdE = \frac{2}{R^2}\left(n\pi + \frac{l\pi}{2} - \delta_l\right)(\pi dn - d(\delta_l)) \approx \frac{2p}{R}(\pi dn - d(\delta_l)) \tag{H.0.7}$$

The phase shift δ_l is a function of E, so we write

$$d(\delta_l) = \frac{d(\delta_l)}{dE}dE \tag{H.0.8}$$

Plugging this in, we find

$$\left(1 + \frac{p}{mR}\frac{d(\delta_l)}{dE}\right)2mdE \approx 2\pi p\frac{dn}{R} \tag{H.0.9}$$

In the limit $R \to \infty$, we can drop the phase shift term. This relates a change in n to a change in E

$$2mdE \approx 2\pi p\frac{dn}{R} \tag{H.0.10}$$

The sum over states involves a discrete sum over n, but for large R we can approximate this sum by an integral. Then we can relate the integral over n to an integral over E

$$\begin{aligned} 1 &= |\text{gs}\rangle\langle\text{gs}| + \sum_n |n\rangle\langle n| \\ &\approx |\text{gs}\rangle\langle\text{gs}| + \int_0^\infty dn\,|n\rangle\langle n| \\ &\approx |\text{gs}\rangle\langle\text{gs}| + \int_0^\infty \frac{2mdE}{2\pi k}R\,|n\rangle\langle n| \\ &= |\text{gs}\rangle\langle\text{gs}| + \int_0^\infty \frac{1}{\pi\sqrt{2mE}}2mdE\,|E\rangle\langle E| \end{aligned} \tag{H.0.11}$$

We have defined a new normalization

$$|E\rangle = \sqrt{\frac{R}{2}}\,|n\rangle \tag{H.0.12}$$

Note that the R in the sum over states has now been compensated by our choice of normalization. The choice of normalization is arbitrary, so long as it is compensated for in the density of states. We have chosen the normalization so that the asymptotic form of the wavefunction is

$$u(E, r) \sim pr\left[\cos(\delta_l)j_l(pr) - \sin(\delta_l)y_l(pr)\right] \tag{H.0.13}$$

Where E is related to p in the standard way

$$E = \frac{p^2}{2m}, \quad 2mdE = 2pdp \tag{H.0.14}$$

We can now write the sum over all states, which is exactly what we needed.

$$1 = |\text{gs}\rangle \langle \text{gs}| + \int_0^\infty \frac{1}{\pi\sqrt{2mE}} 2mdE \, |E\rangle \langle E| \tag{H.0.15}$$

Alternatively, we can write this in terms of an integral over p

$$1 = |\text{gs}\rangle \langle \text{gs}| + \int_0^\infty \frac{2}{\pi} dp \, |E\rangle \langle E| \tag{H.0.16}$$